Univerzita Karlova
1.lékařská fakulta

Studijní program a obor: Preventivní medicína

MUDr. Pavlína Skalická

Geneticky podmíněná onemocnění rohovky: možnosti včasné detekce, ovlivnění vzniku a progrese

Inherited corneal disorders: options for early detection, influencing the onset and progression

Disertační práce

Školitelka: doc. MUDr. Petra Lišková, M.D., Ph.D.

Praha 2020

PROHLÁŠENÍ

Prohlašuji, že jsem předloženou práci vypracovala samostatně a že jsem řádně uvedla a citovala všechny použité prameny a literaturu. Současně prohlašuji, že práce nebyla využita k získání jiného nebo stejného titulu. Souhlasím s trvalým uložením elektronické verze mé práce v databázi systému meziuniverzitního projektu Theses.cz za účelem soustavné kontroly podobnosti kvalifikačních prací.

V Praze 1. 6. 2020 Pavlína Skalická

Podpis

Identifikační záznam:

SKALICKÁ, Pavlína. **Geneticky podmíněná onemocnění rohovky: možnosti včasné detekce, ovlivnění vzniku a progrese**. [Inherited corneal disorders: options for early detection, influencing the onset and progression]. Praha, 2020. 72 stran, 10 příloh. Disertační práce. Univerzita Karlova, 1. lékařská fakulta, Oční klinika 1. LF UK a VFN v Praze. Školitelka: Lišková, Petra.

PODĚKOVÁNÍ

Největší poděkování za vznik této disertační práce patří školitelce doc. MUDr. Petře Liškové, M.D., Ph.D., která připravila podmínky pro rozsáhlé molekulárně genetické testovaní a studium prakticky všech známých dědičných chorob rohovky. Uvedla mne do problematiky této skupiny onemocnění, zvláště zadní polymorfní dystrofie rohovky, a umožnila mi pracovat s rozsáhlým souborem pacientů s tímto onemocněním.

Děkuji také všem zahraničním spolupracovníkům, zvláště prof. Alison J. Hardcastlové a dr. Alici Davidsonové, z UCL Institutu Oftalmologie v Londýně.

Dále musím vyjádřit své poděkování členům skupiny oční genetiky z Laboratoře pro studium vzácných nemocí KDDL, 1. LF UK a VFN v Praze, zejména Ing. Ľubice Ďuďákové, Ph.D. za vedení při laboratorní práci na molekulárně genetické analýze pacientů a za cenné připomínky při psaní publikací. V neposlední řadě děkuji kolegům z Oční kliniky 1. LF UK a VFN v Praze. Děkuji i všem pacientům a jejich rodinám za trpělivost, kterou projevili při jejich rozsáhlém a časově náročném vyšetřování.

Výzkum popsaný v této disertační práci se týká převážně vzácných dědičných chorob rohovky. Problematika přesahuje hranice oftalmologie a prolíná se s genetikou a mnohdy i s interním lékařstvím. Proto se mohou některé kapitoly jevit nevyváženě v závislosti na lékařském oboru, ve kterém je čtenář odborníkem.

Tato práce vznikla za finanční podpory následujících grantových agentur: institucionální podpora Univerzity Karlovy – programy PROGRES-Q26/LF1 a PROGRES-Q25/LF1/2, Grantové agentury Univerzity Karlovy (GAUK) 250361/2017, Specifický vysokoškolský výzkum Univerzity Karlovy (SVV) 260367/2017, Grantové agentury České republiky (GAČR) 17-12355S, Univerzitní výzkumné centrum Univerzity Karlovy (UNCE) 204011.

OBSAH

SOUHRN

Úvod: Rozvoj molekulárně genetických metod vyvolal v řadě oborů potřebu jejich zařazení do běžné klinické praxe, oftalmologii nevyjímaje. Hlavním cílem této disertační práce byla detailní klinická charakterizace českých pacientů s podezřením na dědičná onemocnění rohovky, využití genetického testování ke stanovení nebo upřesnění jejich diagnózy a následně pak i v klinickém a genetickém poradenství, v konečném důsledku vedoucí k preventivním opatřením bránícím ztrátě zrakové ostrosti.

Materiál a metody: Jedinci zařazeni do výzkumu byli buď dlouhodobě sledováni, nebo nově odesláni oftalmology ke konziliárnímu vyšetření na Rohovkovou ambulanci Oční kliniky 1. LF UK a VFN v Praze. Detailní klinické vyšetření zahrnovalo rohovkovou tomografii, zrcadlovou mikroskopii, optickou koherenční tomografii se spektrální doménou, biometrii a genealogickou analýzu. DNA byla izolována z leukocytů venózní krve, popř. buněk bukální sliznice. Příčinné varianty byly hledány pomocí Sangerova a masivně paralelního sekvenování a jejich patogenita prokazována pomocí různých algoritmů, sledováním segregace u rodinných příslušníků. V některých případech bylo přistoupeno i k funkčním studiím, např. analýze sestřihu. U pacientů s Fuchsovou endotelovou dystrofií rohovky (FECD) bylo provedeno genotypování trinukleotidové repetice v genu *TCF4*.

Výsledky: Celkem bylo klinicky charakterizováno a ve formě publikačních výstupů zpracována molekulárně genetická příčina u 44 českých pacientů z 19 rodin s různými monogenně děděnými dystrofiemi a vývojovými anomáliemi rohovky. Studované klinické jednotky zahrnovaly mřížkovou dystrofii, Schnyderovu dystrofii, zadní polymorfní dystrofii (PPCD) typ 3, kongenitální hereditární endotelovou dystrofii, cornea plana a syndrom křehkých rohovek. Nejvýznamnější byl objev *GRHL2* jako nového genu, jehož mutace způsobují PPCD typ 4, což umožnilo prokázat, že společným mechanismem známých typů PPCD je abnormální aktivace epitelo-mezenchymální tranzice rohovkového epitelu. Genotypování 132 českých pacientů s FECD vedlo k průkazu přítomnosti repetic u 107 (81,1 %). Podařilo se také shromáždit z diferenciálně diagnostického hlediska unikátní soubor 6 případů vzácné paraproteinové keratopatie.

Závěr: Správně provedená a interpretovaná molekulárně genetická analýza potvrdila onemocnění u postižených jedinců, identifikovala rodinné příslušníky rizikové pro vznik dědičné nemoci, pomohla v odhadu její prognózy a začlenila se tak do standardní klinické praxe. Získané poznatky byly využity v prevenci rozvoje a progrese této skupiny chorob a jejich komplikací.

Klíčová slova: dědičná onemocnění rohovky, genotypování, genetické poradenství, prevence

SUMMARY

Introduction: The development of molecular genetic methods has in many fields necessitated their inclusion in routine clinical practice, including ophthalmology. The main aim of this thesis was detailed clinical characterization of Czech patients with suspected inherited corneal disorders, followed by genetic testing to determine or specify their clinical diagnosis and subsequently to use the knowledge gained in clinical and genetic counselling and to apply preventive measures in order to avoid loss of vision.

Material and Methods: Individuals included in this research were either followed up or newly referred to the Cornea clinic of the Department of Ophthalmology, First Faculty of Medicine, Charles University and General University Hospital in Prague. Detailed clinical examination included corneal tomography, specular microscopy, spectral domain optical coherence tomography, biometry and genealogical analysis. DNA was extracted from peripheral blood leucocytes or buccal cells. Disease-causing variants were searched for using Sanger or massively parallel sequencing, variant pathogenicity was assessed in silico using various algorithms and by segregation analyses within the families. In some cases assessment of the functional impact on the pre-mRNA splicing process was performed. In patients with Fuchs endothelial corneal dystrophy (FECD) CTG triplet repeat in *TCF4* was genotyped.

Results: In total, 44 Czech patients from 19 families with various monogenic corneal disorders were characterized and their clinical and molecular genetic findings reported in scientific literature. The disorders studied included lattice corneal dystrophy, Schnyder corneal dystrophy, posterior polymorphous corneal dystrophy (PPCD) type 3, congenital hereditary endothelial dystrophy, cornea plana, and brittle cornea syndrome. The most important discovery was that mutations in a novel gene *GRHL2* cause PPCD type 4. This has enabled to prove that abnormal activation of epithelial-to-mesenchymal transition in corneal endothelial cells is a common mechanism implicated in all currently known PPCD types. Genotyping of 132 Czech individuals with FECD found repeat expansion in 107 (81.1%). A unique group of 6 cases with rare paraproteinemic keratopathy was also collected as a part of differential diagnostic procedure.

Conclusion: Correctly performed and interpreted molecular genetic analysis confirmed the suspected diagnoses, identified family members at risk, helped to estimate prognosis and improved clinical counselling. The results were used in the prevention of development and progression of inherited corneal disorders and their complications.

Key words: inherited corneal disorders, genotyping, genetic counselling, preventive measures

SEZNAM ZKRATEK

Tabulka 1. Seznam použitých zkratek

Zkratka	Termín v anglickém jazyce	Termín v českém jazyce
1. LF UK	-	1. lékařská fakulta Univerzity Karlovy
A	Adenine	Adenin
AD	Autosomal dominant	Autozomálně dominantní
AR	Autosomal recessive	Autozomálně recesivní
BCS	Brittle cornea syndrom	Syndrom křehkých rohovek
bp	Base pair	Pár bází
C	Cytosine	Cytosin
CCK	-	Cyklokryokoagulace
CCT	Central corneal thickness	Centrální tloušťka rohovky
cDNA	Complementary DNA	Komplementární DNA
CE	Corneal endothelial	Rohovková endotelová
D	Dioptre	Dioptrie
DALK	Deep anterior lamellar keratoplasty	Hluboká přední lamelární keratoplastika
DM1	Myotonic dystrophy type 1	Myotonická dystrofie typu 1
DMEK	Descemet membrane endothelial keratoplasty	Typ zadní lamelární keratoplastiky
DNA	Deoxyribonucleic acid	Deoxyribonukleová kyselina
EBMD	Epithelial basement membrane dystrophy	Dystrofie bazální membrány epitelu
EMT	Epithelial-to-mesenchymal transition	Epitelo-mezenchymální přeměna
ERED	Epithelial recurrent erosion dystrophy	Dystrofie recidivujících erozí epitelu
FECD	Fuchs endothelial corneal dystrophy	Fuchsova endotelová dystrofie rohovky
G	Guanine	Guanin
GWAS	Genome-wide association study	Celogenomová asociační studie
CHED	Corneal hereditary endothelial dystrophy	Kongenitální hereditární endotelová dystrofie
Ig	Immunoglobulin	Imunoglobulin
iPSC	Induced pluripotent stem cells	Indukované pluripotentní kmenové buňky
K	Keratometry	Keratometrie
KDDL	-	Klinika dětského a dorostového lékařství
M	-	Muž
MBNL	Muscleblind-like protein	Sestřihový protein
MCD	Macular corneal dystrophy	Makulární dystrofie rohovky

MGUS	Monoclonal gammopathy of undetermined significance	Monoklonální gamapatie nejasného významu
mRNA	Messenger RNA	Mediátorová RNA
NKZO	-	Nejlépe korigovaná zraková ostrost
NOT	-	Nitrooční tlak
OL	-	Oko levé
OMIM	Online Mendelian Inheritance in Man	Online mendelovská dědičnost u člověka
OP	-	Oko pravé
PCR	Polymerase chain reaction	Polymerázová řetězová reakce
PKP	-	Perforující keratoplastika
PLK	-	Přední lamelární keratoplastika
PPCD	Posterior polymorphous corneal dystrophy	Zadní polymorfní dystrofie rohovky
PPV	Pars plana vitrectomy	Pars plana vitrektomie
pre-mRNA	Pre-messenger RNA	Pre-mediátorová RNA
RNA	Ribonucleic acid	Ribonukleová kyselina
SD-OCT	Spectral domain optical coherence tomography	Optická koherenční tomografie se spektrální doménou
SNP	Single nucleotide polymorphism	Jednonukleotidový polymorfismus
SO	Silicon iol	Silikonový olej
SP	-	Světelná projekce
STR	Short tandem repeat	Typ PCR metody
T	Thymine	Thymin
TAM	-	Transplantace amniové membrány
TE	Trabeculectomy	Trabekulektomie
U	Uracil	Uracil
VFN	-	Všeobecná fakultní nemocnice
WES	Whole-exome sequencing	Exomové sekvenování
WGS	Whole-genome sequencing	Genomové sekvenování
Ž	-	Žena

1 ÚVOD

1.1 Základní charakteristika rohovky

Fyziologická rohovka je bezcévná a čirá tkáň, která propouští a láme světlo vstupující do oka. Ze všech komponent oka má největší lomivou sílu s hodnotou 40,0 až 44,0 dioptrií. Je spolu se sklérou součástí pevného vnějšího obalu oka. Má vypouklý tvar s průměrným poloměrem zakřivení její přední plochy v centru 7,8 mm. Rozměr rohovky je v horizontální ose přibližně 11,5 mm a ve vertikální 10,5 mm (Eghrari et al. 2015b). Podle studie je centrální tloušťka rohovky (CCT) měřená pomocí předně-segmentové optické koherenční tomografie se spektrální doménou (SD-OCT) 555,50±29,64 µm (Lopez de la Fuente et al. 2016). Rohovka je tvořena pěti základními vrstvami: epitelem a jeho bazální membránou, Bowmanovou vrstvou, stromatem, Descemetovou membránou a endotelem (Obrázek 1). Změna v jejím zakřivení nebo poškození struktury a funkce jednotlivých vrtev rohovky, jež má za následek snížení až ztrátu průhlednosti, vede ke klinicky signifikantnímu poklesu zrakové ostrosti.

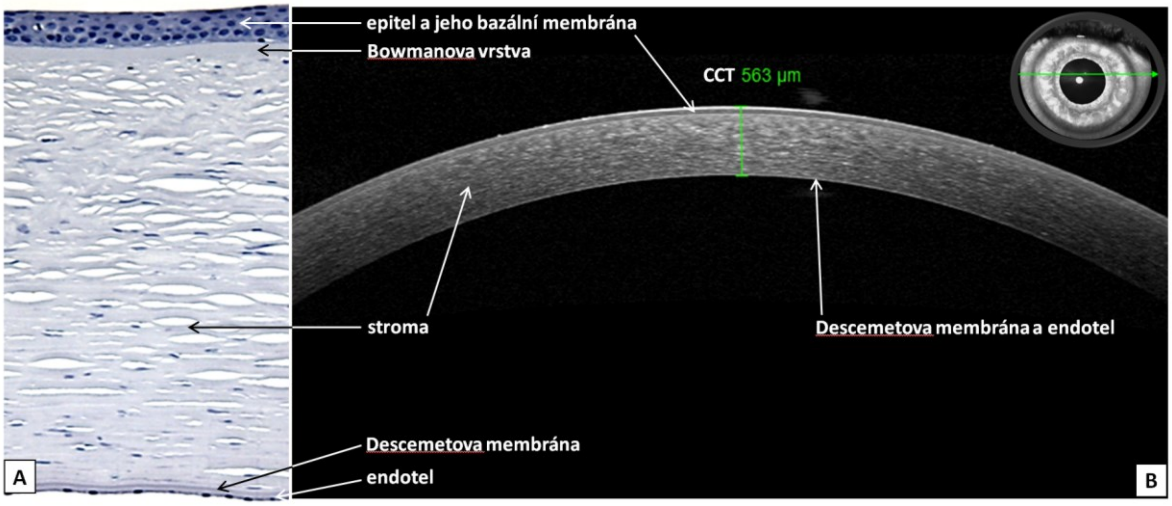

Obrázek 1. Stavba rohovky
(A) Histologický řez lidskou rohovkou obarvenou hematoxylinem-eosinem a (B) její zobrazení pomocí předně-segmentového SD-OCT. CCT – centrální tloušťka rohovky.
Za poskytnutí histologického snímku děkuji doc. Mgr. Kateřině Jirsové, Ph.D. z Laboratoře biologie a patologie oka, Ústav biologie a lékařské genetiky, 1. LF UK a VFN v Praze.

1.2 Dědičná onemocnění rohovky

Hereditární onemocnění rohovky představují heterogenní skupinu chorob, které lze etiologicky rozdělit na monogenně podmíněné řídící se Mendelovými zákony a komplexní. Monogenně dědičné choroby rohovky jsou vzácné, tj. postihují méně než 5 osob na 10 000 obyvatel, a jejich vznik je výsledkem vlivu jedné či dvou patogenních variant v jediném genu (Aronson 2006; Klintworth 2009). Etiopatogeneze častějších komplexních chorob rohovky je dána interakcí mezi genetickými faktory a zevním prostředím (Macek 2019). V současné době rozlišujeme více než třicet různých chorob rohovky s Mendelovským typem dědičnosti, jedná se o rohovkové dystrofie a různé vývojové poruchy ovlivňující její velikost nebo zakřivení. Nejčastějšími představiteli komplexních chorob jsou pak keratokonus a Fuchsova endotelová dystrofie rohovky, která je zároveň i nejvýznamnější indikací k transplantaci této tkáně (Park et al. 2015; Gain et al. 2016; Rock et al. 2017; Flockerzi et al. 2018).

Charakterizace onemocnění rohovky se provádí pomocí detailního očního vyšetření, u některých klinických jednotek se doplňují speciální zobrazovací vyšetřovací metody jako např. konfokální mikroskopie (analyzující všechny vrstvy rohovky), zrcadlová mikroskopie (zobrazující pouze endotel), rohovková tomografie (pomocí SD-OCT nebo Scheimpflugovy kamery umožňující také trojrozměrné modelování rohovky) a fotografie předního segmentu oka.

Molekulárně genetické vyšetření, tj. nález kauzální mutace, jednoznačně potvrdí diagnózu monogenního onemocnění rohovky, která nemusí být vždy klinickým vyšetřením zřejmá, např. u pacientů se značně pokročilými nálezy nebo u jedinců po oboustranných transplantacích této tkáně.

1.2.1 Rohovkové dystrofie

Dystrofie rohovky je skupina chorob, které bývají oboustranně symetrické, pomalu progredující s časnou manifestací (většinou v prvních dvou dekádách života), bez výskytu primární vaskularizace, zánětu a systémového postižení (Klintworth 2009). Rohovkové dystrofie se člení na základě lokalizace nejvýraznějších změn na epitelové a subepitelové, epitelo-stromální, stromální a endotelové (Tabulka 2). Dosud bylo popsáno více než 20 klinických jednotek. Naprostá většina rohovkových dystrofií vykazuje autozomálně dominantní dědičnost (AD) (Weiss et al. 2015; Lisch a Weiss 2019). Mezi dominující symptomy rohovkových dystrofií patří pokles zrakové ostrosti na podkladě zákalů nebo

edému a recidivující eroze. Závažné kongenitální a časně se manifestující dystrofie mohou být provázeny nystagmem a strabismem (Dudakova et al. 2019; Brejchova et al. 2019).

Vzhledem k tomu, že jednotlivé dystrofie nelze někdy spolehlivě odlišit jen na základě klinického obrazu, bere nejmodernější klasifikace v potaz i jejich molekulárně genetickou podstatu (Weiss et al. 2015; Lisch a Weiss 2019). Přehled dystrofií rohovky, o jejichž existenci nejsou v literatuře pochybnosti, uvádí tabulka 2. V tabulce 3 jsou shrnuty a vysvětleny geny asociované s rohovkovými dystrofiemi a vývojovými anomáliemi, které jsou zmiňovány v této práci.

Hlavními klinickými znaky ***epitelových a subepitelových*** dystrofií jsou drobné léze nejrůznějšího vzhledu nacházející se na úrovni epitelu a jeho bazální membrány, případně i Bowmanovy vrstvy (Obrázek 2A). V populaci je nejčastější dystrofie bazální membrány epitelu (Epithelial basement membrane dystrophy; EBMD), také známá jako Coganova dystrofie rohovky nebo „map-dot-fingerprint“ dystrofie (Obrázek 2B). Vzhledem k tomu, že naprostá většina případů je sporadických, jsou projevy v současné době považovány odborníky za degenerativní nebo poúrazové (Weiss et al. 2015). Onemocnění se může projevit náhlým vznikem bolestivých erozí, které se často zahojí do několika hodin, avšak v některých případech je léčba dlouhodobá a komplikovaná. Nejvíce obtěžující jsou recidivy, jež se objevují i několikrát do měsíce. Konzervativní přístup spočívá v pravidelné aplikaci umělých slz. Pokud nedojde k ústupu obtíží, indikujeme fototerapeutickou keratektomii excimer laserem (Wilson et al. 2017; Miller et al. 2019). Díky výzkumu bylo možno nedávno odlišit dystrofii bazální membrány epitelu od dystrofie recidivujících erozí epitelu (Epithelial recurrent erosion dystrophy; ERED), která je monogenním onemocněním a i když se léčí obdobně, znalost molekulárně genetické příčiny dává naději na vývoj cílených terapií (Mohan et al. 2005; Jonsson et al. 2015).

Stromální dystrofie rohovky jsou charakterizované rozmanitě organizovanými zákaly v různých vrstvách stromatu (Obrázek 2C, D a E). V české populaci se lze nejčastěji setkat s makulární dystrofií rohovky (Macular corneal dystrophy; MCD) s autozomálně recesivní dědičností (AR) a s dystrofiemi rohovky asociovanými s mutacemi v genu *TGFBI* (Transforming growth factor β-induced) (Tabulka 2 a 3).

Vzácnější je AD Schnyderova dystrofie rohovky (Schnyder corneal dystrophy; SCD), jejímž základním znakem je hromadění neesterifikovaného cholesterolu a fosfolipidů ve stromatu (Obrázek 2E). Přibližně v 50 % případů mají depozita vzhled podobný krystalům (Weiss 2009). Onemocnění postupně progreduje, na počátku je postižena jen velmi malá plocha rohovky, zhruba od třetí dekády života lze pozorovat *arcus lipoides* v periférii a

později i zkalení ve střední periférii rohovky (Weiss et al. 2015). Schnyderova dystrofie rohovky je podmíněna mutacemi v genu *UBIAD1* (Ubia prenyltransferase domain-containing protein 1), který kóduje membránový protein katalyzující přenos hydrofobního polyprenylového řetězce na celou řadu akceptorových molekul (Weiss et al. 2007; Orr et al. 2007). Do současné doby bylo popsáno nejméně 26 různých mutací zodpovědných za vznik Schnyderovy dystrofie rohovky (Lin et al. 2016).

Znalost zodpovědného genu a identifikace konkrétní mutace je u stromálních dystrofií klíčovým prognostickým faktorem pro volbu léčby a další vývoj stavu po chirurgickém zákroku. Bylo prokázáno, že u některých typů dystrofií může dojít po laserovém ošetření povrhu rohovky k rapidní progresi zákalů (Lee a Kim 2003; Woreta et al. 2015), zatímco u jiných typů je tento postup u nepříliš pokročilých nálezů doporučován (Dinh et al. 1999; Ayres a Rapuano 2006; Vinciguerra et al. 2018). Pro pokročilé nálezy je u stromálních dystrofií rohovky vyhrazeno operační řešení spočívající v transplantaci rohovky a to buď v plné tloušťce, nebo přední lamelární keratoplastika s uchováním vlastní Descemetovy membrány a endotelu (Weiss 2009; Aggarwal et al. 2018).

Endotelové dystrofie rohovky se projevují změnami endotelu a jeho bazální membrány (Descemetovy membrány). Pokud dojde k výraznějšímu poklesu hustoty endotelových buněk anebo ke ztrátě jejich funkce vlivem morfologických změn, projeví se porucha endotelové bariérové funkce, což vede ke vzniku edému rohovky (Eghrari et al. 2015a; Vedana et al. 2016). Pacienti nejprve popisují vidění jako v mlze nebo „přes igelit“, které se typicky objeví po probuzení a během dne se upraví. S progresí onemocnění je zamlžené vidění trvalé v důsledku neustupujícího prosáknutí rohovky (Vedana et al. 2016; Liskova et al. 2010).

U jedinců evropského původů je nejběžnější Fuchsova endotelová dystrofie rohovky (Fuchs endothelial corneal dystrophy; FECD) (Obrázek 2F), která se typicky manifestuje po páté dekádě života a je pomalu progredující (Eghrari a Gottsch 2010; Eghrari et al. 2015a). Onemocnění vykazuje variabilní expresivitu a inkompletní penetranci. Pouze u velmi malé části pacientů lze FECD pozorovat u více členů jedné rodiny, typ přenosu je autozomálně dominantní. Podskupina FECD s časnou manifestací je v literatuře spojována s mutacemi v genu *COL8A2* (Collagen type VIII, α-2) (Magovern et al. 1979; Biswas et al. 2001; Gottsch et al. 2005; Liskova et al. 2007).

Výzkum genetických faktorů podílejících se na etiologii FECD přinesl zcela nový pohled na tuto klinickou jednotku. V roce 2010 byly publikovány výsledky celogenomové asociační studie (genome-wide association study; GWAS), které odhalily silnou souvislost FECD s pozdní manifestací s jednonukleotidovým polymorfismem (single nucleotide polymorphism;

SNP) v genu *TCF4* (Transcription factor 4; transkripční faktor 4), jenž se účastní replikace DNA (Baratz et al. 2010). V roce 2012 bylo zjištěno, že 79 % postižených jedinců má v nekódující části genu *TCF4* (intronu 2) expanzi tripletových repetitivních sekvencí CTG (≥50 kopií na jedné alele nebo obou alelách), zatímco u kontrolní skupiny bez známek FECD se expanze vyskytuje pouze ve 3 % (Wieben et al. 2012). Tato expanze je v literatuře standardně označována jako CTG18.1. Transkripty obsahující expandované kopie CUG repetice se hromadí v endotelových buňkách pacientů s FECD jako oddělená jaderná RNA ohniska, podobně jako u jiných onemocnění s expanzí repetitivních sekvencí, například myotonické dystrofie typu 1 (DM1) (Mahadevan et al. 1992; Taneja et al. 1995; Du et al. 2015).

V české populaci se můžeme relativně často setkat se zadní polymorfní dystrofií rohovky (Posterior polymorphous corneal dystrophy; PPCD) (Tabulka 2 a 3). V současné době sledovaný soubor obsahuje více než 160 jedinců s různými typy této klinické jednotky (nepublikovaná data). Jak vyplývá z názvu, její fenotyp a průběh jsou velmi různorodé (Cibis et al. 1977). V počátečních asymptomatických fázích shledáváme na zadní ploše rohovky polymorfní léze geografického vzhledu, drobné vezikuly a proužkům podobné opacity. V této fázi onemocnění není výjimečná záměna za FECD. S věkem může patologických změn přibývat, postupně dochází k selhání funkce endotelu a vzniká edém celé rohovky, který vyžaduje její transplantaci (Krachmer 1985; Liskova et al. 2018; Studeny et al. 2012). Současně bylo prokázáno, že patologické endotelové buňky proliferují, transformují se v buňky podobné epitelovým a migrují do trámčiny komorového úhlu a duhovky. Tyto změny jsou zodpovědné za adherenci duhovky k rohovce, korektopii zornice a obtížně léčitelný sekundární glaukom (Cibis et al. 1977; Krachmer 1985; Liskova et al. 2010; Liskova et al. 2012). Jde tedy o potenciálně oslepující chorobu s AD dědičností (Krachmer 1985).

Z genetického hlediska rozlišujeme několik typů PPCD: typ 1 je způsoben mutacemi v promotorové regulační oblasti genu *OVOL2* (Ovo-like 2) (Davidson et al. 2016), typ 3 je podmíněn heterozygotními mutacemi v genu kódující transkripční faktor *ZEB1* (Zinc finger e-box-binding homeobox 1) (Krafchak et al. 2005) a typ 4 je dán mutacemi v intronové regulační oblasti genu *GRHL2* (Grainyhead-like 2) (Liskova et al. 2018).

V případě pokročilého nálezu se endotelové dystrofie rohovky léčí jejím nahrazením, přičemž FECD představuje v Evropě a USA v současné době nejčastější indikaci k transplantaci rohovky (Park et al. 2015; Gain et al. 2016; Rock et al. 2017; Flockerzi et al. 2018). Tradiční chirurgická technika perforující keratoplastika byla nedávno nahrazena pro pacienta šetrnější metodou náhrady pouze zadních vrstev, tedy endotelu a Descemetovy

membrány. V dnešní době je v České republice běžně prováděnou a z klinického hlediska nejúspěšnější technikou zadní lamelární keratoplastika typu DMEK (Descemet membrane endothelial keratoplasty) (Melles et al. 2006).

Obecně lze shrnout, že léčba rohovkových dystrofií vždy závisí na subjektivních potížích pacienta, stupni poklesu centrální zrakové ostrosti a míře postižení jednotlivých vrstev rohovky. Chirurgické řešení vyžadují v průběhu života téměř vždy makulární dystrofie, Reisova-Bücklersova dystrofie rohovky, granulární dystrofie rohovky typu 1, želatinózní kapkovitá dystrofie, polovina pacientů se Schnyderovou dystrofií rohovky, přibližně třetina jedinců s PPCD a část pacientů s diagnostikovanou FECD (Weiss 2009; Liskova et al. 2010; Davidson et al. 2016; Gain et al. 2016; Aggarwal et al. 2018; Liskova et al. 2018). Pacienti, zejména po operaci, jsou trvale dispenzarizováni i vzhledem k možnosti vzniku komplikací jako je obtížně řešitelný sekundární glaukom (Franca et al. 2002; Yildirim et al. 2011; Davidson et al. 2016). Jedinci s FECD a nízkým počtem funkčních endotelových buněk jsou ohroženi dekompenzací a edémem rohovky i po nekomplikované operaci katarakty. Takový stav vyžaduje sledování a správné načasování zadní lamelární keratoplastiky (Eghrari et al. 2010; Rosado-Adames a Afshari 2012; Kaup a Pandey 2019).

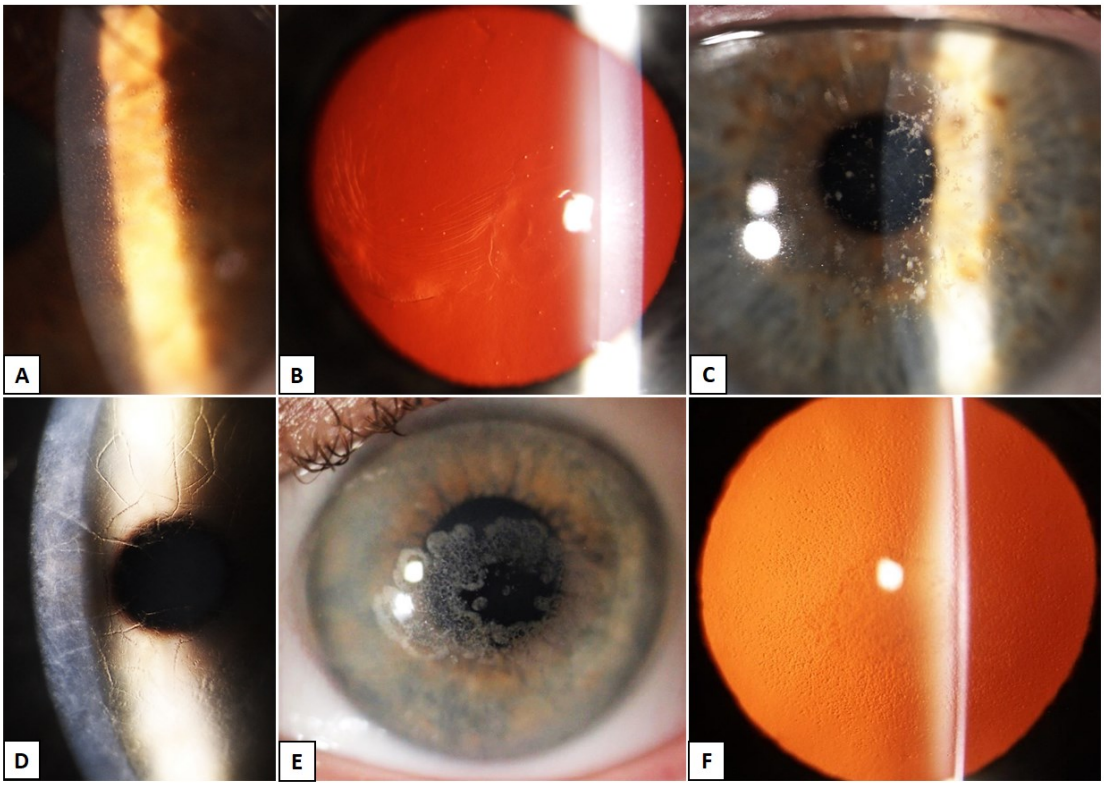

Obrázek 2. Různé fenotypy rohovkových dystrofií
(A) Meesmannova dystrofie rohovky; (B) Dystrofie bazální membrány epitelu; (C) Granulární dystrofie rohovky typu 1; (D) Mřížková dystrofie rohovky typu 1; (E) Schnyderova dystrofie rohovky; (F) Fuchsova endotelová dystrofie rohovky

Tabulka 2. Rozdělení rohovkových dystrofií

Epitelové a subepitelové	Klinický obraz	OMIM č.	Gen	Dědičnost
Meesmannova dystrofie rohovky	Transparentní mikrocysty v epitelu, někdy sektorovitě nebo jednostranně, často asymptomatická	#122100	*KRT3 KRT12*	AD
Dystrofie recidivujících erozí epitelu	Recidivující eroze, povrchové jizvení	#122400	*COL17A1*	AD
Dystrofie bazální membrány epitelu	Recidivující eroze, v epitelu šedobílé opacity ve tvaru map, teček, otisků prstů	#121820	Neznámý a *TGFBI* (malá část)	Sporadický výskyt a AD
Lischova epitelová dystrofie rohovky	Šedé ostře ohraničené opacity v epitelu ve tvaru pruhů, radiálně orientovaných kruhových výsečí, víru	#300778	neznámý	X-vázaná
Želatinózní kapkovitá dystrofie rohovky	Plochá žlutobílá uzlovitá ložiska pod epitelem, nerovnosti povrchu, jizvení, neovaskularizace	#204870	*TACSTD2*	AR
Epitelo-stromální				
Reisova-Bücklersova dystrofie rohovky	Šedobílé geografické opacity v povrchových vrstvách rohovky	#608470	*TGFBI*	AD
Thielova-Behnkeho dystrofie rohovky	Šedobílé šestiboké opacity v povrchových vrstvách rohovky	#602082	*TGFBI*	AD
Granulární dystrofie rohovky, typ 1	Šedobílé hrudkovité opacity v čirém stromatu	#121900	*TGFBI*	AD
Granulární dystrofie rohovky, typ 2	Šedobílé opacity připomínající kruhy, disky, hvězdičky, vločky, případně lineární	#607541	*TGFBI*	AD
Klasická mřížková dystrofie rohovky, typ 1 a její varianty	Vzájemně se křížící lineární opacity	#122200	*TGFBI*	AD
Stromální				
Makulární dystrofie rohovky	Šedobílé opacity s nejasnými okraji, postupné difuzní zkalení i stromatu mezi opacity	#217800	*CHST6*	AR
Schnyderova dystrofie rohovky	Opacity ve tvaru krystalů, velká šedá opacita (bez krystalů) ve tvaru prstence nebo disku	#121800	*UBIAD1*	AD
Kongenitální stromální dystrofie rohovky	Mnohočetné velmi drobné zákalky připomínající peříčka vedoucí ke zkalení stromatu v celé tloušťce	#610048	*DCN*	AD
Flíčková dystrofie rohovky	Desítky až stovky malých bílých opacit ve stromatu	#121850	*PIKFYVE*	AD
Zadní amorfní dystrofie rohovky	Šedobílé opacity připomínající listy papíru, zejména v zadním stromatu a Descemetově membráně	#612868	Delece *EPYC, KERA, LUM, DCN*	AD
Endotelové				
Fuchsova endotelová dystrofie rohovky s pozdní manifestací	Kapkovité útvary prominující do přední komory oka (guttae)	#613267	*TCF4,* neznámý (20-30 %)	Sporadický výskyt a AD
Fuchsova endotelová dystrofie rohovky s časnou manifestací	Kapkovité útvary prominující do přední komory oka (guttae)	#136800	*COL8A2*	AD
Zadní polymorfní dystrofie rohovky 1	Geografické opacity, léze podobné vezikulám a ve tvaru proužků	#122000	*OVOL2*	AD
Zadní polymorfní dystrofie rohovky 3	Geografické opacity, léze podobné vezikulám a ve tvaru proužků, strmé rohovky	#609141	*ZEB1*	AD
Zadní polymorfní dystrofie rohovky 4	Geografické opacity, léze podobné vezikulám a ve tvaru proužků	#618031	*GRHL2*	AD
Kongenitální hereditární dystrofie rohovky	Difuzní edém, granulární vzhled na úrovní endotelu (absence buněk)	#217700	*SLC4A11*	AR
Endotelová dystrofie vázaná na chromozom X	Nerovnosti na úrovni endotelu, kongenitální edém rohovek	%300779	neznámý	X-vázaná

- molekulární podstata onemocnění je známá, % - popis fenotypu, molekulární podstata onemocnění není známa, AD - autozomálně dominantní (50% riziko přenosu na další generace), AR - autozomálně recesivní (minimální riziko přenosu), OMIM - Online Mendelian Inheritance in Man

Tabulka 3. Seznam genů zodpovědných za monogenně podmíněná onemocnění rohovek

Zkratka genu	Anglický název	OMIM č.	Lokalizace	Popis funkce kódovaného proteinu
CHRDL1	Chordin-like 1	*300350	Xq12-q26	Kóduje protein ventroptin, který je antagonistou kostního morfogenetického proteinu 4, má význam během embryonálního vývoje předního segmentu oka.
CHST6	Carbohydrate sulfotransferase 6	*605294	16q23.1	Enzym katalyzující přenos sulfátové skupiny na keratan.
COL8A2	Collagen, type VIII, α-2	*120252	1p34.3	α-2 řetězec kolagenu VIII, tvoří homo a heterodimery s α-1 řetězci kolagenu VIII, který je hlavní součástí Descemetovy membrány.
COL17A1	Collagen, type XVII, α-1	*113811	10q25.1	α-1 řetězec kolagenu XVII tvoří podjednotku kolagenu XVII, který je součástí hemidesmosomů zajišťujících adhezi epitelových buněk k bazální membráně.
DCN	Decorin	*125255	12q21.33	Dekorin patří do skupiny malých proteoglykanů, které se podílejí na pravidelném uspořádání kolagenních vláken ve stromatu rohovky.
EPYC	Epiphycan	*601657	12q21.33	Dermatan patří do skupiny malých proteoglykanů, které se podílejí na pravidelném uspořádání kolagenních vláken ve stromatu rohovky.
GJA1	Gap junction protein, alpha-1	*121014	6q22.31	Konexin-43 je běžný transmembránový protein mezibuněčných kanálů.
GRHL2	Grainyhead-like 2	*608576	8q22.3	Transkripční faktor, který hraje roli v procesu epitelo-mezenchymální přeměny.
KERA	Keratocan	*603288	12q21.33	Keratokan, patří do skupiny malých proteoglykanů, tvoří proteinové jádro keratanu, hraje roli v uspořádání vláken kolagenu, tloušťce a průhlednosti rohovky.
KRT3	Keratin 3	*148043	12q12-q13	Keratiny 3 a 12 jsou součástí vnitřní kostry epitelových buněk rohovky.
KRT12	Keratin 12	*601687	17q21.2	
LUM	Lumican	*600616	12q21.33	Lumikan patří do skupiny malých proteoglykanů bohatých na leucin, stejně jako keratocan, ve velkém množství je obsažen ve stromatu rohovky. Hraje roli v uspořádání vláken kolagenu, tloušťce a průhlednosti rohovky
OVOL2	Ovo-like 2	*616441	20p11.23	Transkripční faktor, který hraje roli v procesu epitelo-mezenchymální přeměny.
PIKFYVE	Phosphoinositide kinase, fyve finger-containing	*609414	2q34	Enzym, patřící do velké skupiny lipidových kináz fosforylujících intracelulární fosfatidylinositoly (součást endozomálních membrán), je důležitý pro udržení integrity membrán uvnitř buňky.
PRDM5	PR domain-containing protein 5	*614161	4q27	Transkripční faktor regulující expresi složek extracelulární matrix stromatu rohovky, především expresi kolagenní vláknech.
SLC4A11	Solute carrier family 4 (sodium borate cotransporter), member 11	*610206	20p13	Transmembránový protein zajišťující oboustranný kotransport iontů Na+ a OH- přes buněčnou membránu endotelových buněk, dále má funkci vodního kanálu a osmolaritou extracelulárního prostředí je regulována reabsorpce vody.
TACSTD2	Tumor-associated calcium signal transducer 2	*137290	1p32.1	Membránový glykoprotein, slouží jako receptor pro vedení kalciového signálu.
TCF4	Transcription factor 4	*602272	18q21.2	Transkripční faktor, hraje roli ve vývoji nervové soustavy, diferenciaci neuronů, vývoji dendritických buněk v plicích, v epitelo-mezenchymální přeměně.
TGFBI	Transforming growth factor ß-induced gene	*601692	5q31.1	Protein, který je vylučován do extracelulárního prostoru a váže se na fibronektin, kolageny I,II, IV a integriny, ovlivňuje adhezi buněk a interakci mezi buňkou a kolagenem.
UBIAD1	Ubia prenyltransferase domain-containing protein 1	*611632	1p36.22	Membránový protein katalyzující přenos hydrofobního polyprenylového řetězce na celou řadu akceptorových molekul, včetně vitaminu K a koenzymu Q.
ZEB1	Zinc finger e-box-binding homeobox 1	*189909	10p11.22	Transkripční faktor hrající roli v procesu epitelo-mezenchymální přeměny.
ZNF469	Zinc finger protein 469	*612078	16q24.2	Transkripčního faktor regulující expresi složek extracelulární matrix stromatu rohovky, především expresi kolagenní vláknech.

OMIM - Online Mendelian Inheritance in Man

1.2.2 Diferenciální diagnostika rohovkových dystrofií

Klinická diferenciální diagnostika rohovkových dystrofií je velmi široká (Weiss a Khemichian 2011). Zahrnuje infekční a postinfekční stavy, ale i některé systémové poruchy se mohou projevit ukládáním různých substancí v rohovce ve formě opacit, krystalů či jiných zákalů. Příkladem je hromadění paraproteinů (tzv. paraproteinová keratopatie) u monoklonální expanze lymfocytů (Milman et al. 2015; Lisch et al. 2012, 2016; Glavey a Leung 2016; Dammacco et al. 2019) a vrozené poruchy metabolismu, jež jsou dány poruchou enzymů podílejících se na metabolické přeměně proteinů, aminokyselin, lipidů a mukopolysacharidů (Poll-The et al. 2003). Oční postižení nebývá izolované jen na rohovku, ale může být asociováno s dalšími projevy např. na sítnici, zrakovém nervu a jedinci jsou ohroženi předčasným vznikem katarakty. Mezi tyto poruchy patří např. mukopolysacharidózy (typ I H, I S, I H/S, II, IV, VI, VII), cystinóza a Wilsonova choroba. Dědičnost je převážně AR a všechna zmíněná onemocnění se řadí ke vzácným chorobám či syndromům (Poll-The et al. 2003).

1.2.3 Vývojové anomálie rohovky

Vrozená vývojová onemocnění rohovky zahrnují klinické jednotky: cornea plana, sklerokornea, megalokornea a mikrokornea (Tabulka 4). Cornea plana je bilaterální, převážně AR, onemocnění vyznačující se plochými rohovkami, jejichž průměrná keratometrie je typicky <36,0 dioptrií. Dalšími klinickými znaky jsou nejasný přechod mezi rohovkou a sklérou, centrální stromální zákal, předčasně vznikající *arcus senilis corneae* a nepravidelná tloušťka rohovky (Forsius et al. 1998; Ebenezer et al. 2005; Dudakova et al. 2014, 2018). Nízká lomivost rohovky je spojena s vysokou hypermetropií, proto nejsou výjimečné hodnoty přes +10,0 dioptrií a stav může být komplikován akomodativním strabismem (Forsius et al. 1998; Khan et al. 2004, 2006b). Znalost projevů onemocnění je důležitá a předejde mylné indikaci k perforující keratoplastice pro centrální rohovkový zákal či k laserovému refrakčnímu výkonu.

V literatuře je někdy cornea plana zaměňována za sklerokorneu, u které však sklerální tkáň přesahuje přes fyziologickou hranici limbu, tedy rozhraní mezi rohovkou a bělimou, což vede k zákalu buď celé rohovky, nebo její periferní části (Khan 2007). Výskyt je většinou izolovaný, případně je dědičnost AR i AD. Sklerokornea může být součástí rozsáhlejších

vývojových vad oka spolu s afakií, mikroftalmií a kolobomy (Quiroz-Casian et al. 2018; Ito a Walter 2014).

Základním charakteristickým znakem pro megalokorneu je průměr rohovek >13,0 mm. Současně nalézáme abnormálně hlubokou přední komoru a v některých případech nižší tloušťku rohovky jak v centru, tak i v periferii. Zraková ostrost je v dětství většinou normální, avšak v průběhu života se může zhoršovat díky presenilní kataraktě, dále se přidružuje mozaikovitá degenerace rohovky a *arcus juvenilis,* případně sekundární glaukom z pigmentové disperze a dislokace čočky. U třetiny pacientů byly popsány fokální, funkčně nevýznamné, demyelinizace bílé hmoty mozkové. Dědičnost je vázaná na chromozom X (Meire et al. 1991; Webb et al. 2012; Davidson et al. 2014).

Druhým onemocněním, které má vztah k velikosti rohovky, je mikrokornea. Průměr rohovek je u pacientů s tímto vývojovým onemocněním <10,0 mm a u většiny případů se jedná o izolovaný výskyt. V rodinách byla pozorována AR i AD dědičnost, nicméně etiologie není vždy jen genetická. Příčinou může být např. i infekce v průběhu těhotenství. Mikrokornea je navíc často součástí dysgeneze předního segmentu nebo i rozsáhlejších vývojových vad oka spolu s mikroftalmem, kataraktou či uveálními kolobomy, nebo může být i jedním z projevů multisystémového postižení, např. syndromu Nanceho-Horanové (Filous et al. 2011; Churchill a Graw 2011; Ito a Walter 2014; Mohamed et al. 2018).

Dalším velmi vzácným geneticky podmíněným systémovým onemocněním s projevy na rohovce je syndrom křehkých rohovek (Brittle cornea syndrom; BCS1 a BCS2) (Tabulka 4). Ztenčování a vyklenování rohovky a její perforace po minimálním traumatu, popř. dokonce i spontánní perforace, je jednou ze základních charakteristik syndromu. Jedná se o AR onemocnění podmíněné mutacemi v genech *ZNF469* (BCS1) a *PRDM5* (BCS2), které se kromě nálezu na rohovkách, také projevuje u části pacientů nedoslýchavostí až hluchotou, hyperelasticitou kůže, hypermobilitou kloubů, kyfoskoliózou a dentálními abnormalitami (Khan et al. 2012; Burkitt Wright et al. 2013; Davidson et al. 2015).

Tabulka 4. Vybrané geneticky definované vrozené anomálie rohovky

Název	Klinický obraz	OMIM č.	Gen	Dědičnost
Cornea plana 1	Ploché rohovky, nejasný přechod mezi rohovkou a sklérou, centrální stromální zákal, předčasně vznikající *arcus senilis,* nepravidelná tloušťka rohovky	%121400	neznámý	AD
Cornea plana 2		#217300	*KERA*	AR
Megalokornea	Průměr rohovek >13 mm, hluboká přední komora, mozaikovitá degenerace rohovek, někdy i tenčí rohovky a *arcus juvenilis*	#309300	*CHRDL1*	X-vázaná
Mikrokornea	Průměr rohovek <10 mm, často součást dysgeneze předního segmentu, rozsáhlejších vývojových vad oka a syndromů	#164200, #257850 #106210 #302200, #302350 #604168 a další	*GJA1 PAX6 NHS CTDP1 a jiné (často neznámé)*	AD, AR, X-vázané
Syndrom křehkých rohovek 1	Ztenčování a vyklenování rohovky, její perforace po minimálním traumatu, popř. i spontánní perforace, „modré skléry“, poruchy sluchu, hyperelasticita kůže, hypermobilita kloubů, kyfoskolióza a zubní abnormality	#229200	*ZNF469*	AR
Syndrom křehkých rohovek 2		#614170	*PRDM5*	AR

- molekulární podstata onemocnění je známá, % - popis fenotypu, molekulární podstata onemocnění není známa, AD - autozomálně dominantní (50% riziko přenosu na další generace), AR - autozomálně recesivní (minimální riziko přenosu), OMIM - Online Mendelian Inheritance in Man

2 HLAVNÍ CÍLE PRÁCE

- Identifikovat v české populaci jedince a rodiny s geneticky podmíněnými chorobami rohovky pomocí klinického vyšetření a zobrazovacích metod
- Charakterizovat specifické klinické znaky rozšiřující poznatky o fenotypu
- Odebrat biologický materiál od postižených jedinců a jejich rodinných příslušníků
- Identifikovat patogenní varianty a prokázat její příčinnou souvislost s popsaným fenotypem
- Zavést molekulárně genetické metody do klinické praxe
- Aplikovat poznatky do výzkumu nových cílených léčebných postupů na buněčné úrovni
- Využít získané poznatky v klinickém a genetickém poradenství

3 MATERIÁL A METODIKA

Studie byla provedena v souladu s Helsinskou deklarací etických zásad v lékařském výzkumu. Před začátkem byl vypracován informovaný souhlas a informace pro pacienty, které byly projednány a schváleny Etickou komisí VFN v Praze. Pokud studie vznikala ve spolupráci se zahraničním pracovištěm, vždy splňovala podmínky dané etickou komisí v příslušném výzkumném nebo klinickém zařízení, např. etickou komisí v Moorfieldské oční nemocnici, (Moorfields Eye Hospital), Londýn, Velká Británie.

Abychom dosáhli vytyčených cílů práce, použili jsme široké spektrum metod. Detailní metodika je popsána v jednotlivých publikacích. Kroky uvedené níže byly plně nebo částečně provedeny autorkou této disertační práce.

3.1 Klinické vyšetření a genealogická analýza

Pacienti a jejich rodinní příslušnici byli buď dlouhodobě sledováni, nebo nově odesláni oftalmology ke konziliárnímu vyšetření na Rohovkovou ambulanci Oční kliniky 1. LF UK a VFN v Praze. Podrobili se detailnímu očnímu vyšetření, které se skládalo z odebrání anamnestických dat, vyšetření nejlépe korigované zrakové ostrosti (NKZO) vyjádřené v decimálních hodnotách, aplanačního měření nitroočního tlaku, fotografie předního segmentu oka a vyšetření fundu v mydriáze. Ze zobrazovacích metod jsme použili bezkontaktní endotelový zrcadlový mikroskop (Noncon ROBO Pachy SP-9000, Konan Medical Inc., Tokyo, Japonsko), rohovkový tomograf (Pentacam, Oculus Inc., Wetzlar, Německo), optickou koherenční tomografii se spektrální doménou (SD-OCT, Spectralis Heidelberg Engineering GmbH, Heidelberg, Německo) a ke zjištění keratometrie, hloubky přední komory, horizontálního rozměru rohovky, axiální délky bulbu přístroj IOLMaster V.5 (Carl Zeiss Meditec AG, Jena, Německo).

Zakreslení rodokmenu probíhalo pomocí programu Haplopainter (http://haplopainter.sourceforge.net/). Použity byly standardní znaky (Tabulka 5; https://www.ncbi.nlm.nih.gov/pubmed/18792771). Mendelovský typ dědičnosti byl odhadován dle rodinné anamnézy a klinického nálezu. U sporadických pacientů vykazující známky dominantního onemocnění byl zvažován možný výskyt mutace *de novo*.

Pacienti a jejich rodinní příslušníci byli žádáni o vzorky biologického materiálu, nejčastěji o vzorek venózní krve na izolaci DNA z leukocytů, popřípadě vzorek slin na izolaci DNA z buněk bukální sliznice. V jedné rodině byl odběr venózní krve použit na izolaci mRNA, její přepis do cDNA s cílem analyzovat transkript exprimovaný v krvi.

Tabulka 5. Základní použité symboly v genealogických schématech

Symbol	Význam
	Nepostižený muž, žena a neznámé pohlaví
	Muž a žena nesoucí daný znak (onemocnění)
	Muž a žena přenašeči
	Nepokrevní sňatek
	Pokrevní sňatek
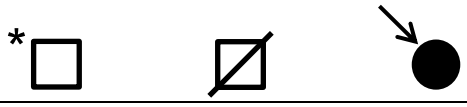	Vyšetřený a zemřelý muž, probandka označená šipkou

3.2 Laboratorní vyšetření

DNA byla izolována ze vzorku venózní krve pomocí kitu Gentra Puregene Blood Kit (Qiagen, Hilden, Germany). Izolace DNA ze vzorku slin probíhala pomocí kitu Oragene kit (Oragene OG-300, DNA Genotek, Canada).

Amplifikace DNA (polymerázová řetězová reakce; PCR) byla provedena pomocí námi navržených nebo již publikovaných primerů (odkazy anebo jejich sekvence jsou uvedeny v jednotlivých přílohách k této práci). Sangerovo sekvenování PCR produktů bylo realizováno na kapilárním sekvenátoru ABI PRISM 3100 Genetic Analyzer (Applied Biosystems, Foster City, USA). Sekvenování nové generace (masivní paralelní sekvenování), tj. exomové sekvenování (screening kódujích úseků všech genů), genomové sekvenování nebo hluboké amplikonové sekvenování bylo odesíláno do velkých servisních laboratoří (např. Macrogen, Jižní Korea a Novogene, Čína). V naší laboratoři probíhalo zpracování dat, anotace a vyhodnocování vlivu detekovaných variant a funkční průkazy jejich patogenity.

Postup použitý při molekulárně genetických analýzách byl vybrán dle již dříve definovaného vztahu mezi fenotypem a genotypem. U onemocnění podmíněných jedním genem bylo většinou voleno cílené přímé (Sangerovo) sekvenování. V některých případech bylo nutné doplnit standardní test paternity k podpoře naší hypotézy *de novo* vzniklé mutace (Ensenberger et al. 2010).

Popis nalezených variant probíhal dle doporučení Human Genome Variation Society (https://www.hgvs.org/), vždy byla uvedena referenční sekvence nebo pozice varianty v konkrétní verzi lidského genomu. V rámci bioinformatického zpracování jsme prováděli filtraci variant na základě jejich frekvence a exprese v tkáních dle veřejně dostupných databází jako např. Genome Aggregation Database (gnomAD) (http://gnomad.broadinstitute.org/). Vzácné sekvenční varianty byly podrobovány dalšímu vyhodnocování pomocí různých softwarových nástrojů (viz seznam webových zdrojů na straně 62). Data získaná sekvenováním nové generace jsme vizualizovali v programu The Integrative Genomics Viewer (IGV, http://gnomad.broadinstitute.org/igv/). Seznam všech při analýze použitých webových zdrojů je uveden v seznamu na straně 61.

Níže uvedené schéma (Obrázek 3) shrnuje vyšetřovací postup u pacientů s podezřením na monogenně podmíněné onemocnění rohovky.

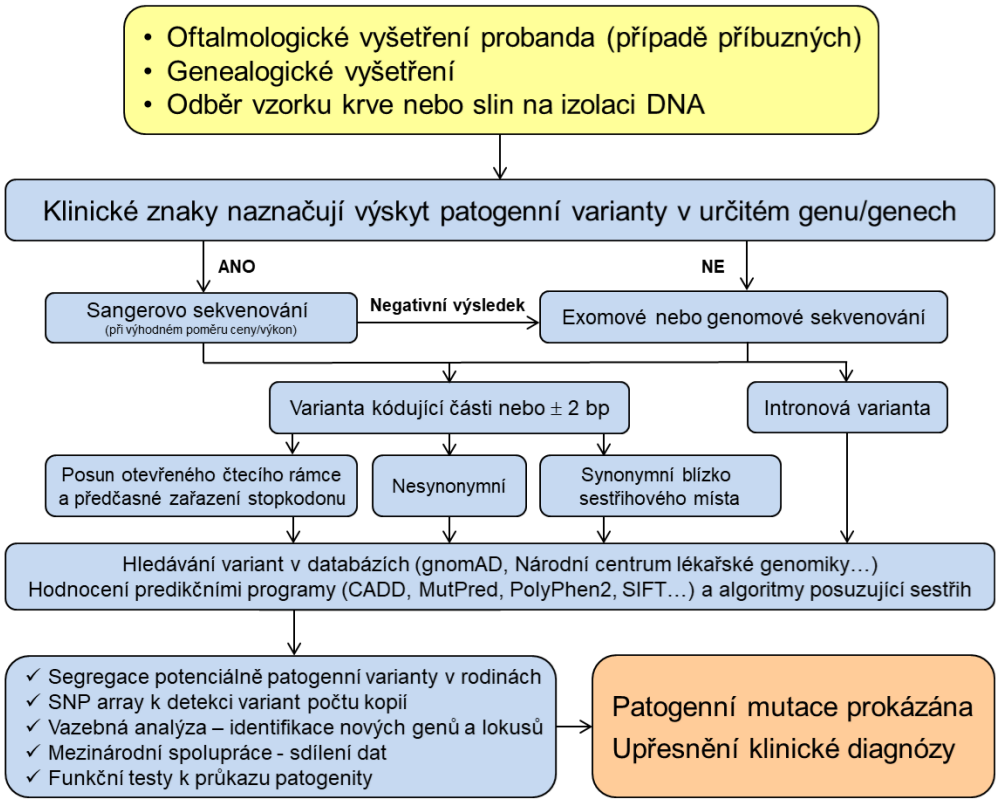

Obrázek 3. Postup vyšetření a diagnostiky u pacientů s podezřením na monogenně podmíněné onemocnění rohovky

4 VÝSLEDKY

V rámci postgraduálního studia se nám podařilo vyhledat, klinicky charakterizovat, identifikovat a ve formě publikačních výstupů zpracovat molekulárně genetickou příčinu u 44 českých pacientů z 19 rodin s různými dystrofiemi a vývojovými anomáliemi rohovky. Celkem jsme odebrali biologický materiál a izolovali DNA od 236 jedinců.

4.1 Mřížková dystrofie rohovky

Příloha 1: Novel *TGFBI* mutation p.(Leu558Arg) in a lattice corneal dystrophy patient

U 53leté probandky českého původu s klinickými znaky mřížkové dystrofie rohovky (Obrázek 4A) byla nalezena nová heterozygotní varianta c.1673T>G v exonu 12 genu *TGFBI* (referenční sekvence NM_000358.2), která byla zodpovědná za aminokyselinovou záměnu p.(Leu558Arg). Predikční programy SIFT, PolyPhen2, MutPred a SNP&GO vyhodnotily tuto variantu jako patogenní. Depozita hromadící se ve všech vrstvách stromatu rohovky (Obrázek 4C) způsobila oboustranný pokles vidění, proto byla provedena transplantace rohovky. Explantovaná rohovková tkáň byla podrobena histopatologickému vyšetření. Barvení Kongo červení a dvojlom v polarizovaném světle potvrdily přítomnost proteinové substance ve stromatu ukládající se ve formě amyloidu (Obrázek 4B a C). Velikost depozit se zvětšovala ve směru od předního k zadnímu stromatu rohovky. V epitelu nebyla přítomna žádná ložiska amyloidu a v Bowmanově vrstvě byla zachycena jen velmi diskrétní fokální depozita (Obrázek 4C). Nízká koncentrace amyloidu v povrchních vrstvách rohovky vysvětlila nepřítomnost typického klinického znaku pro epitelo-stromální dystrofie, kterým je syndrom recidivujících erozí rohovky. Jediný 28letý syn nebyl nositelem této varianty a jeho klinický nález na rohovkách byl v normě.

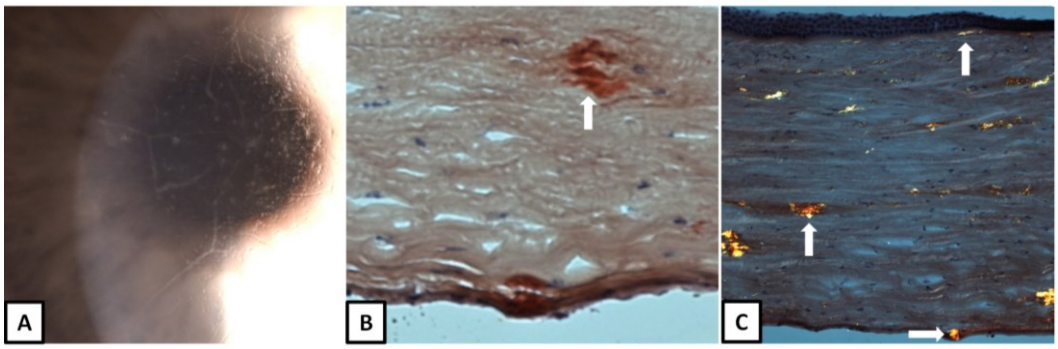

Obrázek 4. Klinický a histopatologický nález u pacientky s mutací c.1673T>G v genu *TGFBI* (A) Rohovka pravého oka s větvícími se liniemi a tečkovitými depozity při vyšetření na štěrbinové lampě, (B) Kongo červení obarvené depozitum amyloidu (šipka) v histologickém řezu explantované rohovky a (C) dvojlom v polarizovaném světle potvrzuje přítomnost amyloidu (šipky) v celém stromatu.

4.2 Schnyderova dystrofie rohovky

Příloha 2: Schnyder corneal dystrophy and associated phenotypes caused by novel and recurrent mutations in the *UBIAD1* gene

Příloha 3: Coincidental occurrence of Schnyder corneal dystrophy and posterior polymorphous corneal dystrophy type 3

Ve dvou českých rodinách jsme identifikovali dva jedince se Schnyderovou dystrofií rohovky (Příloha 2), u jednoho z nich pak byla nalezena v genu *UBIAD1* (NM_013319.2) nová heterozygotní mutace c.527G>A; p.(Gly176Glu). U druhé pacientky, šestiletého dítěte, byla přítomna heterozygotní mutace c.289G>A; p.(Ala97Thr), která vznikla *de novo*, což bylo prokázáno pomocí segregační analýzy v rodině a testováním paternity (Obrázek 5A). Tato varianta byla již v literatuře v souvislosti se Schnyderovou dystrofií rohovky popsána (Nickerson et al. 2013). Dle dostupných informací se celosvětově jedná o teprve druhý případ *de novo* vzniklé mutace v genu *UBIAD1* (Lin et al. 2016). U dalších čtyř jedinců vyšetřených ve Velké Británii našimi spolupracovníky, kteří byli součástí publikované práce, byly rovněž identifikovány již známé mutace.

Klinickým vyšetřením jsme ve všech případech prokázali krystalová depozita na obou očích, mnohdy velmi diskrétní (Obrázek 5B). Pomocí předně-segmentového SD-OCT byla zjištěna jejich akumulace převážně v předním stromatu rohovek (Obrázek 5C). Konfokální mikroskopie, provedená u naší šestileté probandky, přinesla detailní popis změn nejenom v předním stromatu rohovky, ale také v povrchních epitelových vrstvách, zatímco bazální vrstvy epitelu, oblast subepitelového nervového plexu, zadní stroma a endotel byly bez depozit (Obrázek 6). Cílená biochemická analýza navíc odhalila u tří pacientů mírnou dyslipidémii, která je pravděpodobně klinicky nevýznamná.

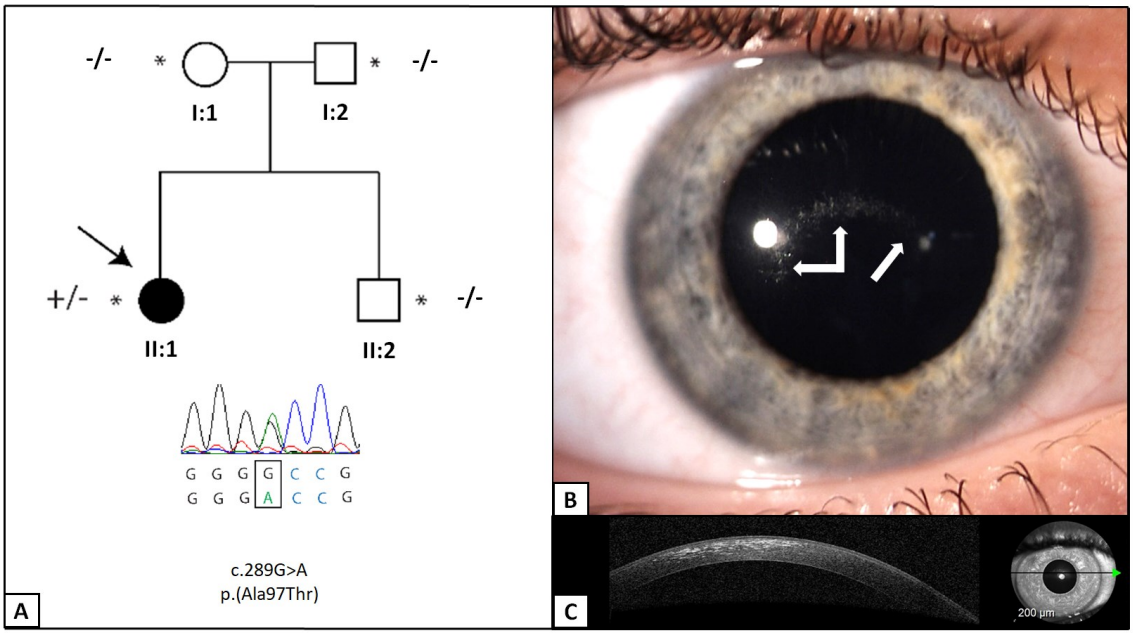

Obrázek 5. Rodokmen, sekvenogram a klinický nález u šestileté dívky se Schnyderovou dystrofií rohovky
(A) *De novo* vzniklá mutace c.289G>A; p.(Ala97Thr) v genu *UBIAD1*. (B) Diskrétní krystalová depozita v rohovce (šipky) a (C) jejich zobrazení v předním stromatu rohovky pomocí předně-segmentového SD-OCT.

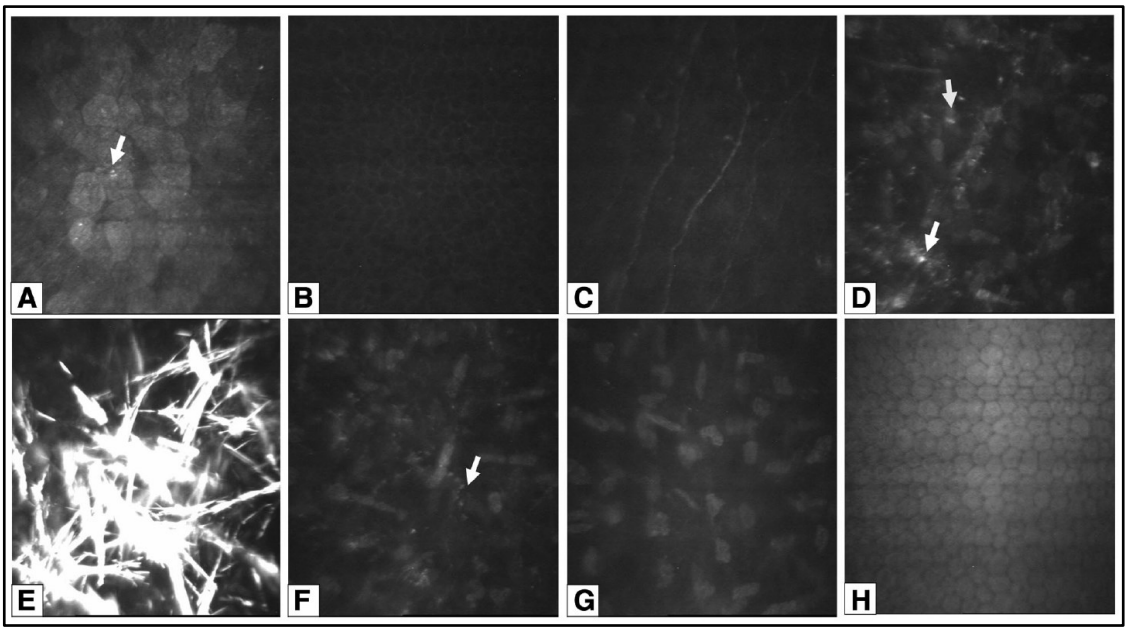

Obrázek 6. Konfokální mikroskopie šestileté dívky se Schnyderovou dystrofií rohovky
(A) Povrchové epitelové buňky s malými kulatými hyperreflektivními depozity (šipka). (B) Normální vzhled bazální vrstvy epitelových buněk a (C) subepitelového nervového plexu. (D) Hyperreflektivní depozita uvnitř a kolem keratocytů (šipky) a (E) jehlicovitý tvar krystalů v předním stromatu rohovky. (F) Hyperreflektivní drobná depozita (šipka) ve střední části stromatu, avšak (G) zadní stroma a (H) endotel jsou bez depozit.

Příkladem nutnosti přesného popisu klinického nálezu v kontextu cíleného genetického testování je případ 30letého muže s již známou mutací pro zadní polymorfní dystrofii typu 3 (PPCD3) c.2157C>G; p.(Tyr719*) v genu *ZEB1* (referenční sekvence NM_030751.5) a současně novou heterozygotní mutací v genu *UBIAD1:* c.569T>C; p.(Ile190Thr) (NM_013319.2) prokazující současně i přítomnost Schnyderovy dystrofie rohovky (Příloha 3) (Obrázek 7).

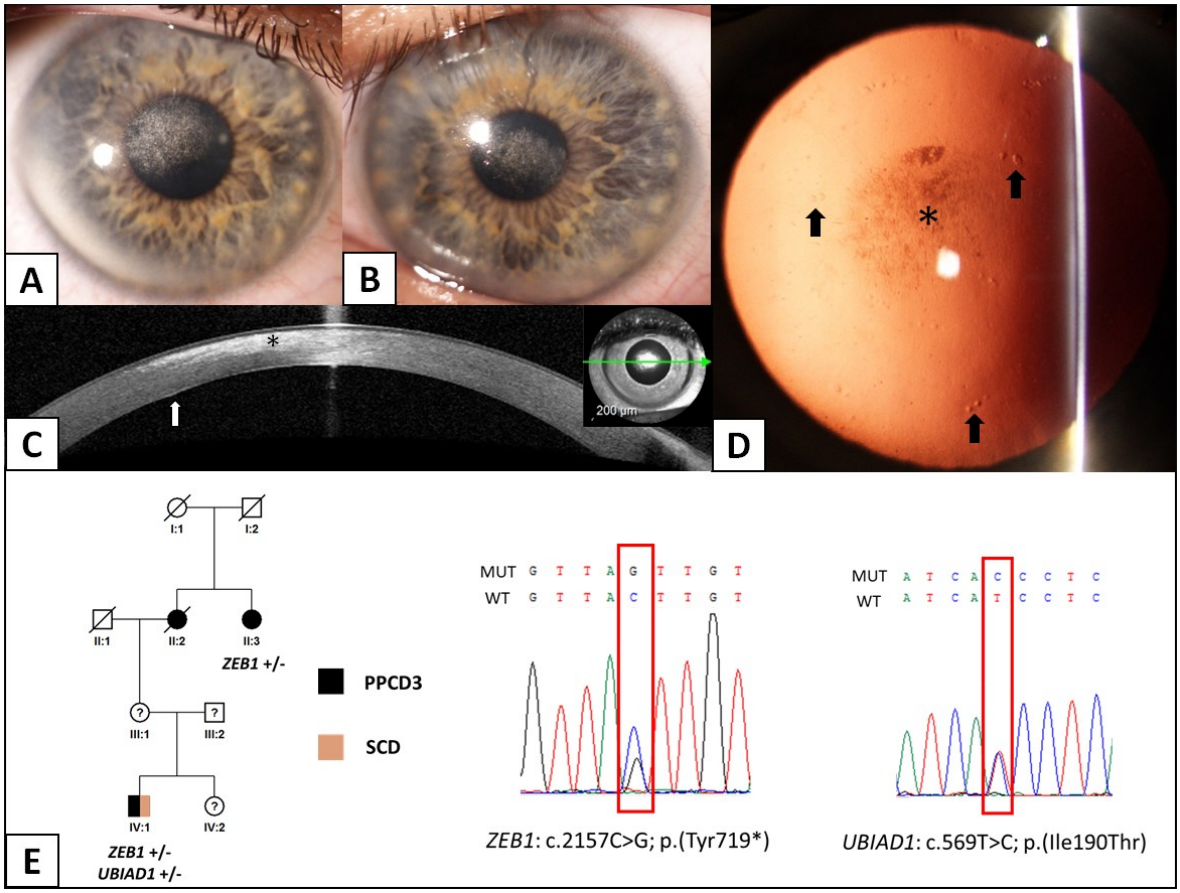

Obrázek 7. Výsledky klinického vyšetření a genetického testování 30letého muže s přítomnými mutacemi pro PPCD3 a Schnyderovu dystrofii rohovky
(A) Pravá rohovka s krystalovými depozity v centru a neúplným *arcus lipoides* v temporální dolní periférii a (B) levá rohovka s menším množstvím krystalových depozit. (C) Řez rohovkou z předně-segmetového SD-OCT dokumentuje změny převážně v předním stromatu (hvězdička) odpovídající krystalovým depozitům a šipka ukazuje na nerovnost zadní plochy rohovky. (D) V retroiluminaci zachycené změny na zadní ploše pravé rohovky typické pro PPCD3 jsou označeny šipkou a změny typické pro Schnyderovu dystrofii rohovky jsou označeny hvězdičkou. (E) Rodokmen a sekvenogram znázorňující zjištěné heterozygotní mutace c.2157C>G; p.(Tyr719*) v genu *ZEB1* způsobující PPCD3 *a* c.569T>C; p.(Ile190Thr) v genu *UBIAD1* způsobující Schnyderovu dystrofii rohovky. PPCD3 – zadní polymorfní dystrofie rohovky typu 3

4.3 Fuchsova endotelová dystrofie rohovky

Příloha 4: Antisense Therapy for a Common Corneal Dystrophy Ameliorates *TCF4* Repeat Expansion-Mediated Toxicity

V letech 2014–2017 jsme vyšetřili a izolovali DNA 132 pacientů s klinickými známkami Fuchsovy endotelové dystrofie rohovky (FECD). Genotypování alely CTG18.1 v intronu 2 genu *TCF4* (referenční sekvence NG_011716.2) probíhalo v laboratoři našich zahraničních spolupracovníků pomocí dříve popsané STR metody (short tandem repeat; PCR metoda využívající jako markery krátké opakující se sekvence) (Wieben et al. 2012). Jako hranice pozitivity byla zvolena hodnota ≥50 opakování tří nukleotidů CTG na jedné alele (Wieben et al. 2012).

Vyšetření společné kohorty 450 českých a britských pacientů (z toho bylo 392 jedinců evropského původu a jen 58 jiného původu) se známkami této dystrofie prokázalo přítomnost expanze CTG18.1 u 76,4 % (344/450) pacientů, z toho ve 4,0 % (18/450) na obou alelách. V kontrolní skupině 550 jedinců s věkem podmíněnou makulární degenerací bez známek FECD byla tripletová expanze na jedné alele prokázána pouze u 4,2 %, na obou alelách nebyla přítomna u žádného jedince.

Na modelu kultivovaných endotelových buněk od pacientů s FECD, který byl generován našimi spolupracovníky, bylo prokázáno, že fluorescenčně označené specifické transkripty RNA (CUG) jsou přítomny pouze v těchto buňkách a nevyskytují se ve fibroblastech získaných kožní biopsií od identických jedinců s FECD. Toto zjištění poskytlo důkaz toho, že porucha se odehrává čistě v endotelových buňkách rohovky postižených osob (Obrázek 8).

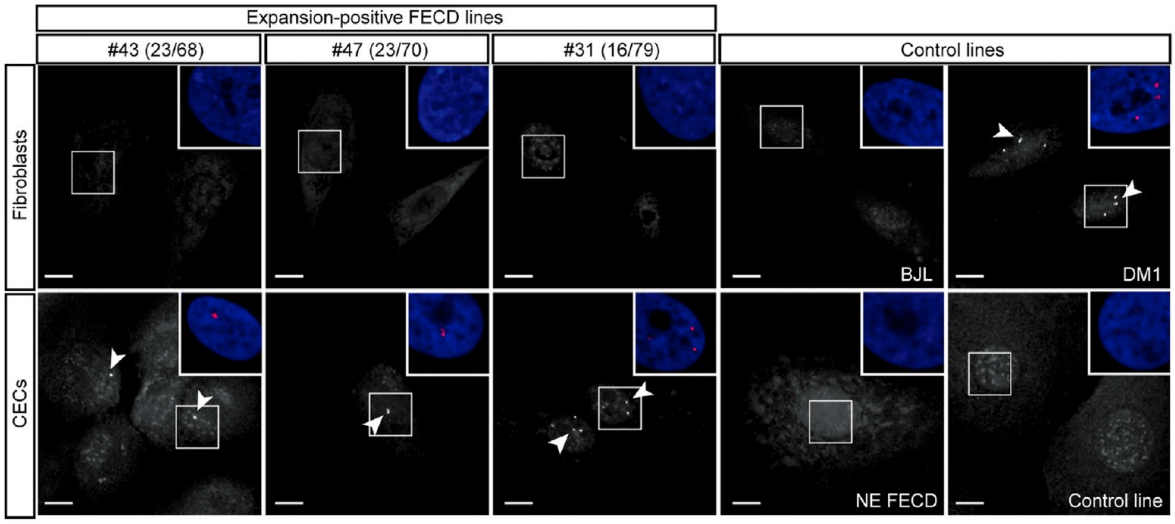

Obrázek 8. Výskyt specifických transkriptů asociovaných s CTG18.1 v různých tkáních
Fluorescenční *in situ* hybridizace byla využita k detekci specifických RNA shluků ve fibroblastech a kultivovaných endotelových buňkách rohovky získaných od tří jedinců s přítomnou CTG expanzí (*Expansion-positive FECD lines*). RNA shluky jsou označeny šipkou a jsou přítomny pouze v endotelových buňkách nikoli ve fibroblastech. Jako negativní kontroly (*Control lines*) sloužily fibroblasty zdravých jedinců (*BJL*), kultivované endotelové buňky od pacientů s klinickými známkami FECD, ale bez CTG expanze (*NE FECD*) a endotelové buňky zcela zdravých osob (*Control line*). Fibroblasty pacientů trpících jiným onemocněním na podkladě tripletové expanze, myotonickou dystrofií typu 1 (DM1), byly využity jako pozitivní kontrola.

Dále byla v jádrech kultivovaných endotelových buněk sledována distribuce sestřihových faktorů MBNL1 a MBNL2 (muscleblind-like protein 1 a 2). Bylo zjištěno, že jejich lokalizace je vázaná na kumulaci RNA shluků obsahujících transkripty s expanzí. To by vysvětlovalo předpoklad, že akumulace toxických transkriptů RNA inhibuje MBNL1 a MBNL2, čímž dochází k ovlivnění celého procesu sestřihu RNA.

Na šesti FECD buněčných kulturách endotelových buněk rohovky byla testována „antisense“ terapie, tj. zda synteticky připravené oligonukleotidy $(CAG)_7$ komplementární k produktu *TCF4* CTG18.1 $(CUG)_n$ mohou snížit množství toxických transkriptů RNA, které vytvářejí shluky v jádře endotelových buněk. Po jejich aplikaci se incidence RNA shluků v porovnání s kontrolami signifikantně snížila. Stejného pozitivního výsledku bylo dosaženo při sledování vlivu „antisense“ terapie na aberantní distribuci MBNL1 v jádře. Deset linií kultivovaných endotelových buněk od dárců s FECD sloužilo k ověření, že použití antisense oligonukleotidů $(CAG)_7$ účinně blokuje abnormální kumulaci transkriptu genu *TCF4*. Tím se zamezí negativnímu vlivu na endotelové buňky, nedochází k jejich apoptóze a progresi FECD.

4.4 Zadní polymorfní dystrofie rohovky typu 4

Příloha 5: Ectopic *GRHL2* Expression Due to Non-coding Mutations Promotes Cell State Transition and Causes Posterior Polymorphous Corneal Dystrophy 4

Identifikovali jsme rozsáhlou rodinu (C15) se známkami zadní polymorfní dystrofie rohovky (PPCD), u které jsme vyloučili dosud známé genetické příčiny pro toto onemocnění (Liskova et al. 2007, 2012). Celkem bylo klinicky vyšetřeno 32 jedinců a genetický materiál odebrán od 18 postižených rodinných příslušníků, 10 nepostižených příbuzných prvního stupně a čtyř partnerů (Obrázek 9). Dále jsme vyšetřili tři další menší rodiny, které neudávaly příbuznost s rodinou C15, včetně rozdílného geografického původu. Screening známých oblastí pro PPCD1 a PPCD3 byl v těchto rodinách také negativní. Konkrétně jsme u všech zástupců těchto čtyř rodin provedli Sangerovo sekvenování genu *ZEB1* a promotoru genu *OVOL2*.

Při hledání genetické příčiny jsme tedy dále pokračovali metodou masivního paralelního sekvenování, nejprve jsme provedli exomové sekvenování a to celkem 8 postižených a tří nepostižených jedinců, avšak ani poté nebyla nalezena patogenní mutace, proto jsme přistoupili k vazebné analýze a genomovému sekvenování (Obrázek 9).

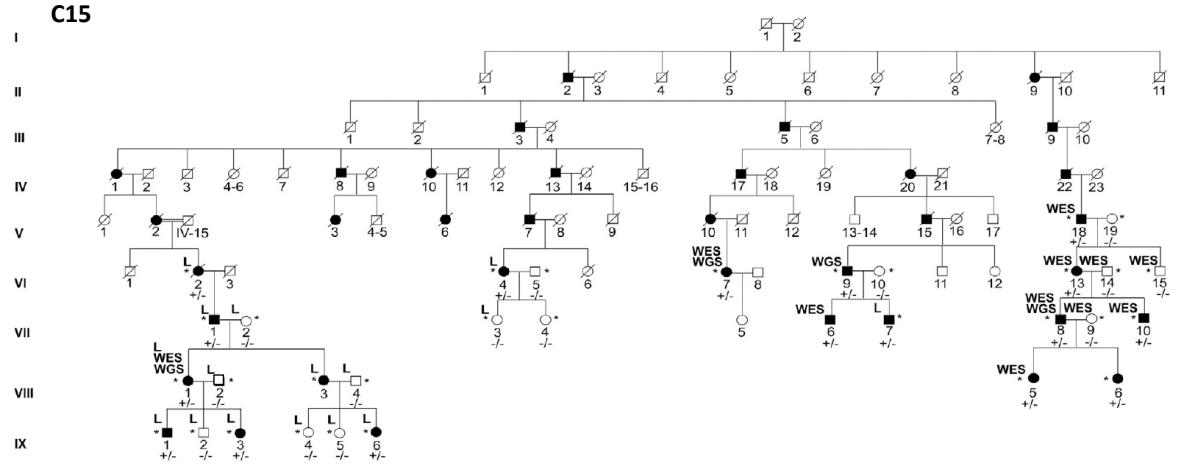

Obrázek 9. Rodokmen rodiny českého původu C15 s PPCD4
Velkým L jsou označeni jedinci, kteří byli zařazeni do vazebné analýzy. WES značí exomové a WGS genomové sekvenování. Heterozygoti s patogenní mutací c.20+544G>T v genu *GRHL2* jsou označeni +/- a jedinci bez přítomné mutace -/-. Klinicky vyšetření jedinci jsou označeni hvězdičkou.
PPCD - zadní polymorfní dystrofie rohovky

Vazebná analýza byla provedena v jedné větvi rodiny pomocí mikročipu Illumina Omni2.5 Exome-8 u 9 postižených a 7 nepostižených jedinců. Statisticky byla zjištěna vazba na chromozom 8, konkrétně do oblasti 8q22.3-q24.12 (chr8.hg38:100 821 039-119 725 923), což jednoznačně prokázalo existenci nového typu PPCD, který jsme označili jako 4.

Genomové sekvenování bylo provedeno u čtyř velmi vzdálených příbuzných jedinců s typickými známkami PPCD (Obrázek 9 a 10). Tento postup nám umožnil zjistit, jaké heterozygotní varianty tito jedinci sdílejí v mapované oblasti pro PPCD4. Vzhledem k tomu, že onemocnění je vzácné, byly primárně hledány především unikátní varianty, která nejsou přítomny v žádných kontrolních databázích. Celkem byly nalezeny tři, jejich přítomnost pak byla potvrzena Sangerovým sekvenováním. Dvě varianty byly v nekódujících oblastech mezi geny a jedna se nalézala v intronu 1 genu *GRHL2* (referenční sekvence NM_024915). Tato intronová varianta c.20+544G>T (chr.8.hg38:101 493 333G>T) byla vyhodnocena, na základě funkce proteinu kódovaným genem *GRHL2*, tj. jeho role v procesu epitelo-mezenchymové tranzice a vzájemnou regulací s již známými geny uplatňujícími se v patogenezi PPCD, jako pravděpodobně patogenní. Její přítomnost byla ověřena Sangerovým sekvenováním (Obrázek 10). Tato mutace byla dále zjištěna u dalších nevyřešených PPCD případů, konkrétně ve 3 rodinách českého původu (C23, C26 a C33) bez příbuzenského sňatku. V rodině C33 se varianta objevila *de novo* a toto zjištění bylo podpořeno i testem paternity (Obrázek 11).

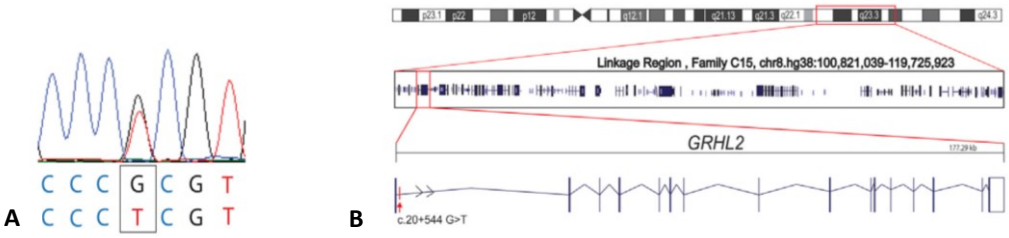

Obrázek 10. Identifikace lokusu pro PPCD4 v rodině C15 v oblasti 8q22.3-q24.12 (chr8.hg38:100 821 039-119 725 923) a unikátní varianty v intronu 1 genu *GRHL2* (A) Heterozygotní varianta c.20+544G>T odhalená pomocí genomového sekvenování, lokalizovaná v intronu 1 *GRHL2*, byla potvrzena Sangerovým sekvenováním. (B) Zvětšená oblast chr8.hg38:100 821 039-119 725 923 a zobrazeno místo intronové mutace c.20+544G>T. PPCD - zadní polymorfní dystrofie rohovky

Genotypováním několika nízce frekventních SNPs (jednonukleotidových polymorfismů) v mapované oblasti PPCD4 u členů všech čtyř zkoumaných rodin českého původu nesoucích c.20+544G>T v *GRHL2* bylo zjištěno, na základě sdílení společného haplotypu, že rodiny C15, C23, C26 sdílejí tuto patogenní mutaci od vzdáleného předka, zatímco u probandky z rodiny C33, u které mutace vznikla nově, tento haplotyp přítomen není (Obrázek 11).

Patogenní varianty v oblasti intronu 1 genu *GRHL2* jsme dále hledali v rámci mezinárodní spolupráce i u pacientů Moorfieldské oční nemocnice. Tímto způsobem byly identifkovány další dvě rodiny s heterozygotními variantami c.20+257delT a c.20+133delA, které byly vyhodnoceny jako patogenní (Obrázek 11).

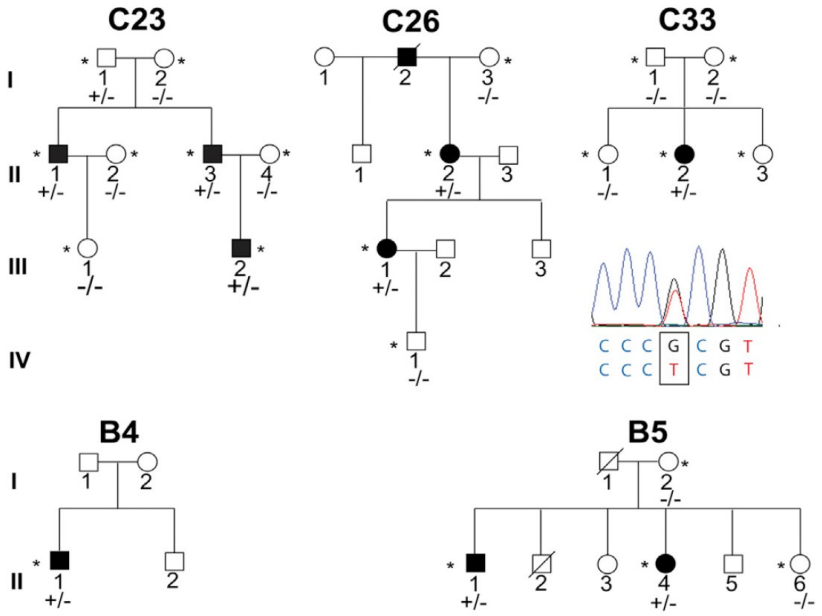

Obrázek 11. Rodokmen rodin C23, C26, C33, B4 a B5 s mutacemi v regulační oblasti *GRHL2*. Heterozygotní varianta v intronu 1 genu *GRHL2,* c.20+544G>T, byla segregací nalezena i v rodinách C23 a C26, které sdílejí zděděný haplotyp od společného vzdáleného předka s rodinou C15. V rodině C33 byla tato varianta nalezena *de novo.* V britských rodinách byly identifikovány další dvě mutace v intronu 1 genu *GRHL2* a to c.20+257delT v rodině B4 a c.20+133delA v rodině B5.

Vzhledem k tomu, že na základě údajů v databázích se oblast, kde se nacházely zjištěné mutace, jevila jako regulační, provedli jsme bioinformatické vyhodnocení jejich možného vlivu predikčními nástroji MatInspector a AliBaba 2.1. Z této analýzy vyplynulo, že přítomnost varianty c.20+544G>T porušuje vazebné místo pro transkripční faktor, což navozuje odblokování suprese *GRHL2* a tím dochází k dysregulaci procesu epitelo-mezenchymální tranzice. V konečném důsledku pak dochází ke změně fenotypu endotelových buněk. Expresi *GRHL2*, ke které v normálním endotelu nedochází, jsme prokázali imunohistochemickým vyšetřením rohovkové tkáně získané od jednoho pacienta, nositele c.20+544G>T mutace z rodiny C23, který prodělal perforující keratoplastiku (Obrázek 12H).

Současně jsme popsali i klinické nálezy u 27 nositelů *GRHL2* mutace c.20+544G>T. Většina (26 jedinců) měla typické znaky PPCD, tj. nepravidelnosti zadní plochy rohovky, opacity různé velikosti a tvaru, které jsou popisovány jako proužky, vezikuly a geografické léze (Obrázek 12). Čtyři jedinci zaznamenali zhoršené a zamlžené vidění v důsledku edému rohovky. U dvou dětí byl otok rohovky diagnostikován již v době dvou až tří měsíců po narození. Sekundární glaukom, jako iniciální projev PPCD4, byl přítomen u pěti pacientů, celkově byl diagnostikován u 7 jedinců bilaterálně a u jednoho muže pouze na jednom oku. V souvislosti se sekundárním glaukomem byla popsána u čtyř očí tří jedinců korektopie zornice. Od dětství mělo nízkou zrakovou ostrost na jednom či obou očích bez dalšího

významného poklesu v průběhu života celkem pět postižených, jeden si všiml horšího vidění ve druhé dekádě svého života, 9 jedinců nevnímalo při poslední kontrole žádné obtíže a od jednoho pacienta nemáme klinické informace.

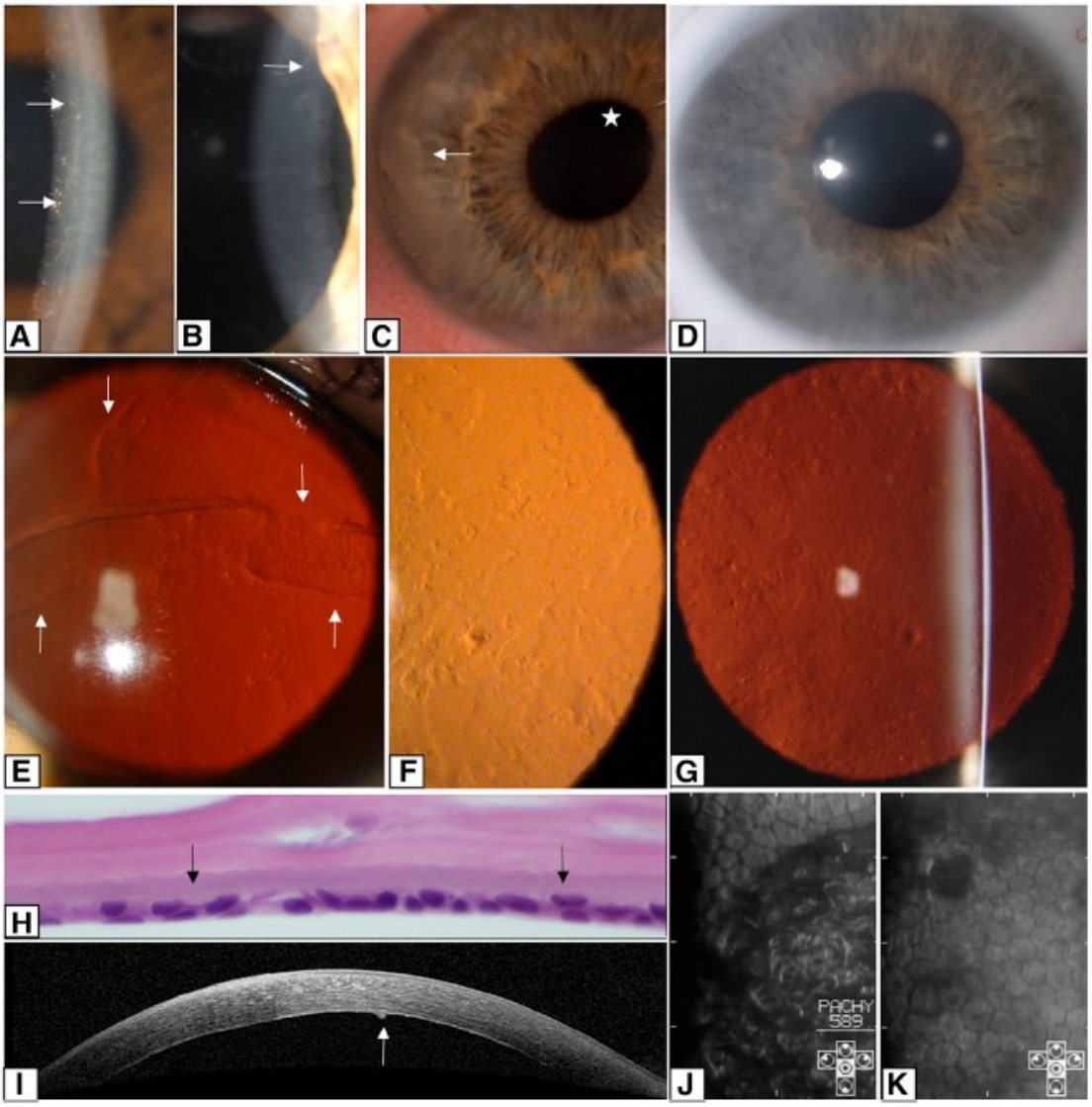

Obrázek 12. Příklady klinických nálezů u pacientů s PPCD4 zapříčiněnou mutacemi v regulační oblasti genu *GRHL2*
(A) Proužky a vezikuly (šipky) rohovky u 30leté ženy II:4 z rodiny B5. (B) Prominující proužky na zadní ploše rohovky u 46letého muže II:3 z rodiny C23. (C) Subepitelově uložená depozita vápníku (šipka) a korektopie (hvězdička) u 29letého muže VII:6 z C15. (D) Difuzní stromální zašednutí rohovky u 11letého chlapce III:2 z C23. (E-G) V retroiluminaci patrné pruhy (šipky), vezikuly a geografické léze (E) u 53letého muže II:1 z B4, (F) 30leté ženy II:4 z B5, (G) 58letého muže VI:9 z C15. (H) Histologický řez (barvení hematoxylin-eosin, zvětšení 600krát) explantované rohovky 8,5letého chlapce III:2 z C23; endotelové buňky formují dvojitou vrstvu (šipka). (I) Rohovka 58letého muže VI:9 z rodiny C15 zobrazena pomocí předně-segmentového SD-OCT; nepravidelnosti zadní plochy rohovky a šipka ukazuje prominenci na úrovni Descemetovy membrány a endotelu. (J a K) Obrázky endotelu získané pomocí zrcadlového mikroskopu ukazují změny tvaru a velikosti endotelových buněk u (J) 37leté ženy VIII:3 z C15 a (K) 5,5leté dívky II:2 z rodiny C33. Tmavé okrsky bez přítomných endotelových buněk velmi pravděpodobně odpovídají prominencím a nepravidelnostem zadní plochy rohovky. PPCD - zadní polymorfní dystrofie rohovky

Transplantace rohovky byla provedena u 7 z 27 (25,9 %) jedinců, z nich tři podstoupili operaci na obou očích. Průměrný věk jejich první transplantace byl 34,9±17,9 let (v rozmezí od 8,5 do 59 let). Dvě oči byly eviscerovány pro bolest, jedno ve věku 25 let, druhé v 70 letech. Zonulární keratopatie se objevila u dvou pacientů oboustranně. U jednoho pacienta se ve věku 79 let onemocnění projevilo pouze jako snížená hustota endotelových buněk s hodnotami 1295 buněk/mm^2 na pravém oku a 1309 buněk/mm^2 na levém oku (normální hodnoty pro danou věkovou kategorii 2400–2600 buněk/mm^2) (McCarey et al. 2008).

4.5 Zadní polymorfní dystrofie rohovky typu 3

Příloha 6: The utility of massively parallel sequencing for posterior polymorphous corneal dystrophy type 3 molecular diagnosis

Část výzkumu byla zaměřena na PPCD typ 3, která je podmíněna haploinsuficiencí a následnou sníženou expresí *ZEB1* v endotelových buňkách rohovky (Liskova et al. 2016). Celkem bylo studováno 19 postižených jedinců ze 12 rodin: 4 české rodiny, 4 britské, jedna britská původem z Asie, jedna rodina slovenského původu a dvě rodiny ze Švýcarska. Nejprve byly pomocí Sangerova sekvenování vyloučeny všechny patogenní varianty v regulačních oblastech *OVOL2* a *GRHL2*. U části probandů byla dále přímo sekvenována oblast *ZEB1* a přilehlé intronové sekvence. U 5 probandů bylo provedeno exomové sekvenování a u tří jedinců sekvenování celého genomu.

Celkem bylo v *ZEB1* identifikováno 10 nových heterozygotních variant, které jsme vyhodnotili jako patogenní, a dvě známé mutace. U dvou probandů českého původu bylo prokázáno, že dvě mutace vznikly *de novo.* K podpoře tohoto zjištění byl proveden test paternity.

U jedné probandky českého původu (rodina C31, II:1) byla molekulárně genetická analýza obzvláště rozsáhlá. Nejprve podstoupila Sangerovo sekvenování, potom exomové a posléze i genomové sekvenování. Až touto poslední metodou byla odhalena částečná delece zahrnující exony 1-7 a část exonu 8 v genu *ZEB1* (Obrázek 13).

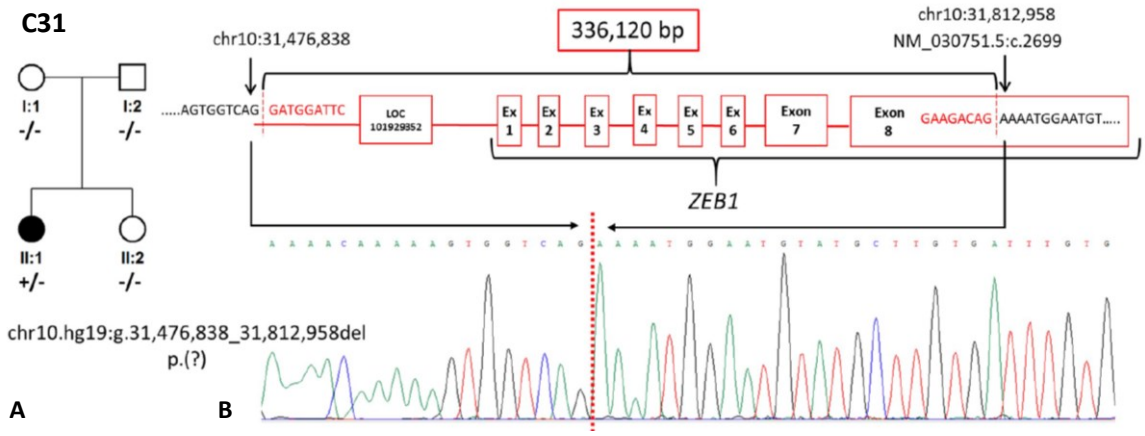

Obrázek 13. Rodina C31
(A) Genealogické schéma rodiny C31 s *de novo* vzniklou mutací v *ZEB1;* (B) Sekvenogram dokumentuje částečnou deleci chr.10.hg19:g.31 476 838_31 812 958del zahrnující exony 1-7 a část exonu 8.

V další české rodině (C36) bylo díky analýze mRNA *ZEB1* transkriptu exprimovaného v krvi a přepsaného do cDNA prokázáno, že mutace c.482-2A>G narušuje sestřih. Výsledkem je přeskočení exonu 5 a předčasné zařazení terminačního kodonu (Obrázek 14).

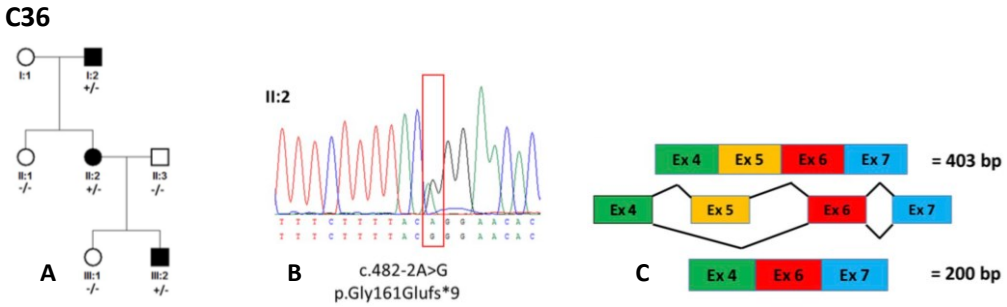

Obrázek 14. Rodina C36
(A) Genealogické schéma rodiny C36 s mutací; (B) c.482-2A>G zobrazené na sekvenogramu; (C) Pomocí mRNA transkriptu přepsaného do cDNA bylo prokázáno, že tato mutace porušuje sestřih pre-mRNA a výsledkem je přeskočení exonu 5.

U všech 19 pacientů (38 očí) byly přítomny charakteristické klinické znaky pro PPCD3. Deset očí 7 jedinců mělo pokles zrakové ostrosti <0,33, čtyři pacienti podstoupili transplantaci rohovky alespoň na jednom oku, dva pacienti měli nystagmus a jen 9 očí mělo zrakovou ostrost 1,0. U nikoho nebyl zjištěn glaukom.

4.6 Kongenitální hereditární endotelová dystrofie rohovky

Příloha 7: IPSC-derived corneal endothelial-like cells act as an appropriate model system to assess the impact of *SLC4A11* variants on pre-mRNA splicing

Studovali jsme šest probandů, ze čtyř českých (C2–5) a dvou britských rodin (B1 a 2), s prokazatelnými klinickými známkami kongenitální hereditární endotelové dystrofie rohovky (CHED) (Obrázek 15). Edém rohovky, který způsobil oboustranné difuzní zašednutí celé rohovky, byl pozorován u pěti jedinců od narození.

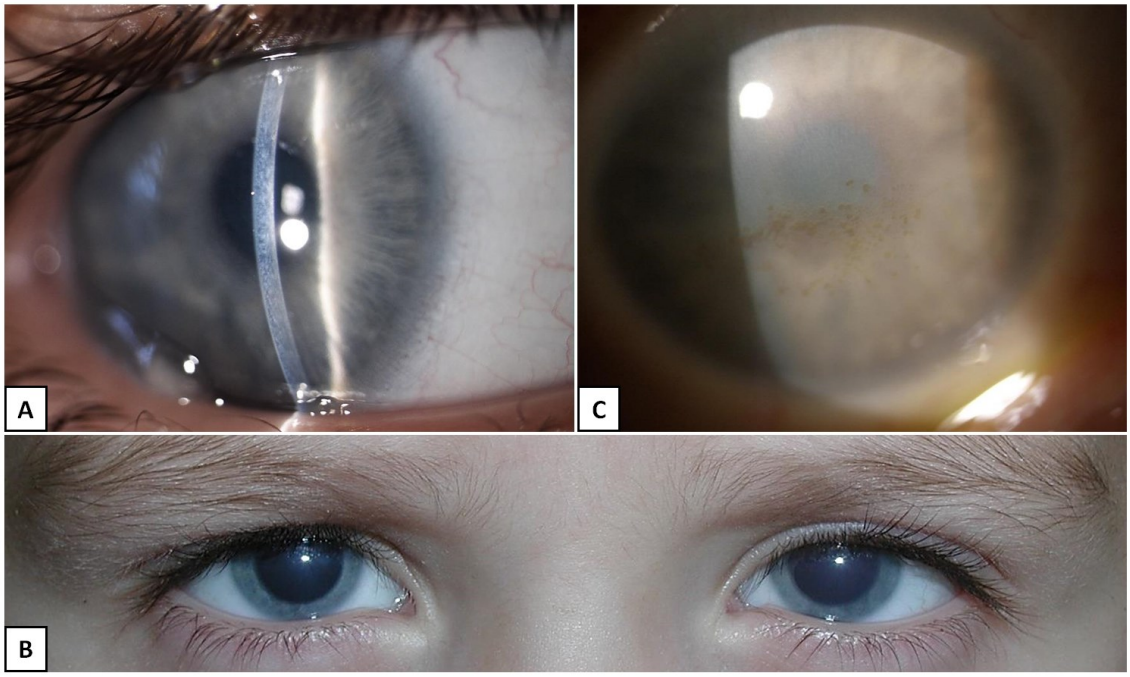

Obrázek 15. Klinické nálezy u jedinců s kongenitální hereditární endotelovou dystrofií rohovky (CHED) z rodin C2 a C3
(A) Edém a zašednutí stromatu pravé rohovky a (B) makroskopicky zjevné zašednutí rohovek bilaterálně u pětiletého chlapce z rodiny C2. (C) Pravé oko 70leté ženy z rodiny C3 s edémem a zašednutím celé rohovky až do její periférie a přítomnou paracentrální sferoidální degenerací.

U jednoho chlapce z české rodiny C5 bylo postižení zjištěno náhodně až při pravidelné kontrole ve věku pěti let. Tuto skutečnost lze vysvětlit tím, že nižší úroveň NKZO na dálku (0,4) byla kompenzována normálním viděním do blízka. Zraková ostrost očí, které nepodstoupily transplantaci rohovky, se pohybovala od 0,64 u nejmladšího tříletého probanda do 0,01 u 70leté ženy. U poloviny očí se podařilo zdokumentovat významně ztluštělou rohovku v rozmezí od 1032 do 1098 µm (normální hodnoty 510–624 µm) (Lopez de la Fuente et al. 2016). U čtyř ze šesti jedinců bylo oční postižení kombinováno se sluchovým, přičemž u chlapce z rodiny C5 percepční neprogresivní porucha sluchu vyžadovala od 8,5 let naslouchadla. Klinické nálezy všech studovaných pacientů jsou shrnuty v tabulce 6.

Tabulka 6. Klinická a demografická data šesti probandů s CHED

Rodina/ jedinec	Věk (roky)*	NKZO		CCT (μm)		Doplňující informace	Porucha sluchu
		OP	OL	OP	OL		
C2/II:1	5	0,5	0,4	1098	1078	OL konvergentní strabismus	Ano – mírná, začátek v pěti letech
C3/II:1	70	0,01	0	N	PKP	OL PKP v 10 letech, poúrazová ztráta vidění v 36 letech	Ano
C4/II:2	7	0,02#	0,03#	N	N	Horizontální nystagmus OP PKP v 7 letech OL PKP v 8,5 letech, rePKP	Ano – mírná, začátek ve 14 letech
	35	HM	0,05	PKP	PKP		
C5/II:2	10	0,4	0,4	1032	1032	Nižší NKZO na dálku zjištěna v pěti letech, vidění na blízko bez poruchy	Ano – začátek v 6 letech, naslouchadla od 8,5 let
B1/II:1	3	0,54	0,64	1046	1036	Žádná	Ne
B2/II:1	6	0,25#	0,25#	N	N	OP exotropia	Ne
	10	0,05#	0,66	N	PKP	OP PKP v 10 letech, rePKP, rePKP + operace katarakty	
	47	0,66	0,66	PKP	PKP + DMEK	OL PKP v 7 letech, DMEK + operace katarakty	

B - rodina britského původu, C - rodina českého původu, DMEK - Descemet membrane endothelial keratoplasty (typ zadní lamelární keratoplastiky), N - nezjištěno, NKZO - nejlépe korigovaná zraková ostrost vyjádřená decimálně, OL - oko levé, OP - oko pravé, PKP - perforující keratoplastika, rePKP - rekeratoplastika, * - v době vyšetření, # - před PKP

Celkem se genetické analýze podrobilo 18 jedinců, včetně šesti klinicky postižených pacientů. V genu *SLC4A11* (referenční sekvence NM_032034.3) bylo identifikováno 11 různých variant vyhodnocených jako patogenní pro CHED, z toho byly čtyři mutace nové. Segregace v rodinách C2, C4, C5 a B1 prokázala, že postižení jedinci jsou složenými heterozygoty (Obrázek 16). Ve dvou rodinách (C3 a B2) nebylo možné segregaci provést pro nedostupnost vzorků od příbuzných prvního stupně.

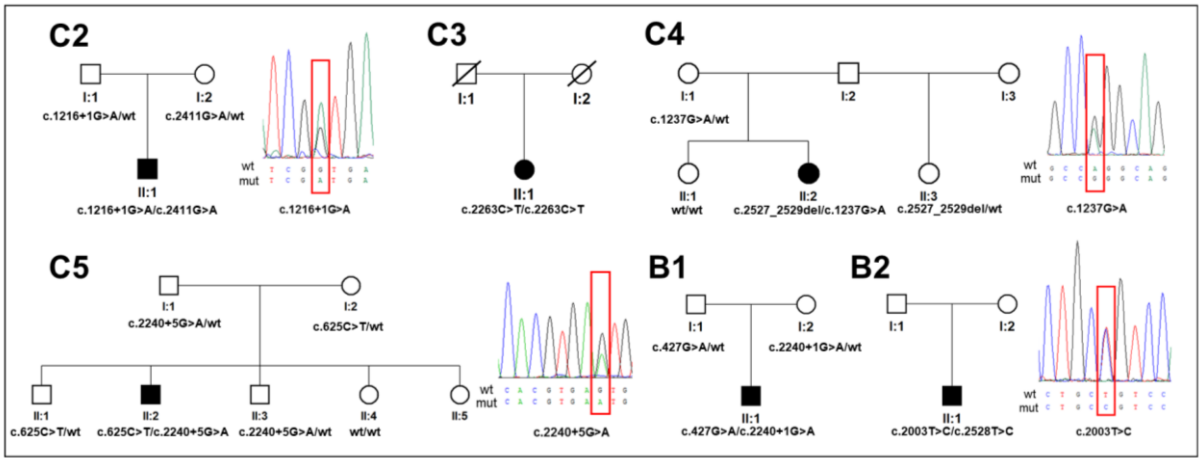

Obrázek 16. Rodokmeny šesti rodin s výskytem kongenitální hereditární endotelové dystrofie rohovky (CHED) a sekvenogramy čtyř nových mutací v rodinách C2, C4, C5 a B2

Účinek nových nesynonymních mutací c.1237G>A, p.(Gly413Arg), a c.2003T>C, p.(Leu668Pro), byl testován pomocí šesti predikčních nástrojů, které vyhodnotily obě varianty jako patogenní nebo pravděpodobně patogenní. Další nová mutace c.1216+1G>A zasahovala kanonické sestřihové místo a není známo, k jaké změně na úrovni proteinu by mohla vést. Poslední nová mutace c.2240+5G>A se nacházela blízko rozhraní intronu a exonu mimo donorové sestřihové místo. Vliv mutace c.1216+1G>A a c.2240+5G>A na pre-mRNA sestřih byl ověřován *in silico* za použití čtyř různých nástrojů.

Jelikož se varianta c.2240+5G>A nacházela mimo kanonické sestřihové místo, bylo třeba k ověření její patogenity vytvořit experimentální buněčný model a provést funkční analýzu, tj. experimentálně zjistit, zda vede ke vzniku aberantního transkriptu *SLC4A11*. Protože gen *SLC4A11* není exprimován v tkáni přístupné pro biopsii, vytvořili jsme z autologních indukovaných pluripotentních kmenových buněk (induced pluripotent stem cells; iPSC) model buněk podobajících se endotelu rohovky, jejich mRNA pak byla reverzní transkripcí přepsána do cDNA. Pomocí primerů komplementárních se sekvencí v přilehlých exonech jsme provedli PCR amplifikaci. Sangerovým sekvenováním bylo poté prokázáno, že vznikají dva produkty: wild-type (divoká alela, která se vyskytuje ve zdravé běžné populaci) a aberantní transkript, u kterého došlo vlivem mutace c.2240+5G>A k začlenění šesti nukleotidů a následně předčasnému ukončení translace proteinu (tj. zařazení stop kodonu na pozici 747; p.Thr747*). Přítomnost tohoto aberantního transkriptu jsme dále ověřovali pomocí hlubokého amplikonového sekvenování. Kromě aberantního transkriptu prokázaného již Sangerovým sekvenovaním, byla ve velmi malém procentu odhalena i přítomnost dalšího transkriptu začleňujícího 130 nukleotidů, což na úrovni proteinu vedlo opět k předčasnému vmezeření terminačního kodonu.

4.7 Paraproteinová keratopatie

Příloha 8: Paraproteinemic keratopathy associated with monoclonal gammopathy of undetermined significance (MGUS): clinical findings in twelve patients including recurrence after keratoplasty)

V průběhu výzkumu bylo laboratorně vyšetřeno 18 pacientů s klinickým podezřením na ukládání paraproteinů v rohovkách. Z celkového počtu bylo nakonec zjištěno, že 12 jedinců (9 mužů a 3 ženy) splňuje kritéria pro monoklonální gamapatii nejasného významu (MGUS) manifestující se jako paraproteinová keratopatie, z toho 6 pacientů bylo vyšetřeno v Moorfieldské oční nemocnici. Průměrný věk pacientů byl 52,2 roku v rozmezí od 24 do 63 roků.

Klinické obrazy u tří pacientů natolik připomínaly stromální rohovkové dystrofie podmíněné mutacemi v genu *TGFBI*, že bylo nejprve provedeno Sangerovo sekvenování exonů 4, 11–14 (referenční sekvence NM_000358.2) (Liskova et al. 2008) u případů #1 a #2 k vyloučení mřížkové dystrofie rohovky typu 1 a u případu #3 Thielovy-Behnkeho dystrofie (Obrázek 17A a B). Oční nálezy dalších tří pacientů (#6, #8 a #9) byly mylně považovány za cystinózu a u jednoho pacienta (#5) bylo onemocnění spojeno s hyperémií spojivek a recidivujícími episkleritidami (Obrázek 17D). Charakter depozit byl velmi rozmanitý a klinicky se jevily jako lineární, retikulární a granulární, popř. tečkovité a numulární léze (#1, #2, #3 a #12) (Obrázek 17A, B, F a G). U pacienta #4 bylo pozorováno difuzní zašednutí stromatu rohovky, u dalších jedinců jsme pak zdokumentovali cirkulární prstencovité zašednutí (#5 a #11) (Obrázek 17D), depozita podobná krystalům (#5, #6, #7, #8, #9 a #11) (Obrázek 17E) a povrchní zašednutí rohovky (#10) (Tabulka 7). Pomocí předně-segmentového SD-OCT (Obrázek 17C) a konfokálního mikroskopu se prokázalo variabilní střádání paraproteinů ve všech vrstvách rohovky, vyjma endotelu, a to jak extracelulárně, tak intracelulárně.

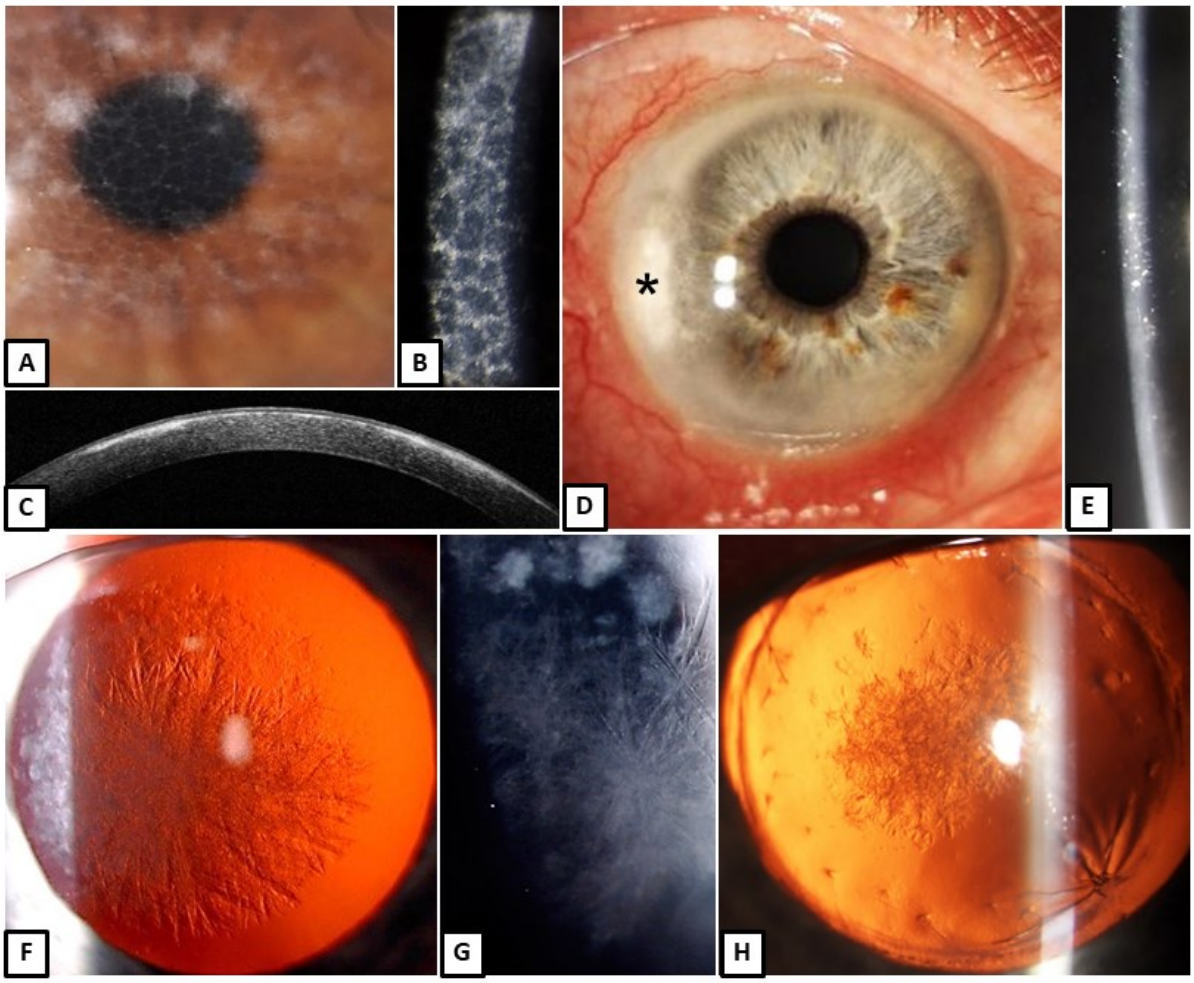

Obrázek 17. Příklady různorodých klinických očních nálezů u pacientů s paraproteinovou keratopatií asociovanou s monoklonální gamapatií nejasného významu (MGUS)
(A a B) Retikulární a numulární léze a (C) jejich uložení převážně v předním stromatu rohovky (zobrazeno na předně-segmentovém SD-OCT) (#3). (D) Periferní cirkulární prstencovité zašednutí rohovky (D, E) s krystalovými depozity v temporálním okraji stromatu rohovky (hvězdička) (#5). (F a G) Větvící se lineární a granulární opacity postihující centrální část rohovky a (H) recidiva podobných depozit na rohovkovém transplantátu (#12).

Ukládání paraproteinů (M-protein) v rohovce zapříčinilo pokles zrakové ostrosti pod 0,66 alespoň na jednom oku u pěti pacientů (#1, #2, #7, #10 a #12), zatímco tři jedinci (#3, #4 a #6) neměli žádné obtíže a depozita byla zachycena náhodně při běžné oční prohlídce. První pacient (#1) zaznamenal snížení zrakové ostrosti v důsledku rohovkových opacit již v jeho 24 letech, avšak správná diagnóza byla stanovena až ve 40 letech. Během 17leté sledovací doby vidění vpravo pokleslo z 0,8 na 0,5 a vlevo z 0,66 na 0,3. Ze souboru pacientů pouze dva podstoupili perforující keratoplastiku, přičemž případ #2 pouze na pravém oku a případ #12 na obou očích. Recidiva onemocnění nastala na rohovkovém transplantátu u případu #12, a to i přestože nemocný byl zajištěn systémovou hematologickou léčbou (Obrázek 17H).

Paraprotein třídy IgGκ (kappa) byl nalezen u 10 pacientů, IgGλ (lambda) a IgAλ u zbývajících dvou pacientů. Sérové hladiny monoklonálních imunoglobulinů nepřesáhly hodnotu 13,3 g/l (norma <0,4 g/l). U žádného pacienta se v průběhu sledování neobjevily známky systémového postižení. Všechny další údaje o souboru pacientů jsou přehledně uvedeny v tabulce 7.

Tabulka 7. Charakteristika 12 pacientů s paraproteinovou keratopatií jako projev monoklonální gamapatie nejasného významu

Případ	Věk*(roky) Pohlaví	M-protein	Sérová hladina M-proteinu (g/l)**	NKZO***		Iniciální klinická diagnóza	Klinický popis	Lokalizace	CCT*** (µm)		Operace	Sledo-vací doba (roky)
				OP	OL				OP	OL		
1	24/M	IgGκ	5,1	0,5	0,3	Mřížková dystrofie rohovky typu 1	Lineární opacity se zašednutím okolního stromatu a numulární léze	Celé stroma (lineární opacity) a povrchní stroma (numulární léze)	530	525	Žádná	17
2	63/M	IgGκ	6,9	0,32$	0,5	Mřížková dystrofie rohovky typu 1	Lineární a retikulární opacity se zašednutím okolního stromatu	Hlavně povrchní stroma	515	501	OP PKP	5
3	53/M	IgGκ	1,5	1,0	1,0	Thielova-Behnkeho dystrofie rohovky	Retikulární opacity, tečky a numulární léze	Hlavně povrchní stroma v centru	543	535	Žádná	2
4	47/Ž	IgGλ	0,7	1,0	1,0	Centrální zašednutí rohovky	Difuzní zašednutí	Hluboké stroma v centru	N	N	Žádná	0
5	48/M	IgAλ	13,3	1,0	1,0	Paraproteinová keratopatie	Cirkulární prstencovité zašednutí s okrsky krystalů a hyperémie spojivek	Hluboké stroma v periférii	514	535	Žádná	15
6	45/M	IgGκ	10,6	1,25	1,25	Cystinóza	Krystalová depozita	Celé stroma	N	N	Žádná	1
7	57/M	IgGκ	9,0	0,63	1,0	Paraproteinová keratopatie	Krystalová depozita	Okrsky v povrchním stromatu	530	528	Žádná	9
8	59/Ž	IgGκ	12,9	0,05#	0,05#	Cystinóza	Krystalová depozita	Celé stroma	536	528	Žádná	3
9	61/M	IgGκ	8,89	0,66	1,0	Cystinóza	Krystalová depozita	Epitel a celé stroma	552	664	Žádná	1
10	60/M	IgGκ	4,0	0,16#	0,1$#	Příčina neznámá	Zašednutí v tenké vrstvě	Povrchní stroma	615	625	OL PLK	2
11	48/Ž	IgGk	10,0	0,66	1,0	Paraproteinová keratopatie	Hypertrofický periferní prstenec a krystalová depozita	Povrchní stroma (prstenec) a celé stroma (krystaly)	487	470	OP a OL periferní keratektomie	12
12	61/M	IgGκ	6,5	0,33$	0,33$	Paraproteinová keratopatie	Větvící se lineární a granulární opacity	Hluboké stroma v centru	N	N	OP a OL PKP	10

* - věk, ve kterém byla depozita poprvé diagnostikována, ** - nejvyšší zaznamenaná hladina, *** - při poslední návštěvě, # -pokles vidění díky kataraktě, $ - zraková ostrost před keratoplastikou
Normální hladina M-proteinu <0.4 g/l (paraprotein),
CCT - centrální tloušťka rohovky, Ig - imunoglobulin, M - muž, N - neprovedeno, NKZO - nejlépe korigovaná zraková ostrost vyjádřená decimálně, OL - oko levé, OP - oko pravé, PLK - přední lamelární keratoplastika, PKP - perforující keratoplastika, Ž - žena, κ - kappa, λ - lambda,

4.8 Cornea plana

Příloha 9: Analysis of *KERA* in four families with cornea plana identifies two novel mutations

V rámci postgraduálního studia byli na ambulanci pro onemocnění rohovky a spojivky vyšetřeni tři jedinci ze dvou rodin českého původu s cornea plana, konkrétně v první rodině dva sourozenci mužského pohlaví ve věku 13 a 20 let a v druhé rodině 70letá žena. U všech vyšetřených osob jsme nalezli charakteristické klinické znaky pro diagnózu cornea plana, tj. ploché rohovky s nízkými hodnotami keratometrie (průměrná hodnota 29,63 dioptrií) zodpovědné za hypermetropickou korekci, nejasný přechod mezi rohovkou a sklérou, centrální rohovkové plaky lemované ztenčením a mělké přední komory (Obrázek 18A a B).

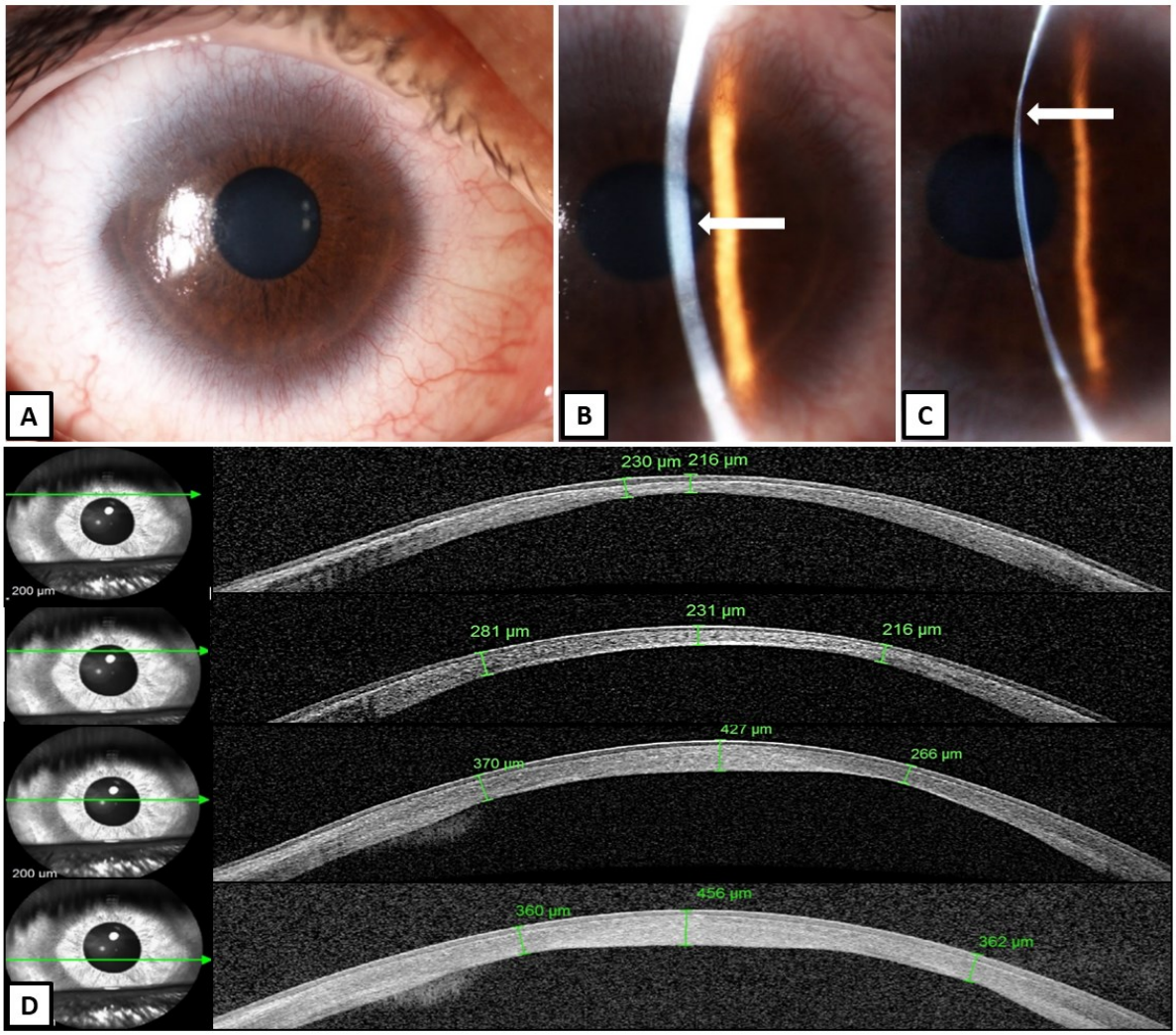

Obrázek 18. Klinický nález na předním segmentu očí 20letého probanda s cornea plana
(A) Nejasný přechod mezi rohovkou a sklérou, (B) centrální rohovkový plak (šipka) a mělká přední komora na pravém oku. (C) Vyklenutí a ztenčení levé rohovky (šipka), které je největší v její horní části a (D) je dokumentováno na řezech rohovky pomocí předně-segmentového SD-OCT.

Výjimkou bylo levé oko 20letého muže, u kterého byly naměřeny abnormálně vysoké hodnoty keratometrie (K1/K2 44,47/49,93 dioptrie) a tomu odpovídala myopická a cylindrická korekce (Tabulka 8). Z dostupné dokumentace vyplynulo, že mezi jeho 18. a 20. rokem života poklesla zraková ostrost z 0,5 na 0,3 a změnila se refrakce v cykloplegii z +3,00/−4,50 x 90° na −4,75/ −6,75 x 53°. Vysoká keratometrie byla vysvětlena biomikroskopicky patrným ztenčením a ektázií rohovky (Obrázek 18C), která byla potvrzena pomocí předně-segmentového SD-OCT. Největší ztenčení rohovky bylo naměřeno v její horní periférii (216 μm) (Obrázek 18D). U ženy z druhé rodiny byl navíc popsán rotační nystagmus a *arcus senilis corneae*.

Tabulka 8. Výsledky jednotlivých měření u třech jedinců českého původu s cornea plana

Pohlaví/ věk/označení	NKZO		Refrakce (DS, DC)		CCT (μm)		NOT (mmHg)		Délka bulbu (mm)		K1/K2 (D)	
	OP	OL	OP	OL	OP	OL	OP	OL	OP	OL	OP	OL
Muž/20 let II:1	0,5	0,3	+3,75/ -5,75x90°	-4,75/ -6,75x53°	456	427	16	16	24,21	24,72	35,87/40,23	44,47/49,93
Muž/13 let II:2	0,9	0,9	+12,0	+11,0	518	511	20	20	24,16	24,05	24,83/26,22	25,41/26,79
Žena/70 let II:1	0,2	0,3	+2,75	+1,5	402	418	20	18	25,77	26,26	27,37/30,24	29,25/30,11

CCT - centrální tloušťka rohovky, D - dioptrie, DC - dioptrie cylindrická, DS - dioptrie sférická, K1 - keratometrie plochý meridián, K2 - keratometrie strmý meridián, NKZO - nejlépe korigovaná zraková ostrost vyjádřená decimálně, NOT - nitrooční tlak, OL - oko levé, OP - oko pravé

V první rodině přímé sekvenování genu *KERA* (referenční sekvence NM_007035.3 a NG_021223.1) (Liskova et al. 2007) odhalilo dvě nové mutace c.209C>T p.(Pro70Leu) a c.887-1G>A v heterozygotním stavu shodně u obou sourozenců. První způsobuje aminokyselinovou záměnu a druhá poruchu sestřihu. Rodiče byli zcela bez příznaků, v souladu s AR dědičností genetická analýza identifikovala u každého z nich jednu variantu (Obrázek 19). Ve druhé rodině byla u ženy zjištěna již známá mutace c.835C>T; p.(Arg279*) v homozygotním stavu.

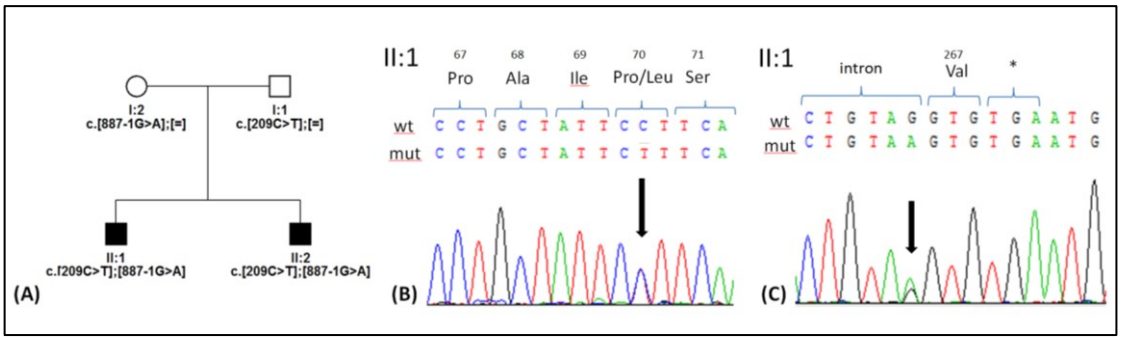

Obrázek 19. Rodina 1 českého původu s cornea plana
(A) Genealogické schéma znázorňující postižené bratry (černé čtverce), jež jsou nositeli dvou nových mutací c.209C>T a c.887-1G>A v genu *KERA*. (B) Sekvenogram mutace c.209C>T způsobující aminokyselinovou záměnu prolinu na leucin pozici 70. (C) Sekvenogram mutace c.887-1G>A, která se nachází v intronu a pravděpodobně vede k poruše sestřihu.

Sourozenci z první rodiny byli od raného dětství sledováni a antiglaukomatiky léčeni pro podezření na glaukom. Toto podezření jsme pomocnými vyšetřovacími metodami vyvrátili, tj. nitrooční tlak byl po vysazení antiglaukomové terapie v normě, nebyly přítomny výpady zorného pole a vrstva nervových vláken byla normální tloušťky. V českých rodinách jsme nezaznamenali příbuzenské sňatky na rozdíl od dvou zbylých jedinců tureckého původu, jejichž DNA byla vyšetřena belgickými spolupracovníky v rámci společného publikovaného souboru.

4.9 Syndrom křehkých rohovek

Příloha 10: Brittle cornea syndrome: A systemic review of disease-causing mutations in *ZNF469* and two novel variants identified in a patient followed for 26 years

Proband česko-polského původu byl sledován od tří let věku, kdy byla zjištěna myopie, která v pozdějším dětském věku dosáhla hodnot až −23,0 dioptrií na obou očích. Onemocnění bylo klasifikováno jako oboustranná ektázie a pro hydrops levé rohovky byla ve věku 16,5 let provedena první perforující keratoplastika (Obrázek 20A a B, Tabulka 9). Vzhledem k selhávání transplantátů následovaly další dvě rekeratoplastiky (Obrázek 20D). Pravé oko bylo poprvé operováno ve věku 26 let pro rozsáhlou perforaci rohovky způsobenou nevelkým tupým traumatem, avšak pooperační období bylo komplikováno netěsností rány a odchlípením sítnice, které vyžadovalo další operace (Tabulka 9). Také díky refrakternímu glaukomu na obou očích bylo pravé oko ve 32 letech zcela slepé a levé vnímalo pouze zbytky světla při poslední kontrole ve 42 letech. Jedním z dalších očních klinických znaků syndromu křehkých rohovek je okrskově ztenčená skléra namodralé barvy, jež byla u našeho probanda popsána na obou očích (Obrázek 20C).

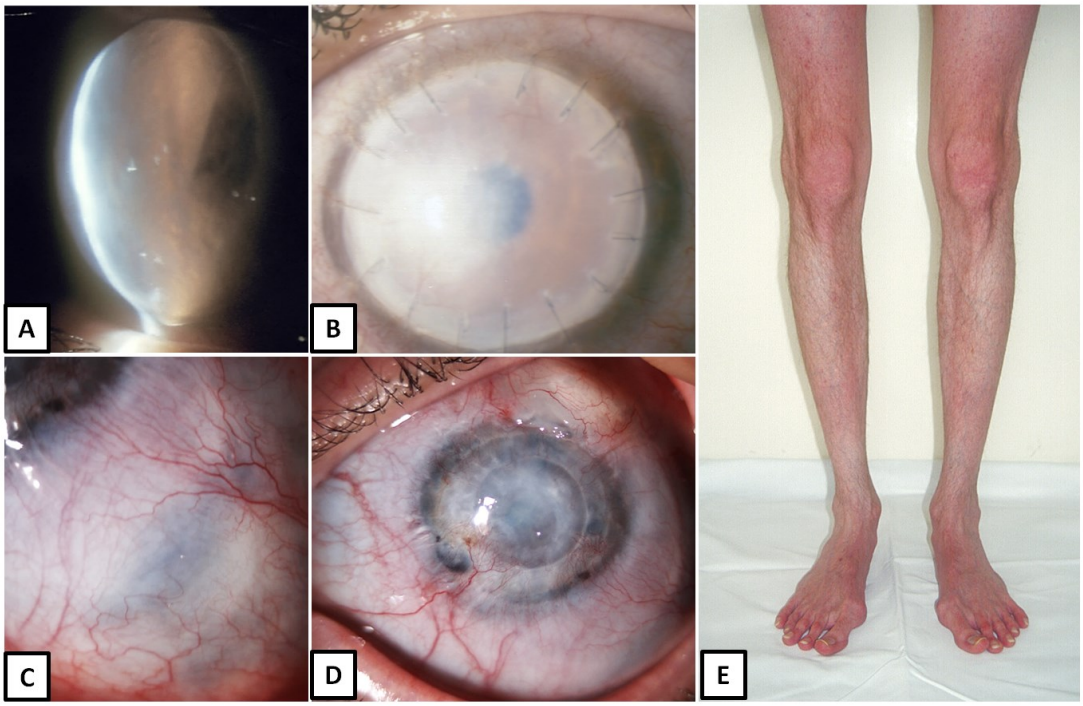

Obrázek 20. Příklady očních a ostatních klinických znaků u muže se syndromem křehkých rohovek způsobených mutacemi v genu *ZNF469*
(A) Akutní hydrops rohovky levého oka (věk 16,5 let), (B) selhání transplantátu jeden rok po první transplantaci rohovky levého oka, (C) detail na tenkou skléru s prosvítající uveou a (D) vaskularizovaný zašedlý transplantát po třetí transplantaci rohovky levého oka. (E) Astenický habitus a vbočené palce.

Tabulka 9. Seznam očních operací provedených u probanda během 26leté sledovací doby

Oko	Věk (roky)	Typ operace	Důvod operace	NKZO před operací	NKZO tři měsíce po operaci	Doplňující informace
pravé	26,0	Tektonická PKP	Velká perforace rohovky po tupém poranění oka	SP	0,16	Velikost transplantátu 8,5 mm, afakie (čočka ztracena během úrazu)
	26,0	TAM	Netěsnost a filtrace rány	0,16	0,16	-
	26,5	PPV + SO	Odchlípení sítnice	0,10	0,25	-
	28,5	CCK	Sekundární glaukom	SP	SP	-
levé	16,5	PKP	Hydrops rohovky	SP	0,16	Velikost transplantátu 9,0 mm
	17,5	rePKP	Selhání rohovkového transplantátu	0,01	0,01	-
	17,5	TE	Sekundární glaukom	0,01	nevyšetřeno	Operace provedena 11 dní po rePKP
	20,0	rePKP	Selhání rohovkového transplantátu	SP	0,16	Velikost transplantátu 6,2 mm

TAM - transplantace amniové membrány, NKZO - nejlépe korigovaná zraková ostrost (vyšetřena pomocí Snellenových optotypů a převedena na decimální hodnoty), CCK - cyklokryokoagulace, SP - světelná projekce, PKP - perforující keratoplastika, PPV - pars plana vitrektomie, rePKP - perforující rekeratoplastika, SO - tamponáda silikonovým olejem, TE - trabekulektomie

Ze systémových klinických znaků jsme zdokumentovali astenický habitus, mírnou kyfoskoliózu, klinodaktylii, hallux valgus, skrotální hernii, poruchu sluchu a funkčně nevýznamné postižení srdce, tj. mitrální a trikuspidální insuficienci a nekompletní blok pravého Tawarova raménka (Obrázek 20E). Celkové a oční projevy onemocnění byly příčinou nesprávné diagnózy *de novo* vzniklého Sticklerova syndromu, pod kterou byl veden od 13 do 40 let věku.

Genomové sekvenování odhalilo dvě nové mutace v genu *ZNF469,* jež podpořily námi zamýšlenou změnu diagnózy vysvětlující vzácný rohovkový nález a obtížně řešitelné oční komplikace syndromu křehkých rohovek. Konkrétně jsme identifikovali c.1402_1411del; p.(Pro468Alafs*31) a c.1705C>T; p.(Gln569*) (Obrázek 21). Sangerovým sekvenováním jsme přítomnost obou patogenních mutací u probanda potvrdili a dále zjistili, že c.1402_1411del v heterozygotním stavu byla zděděna od otce a její nositelkou je také jedna sestra probanda. U druhé sestry a matky byla nalezena mutace c.1705C>T také v heterozygotním stavu (Obrázek 21). Sledováním segregace patogenních variant v rodině jsme tedy prokázali, že proband je složeným heterozygotem, což je v souladu s AR dědičností syndromu křehkých rohovek. V rámci publikované práce jsme také shrnuli všechny patogenní varianty v genu *ZNF469*, které byly dosud celosvětově identifikovány jako příčinné pro syndrom křehkých rohovek. Včetně naší práce bylo celkem popsáno 22 mutací, většina jedinců byla homozygoty a pocházela z příbuzenských sňatků.

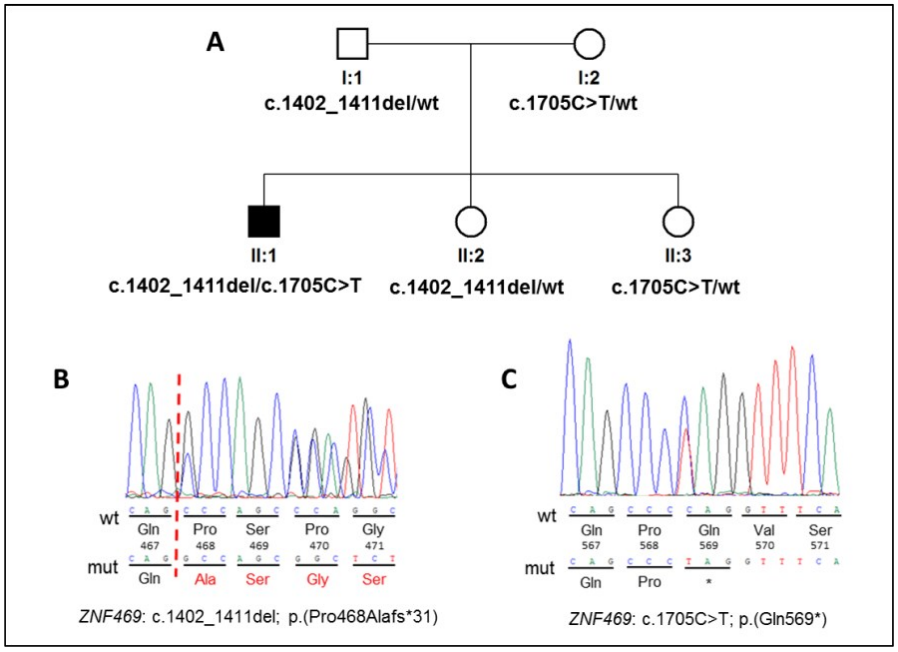

Obrázek 21. Rodokmen a výsledky molekulárně genetického testování
(A) Rodokmen vyšetřované rodiny. Sekvenční chromatogramy mutací identifikovaných v genu *ZNF469* (B) c.1402_1411del a (C) c.1705C>T.

5 DISKUZE

Cílem této disertační práce byl souhrn výsledků studia geneticky podmíněných chorob rohovky s důrazem na využití získaných poznatků v léčebně preventivní péči. Znalost vzácných fenotypů spolu s genetickým testováním napomohla zpřesnění či potvrzení diagnózy, což vytvořilo základ pro lepší odhad prognózy vývoje onemocnění a včasnou intervenci jako prevenci následných komplikací, a tím pozitivně ovlivnila život postižených jedinců a jejich rodin. V průběhu postgraduálního studia se molekulárně genetická analýza stala u mnoha pacientů nezbytným článkem v diferenciálně diagnostickém procesu a byla postupně zařazena do běžné klinické praxe.

5.1 Charakterizované klinické jednotky

Celkem bylo v rámci této práce klinicky vyšetřeno a v publikačních výstupech zdokumentováno 107 jedinců z 19 rodin, včetně 44 pacientů s klinickými znaky vzácných monogenně podmíněných chorob rohovky. Biologický materiál byl odebrán od 104 osob, nalezeno bylo 14 nových a 7 známých mutací. Předpokládaná diagnóza byla genetickým testováním potvrzena u 40 jedinců. Zjištěná molekulárně genetická příčina zcela změnila diagnózu ve čtyřech případech. Negativní nález při genetickém testování napomohl stanovit diagnózu paraproteinové keratopatie namísto zvažované rohovkové dystrofie.

Ze skupiny komplexních dědičných chorob rohovky byla DNA izolována od 132 pacientů s Fuchsovou endotelovou dystrofií rohovky (FECD), z toho u 107 byla prokázána přítomnost expanze tří nukleotidů CTG18.1 v intronu 2 genu *TCF4*.

Před započetím výzkumu popsaného v této práci byla v české populaci klinicky a současně i na molekulárně genetické úrovni charakterizována následující monogenně podmíněná onemocnění rohovky: Reisova-Bücklersova dystrofie, Thieleho-Benkeho dystrofie, granulární dystrofie typ 1, mřížková dystrofie typ 1 (Liskova et al. 2008), makulární dystrofie (Liskova et al. 2008; Dudakova et al. 2014), Schnyderova dystrofie (Weiss et al. 2008), zadní polymorfní dystrofie (PPCD) typ 1 a 3 (Gwilliam et al. 2005; Liskova et al. 2007, 2010, 2012, 2013; Davidson et al. 2016), kongenitální hereditární endotelová dystrofie (CHED) asociovaná s percepční hluchotou, tzv. Harboyanův syndrom (Liskova et al. 2015) a cornea plana (Dudakova et al. 2014). Tato práce rozšiřuje spektrum této skupiny chorob, poprvé jsme na území České republiky popsali a geneticky ověřili diagnózu PPCD4 a syndromu křehkých rohovek (Liskova et al. 2018; Skalicka et al. 2019). Objevením variant v novém genu *GRHL2*

asociovaném s PPCD4 vedlo k vyčlenění této dystrofie jako samostatné klinické jednotky a přiřazení vlastního čísla v databázi OMIM (Liskova et al. 2018). Detekována byla řada nových mutací v různých genech (Dudakova et al. 2016, 2018, 2019; Evans et al. 2018; Brejchova et al. 2019; Skalicka et al. 2019).

5.2 Fenotypová variabilita a korelace s genotypem

Pokud je klinický obraz natolik specifický, že je asociován pouze s mutacemi v jednom genu, lze přikročit k jeho cílenému testování. Příkladem je námi popsaný případ 53leté ženy s mřížkovou dystrofií rohovky, u které bylo provedeno přímé sekvenování vybraných exonů genu *TGFBI*. V souladu s fenotypem, histopatologickým a genetickým vyšetřením byla stanovena diagnóza mřížkové dystrofie rohovky na podkladě nové, dosud nepopsané heterozygotní mutace p.(Leu558Arg) (Dudakova et al. 2016).

Schnyderova dystrofie rohovky je dalším příkladem onemocnění, kdy lze na základě fenotypových projevů přímo přistoupit ke screeningu konkrétního genu. Tato dystrofie byla před započetím této práce popsána s určením příčinné mutace pouze v jedné české rodině (Weiss et al. 2008). V rámci postgraduálního studia jsme detekovali další tři pacienty ze tří rodin a provedli u nich screening genu *UBIAD1*, u dvou z nich byla nalezena nová, dosud nepopsaná mutace (Evans et al. 2018; Dudakova et al. 2019). Detailní klinická charakterizace našeho souboru pacientů vedla ke zjištění, že u všech bylo možno nalézt alespoň ve velmi malém okrsku krystaly v rohovkách, což je v kontrastu s literaturou, která udává jejich přítomnost pouze u 54 % jedinců (Weiss 2009). Tuto skutečnost lze vysvětlit malých počtem osob v našem souboru. U jedné probandky vznikla mutace v genu *UBIAD1 de novo* a dle dostupné literatury je to teprve druhý případ na světě (Lin et al. 2016; Evans et al. 2018; Dudakova et al. 2019).

U jednoho muže byla pozorována unikátní duální diagnóza dvou vzácných dystrofií rohovek, PPCD3 a Schnyderovy dystrofie. Jde o první popsaný případ výskytu dvou vzácných monogenních rohovkových dystrofií u jednoho jedince (Dudakova et al. 2019).

Podrobně jsme zdokumentovali rohovkový nález, zejména centrální zákal a nepravidelnou tloušťku rohovky, u dvou sourozenců, složených heterozygotů pro dvě nové mutace v genu *KERA*. Přesná přístrojová vyšetření zobrazila plaky v centru rohovky lemované ztenčením, jež rovněž pomocí předně-segmentového SD-OCT popsal Rantala u dvou nepříbuzných finských dětí (Rantala a Majander 2015). Navíc jsme u staršího sourozence zjistili, pro cornea plana, výjimečný klinický nález ektázie v horní části rohovky projevující se i změnou refrakce.

Tento méně obvyklý nález byl v literatuře zaznamenán u jedné ze sester britského původu s recesivně dědičnou cornea plana (Liskova et al. 2007). Také Khan popsal případ 16letého chlapce s ektázií v horní periférii rohovky a vznikem hydropsu, který spontánně ustoupil po konzervativní léčbě. Prokázal progresi nálezu a vznik astigmatismu s nárůstem cylindrických dioptrií během chlapcova života (Khan et al. 2006a). Stejný autor publikoval případ 24leté ženy s oboustranným ztenčením rohovky provázeným astigmatismem a stav vyhodnotil jako horní marginální pelucidní degeneraci (Khan et al. 2005). Až další sledování v čase ukáže, zda bude ztenčení rohovky u našeho 20letého probanda progredovat.

U obou mužů byly naměřeny normální hustoty endotelových buněk. Důvodem pro hodnocení tohoto parametru byla skutečnost, že v literatuře byla u jedné pacientky pozorována nižší hustota endotelových buněk s nálezem *guttae* (Dudakova et al. 2014) a u jiného pacienta selhání endotelu bez zjevné příčiny s edémem rohovky (Khan et al. 2009). Dále byla dalšími autory zdokumentována celá škála abnormalit duhovky od drobných periferních předních adherencí duhovky až po okluze zornice (Forsius et al. 1998; Khan et al. 2005; Dudakova et al. 2014). V největší finské kohortě s recesivně dědičnou cornea plana (78 postižených osob) Forsius, kromě již zmíněných změn, dále popsal 23 jedinců se strabismem, 9 s vrozenou ptózou horního víčka a čtyři s glaukomem (Forsius et al. 1998). Na rozdíl od finských pacientů námi zkoumaní jedinci nevykazovali ani známky strabismu, ptózy a glaukomu, ani výše popsané duhovkové změny (Dudakova et al. 2018).

Nicméně u 70leté ženy z druhé rodiny byl přítomen manifestní rotační nystagmus, který nebyl dosud popsán u žádného pacienta s autozomálně recesivní cornea plana. U této probandky byla identifikována známá mutace c.835C>T; p.(Arg279*) v homozygotním stavu. Tato mutace byla již dříve zjištěna u jiné české pacientky, ovšem v heterozygotním stavu (Dudakova et al. 2014) a v souboru ze Saudské Arábie v homozygotním stavu (Khan et al. 2005). Hypoteticky lze zvažovat, v rámci české populace, možnost přenosu této mutace od společného předka, ovšem průkaz tohoto předpokladu by musel být předmětem dalšího zkoumání (Dudakova et al. 2018).

5.3 Přínos molekulárně genetického vyšetření v diferenciální diagnostice

Společným znakem vzácných chorob, rohovku nevyjímaje, je často pozdní stanovení správné diagnózy. Situaci komplikuje i fakt, že v průběhu let může dojít ke změně fenotypu po opakovaných operacích nebo klinický nález není před transplantací rohovky podrobně zdokumentován a původní diagnózu tak nelze objektivně posoudit. Příkladem je prezentovaný

případ muže česko-polského původu, který byl do 13 let sledován s diagnózou keratokonus či jiná ektázie rohovky a následně do 40 let jako Sticklerův syndrom (Skalicka et al. 2019). V klinickém obraze dominovala progredující extrémní myopie na obou očích, ztenčené vyklenující se rohovky a namodralé skléry s prosvítající uveou. V jeho 16,5 letech se projevily první závažné obtíže ve formě akutního hydropsu levé rohovky a ve 26 letech vznikla po nevelkém tupém poranění pravého oka rozsáhlá perforace. Na obou očích následovala série operací na předním i zadním segmentu, jejichž sekundární komplikace vedly ke slepotě.

Nepříznivý průběh onemocnění, poruchy sluchu a celkový habitus pacienta nás vedl k podezření na syndrom křehkých rohovek (BCS), nicméně dle dokumentace byl zvažován i Marfanův syndrom a Ehlersův-Danlosův syndrom, se kterým je BCS často zaměňován (Ramappa et al. 2014). S cílem vyloučit i jiná systémová onemocnění pojiva, bylo zvoleno genomové sekvenování, které identifikovalo dvě zcela nové mutace v genu *ZNF469* potvrzující naše klinické podezření. Je třeba ale dodat, že v době, kdy tento pacient onemocněl, nebyla klinická jednotka křehkých rohovek vyčleněná a nebylo na ní tedy cíleně pomýšleno. Pacient zůstává, dle našich informací, s tímto syndromem jediný diagnostikovaný případ na území České republiky (Skalicka et al. 2019).

Léčba komplikací BCS je velmi kontroverzní a standardní metody, u jiných chorob úspěšné, zde selhávají (Izquierdo et al. 1999; Burkitt Wright et al. 2013). Proto je důležité rozpoznat onemocnění včas a doporučit preventivní opatření k zabránění vzniku spontánní ruptury rohovky (Burkitt Wright et al. 2013). Kromě nošení protektivních polykarbonátových brýlí se jeví nadějně corneal cross-linking. Byl publikován případ 11letého dítěte, u kterého bylo dosaženo stabilizace ve dvouletém sledovacím období po provedení modifikované metody corneal cross-linking (Kaufmann et al. 2015).

Lze se domnívat, že řada rohovkových nálezů, včetně paraproteinové keratopatie, byla v minulosti publikována a označena jako rohovkové dystrofie mylně, a to i proto, že nebylo možné prokázat příčinnou mutaci. V české populaci jsme se setkali s paraproteinovou keratopatií asociovanou s monoklonální gamapatií nejasného významu (MGUS) u šesti pacientů, z toho tři byli iniciálně diagnostikováni jako rohovkové dystrofie a jedna žena jako cystinóza. Nejdéle byl s nepřesnou diagnózou sledován muž, u kterého bylo 16 let podezření na mřížkovou dystrofii rohovky, a až přímé sekvenování genu *TGFBI* tuto dystrofii vyloučilo. První změny byly zaznamenány v jeho 24 letech, což je dle údajů z literatury nejnižší dokumentovaný věk manifestace paraproteinové keratopatie u MGUS (Skalicka et al. 2019).

Depozita monoklonálních imunoglobulinů se ukládala v různých částech a vrstvách rohovky, vyjma endotelu. Pozorovali jsme, stejně jako autoři jiných publikací, velkou variabilitu očních nálezů a stále je možné nalézt nové, dosud nepopsané kombinace projevů (Lisch et al. 2012; Milman et al. 2015; Lisch et al. 2016; Wasielica-Poslednik et al. 2019). Prokázali jsme tedy, že diferenciální diagnostika rohovkových dystrofií a paraproteinové keratopatie může být komplikovaná, proto jsme do vyšetřovacího postupu nevysvětlitelných bilaterálních depozit zařadili i krevní testy k vyloučení paraproteinémie (monoklonální gamapatie).

Jedinci s paraproteinovou keratopatií jsou často asymptomatičtí a depozita v rohovce mohou být zjištěna při běžné oční kontrole, např. při předpisu brýlové korekce na čtení. U poloviny českých pacientů však byla zjištěna zraková ostrost 0,5 a nižší. V jednom případě si pokles vidění vyžádal transplantaci rohovky na obou očích. Proto se v případě poklesu zrakové ostrosti, přikláníme k novému konceptu „klinicky signifikantní monoklonální gamapatie“ (Fermand et al. 2018). Dále z našeho pozorování vyplývá, že postiženou skupinou není jen starší populace, ale i jedinci v mladším produktivním věku.

I přes pokroky v diagnostice, není uspokojivě vyřešena léčba paraproteinové keratopatie. Podobně jako jiní autoři, i my jsme pozorovali recidivy depozit v rohovkových transplantátech v různém časovém odstupu od keratoplastiky (Lisch et al. 2016; Milman et al. 2015). Role systémově podávané cytostatické léčby je nejasná a konkrétně u našeho pacienta nepředešla recidivě depozit (Skalicka et al. 2019).

Vzhledem k tomu, že rohovka je snadno přístupný orgán k neinvazivnímu vyšetření, může být oftalmolog první lékař, který odhalí depozita monoklonálních imunoglobulinů a upozorní na paraproteinémii, což může mít pro pacienta zásadní význam v prevenci pozdějších systémových komplikací. Spektrum hematologických chorob, které se vyznačují produkcí monoklonálních imunoglobulinů, je totiž široké, od benigních po maligní: monoklonální gamapatie nejasného významu (monoclonal gammopathy of undetermined significance; MGUS), mnohočetný myelom, plazmacytom, Waldenströmova makroglobulinémie, chronický lymfocytární lymfom a jiné low grade lymfomy (Kyle et al. 2006).

U všech pacientů v našem souboru byla prokázána MGUS, obecně vnímána jako benigní porucha, jelikož riziko maligního zvratu je nízké, přibližně 1 % pacientů za rok (Kyle et al. 2018). Avšak při přepočtu na kumulativní pravděpodobnost je to již 12 % při desetiletém trvání onemocnění a 30 % po 25 letech (Kyle et al. 2002). Toto je další důvod pro přijetí označení „klinicky signifikantní monoklonální gamapatie“ (Fermand et al. 2018).

5.4 Význam masivního paralelního sekvenování

Možnosti molekulárně genetického vyšetření se neustále vyvíjejí. Primární zvolená metoda by měla respektovat nejlepší poměr ceny a výkonu. U vybraných klinických jednotek podmíněných mutacemi v malém genu lze zvolit Sangerovo sekvenování, které se provádí převážně manuálně a v současné době představuje zlatý standard v diagnostice. Příkladem onemocnění, kde je vhodný screening touto konvenční metodou, je Schnyderova dystrofie rohovky a cornea plana (Dudakova et al. 2018; Evans et al. 2018).

U onemocnění způsobených mutacemi v mnoha genech nebo v genech extrémně dlouhých se v poslední době využívá masivní paralelní sekvenování, které umožňuje vyšetření mnoha úseků genomu a současně nad určitou velikost je ekonomicky výhodnější. Diagnostické laboratoře nabízejí často panel známých genů pro určitou konkrétní skupinu chorob. Ve výzkumu se pak spíše uplatňuje exomové nebo genomové sekvenování, které bylo použito i v této práci. Prokázali jsme přínos masivního paralelního sekvenování při identifikaci mutací způsobujících BCS a PPCD3 a 4 (Liskova et al. 2018; Dudakova et al. 2019; Skalicka et al 2019).

Díky exomovému a genomovému sekvenování byly zjištěny příčinné mutace v genu *ZEB1* u 19 jedinců z 12 rodin s PPCD3, celkem 10 nových mutací v heterozygotním stavu, z toho dvě *de novo* (Dudakova et al. 2019). Bez sekvenování celého genomu by nebyla určena příčina PPCD3 u 30leté ženy z české rodiny C31, jejíž rodiče nevykazovali žádné známky tohoto autozomálně dominantního onemocnění a screening pomocí Sangerova a exomového sekvenování nevedl k detekci patogenní mutace. Nakonec byla právě díky genomovému sekvenování zjištěna *de novo* částečná delece zasahující exony 1-7 a část exonu 8 v genu *ZEB1*. Velké delece byly popsány v 10 % ze všech 49 mutací v genu *ZEB1* (Liskova et al. 2016; Chaudhry et al. 2017). Jejich délka je variabilní a při použití Sangerova či exomového sekvenování, SNP-mikročipu nebo qPCR analýzy nemusí být detekovány. Genomové sekvenování se s podobnými limity nepotýká a dokáže přesně vizualizovat a mapovat chybějící úseky.

V případě hledání nových genů, které nebyly doposud s konkrétním onemocněním asociovány, se s výhodou provádí nejprve určení chromozomálního lokusu, ve kterém se neznámý gen nachází, pomocí tzv. vazebné analýzy, dnes standardně použitím genotypovacích mikročipů, tak jak jsme provedli i my rodině C15. Tím jsme prokázali existenci nového, dosud nepopsaného genu pro PPCD4 (Liskova et al. 2018). Konkrétní příčinná mutace pak byla nalezena genomovým sekvenováním (Liskova et al. 2018).

Ukazuje se, že v diagnostice PPCD nebo jiných neobjasněných případů se může genomové sekvenování uplatnit jako metoda první volby, jelikož uspoří jak výdaje za předchozí negativní genetické analýzy, tak i celkový vyšetřovací čas.

5.5 Průkaz příčinné souvislosti mezi variantou a fenotypem

Všechny níže uvedené logické kroky při prokazování fenotypu byly v roce 2015 sepsány a vydány jako doporučení Americké společnosti lékařské genetiky a genomiky. Bylo doporučeno hodnotit zjištěné varianty na pětistupňové škále jako patogenní, pravděpodobně patogenní, varianty neznámého významu, pravděpodobně benigní a benigní (Richards et al. 2015).

Prvním krokem při zjištění varianty je její hledání v populačních databázích, které obsahují vzorky nepříbuzných, předpokládá se, zdravých jedinců. Mezi největší, a námi nejčastěji používané, patří Genome Aggregation Database (gnomAD), která zahrnuje 125 748 exomů a 71 702 genomů, a česká databáze se 2 264 vzorky spravovaná Národním centrem lékařské genomiky (http://ncmg.cz/en) (Skalicka et al. 2019). Vyskytuje-li se varianta, o které se snažíme zjistit, zda má vliv na vznik monogenně podmíněného onemocnění, v populaci s vysokou frekvencí, potom je její zásadní vliv na pozorovaný fenotyp vyloučen. V opačném případě je vhodné provést segregační analýzu u dostupných členů rodiny, nejlépe společně s klinickým vyšetřením. Tímto relativně jednoduchým krokem zjistíme, např. u recesivních onemocnění, zda se obě nalezené varianty nachází v poloze trans, tedy každá na jiném chromozomu zděděném po jednom od obou rodičů. U dominantně dědičných chorob jsou pak všichni klinicky postižení jedinci nositelé varianty, o které se domníváme, že je patogenní.

Druhým krokem je hledání v literatuře a různých internetových databázích (např. Human Gene Mutation Database, Clivar či lokus specifických), zda již byla zjištěná varianta popsána v souvislosti s nalezeným fenotypem. Pokud ano, je vysoce pravděpodobné, že je zodpovědná za popsaný klinický obraz. Je-li zjištěna nová, dosud nepopsaná varianta, je nutné za pomoci predikčních algoritmů (MutPred, SIFT, PolyPhen2 apod.) zhodnotit její vliv na fenotyp. Tyto a další podobné programy jsou vhodné pro posuzování aminokyselinových záměn a jejich spolehlivost je okolo 70 %. Pro zhodnocení možného vlivu na pre-mRNA sestřih se pak používají jiné algoritmy (např. HSF, NetGene, NNSPLICE, MaxEntScan).

Proto třetím krokem, který nejenže zvýší spolehlivost předchozích procesů, ale zkoumá i patogenetické mechanismy, je funkční analýza.

Jelikož neexistuje zvířecí model věrně simulující kongenitální hereditární endotelovou dystrofii rohovky (CHED), byl vyvinut model buněčný. Diferenciace indukovaných pluripotentních kmenových buněk (autologous induced pluripotent stem cells; iPSC) v různé buňky je atraktivní možností, jak testovat choroby (Ebert et al. 2012). V našem případě byl k ověření patogenity nové varianty c.2240+5G>A v genu *SLC4A11* u CHED použit model buňky podobné endotelové (CE-like cells). Leukocyty, získané od asymptomatického otce, byly přeprogramovány do stadia pluripotentních buněk a dále diferenciovány do endotelu se podobajících buněk, které exprimovaly *SLC4A11*. Bylo prokázáno, že nová varianta c.2240+5G>A indukuje aberantní *SLC4A11* pre-mRNA sestřih (Brejchova et al. 2019). Do dnešní doby byly publikovány jen tři studie (Ali et al. 2018; Wagoner et al. 2018; Zhao a Afshari 2016), které diferencovaly iPSC do endotelových buněk rohovky, avšak na rozdíl od naší práce, ještě nikdy nebyly využity pro studium chorob asociovaných s variantami v genu *SLC4A11*.

U nové mutace 482-2A>G v genu *ZEB1*, jsme prokazovali její vliv na sestřih pomocí izolace mRNA a jejím přepisem do cDNA z čerstvého vzorku krve. Takto jsme prokázali, že mutace vede k vynechání exonu 5 (Dudakova et al. 2019).

V případě identifikace variant v genu, který nebyl doposud s daným onemocněním spojován, je třeba také vycházet ze známých mechanismů vzniku obdobných onemocnění. Na základě znalosti jeho funkce je nutné si položit otázku, zda se jedná o vhodný kandidátní gen. Například u genu *GRHL2*, jsme usoudili, že jeho změny by se mohly podílet na etiologii PPCD, neboť se jedná o transkripční faktor, který hraje roli v diferenciaci epitelu a supresi epitelo-mezenchymální tranzice (EMT) (Kitazawa et al. 2016; Xiang et al. 2017). *GRHL2* působí jako přímý transkripční represor ZEB1 (Frisch et al. 2017). Také se předpokládá, že *GRHL2* se podílí na aktivaci exprese *OVOL2*, je součástí signalizační sítě, která reguluje EMT a stabilizuje specifickou expresi genů v epitelu (Aue et al. 2015). Jelikož se v patogenezi PPCD uplatňuje *ZEB1* haploinsuficience a aberantní ektopická exprese *OVOL2*, jevila se varianta c.20+544G>T v *GRHL2* jako příčina onemocnění PPCD4, což bylo ověřeno funkční studií a nálezem dalších mutací u jiných pacientů. Identifikace nových patogenních variant, včetně mutací v novém genu pro PPCD4, prokázala, že společným mechanismem všech doposud známých typů PPCD je abnormální aktivace EMT rohovkového epitelu. Doufáme, že tento poznatek bude také využit k návrhu cílené léčby, která by mohla spočívat například v zabránění abnormální exprese daného genu.

5.6 Aplikace poznatků do výzkumu cílených léčebných postupů na buněčné úrovni

Znalost příčinné mutace otevírá cestu k budoucím cíleným terapiím, které mohou spočívat v náhradě funkce chorobné alely dodáním alely zdravé genovou terapií nebo zablokováním jejího přepisu pomocí antisense oligonukleotidů. Pro mnoho pacientů s dosud nevyléčitelnými onemocněními představují tyto terapie novou naději, jedná se totiž o léčbu kauzální, která se neomezuje pouze na zmírňování příznaků.

Rohovka se z hlediska kauzálních terapií geneticky podmíněných chorob jeví jako ideální tkáň, jednak kvůli relativnímu imunologickému privilegiu a také proto, že vpravení vektoru nesoucího gen nebo antisense oligonukleotidy by mělo být díky její anatomické dostupnosti mnohem jednodušší ve srovnání se sítnicí, na které v současné době probíhá řada výzkumných projektů. Proč není rohovka v centru zájmu, je opět dáno její strukturou a polohou. Transplantací rohovky lze, i přes nejrůznější komplikace, léčit převážnou část dědičných onemocnění této tkáně, zatímco u onemocnění sítnice, která vedou často k úplné slepotě, představuje genová terapie v naprosté většině případů jedinou naději na zachování zrakových funkcí. Nicméně je třeba si uvědomit, že vlivem stárnoucí populace se budeme již brzy potýkat s nedostatkem vhodné dárcovské tkáně (Golchet et al. 2000). A nové možnosti předejití nutnosti transplantace rohovky u pacientů s dystrofiemi budou nabývat na významu.

Jedním ze základních cílů současného výzkumu je zabránit u pacientů s endotelovými dystrofiemi rohovky selhání bariérové funkce endotelu. V tomto ohledu naše práce přispěla v mnoha rovinách. Potvrdili jsme, podobně jako Wieben a kol., že CTG18.1 expanze významně zvyšuje riziko rozvoje FECD u jedinců evropského původu (Wieben et al. 2012; Zarouchlioti et al. 2018). V endotelových buňkách jsme prokázali hromadění transkriptů s expanzí, které vede k ložiskovému vychytávání faktorů účastnících se sestřihu, což se v konečném důsledku pravděpodobně podílí na apoptóze endotelové buňky. Na modelu kultivovaných endotelových buněk získaných od pacientů s klinickými projevy FECD a expanzí CTG18.1 bylo ověřeno, že navázání synteticky připravených oligonukleotidů do krátkého úseku toxického produktu genu *TCF4* vede k jeho vyřazení („antisense“ terapie). Jinými slovy, „antisense“ terapie snížila výskyt toxických RNA ohnisek. Význam tohoto procesu spočívá v prevenci úbytku endotelových buněk, tím je zachována jejich základní bariérová funkce a nedochází ke klinické progresi FECD (Zarouchlioti et al. 2018).

5.7 Preventivní aspekty využití získaných poznatků

Během posledních několika let se genetické testování očních chorob velmi změnilo. Zatímco dříve bylo dostupné pouze na výzkumné bázi pro několik málo onemocnění, dnes jsou specifické testy nabízeny řadou akreditovaných laboratoří a toto se týká i onemocnění postihujících rohovku. Výsledkem je zlepšení klinického a genetického poradenství pacientům a jejich rodinám.

Včasná detekce geneticky podmíněných onemocnění rohovky je rozhodující pro další péči o postiženého jedince či celou jeho rodinu, nabízí totiž možnost, dle závažnosti nálezu, přizpůsobit frekvenci klinických kontrol. U dětí hraje významnou roli v prevenci vzniku amblyopie (tupozrakosti) možnost záchytu onemocnění spojeného s refrakční vadou, jako je například PPCD3 a cornea plana. Nastavení nebo úprava korekce umožňuje snížit stupeň tupozrakosti na nejnižší možnou míru. U dětí s CHED je pak nutno myslet na možný výskyt poruchy sluchu, její včasnou detekci a řešení např. naslouchadly. To má nemalý význam při začleňování dítěte do kolektivu a vzdělávacího systému státu. Na celý proces navazuje vhodný výběr povolání s ohledem na správně stanovenou oční diagnózu a jejího dalšího očekávaného vývoje.

Konkrétním příkladem včasné a přesné diagnostiky je případ šestileté dívky se Schnyderovou dystrofií rohovky, u které byla zjištěna *de novo* vzniklá mutace (Evans et al. 2018). Němá rodinná anamnéza a záchyt jen diskrétních krystalových depozit ve velmi raném věku by mohl bez genetického vyšetření vést k mylné diagnóze infantilní cystinózy. Dalšími diagnózami, které jsme odhalili v předškolním věku, jsou CHED a PPCD3 a 4 (Liskova et al. 2018; Brejchova et al. 2019; Dudakova et al. 2019).

Důkazem nezbytnosti přesné diagnózy vedoucí k zamezení zbytečné léčby s možnými vedlejšími účinky jsou dva bratři, kteří byli od narození sledováni pod jinou diagnózou, dysgeneze předního segmentu oka. Obavy z glaukomu zapříčinily neopodstatněné předepisování kombinované antiglaukomové terapie od raného věku (Dudakova et al. 2018). Potvrzení diagnózy cornea plana na genové úrovni a vyloučení jiných klinických jednotek přispělo ke změně terapeutického plánu, včetně možnosti správně informovat jedince a jejich rodinu o dalším vývoji onemocnění.

Včasná a správná diagnostika je důležitá nejenom z hlediska plánování kariéry a rodičovství, ale může mít i další socioekonomické dopady, např. v podobě redukce nákladů na zbytečná vyšetření, nezřídka opakovaně prováděná.

Pro zvláště závažná onemocnění způsobující výrazné snížení zrakové ostrosti a slepotu, v případě monogenních onemocnění rohovky např. BCS nebo CHED, lze uvažovat o preimplantační genetické diagnostice (Hlavata et al. 2016). Předpokladem je právě dokonalé zmapování mutací. Je třeba mít ale na paměti, že současné metody detekce neodhalí všechny možné patogenní varianty a řada pacientů, především s retinálními onemocněními, zůstává bez molekulárně genetické diagnózy i přes absolvování všech dostupných molekulárně genetických vyšetření.

Stanovení příčinné mutace(í) umožňuje poskytnout pacientovi informaci stran přenosu onemocnění v dalších generacích. To je zvlášť důležité např. u sporadických pacientů s klinickou charakteristikou AD dědičností, kdy je třeba vysvětlit, proč se onemocnění nevyskytovalo v žádné předcházející generaci. V minulosti tyto případy vedly i k úvahám, že by se mohlo jednat o podtyp onemocnění s recesivním typem dědičnosti (Soukup 1964). Lze zvažovat tzv. nonpenetranci, kdy jedinec je nositelem vlohy pro onemocnění, ale zjevné klinické známky se u něj neprojeví. Další možností je vznik mutace *de novo*, jak jsme pozorovali např. v jednom případě PPCD4 a u jedné dívky se Schnyderovou dystrofií rohovky.

Nové poznatky o genetické etiologii FECD boří tradiční rozdělení dědičných chorob na komplexní a řídící se Mendelovými zákony. Tato dystrofie byla ve starší literatuře považována za jednoznačně AD dědičné onemocnění (Rosenblum et al. 1980; Aldave et al. 2006), což podporovaly i nálezy bodových mutací v různých genech (Biswas et al. 2001; Sundin et al. 2006; Vithana et al. 2008; Riazuddin et al. 2010, 2012, 2013). Později došlo ke změně názoru a na FECD bylo nahlíženo jako na onemocnění komplexní. Objevení přítomnosti expanze tří nukleotidů CTG18.1 v intronu 2 genu *TCF4* opět vedlo k úvaze, zda by neměl být typ přenosu označen za AD (Wieben et al. 2012). Vzhledem k tomu, že dosud nebylo uspokojivě vysvětleno, proč existují rozdíly mezi pohlavími, že expanze CTG18.1 může vykazovat instabilitu (tj. počet repetic se může lišit v následujících generacích) v kombinaci s tím, že u 20–30 % pacientů je podstata onemocnění nevysvětlena, není zatím opodstatněné přehodnocení konceptu FECD z komplexního onemocnění na AD poruchu.

6 ZÁVĚR

Tato práce se zabývala zpracováním výskytu, popisem fenotypu a molekulárně genetickou analýzou různých dystrofií a některých vývojových anomálií rohovky na území České republiky. Zdůrazněn byl dále dopad získaných dat na využití v prevenci vzniku, rozvoje a progrese této skupiny chorob a jejich komplikací s cílem zabránit poklesu či ztrátě zrakové ostrosti.

Genetické testování při správném provedení a interpretaci napomáhá k lepšímu odhadu prognózy vývoje onemocnění, dále vede k identifikaci členů rodiny rizikových pro vznik určitého onemocnění a napomáhá k vývoji a zavedení cílených terapií reflektujících mechanismus vzniku dané choroby. Rohovka, jako snadno přístupná tkáň, se jeví obzvláště vhodná pro tyto nové metody léčby.

Podařilo se učinit několik významných objevů včetně identifikace nového genu, jehož mutace podmiňují PPCD typ 4. Naše práce také prokázala, že všechny typy PPCD mají poruchu na úrovni regulovaných transkripčních faktorů zapojených do epitelo-mezenchymální přeměny. Nastínili jsme i možnosti nových terapií pro geneticky podmíněná onemocnění rohovky.

Výsledky postgraduálního studia byly přímo implementovány do klinické praxe zavedením cíleného genetického testování u vybraných pacientů, upřesněním genetického poradenství postiženým jedincům a jejich rodinám a stanovením konkrétních doporučení z hlediska sledování jako prevence vývoje možných sekundárních komplikací.

SEZNAM WEBOVÝCH ZDROJŮ

1000 Genomes, http://www.internationalgenome.org/
Alibaba 2.1, http://www.gene-regulation.com/pub/programs/alibaba2/index.html
ClinVar, https://www.ncbi.nlm.nih.gov/clinvar/
dbSNP, https://www.ncbi.nlm.nih.gov/projects/SNP/
ENCODE, https://genome.ucsc.edu/ENCODE/
Ensembl Genome Browser, http://www.ensembl.org/index.html
Exome Aggregation Consortium (ExAC) Browser, http://exac.broadinstitute.org/
ExomeDepth, http://cran.r-project.org/web/packages/ExomeDepth/index.html
GeneCards, https://www.genecards.org/
GeneMarker Software (SoftGenetics), https//softgenetics.com/GeneMarker.php
Genome Analysis Toolkit (GATK), https://software.broadinstitute.org/gatk/
Genome Aggregation Database (gnomAD) Browser, http://gnomad.broadinstitute.org/
Genomes of the Netherlands (GoNL), http://www.nlgenome.nl/search/
Haplopainter, http://haplopainter.sourceforge.net/
Human Gene Mutation Database (HGMD), http://www.hgmd.cf.ac.uk/ac/index.php
Human Genome Variation Society, https://www.hgvs.org/
Human Splicing Finder (HSF), https://www.genomnis.com/access-hsf
Interactive Genomics Viewer (IGV), http://www.broadinstitute.org/software/igv/
Kaviar Browser, http://db.systemsbiology.net/kaviar/
Locus Specific Database, https://databases.lovd.nl/shared/genes/SLC4A11
MatInspector, http://www.genomatix.de/index.html
MaxEntScan, http://hollywood.mit.edu/burgelab/maxent/Xmaxentscan_scoreseq.html
MutationTaster, http://www.mutationtaster.org/
MutPred2, http://mutpred.mutdb.org/
Národní centrum lékařské genomiky (The Czech National Center for Medical Genomics), http://ncmg.cz/en
NCBI Genome build GRCh38, https://www.ncbi.nlm.nih.gov/assembly?term=GRCh38&cmd=DetailsSearch
NetGene, http://www.cbs.dtu.dk/services/NetGene2/
NHLBI Exome Sequencing Project (ESP) Exome Variant Server, http://evs.gs.washington.edu/EVS/
NNSplice, http://www.fruitfly.org/seq_tools/splice.html
Novoalign, http://www.novocraft.com/products/novoalign/
Online Mendelian Inheritance in Man (OMIM), http://www.omim.org/
PolyPhen2, http://genetics.bwh.harvard.edu/pph2/
PROVEAN and SIFT, http://provean.jcvi.org/index.php
PubMed, https://www.ncbi.nlm.nih.gov/pubmed
RefSeq, http://www.ncbi.nlm.nih.gov/RefSeq/
SAMtools, http://www.htslib.org/
Scopus, https://www.scopus.com/
SeattleSeq Annotation, http://snp.gs.washington.edu/SeattleSeqAnnotation150/
Sequence Variant Nomenclature, http://varnomen.hgvs.org/
SNP&GO, http://snps.biofold.org/snps-and-go/snps-and-go.html
UCSC Genome Browser, https://genome.ucsc.edu/
UK10K Consortium, http://www.uk10k.org/
UniProt, https://www.uniprot.org/
Variant Effect Predictor, http://useast.ensembl.org/Homo_sapiens/Tools/VEP

LITERATURA

Aggarwal, S., T. Peck, J. Golen, and Z. A. Karcioglu. 2018. 'Macular corneal dystrophy: A review', *Surv Ophthalmol*, 63: 609-17.

Aldave, A. J., S. A. Rayner, A. K. Salem, G. L. Yoo, B. T. Kim, M. Saeedian, B. Sonmez, and V. S. Yellore. 2006. 'No pathogenic mutations identified in the COL8A1 and COL8A2 genes in familial Fuchs corneal dystrophy', *Invest Ophthalmol Vis Sci*, 47: 3787-90.

Ali, M., S. Y. Khan, S. Vasanth, M. R. Ahmed, R. Chen, C. H. Na, J. J. Thomson, C. Qiu, J. D. Gottsch, and S. A. Riazuddin. 2018. 'Generation and Proteome Profiling of PBMC-Originated, iPSC-Derived Corneal Endothelial Cells', *Invest Ophthalmol Vis Sci*, 59: 2437-44.

Aronson, J. K. 2006. 'Rare diseases and orphan drugs', *Br J Clin Pharmacol*, 61: 243-5.

Aue, A., C. Hinze, K. Walentin, J. Ruffert, Y. Yurtdas, M. Werth, W. Chen, A. Rabien, E. Kilic, J. D. Schulzke, M. Schumann, and K. M. Schmidt-Ott. 2015. 'A Grainyhead-Like 2/Ovo-Like 2 Pathway Regulates Renal Epithelial Barrier Function and Lumen Expansion', *J Am Soc Nephrol*, 26: 2704-15.

Ayres, B. D., and C. J. Rapuano. 2006. 'Excimer laser phototherapeutic keratectomy', *Ocul Surf*, 4: 196-206.

Baratz, K. H., N. Tosakulwong, E. Ryu, W. L. Brown, K. Branham, W. Chen, K. D. Tran, K. E. Schmid-Kubista, J. R. Heckenlively, A. Swaroop, G. Abecasis, K. R. Bailey, and A. O. Edwards. 2010. 'E2-2 protein and Fuchs's corneal dystrophy', *N Engl J Med*, 363: 1016-24.

Biswas, S., F. L. Munier, J. Yardley, N. Hart-Holden, R. Perveen, P. Cousin, J. E. Sutphin, B. Noble, M. Batterbury, C. Kielty, A. Hackett, R. Bonshek, A. Ridgway, D. McLeod, V. C. Sheffield, E. M. Stone, D. F. Schorderet, and G. C. Black. 2001. 'Missense mutations in COL8A2, the gene encoding the alpha2 chain of type VIII collagen, cause two forms of corneal endothelial dystrophy', *Hum Mol Genet*, 10: 2415-23.

Brejchova, K., L. Dudakova, P. Skalicka, R. Dobrovolny, P. Masek, M. Putzova, M. Moosajee, S. J. Tuft, A. E. Davidson, and P. Liskova. 2019. 'IPSC-Derived Corneal Endothelial-like Cells Act as an Appropriate Model System to Assess the Impact of SLC4A11 Variants on Pre-mRNA Splicing', *Invest Ophthalmol Vis Sci*, 60: 3084-90.

Burkitt Wright, E. M., L. F. Porter, H. L. Spencer, J. Clayton-Smith, L. Au, F. L. Munier, S. Smithson, M. Suri, M. Rohrbach, F. D. Manson, and G. C. Black. 2013. 'Brittle cornea syndrome: recognition, molecular diagnosis and management', *Orphanet J Rare Dis*, 8: 68.

Cibis, G. W., J. A. Krachmer, C. D. Phelps, and T. A. Weingeist. 1977. 'The clinical spectrum of posterior polymorphous dystrophy', *Arch Ophthalmol*, 95: 1529-37.

Dammacco, R., G. Merlini, W. Lisch, T. T. Kivela, E. Giancipoli, A. Vacca, and F. Dammacco. 2019. 'Amyloidosis and Ocular Involvement: an Overview', *Semin Ophthalmol*: 1-20.

Davidson, A. E., E. Borasio, P. Liskova, A. O. Khan, H. Hassan, M. E. Cheetham, V. Plagnol, F. S. Alkuraya, S. J. Tuft, and A. J. Hardcastle. 2015. 'Brittle cornea syndrome ZNF469 mutation carrier phenotype and segregation analysis of rare ZNF469 variants in familial keratoconus', *Invest Ophthalmol Vis Sci*, 56: 578-86.

Davidson, A. E., S. S. Cheong, P. G. Hysi, C. Venturini, V. Plagnol, J. B. Ruddle, H. Ali, N. Carnt, J. C. Gardner, H. Hassan, E. Gade, L. Kearns, A. M. Jelsig, M. Restori, T. R. Webb, D. Laws, M. Cosgrove, J. M. Hertz, I. Russell-Eggitt, D. T. Pilz, C. J. Hammond, S. J. Tuft, and A. J. Hardcastle. 2014. 'Association of CHRDL1 mutations and variants with X-linked megalocornea, Neuhauser syndrome and central corneal thickness', *PLoS One*, 9: e104163.

Davidson, A. E., P. Liskova, C. J. Evans, L. Dudakova, L. Noskova, N. Pontikos, H. Hartmannova, K. Hodanova, V. Stranecky, Z. Kozmik, H. J. Levis, N. Idigo, N. Sasai, G. J. Maher, J. Bellingham, N. Veli, N. D. Ebenezer, M. E. Cheetham, J. T. Daniels, C. M. Thaung, K. Jirsova, V. Plagnol, M. Filipec, S. Kmoch, S. J. Tuft, and A. J. Hardcastle. 2016. 'Autosomal-Dominant Corneal Endothelial Dystrophies CHED1 and PPCD1 Are Allelic Disorders Caused by Non-coding Mutations in the Promoter of OVOL2', *Am J Hum Genet*, 98: 75-89.

Dinh, R., C. J. Rapuano, E. J. Cohen, and P. R. Laibson. 1999. 'Recurrence of corneal dystrophy after excimer laser phototherapeutic keratectomy', *Ophthalmology*, 106: 1490-7.

Du, J., R. A. Aleff, E. Soragni, K. Kalari, J. Nie, X. Tang, J. Davila, J. P. Kocher, S. V. Patel, J. M. Gottesfeld, K. H. Baratz, and E. D. Wieben. 2015. 'RNA toxicity and missplicing in the common eye disease fuchs endothelial corneal dystrophy', *J Biol Chem*, 290: 5979-90.

Dudakova, L., C. J. Evans, N. Pontikos, N. J. Hafford-Tear, F. Malinka, P. Skalicka, A. Horinek, F. L. Munier, N. Voide, P. Studeny, L. Vanikova, T. Kubena, K. E. Rojas Lopez, A. E. Davidson, A. J. Hardcastle, S. J. Tuft, and P. Liskova. 2019. 'The utility of massively parallel sequencing for posterior polymorphous corneal dystrophy type 3 molecular diagnosis', *Exp Eye Res*, 182: 160-66.

Dudakova, L., M. Palos, A. J. Hardcastle, and P. Liskova. 2014. 'Corneal endothelial findings in a Czech patient with compound heterozygous mutations in KERA', *Ophthalmic Genet*, 35: 252-4.

Dudakova, L., M. Palos, K. Jirsova, P. Skalicka, P. Dundr, and P. Liskova. 2016. 'Novel TGFBI mutation p.(Leu558Arg) in a lattice corneal dystrophy patient', *Ophthalmic Genet*, 37: 473-74.

Dudakova, L., M. Palos, M. Svobodova, J. Bydzovsky, L. Huna, K. Jirsova, A. J. Hardcastle, S. J. Tuft, and P. Liskova. 2014. 'Macular corneal dystrophy and associated corneal thinning', *Eye (Lond)*, 28: 1201-5.

Dudakova, L., P. Skalicka, A. E. Davidson, and P. Liskova. 2019. 'Coincidental Occurrence of Schnyder Corneal Dystrophy and Posterior Polymorphous Corneal Dystrophy Type 3', *Cornea*, 38: 758-60.

Dudakova, L., J. H. J. Vercruyssen, I. Balikova, L. Postolache, B. P. Leroy, P. Skalicka, and P. Liskova. 2018. 'Analysis of KERA in four families with cornea plana identifies two novel mutations', *Acta Ophthalmol*, 96: e87-e91.

Ebenezer, N. D., C. B. Patel, S. M. Hariprasad, L. L. Chen, R. J. Patel, A. J. Hardcastle, and R. C. Allen. 2005. 'Clinical and molecular characterization of a family with autosomal recessive cornea plana', *Arch Ophthalmol*, 123: 1248-53.

Ebert, A. D., P. Liang, and J. C. Wu. 2012. 'Induced pluripotent stem cells as a disease modeling and drug screening platform', *J Cardiovasc Pharmacol*, 60: 408-16.

Eghrari, A. O., Y. J. Daoud, and J. D. Gottsch. 2010. 'Cataract surgery in Fuchs corneal dystrophy', *Curr Opin Ophthalmol*, 21: 15-9.

Eghrari, A. O., and J. D. Gottsch. 2010. 'Fuchs' corneal dystrophy', *Expert Rev Ophthalmol*, 5: 147-59.

Eghrari, A. O., S. A. Riazuddin, and J. D. Gottsch. 2015a. 'Fuchs Corneal Dystrophy', *Prog Mol Biol Transl Sci*, 134: 79-97.

Eghrari, A. O. 2015b. 'Overview of the Cornea: Structure, Function, and Development', *Prog Mol Biol Transl Sci*, 134: 7-23.

Ensenberger, M. G., J. Thompson, B. Hill, K. Homick, V. Kearney, K. A. Mayntz-Press, P. Mazur, A. McGuckian, J. Myers, K. Raley, S. G. Raley, R. Rothove, J. Wilson, D. Wieczorek, P. M. Fulmer, D. R. Storts, and B. E. Krenke. 2010. 'Developmental validation of the PowerPlex 16 HS System: an improved 16-locus fluorescent STR multiplex', *Forensic Sci Int Genet*, 4: 257-64.

Evans, C. J., L. Dudakova, P. Skalicka, G. Mahelkova, A. Horinek, A. J. Hardcastle, S. J. Tuft, and P. Liskova. 2018. 'Schnyder corneal dystrophy and associated phenotypes caused by novel and recurrent mutations in the UBIAD1 gene', *BMC Ophthalmol*, 18: 250.

Fermand, J. P., F. Bridoux, A. Dispenzieri, A. Jaccard, R. A. Kyle, N. Leung, and G. Merlini. 2018. 'Monoclonal gammopathy of clinical significance: a novel concept with therapeutic implications', *Blood*, 132: 1478-85.

Filous, A., J. Osmera, M. Hlozanek, and G. Mahelkova. 2011. 'Central corneal thickness in microphthalmic eyes with or without history of congenital cataract surgery', *Eur J Ophthalmol*, 21: 374-8.

Flockerzi, E., P. Maier, D. Bohringer, H. Reinshagen, F. Kruse, C. Cursiefen, T. Reinhard, G. Geerling, N. Torun, B. Seitz, and Contributors all German Keratoplasty Registry. 2018. 'Trends in Corneal Transplantation from 2001 to 2016 in Germany: A Report of the DOG-Section Cornea and its Keratoplasty Registry', *Am J Ophthalmol*, 188: 91-98.

Forsius, H., M. Damsten, A. W. Eriksson, J. Fellman, S. Lindh, and E. Tahvanainen. 1998. 'Autosomal recessive cornea plana. A clinical and genetic study of 78 cases in Finland', *Acta Ophthalmol Scand*, 76: 196-203.

Franca, E. T., E. S. Arcieri, R. S. Arcieri, and F. J. Rocha. 2002. 'A study of glaucoma after penetrating keratoplasty', *Cornea*, 21: 284-8.
Frisch, S. M., J. C. Farris, and P. M. Pifer. 2017. 'Roles of Grainyhead-like transcription factors in cancer', *Oncogene*, 36: 6067-73.
Gain, P., R. Jullienne, Z. He, M. Aldossary, S. Acquart, F. Cognasse, and G. Thuret. 2016. 'Global Survey of Corneal Transplantation and Eye Banking', *JAMA Ophthalmol*, 134: 167-73.
Glavey, S. V., and N. Leung. 2016. 'Monoclonal gammopathy: The good, the bad and the ugly', *Blood Rev*, 30: 223-31.
Golchet, G., J. Carr, and M. G. Harris. 2000. 'Why don't we have enough cornea donors? A literature review and survey', *Optometry*, 71: 318-28.
Gottsch, J. D., O. H. Sundin, S. H. Liu, A. S. Jun, K. W. Broman, W. J. Stark, E. C. Vito, A. K. Narang, J. M. Thompson, and M. Magovern. 2005. 'Inheritance of a novel COL8A2 mutation defines a distinct early-onset subtype of fuchs corneal dystrophy', *Invest Ophthalmol Vis Sci*, 46: 1934-9.
Gwilliam, R., P. Liskova, M. Filipec, S. Kmoch, K. Jirsova, E. J. Huckle, C. L. Stables, S. S. Bhattacharya, A. J. Hardcastle, P. Deloukas, and N. D. Ebenezer. 2005. 'Posterior polymorphous corneal dystrophy in Czech families maps to chromosome 20 and excludes the VSX1 gene', *Invest Ophthalmol Vis Sci*, 46: 4480-4.
Hlavata, L., L. Dudakova, M. Trkova, I. Soldatova, P. Skalicka, B. Kousal, and P. Liskova. 2016. 'Preimplantation genetic diagnosis and monogenic inherited eye diseases', *Cesk Slov Oftalmol*, 72: 167-71.
Chaudhry, A., B. H. Chung, D. J. Stavropoulos, M. P. Araya, A. Ali, E. Heon, and D. Chitayat. 2017. 'Agenesis of the corpus callosum, developmental delay, autism spectrum disorder, facial dysmorphism, and posterior polymorphous corneal dystrophy associated with ZEB1 gene deletion', *Am J Med Genet A*, 173: 2467-71.
Churchill, A., and J. Graw. 2011. 'Clinical and experimental advances in congenital and paediatric cataracts', *Philos Trans R Soc Lond B Biol Sci*, 366: 1234-49.
Ito, Y. A., and M. A. Walter. 2014. 'Genomics and anterior segment dysgenesis: a review', *Clin Exp Ophthalmol*, 42: 13-24.
Izquierdo, L., Jr., M. J. Mannis, P. B. Marsh, S. P. Yang, and J. M. McCarthy. 1999. 'Bilateral spontaneous corneal rupture in brittle cornea syndrome: a case report', *Cornea*, 18: 621-4.
Jonsson, F., B. Bystrom, A. E. Davidson, L. J. Backman, T. G. Kellgren, S. J. Tuft, T. Koskela, P. Ryden, O. Sandgren, P. Danielson, A. J. Hardcastle, and I. Golovleva. 2015. 'Mutations in collagen, type XVII, alpha 1 (COL17A1) cause epithelial recurrent erosion dystrophy (ERED)', *Hum Mutat*, 36: 463-73.
Kaufmann, C., G. Schubiger, and M. A. Thiel. 2015. 'Corneal Cross-Linking for Brittle Cornea Syndrome', *Cornea*, 34: 1326-8.
Kaup, S., and S. K. Pandey. 2019. 'Cataract surgery in patients with Fuchs' endothelial corneal dystrophy', *Community Eye Health*, 31: 86-87.
Khan, A., A. Al-Saif, and M. Kambouris. 2004. 'A novel KERA mutation associated with autosomal recessive cornea plana', *Ophthalmic Genet*, 25: 147-52.
Khan, A. O. 2007. 'Sclerocornea and cornea plana are distinct entities', *Surv Ophthalmol*, 52: 325; author reply 25-6.
Khan, A. O., M. A. Aldahmesh, S. Al-Gehedan, B. F. Meyer, and F. S. Alkuraya. 2009. 'Corneal decompensation in recessive cornea plana', *Ophthalmic Genet*, 30: 142-5.
Khan, A. O., M. A. Aldahmesh, and F. S. Alkuraya. 2012. 'Brittle cornea without clinically-evident extraocular findings in an adult harboring a novel homozygous ZNF469 mutation', *Ophthalmic Genet*, 33: 257-9.
Khan, A. O., M. Aldahmesh, A. Al-Saif, and B. Meyer. 2005. 'Pellucid marginal degeneration coexistent with cornea plana in one member of a family exhibiting a novel KERA mutation', *Br J Ophthalmol*, 89: 1538-40.
Khan, A. O., M. Aldahmesh, and B. Meyer. 2006a. 'Corneal ectasia and hydrops in a patient with autosomal recessive cornea plana', *Ophthalmic Genet*, 27: 99-101.
Khan, A. O. 2006b. 'Recessive cornea plana in the Kingdom of Saudi Arabia', *Ophthalmology*, 113: 1773-8.

Kitazawa, K., T. Hikichi, T. Nakamura, K. Mitsunaga, A. Tanaka, M. Nakamura, T. Yamakawa, S. Furukawa, M. Takasaka, N. Goshima, A. Watanabe, K. Okita, S. Kawasaki, M. Ueno, S. Kinoshita, and S. Masui. 2016. 'OVOL2 Maintains the Transcriptional Program of Human Corneal Epithelium by Suppressing Epithelial-to-Mesenchymal Transition', *Cell Rep*, 15: 1359-68.

Klintworth, G. K. 2009. 'Corneal dystrophies', *Orphanet J Rare Dis*, 4: 7.

Krafchak, C. M., H. Pawar, S. E. Moroi, A. Sugar, P. R. Lichter, D. A. Mackey, S. Mian, T. Nairus, V. Elner, M. T. Schteingart, C. A. Downs, T. G. Kijek, J. M. Johnson, E. H. Trager, F. W. Rozsa, M. N. Mandal, M. P. Epstein, D. Vollrath, R. Ayyagari, M. Boehnke, and J. E. Richards. 2005. 'Mutations in TCF8 cause posterior polymorphous corneal dystrophy and ectopic expression of COL4A3 by corneal endothelial cells', *Am J Hum Genet*, 77: 694-708.

Krachmer, J. H. 1985. 'Posterior polymorphous corneal dystrophy: a disease characterized by epithelial-like endothelial cells which influence management and prognosis', *Trans Am Ophthalmol Soc*, 83: 413-75.

Kyle, R. A., D. R. Larson, T. M. Therneau, A. Dispenzieri, S. Kumar, J. R. Cerhan, and S. V. Rajkumar. 2018. 'Long-Term Follow-up of Monoclonal Gammopathy of Undetermined Significance', *N Engl J Med*, 378: 241-49.

Kyle, R. A., T. M. Therneau, S. V. Rajkumar, D. R. Larson, M. F. Plevak, J. R. Offord, A. Dispenzieri, J. A. Katzmann, and L. J. Melton, 3rd. 2006. 'Prevalence of monoclonal gammopathy of undetermined significance', *N Engl J Med*, 354: 1362-9.

Kyle, R. A., T. M. Therneau, S. V. Rajkumar, J. R. Offord, D. R. Larson, M. F. Plevak, and L. J. Melton, 3rd. 2002. 'A long-term study of prognosis in monoclonal gammopathy of undetermined significance', *N Engl J Med*, 346: 564-9.

Lee, E. S., and E. K. Kim. 2003. 'Surgical do's and don'ts of corneal dystrophies', *Curr Opin Ophthalmol*, 14: 186-91.

Lin, B. R., R. F. Frausto, R. C. Vo, S. Y. Chiu, J. L. Chen, and A. J. Aldave. 2016. 'Identification of the First De Novo UBIAD1 Gene Mutation Associated with Schnyder Corneal Dystrophy', *J Ophthalmol*, 2016: 1968493.

Lisch, W., P. Saikia, S. Pitz, U. Pleyer, C. Lisch, M. Jaeger, and J. M. Rohrbach. 2012. 'Chameleon-like appearance of immunotactoid keratopathy', *Cornea*, 31: 55-8.

Lisch, W., J. Wasielica-Poslednik, T. Kivela, U. Schlotzer-Schrehardt, J. M. Rohrbach, W. Sekundo, U. Pleyer, C. Lisch, A. Desuki, H. Rossmann, and J. S. Weiss. 2016. 'The Hematologic Definition of Monoclonal Gammopathy of Undetermined Significance in Relation to Paraproteinemic Keratopathy (An American Ophthalmological Society Thesis)', *Trans Am Ophthalmol Soc*, 114: T7.

Lisch, W., and J. S. Weiss. 2019. 'Clinical and genetic update of corneal dystrophies', *Exp Eye Res*, 186: 107715.

Liskova, P., L. Dudakova, C. J. Evans, K. E. Rojas Lopez, N. Pontikos, D. Athanasiou, H. Jama, J. Sach, P. Skalicka, V. Stranecky, S. Kmoch, C. Thaung, M. Filipec, M. E. Cheetham, A. E. Davidson, S. J. Tuft, and A. J. Hardcastle. 2018. 'Ectopic GRHL2 Expression Due to Non-coding Mutations Promotes Cell State Transition and Causes Posterior Polymorphous Corneal Dystrophy 4', *Am J Hum Genet*, 102: 447-59.

Liskova, P., L. Dudakova, V. Tesar, V. Bednarova, J. Kidorova, K. Jirsova, A. E. Davidson, and A. J. Hardcastle. 2015. 'Detailed assessment of renal function in a proband with Harboyan syndrome caused by a novel homozygous SLC4A11 nonsense mutation', *Ophthalmic Res*, 53: 30-5.

Liskova, P., C. J. Evans, A. E. Davidson, M. Zaliova, L. Dudakova, M. Trkova, V. Stranecky, N. Carnt, V. Plagnol, A. L. Vincent, S. J. Tuft, and A. J. Hardcastle. 2016. 'Heterozygous deletions at the ZEB1 locus verify haploinsufficiency as the mechanism of disease for posterior polymorphous corneal dystrophy type 3', *Eur J Hum Genet*, 24: 985-91.

Liskova, P., M. Filipec, S. Merjava, K. Jirsova, and S. J. Tuft. 2010. 'Variable ocular phenotypes of posterior polymorphous corneal dystrophy caused by mutations in the ZEB1 gene', *Ophthalmic Genet*, 31: 230-4.

Liskova, P., R. Gwilliam, M. Filipec, K. Jirsova, S. Reinstein Merjava, P. Deloukas, T. R. Webb, S. S. Bhattacharya, N. D. Ebenezer, A. G. Morris, and A. J. Hardcastle. 2012. 'High prevalence of

posterior polymorphous corneal dystrophy in the Czech Republic; linkage disequilibrium mapping and dating an ancestral mutation', *PLoS One*, 7: e45495.

Liskova, P., P. G. Hysi, D. Williams, J. R. Ainsworth, S. Shah, A. de la Chapelle, S. J. Tuft, and S. S. Bhattacharya. 2007. 'Study of p.N247S KERA mutation in a British family with cornea plana', *Mol Vis*, 13: 1339-47.

Liskova, P., G. K. Klintworth, B. L. Bowling, M. Filipec, K. Jirsova, S. J. Tuft, S. S. Bhattacharya, A. J. Hardcastle, and N. D. Ebenezer. 2008. 'Phenotype associated with the H626P mutation and other changes in the TGFBI gene in Czech families', *Ophthalmic Res*, 40: 105-8.

Liskova, P., M. Palos, A. J. Hardcastle, and A. L. Vincent. 2013. 'Further genetic and clinical insights of posterior polymorphous corneal dystrophy 3', *JAMA Ophthalmol*, 131: 1296-303.

Liskova, P., Q. Prescott, S. S. Bhattacharya, and S. J. Tuft. 2007. 'British family with early-onset Fuchs' endothelial corneal dystrophy associated with p.L450W mutation in the COL8A2 gene', *Br J Ophthalmol*, 91: 1717-8.

Liskova, P., S. J. Tuft, R. Gwilliam, N. D. Ebenezer, K. Jirsova, Q. Prescott, R. Martincova, M. Pretorius, N. Sinclair, D. L. Boase, M. J. Jeffrey, P. Deloukas, A. J. Hardcastle, M. Filipec, and S. S. Bhattacharya. 2007. 'Novel mutations in the ZEB1 gene identified in Czech and British patients with posterior polymorphous corneal dystrophy', *Hum Mutat*, 28: 638.

Liskova, P., B. Veraitch, K. Jirsova, M. Filipec, A. Neuwirth, N. D. Ebenezer, P. G. Hysi, A. J. Hardcastle, S. J. Tuft, and S. S. Bhattacharya. 2008. 'Sequencing of the CHST6 gene in Czech macular corneal dystrophy patients supports the evidence of a founder mutation', *Br J Ophthalmol*, 92: 265-7.

Lopez de la Fuente, C., A. Sanchez-Cano, F. Segura, E. O. Hospital, and I. Pinilla. 2016. 'Evaluation of Total Corneal Thickness and Corneal Layers With Spectral-Domain Optical Coherence Tomography', *J Refract Surg*, 32: 27-32.

Macek, M., Jr. 2019. 'Rare diseases in the year 2019 - the Czech and international context', *Cas Lek Cesk*, 158: 33-37.

Magovern, M., G. R. Beauchamp, J. W. McTigue, B. S. Fine, and R. C. Baumiller. 1979. 'Inheritance of Fuchs' combined dystrophy', *Ophthalmology*, 86: 1897-923.

Mahadevan, M., C. Tsilfidis, L. Sabourin, G. Shutler, C. Amemiya, G. Jansen, C. Neville, M. Narang, J. Barcelo, K. O'Hoy, and et al. 1992. 'Myotonic dystrophy mutation: an unstable CTG repeat in the 3' untranslated region of the gene', *Science*, 255: 1253-5.

McCarey, B. E., H. F. Edelhauser, and M. J. Lynn. 2008. 'Review of corneal endothelial specular microscopy for FDA clinical trials of refractive procedures, surgical devices, and new intraocular drugs and solutions', *Cornea*, 27: 1-16.

Meire, F. M., E. M. Bleeker-Wagemakers, M. Oehler, A. Gal, and J. W. Delleman. 1991. 'X-linked megalocornea. Ocular findings and linkage analysis', *Ophthalmic Paediatr Genet*, 12: 153-7.

Melles, G. R., T. S. Ong, B. Ververs, and J. van der Wees. 2006. 'Descemet membrane endothelial keratoplasty (DMEK)', *Cornea*, 25: 987-90.

Miller, D. D., S. A. Hasan, N. L. Simmons, and M. W. Stewart. 2019. 'Recurrent corneal erosion: a comprehensive review', *Clin Ophthalmol*, 13: 325-35.

Milman, T., A. A. Kao, D. Chu, M. Gorski, A. Steiner, C. Z. Simon, C. Shih, A. J. Aldave, R. C. Eagle, Jr., F. A. Jakobiec, and I. Udell. 2015. 'Paraproteinemic Keratopathy: The Expanding Diversity of Clinical and Pathologic Manifestations', *Ophthalmology*, 122: 1748-56.

Mohamed, A., S. Chaurasia, M. Ramappa, and S. Jalali. 2018. 'Corneal thickness in uveal coloboma with microcornea', *Eye (Lond)*, 32: 586-89.

Mohan, R. R., A. Sharma, M. V. Netto, S. Sinha, and S. E. Wilson. 2005. 'Gene therapy in the cornea', *Prog Retin Eye Res*, 24: 537-59.

Nickerson, M. L., A. D. Bosley, J. S. Weiss, B. N. Kostiha, Y. Hirota, W. Brandt, D. Esposito, S. Kinoshita, L. Wessjohann, S. G. Morham, T. Andresson, H. S. Kruth, T. Okano, and M. Dean. 2013. 'The UBIAD1 prenyltransferase links menaquinone-4 [corrected] synthesis to cholesterol metabolic enzymes', *Hum Mutat*, 34: 317-29.

Orr, A., M. P. Dube, J. Marcadier, H. Jiang, A. Federico, S. George, C. Seamone, D. Andrews, P. Dubord, S. Holland, S. Provost, V. Mongrain, S. Evans, B. Higgins, S. Bowman, D. Guernsey, and M. Samuels. 2007. 'Mutations in the UBIAD1 gene, encoding a potential prenyltransferase, are causal for Schnyder crystalline corneal dystrophy', *PLoS One*, 2: e685.

Park, C. Y., J. K. Lee, P. K. Gore, C. Y. Lim, and R. S. Chuck. 2015. 'Keratoplasty in the United States: A 10-Year Review from 2005 through 2014', *Ophthalmology*, 122: 2432-42.

Poll-The, B. T., L. J. Maillette de Buy Wenniger-Prick, P. G. Barth, and M. Duran. 2003. 'The eye as a window to inborn errors of metabolism', *J Inherit Metab Dis*, 26: 229-44.

Quiroz-Casian, N., O. F. Chacon-Camacho, T. Barragan-Arevalo, J. Nava-Valdez, E. Lieberman, A. Salgado-Medina, A. Navas, E. O. Graue-Hernandez, and J. C. Zenteno. 2018. 'Sclerocornea-Microphthalmia-Aphakia Complex: Description of Two Additional Cases Associated With Novel FOXE3 Mutations and Review of the Literature', *Cornea*, 37: 1178-81.

Ramappa, M., M. E. Wilson, R. C. Rogers, and R. H. Trivedi. 2014. 'Brittle cornea syndrome: a case report and comparison with Ehlers Danlos syndrome', *J AAPOS*, 18: 509-11.

Rantala, E., and A. Majander. 2015. 'Anterior segment optical coherence tomography in autosomal recessive cornea plana', *Acta Ophthalmol*, 93: e232-3.

Riazuddin, S. A., D. S. Parker, E. J. McGlumphy, E. C. Oh, B. W. Iliff, T. Schmedt, U. Jurkunas, R. Schleif, N. Katsanis, and J. D. Gottsch. 2012. 'Mutations in LOXHD1, a recessive-deafness locus, cause dominant late-onset Fuchs corneal dystrophy', *Am J Hum Genet*, 90: 533-9.

Riazuddin, S. A., S. Vasanth, N. Katsanis, and J. D. Gottsch. 2013. 'Mutations in AGBL1 cause dominant late-onset Fuchs corneal dystrophy and alter protein-protein interaction with TCF4', *Am J Hum Genet*, 93: 758-64.

Riazuddin, S. A., N. A. Zaghloul, A. Al-Saif, L. Davey, B. H. Diplas, D. N. Meadows, A. O. Eghrari, M. A. Minear, Y. J. Li, G. K. Klintworth, N. Afshari, S. G. Gregory, J. D. Gottsch, and N. Katsanis. 2010. 'Missense mutations in TCF8 cause late-onset Fuchs corneal dystrophy and interact with FCD4 on chromosome 9p', *Am J Hum Genet*, 86: 45-53.

Richards, S., N. Aziz, S. Bale, D. Bick, S. Das, J. Gastier-Foster, W. W. Grody, M. Hegde, E. Lyon, E. Spector, K. Voelkerding, H. L. Rehm, and Acmg Laboratory Quality Assurance Committee. 2015. 'Standards and guidelines for the interpretation of sequence variants: a joint consensus recommendation of the American College of Medical Genetics and Genomics and the Association for Molecular Pathology', *Genet Med*, 17: 405-24.

Rock, T., J. Landenberger, M. Bramkamp, K. U. Bartz-Schmidt, and D. Rock. 2017. 'The Evolution of Corneal Transplantation', *Ann Transplant*, 22: 749-54.

Rosado-Adames, N., and N. A. Afshari. 2012. 'The changing fate of the corneal endothelium in cataract surgery', *Curr Opin Ophthalmol*, 23: 3-6.

Rosenblum, P., W. J. Stark, I. H. Maumenee, L. W. Hirst, and A. E. Maumenee. 1980. 'Hereditary Fuchs' Dystrophy', *Am J Ophthalmol*, 90: 455-62.

Skalicka, P., L. Dudakova, M. Palos, L. J. Huna, C. J. Evans, G. Mahelkova, M. Meliska, T. Stopka, S. Tuft, and P. Liskova. 2019. 'Paraproteinemic keratopathy associated with monoclonal gammopathy of undetermined significance (MGUS): clinical findings in twelve patients including recurrence after keratoplasty', *Acta Ophthalmol*, 97: e987-e92.

Skalicka, P., L. F. Porter, K. Brejchova, F. Malinka, L. Dudakova, and P. Liskova. 2019. 'Brittle cornea syndrome: A systemic review of disease-causing mutations in ZNF469 and two novel variants identified in a patient followed for 26 years', *Biomed Pap Med Fac Univ Palacky Olomouc Czech Repub*.

Studeny, P., K. Jirsova, P. Kuchynka, and P. Liskova. 2012. 'Descemet membrane endothelial keratoplasty with a stromal rim in the treatment of posterior polymorphous corneal dystrophy', *Indian J Ophthalmol*, 60: 59-60.

Sundin, O. H., K. W. Broman, H. H. Chang, E. C. Vito, W. J. Stark, and J. D. Gottsch. 2006. 'A common locus for late-onset Fuchs corneal dystrophy maps to 18q21.2-q21.32', *Invest Ophthalmol Vis Sci*, 47: 3919-26.

Taneja, K. L., M. McCurrach, M. Schalling, D. Housman, and R. H. Singer. 1995. 'Foci of trinucleotide repeat transcripts in nuclei of myotonic dystrophy cells and tissues', *J Cell Biol*, 128: 995-1002.

Vedana, G., G. Villarreal, Jr., and A. S. Jun. 2016. 'Fuchs endothelial corneal dystrophy: current perspectives', *Clin Ophthalmol*, 10: 321-30.

Vinciguerra, P., R. Vinciguerra, J. B. Randleman, I. Torres, E. Morenghi, and F. I. Camesasca. 2018. 'Sequential Customized Therapeutic Keratectomy for Reis-Bucklers' Corneal Dystrophy: Long-term Follow-up', *J Refract Surg*, 34: 682-88.

Vithana, E. N., P. E. Morgan, V. Ramprasad, D. T. Tan, V. H. Yong, D. Venkataraman, A. Venkatraman, G. H. Yam, S. Nagasamy, R. W. Law, R. Rajagopal, C. P. Pang, G. Kumaramanickevel, J. R. Casey, and T. Aung. 2008. 'SLC4A11 mutations in Fuchs endothelial corneal dystrophy', *Hum Mol Genet*, 17: 656-66.

Wagoner, M. D., L. R. Bohrer, B. T. Aldrich, M. A. Greiner, R. F. Mullins, K. S. Worthington, B. A. Tucker, and L. A. Wiley. 2018. 'Feeder-free differentiation of cells exhibiting characteristics of corneal endothelium from human induced pluripotent stem cells', *Biol Open*, 7.

Wasielica-Poslednik, J., A. Gericke, N. Pfeiffer, and W. Lisch. 2019. '[Paraproteinemic Keratopathy as a Clinical Sign of Monoclonal Gammopathy]', *Klin Monbl Augenheilkd*, 236: 289-94.

Webb, T. R., M. Matarin, J. C. Gardner, D. Kelberman, H. Hassan, W. Ang, M. Michaelides, J. B. Ruddle, C. E. Pennell, S. Yazar, C. C. Khor, T. Aung, M. Yogarajah, A. G. Robson, G. E. Holder, M. E. Cheetham, E. I. Traboulsi, A. T. Moore, J. C. Sowden, S. M. Sisodiya, D. A. Mackey, S. J. Tuft, and A. J. Hardcastle. 2012. 'X-linked megalocornea caused by mutations in CHRDL1 identifies an essential role for ventroptin in anterior segment development', *Am J Hum Genet*, 90: 247-59.

Weiss, J. S. 2009. 'Schnyder corneal dystrophy', *Curr Opin Ophthalmol*, 20: 292-8.

Weiss, J. S., and A. J. Khemichian. 2011. 'Differential diagnosis of Schnyder corneal dystrophy', *Dev Ophthalmol*, 48: 67-96.

Weiss, J. S., H. S. Kruth, H. Kuivaniemi, G. Tromp, J. Karkera, S. Mahurkar, W. Lisch, W. J. Dupps, Jr., P. S. White, R. S. Winters, C. Kim, C. J. Rapuano, J. Sutphin, J. Reidy, F. R. Hu, D. W. Lu, N. Ebenezer, and M. L. Nickerson. 2008. 'Genetic analysis of 14 families with Schnyder crystalline corneal dystrophy reveals clues to UBIAD1 protein function', *Am J Med Genet A*, 146A: 271-83.

Weiss, J. S., H. S. Kruth, H. Kuivaniemi, G. Tromp, P. S. White, R. S. Winters, W. Lisch, W. Henn, E. Denninger, M. Krause, P. Wasson, N. Ebenezer, S. Mahurkar, and M. L. Nickerson. 2007. 'Mutations in the UBIAD1 gene on chromosome short arm 1, region 36, cause Schnyder crystalline corneal dystrophy', *Invest Ophthalmol Vis Sci*, 48: 5007-12.

Weiss, J. S., H. U. Moller, A. J. Aldave, B. Seitz, C. Bredrup, T. Kivela, F. L. Munier, C. J. Rapuano, K. K. Nischal, E. K. Kim, J. Sutphin, M. Busin, A. Labbe, K. R. Kenyon, S. Kinoshita, and W. Lisch. 2015. 'IC3D classification of corneal dystrophies--edition 2', *Cornea*, 34: 117-59.

Wieben, E. D., R. A. Aleff, N. Tosakulwong, M. L. Butz, W. E. Highsmith, A. O. Edwards, and K. H. Baratz. 2012. 'A common trinucleotide repeat expansion within the transcription factor 4 (TCF4, E2-2) gene predicts Fuchs corneal dystrophy', *PLoS One*, 7: e49083.

Wilson, S. E., G. K. Marino, C. S. Medeiros, and M. R. Santhiago. 2017. 'Phototherapeutic Keratectomy: Science and Art', *J Refract Surg*, 33: 203-10.

Woreta, F. A., G. W. Davis, and K. S. Bower. 2015. 'LASIK and surface ablation in corneal dystrophies', *Surv Ophthalmol*, 60: 115-22.

Xiang, J., X. Fu, W. Ran, and Z. Wang. 2017. 'Grhl2 reduces invasion and migration through inhibition of TGFbeta-induced EMT in gastric cancer', *Oncogenesis*, 6: e284.

Yildirim, N., H. Gursoy, A. Sahin, A. Ozer, and E. Colak. 2011. 'Glaucoma after penetrating keratoplasty: incidence, risk factors, and management', *J Ophthalmol*, 2011: 951294.

Zarouchlioti, C., B. Sanchez-Pintado, N. J. Hafford Tear, P. Klein, P. Liskova, K. Dulla, M. Semo, A. A. Vugler, K. Muthusamy, L. Dudakova, H. J. Levis, P. Skalicka, P. Hysi, M. E. Cheetham, S. J. Tuft, P. Adamson, A. J. Hardcastle, and A. E. Davidson. 2018. 'Antisense Therapy for a Common Corneal Dystrophy Ameliorates TCF4 Repeat Expansion-Mediated Toxicity', *Am J Hum Genet*, 102: 528-39.

Zhao, J. J., and N. A. Afshari. 2016. 'Generation of Human Corneal Endothelial Cells via In Vitro Ocular Lineage Restriction of Pluripotent Stem Cells', *Invest Ophthalmol Vis Sci*, 57: 6878-84.

SEZNAM PUBLIKACÍ AUTORKY

Publikace k tématu studia

Brejchova, K., L. Dudakova, **P. Skalicka**, R. Dobrovolny, P. Masek, M. Putzova, M. Moosajee, S. J. Tuft, A. E. Davidson, and P. Liskova. 2019. 'IPSC-Derived Corneal Endothelial-like Cells Act as an Appropriate Model System to Assess the Impact of SLC4A11 Variants on Pre-mRNA Splicing', *Invest Ophthalmol Vis Sci*, 60: 3084-90. IF: 3,812

Dudakova, L., C. J. Evans, N. Pontikos, N. J. Hafford-Tear, F. Malinka, **P. Skalicka**, A. Horinek, F. L. Munier, N. Voide, P. Studeny, L. Vanikova, T. Kubena, K. E. Rojas Lopez, A. E. Davidson, A. J. Hardcastle, S. J. Tuft, and P. Liskova. 2019. 'The utility of massively parallel sequencing for posterior polymorphous corneal dystrophy type 3 molecular diagnosis', *Exp Eye Res*, 182: 160-66. IF: 2,998

Dudakova, L., S. S. Cheong, S. R. Merjava, **P. Skalicka**, M. Michalickova, M. Palos, G. Mahelkova, D. Krizova, M. Hlozanek, M. Trkova, J. L. Chojnowski, E. Hrdlickova, N. Pontikos, V. Plagnol, V. Vesela, K. Jirsova, A. J. Hardcastle, M. Filipec, J. D. Lauderdale, and P. Liskova. 2018. 'Familial Limbal Stem Cell Deficiency: Clinical, Cytological and Genetic Characterization', *Stem Cell Rev Rep*, 14: 148-51. IF: 4,697

Dudakova, L., M. Palos, K. Jirsova, **P. Skalicka**, P. Dundr, and P. Liskova. 2016. 'Novel *TGFBI* mutation p.(Leu558Arg) in a lattice corneal dystrophy patient', *Ophthalmic Genet*, 37: 473-74. IF: 1,277

Dudakova, L., **P. Skalicka**, A. E. Davidson, and P. Liskova. 2019. 'Coincidental Occurrence of Schnyder Corneal Dystrophy and Posterior Polymorphous Corneal Dystrophy Type 3', *Cornea*, 38: 758-60. IF: 2,000

Dudakova, L., J. H. J. Vercruyssen, I. Balikova, L. Postolache, B. P. Leroy, **P. Skalicka**, and P. Liskova. 2018. 'Analysis of *KERA* in four families with cornea plana identifies two novel mutations', *Acta Ophthalmol*, 96: e87-e91. IF: 3,153

Evans, C. J., L. Dudakova, **P. Skalicka**, G. Mahelkova, A. Horinek, A. J. Hardcastle, S. J. Tuft, and P. Liskova. 2018. 'Schnyder corneal dystrophy and associated phenotypes caused by novel and recurrent mutations in the *UBIAD1* gene', *BMC Ophthalmol*, 18: 250. IF: 1,431

Hlavata, L., L. Dudakova, M. Trkova, I. Soldatova, **P. Skalicka**, B. Kousal, and P. Liskova. 2016. 'Preimplantation genetic diagnosis and monogenic inherited eye diseases', *Cesk Slov Oftalmol*, 72: 167-71. bez IF

Liskova, P., L. Dudakova, C. J. Evans, K. E. Rojas Lopez, N. Pontikos, D. Athanasiou, H. Jama, J. Sach, **P. Skalicka**, V. Stranecky, S. Kmoch, C. Thaung, M. Filipec, M. E. Cheetham, A. E. Davidson, S. J. Tuft, and A. J. Hardcastle. 2018. 'Ectopic *GRHL2* Expression Due to Non-coding Mutations Promotes Cell State Transition and Causes Posterior Polymorphous Corneal Dystrophy 4', *Am J Hum Genet*, 102: 447-59. IF: 8,855

Skalicka, P., L. Dudakova, M. Palos, L. J. Huna, C. J. Evans, G. Mahelkova, M. Meliska, T. Stopka, S. Tuft, and P. Liskova. 2019. 'Paraproteinemic keratopathy associated with monoclonal gammopathy of undetermined significance (MGUS): clinical findings in twelve patients including recurrence after keratoplasty', *Acta Ophthalmol*, 97: e987-e92. IF: 3,153

Skalicka, P., L. F. Porter, K. Brejchova, F. Malinka, L. Dudakova, and P. Liskova. 2019. 'Brittle cornea syndrome: A systemic review of disease-causing mutations in *ZNF469* and two novel variants identified in a patient followed for 26 years', *Biomed Pap Med Fac Univ Palacky Olomouc Czech Repub*. IF: 1,141

Stadnikova, A., L. Dudakova, **P. Skalicka**, Z. Valenta, M. Filipec, and K. Jirsova. 2017. 'Active transforming growth factor-beta2 in the aqueous humor of posterior polymorphous corneal dystrophy patients', *PLoS One*, 12: e0175509. IF: 2,766

Zarouchlioti, C., B. Sanchez-Pintado, N. J. Hafford Tear, P. Klein, P. Liskova, K. Dulla, M. Semo, A. A. Vugler, K. Muthusamy, L. Dudakova, H. J. Levis, **P. Skalicka**, P. Hysi, M. E. Cheetham, S. J. Tuft, P. Adamson, A. J. Hardcastle, and A. E. Davidson. 2018. 'Antisense Therapy for a Common Corneal Dystrophy Ameliorates TCF4 Repeat Expansion-Mediated Toxicity', *Am J Hum Genet*, 102: 528-39. IF: 8,855

Ostatní recenzované publikace

Brejchova, K., P. Trosan, P. Studeny, **P. Skalicka**, T. P. Utheim, J. Bednar, and K. Jirsova. 2018. 'Characterization and comparison of human limbal explant cultures grown under defined and xeno-free conditions', *Exp Eye Res*, 176: 20-28. IF: 2,998

Gkalpakiotis, S., P. Arenberger, **P. Skalicka**, and M. Arenbergerova. 2020. 'Dupilumab therapy in a patient with atopic dermatitis and severe atopic keratoconjunctivitis', *J Eur Acad Dermatol Venereol*. IF: 5,113

Kousal, B., **P. Skalicka**, P. Diblik, P. Kuthan, H. Langrova, and P. Liskova. 2013. 'Clinical findings in members of a Czech family with retinitis pigmentosa caused by the c.2426_2427delAG mutation in RPGR', *Cesk Slov Oftalmol*, 69: 8-15. bez IF

Kousal, B., **P. Skalicka**, L. Valesova, T. Fletcher, N. Hart-Holden, A. O'Grady, C. F. Chakarova, M. Michaelides, A. J. Hardcastle, and P. Liskova. 2014. 'Severe retinal degeneration in women with a c.2543del mutation in ORF15 of the RPGR gene', *Mol Vis*, 20: 1307-17. IF: 2,365

Liskova, P., T. Colclough, N. Hart-Holden, C. F. Chakarova, A. O'Grady, L. Kondrova, **P. Skalicka**, P. Diblik, and A. J. Hardcastle. 2011. 'Molecular genetic cause of X-linked retinitis pigmentosa in a Czech family', *Acta Ophthalmol*, 89: e213-5. IF: 2,629

Mahelkova, G., V. Vesela, P. Seidler Stangova, A. Zidlicka, D. Dotrelova, I. Fales, **P. Skalicka**, and K. Jirsova. 2015. 'Tear Osmolarity in Patients with Severe Dry Eye Syndrome Before and After Autologous Serum Treatment: a Comparison with Tear Osmolarity in Healthy Volunteers', *Cesk Slov Oftalmol*, 71: 184-8. bez IF

Rihova, Z., M. Merta, R. Rysava, P. Bezdicek, V. Danzig, K. Gorican, J. Lukas, **P. Skalicka**, Z. Vernerova, and V. Tesar. 2001. 'Multiple extrarenal complications in Wegener granulomatosis', *Cas Lek Cesk*, 140: 503-5. IF: 0,140

Rybickova, I., V. Vesela, I. Fales, **P. Skalicka**, and K. Jirsova. 2016. 'Apoptosis of conjunctival epithelial cells before and after the application of autologous serum eye drops in severe dry eye disease', *Biomed Pap Med Fac Univ Palacky Olomouc Czech Repub*, 160: 271-5. IF: 0,894

Siskova, A., E. Rihova, **P. Skalicka**, J. Jandusova, and D. Dotrelova. 2003. 'Importance of pars plana vitrectomy in the diagnosis of ocular toxocariasis', *Cesk Slov Oftalmol*, 59: 304-11. bez IF

Skalicka, P., and B. Kalvodova. 2013. 'Problematic issues related to screening for diabetic retinopathy', *Vnitr Lek*, 59: 218-23. IF: 0,360

Stadnikova, A., P. Trosan, **P. Skalicka**, T. P. Utheim, and K. Jirsova. 2019. 'Interleukin-13 maintains the stemness of conjunctival epithelial cell cultures prepared from human limbal explants', *PLoS One*, 14: e0211861. IF: 2,776

Szabo, E., M. Palos, and **P. Skalicka**. 2016. 'Ocular Cicatricial Pemphigoid - a Retrospective Study', *Cesk Slov Oftalmol*, 72: 283-92. bez IF

Ostatní publikace

Klímová, A., P. Svozílková, **P. Skalická**. Konjunktivitidy. Remedia. 2015, 25(4), 259-263. ISSN 0862-8947.

Kalvodová, B., **P. Skalická**. Diabetická retinopatie - možnosti farmakoterapie a pokroky v léčbě. Remedia. 2014, 24(1), 21-24. ISSN 0862-8947.

Kapitoly v knihách

Svozílková, P., J. Heissigerová, P. Diblík, J. Becková, A. Beňová, J. Betková, M. Brichová, Z. Dubská, J. Dvořák, M. Fichtl, J. Glezgová, L. Huňa, M. Janek, I. Kaincová, B. Kalvodová, E. Klofáčová, B. Kousal, M. Kováčová, P. Kuthan, M. Meliška, M. Michaličková, M. Palos, E. Růžičková, E. Říhová, K. Sedláková, **P. Skalická**, P. Sklenka, M. Vajter, et al.. Diferenciální diagnostika v oftalmologii v obrazech. 1 vyd. Praha: Mladá fronta, 2015. 222 s. ISBN 978-80-204-3393-0.

Heissigerová, J., M. Brichová, P. Diblík, Z. Dubská, M. Fichtl, J. Glezgová, L. Huňa, B. Kalvodová, A. Klímová, B. Kousal, P. Kuthan, P. Lišková, M. Michaličková, P. Novák, L. Rezková,

E. Růžičková, **P. Skalická**, P. Sklenka, P. Svozílková. Oftalmologie: pro pregraduální i postgraduální přípravu. 1 vyd. Praha: Maxdorf, 2018. 380 s. ISBN 978-80-7345-580-4.

Stať ve sborníku prací (nekonferenčním)

Skalická, P. Recidivující eroze rohovky a současné možnosti léčby v běžné klinické praxi. In: Oftalmologie pro praxi. Olomouc: Solen, Medical education, 2017. s. 6-8. ISBN 978-80-7471-211-1.

Skalická, P., L. Huňa, N. Járová. Komplikace syndromu suchého oka a jejich řešení. In: Trendy soudobé oftalmologie. Svazek 11. 1. vyd. Praha: Galén, 2018. s. 85-96. ISBN 978-80-7492-377-7.

PŘÍLOHY

Příloha 1. Novel *TGFBI* mutation p.(Leu558Arg) in a lattice corneal dystrophy patient

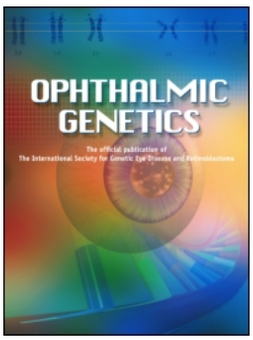

Ophthalmic Genetics

ISSN: 1381-6810 (Print) 1744-5094 (Online) Journal homepage: http://www.tandfonline.com/loi/iopg20

Novel TGFBI mutation p.(Leu558Arg) in a lattice corneal dystrophy patient

Lubica Dudakova, Michalis Palos, Katerina Jirsova, Pavlina Skalicka, Pavel Dundr & Petra Liskova

To cite this article: Lubica Dudakova, Michalis Palos, Katerina Jirsova, Pavlina Skalicka, Pavel Dundr & Petra Liskova (2016): Novel TGFBI mutation p.(Leu558Arg) in a lattice corneal dystrophy patient, Ophthalmic Genetics

To link to this article: http://dx.doi.org/10.3109/13816810.2015.1126615

Published online: 30 Mar 2016.

OPHTHALMIC GENETICS
http://dx.doi.org/10.3109/13816810.2015.1126615

Taylor & Francis
Taylor & Francis Group

LETTER TO THE JOURNAL

Novel *TGFBI* mutation p.(Leu558Arg) in a lattice corneal dystrophy patient

Lubica Dudakova[a], Michalis Palos[b], Katerina Jirsova[a], Pavlina Skalicka[b], Pavel Dundr[c], and Petra Liskova[a,b]

[a]Laboratory of the Biology and Pathology of the Eye, Institute of Inherited Metabolic Disorders, First Faculty of Medicine, Charles University in Prague and General University Hospital in Prague, Prague, Czech Republic; [b]Department of Ophthalmology, First Faculty of Medicine, Charles University in Prague and General Teaching Hospital in Prague, Prague, Czech Republic; [c]Institute of Pathology, First Faculty of Medicine, Charles University in Prague and General University Hospital in Prague, Prague, Czech Republic

Mutations in the human transforming growth factor beta–induced gene (*TGFBI*) have been identified as disease-causing in several clinically distinct epithelial-stromal corneal dystrophies.[1,2] Most common are classical lattice corneal dystrophy (LCD); granular corneal dystrophy type 1 and granular corneal dystrophy type 2.[1,2] Several distinct heterozygous mutations lead to LCD variants with delayed onset and differences in lattice line appearance compared to classical LCD.[1] In this study, a female of Czech origin clinically diagnosed with LCD was investigated. Ophthalmological examination, histopathological study of an explanted corneal disc and conventional Sanger sequencing of *TGFBI* exons 4, 11, 12, 13, 14 (NM_000358.2) were performed.[3]

The proband has been wearing glasses since the age of 15 years. She has never experienced symptoms suggestive of recurrent corneal erosions and she has only noticed decrease of her best corrected visual acuity (BCVA) at the age of 52 years. Upon the first examination at the age of 53 years, BCVA was 0.33 and 0.25 in the right and left eye, respectively. Fine translucent gray-white branching lines and dot deposits were observed bilaterally at all depths of the corneal stroma (Figure 1a, b). Rotating Scheimpflug imaging (Pentacam; Oculus Optikgeräte GmbH, Wetzlar, Germany) revealed in both corneas slightly irregular anterior surface but no ectasia. Central corneal thickness was 539 μm and 525 μm in the right and left eye, respectively. The patient underwent penetrating keratoplasty (PK) in the left eye at the age of 53 years. At the last examination, 2 years after the surgery, the graft remained clear.

Histopathological examination of 6 μm sections from the corneal disc obtained after PK demonstrated multiple stromal amyloid deposits staining with Congo-red, with birefringence and dichroism under polarized light (Figure 1c, d, e, f). The size of the stromal deposits increased in anterior to posterior direction where they measured up to 50 μm in diameter. The epithelium appeared normal with 5–6 layers (Figure 1g). Very little amyloid deposition was detected focally in the Bowman layer which appeared otherwise also intact (Figure 1c, d, e, g). No changes of the Descemet membrane and the endothelium were found. The proband's deceased father was known to suffer from an ocular disorder however medical notes confirming the presence of corneal dystrophy were not available.

A novel heterozygous *TGFBI* mutation was identified in the proband, c.1673T>G in exon 12 (Figure 1h) that leads to a p.(Leu558Arg) change at the protein level. The unaffected 28-year-old son of the proband did not inherit the mutation and this was consistent in not showing any clinical corneal findings. No other relatives were known to suffer from a corneal disease. The c.1673T>G in *TGFBI* is not listed in the dataset of the Exome Aggregation Consortium (ExAC), Cambridge, MA (http://exac.braoadinstitute.org) version 0.3, showing data from 60,706 unrelated individuals of different origins. Four algorithms were used; SIFT,[4] PolyPhen2,[5] MutPred[6] and SNPs&GO,[7] which predicted that the p.(Leu558Arg) change was likely to be deleterious. Leucine at amino acid position 558 is highly conserved in mammals as well as in other animal classes.

Clinical and histopathological findings suggest that the observed mutation leads to LCD. The low level of amyloid deposition within the Bowman layer may explain the lack of recurrent corneal erosions typically observed in classic LCD.[1] However, as diverse phenotypes for identical *TGFBI* pathogenic changes have been observed previously,[8] and as we only report one individual, it cannot be excluded that features associated with p.(Leu558Arg) may vary in other patients.

In summary, our study expands the spectrum of pathogenic mutations associated with LCD and although we cannot show segregation of c.1673T>G in *TGFBI* within the family, it is likely that the change identified is pathogenic and this is supported by prediction algorithms, conservation of the affected residue across multiple species, and an absence in variant databases.

Declaration of interest

The authors report no conflicts of interest. The authors alone are responsible for the content and writing of this article.

Funding

Institutional support was provided by the UNCE 204011 and PRVOUK-P24/LF1/3 programs of the Charles University in Prague. KJ and PD were supported by project LM 2010004 BBMRI_CZ and LD by SVV 260148/2015. Dr. Reshma Malviya performed English language editing.

CONTACT Petra Liskova petra.liskova@lf1.cuni.cz Laboratory of the Biology and Pathology of the Eye, Institute of Inherited Metabolic Disorders, First Faculty of Medicine, Charles University in Prague and General University Hospital in Prague, Ke Karlovu 2, Prague 128 08, Czech Republic.

Color versions of one or more figures in the article can be found online at http://www.tandfonline.com/iopg.

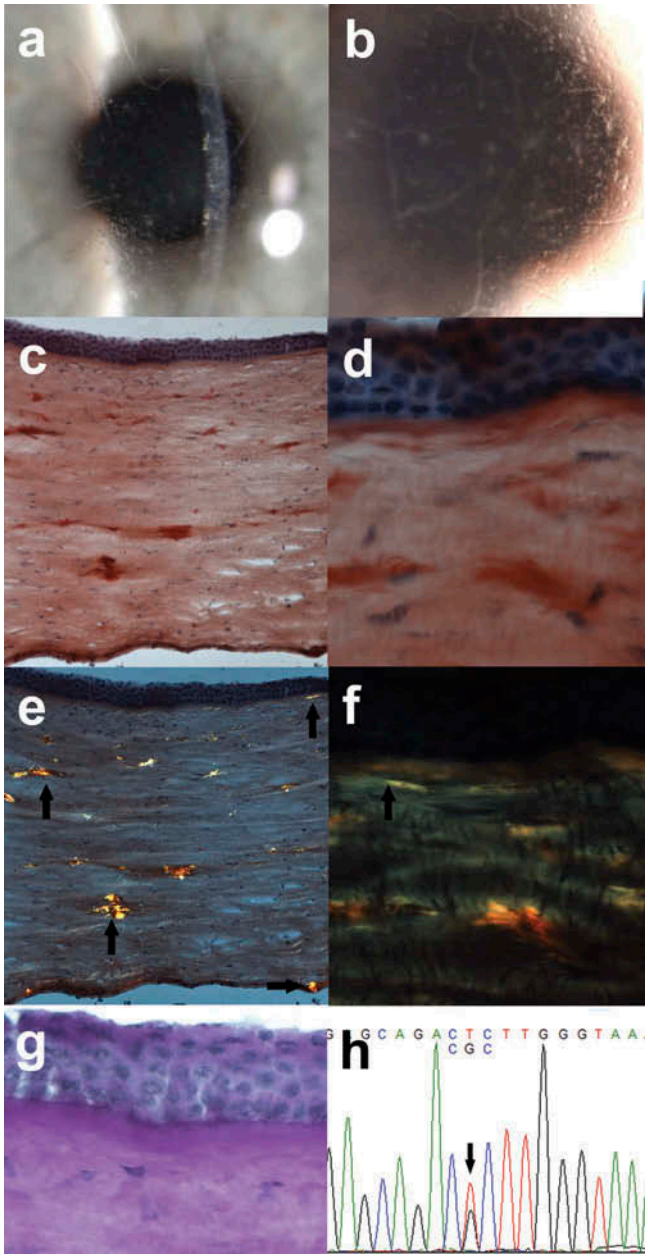

Figure 1. Clinical, histopathological and molecular genetic findings in a proband with a c.1673T>G; p.(Leu558Arg) mutation in the *TGFBI* gene. (a) Slit-lamp image of the right and (b) left cornea showing corneal stromal branching thin translucent lines and small dot deposits. (c) Corneal tissue section with Congo-red stained amyloid deposits (original magnification ×100) and (d) detailed view of an area with amyloid deposition in the Bowman layer (original magnification ×200). (e) Green birefringence of amyloid deposits under polarized light located throughout the entire stroma (arrows) including Bowman layer and deep stromal lamellae adjacent to Descemet membrane (original magnification ×100). (f) Congo-red positive material under polarized light in the Bowman layer (arrow). (g) Periodic acid-Schiff staining showing normal corneal epithelium, intact epithelial basement membrane and Bowman layer appearing morphologically also normal (original magnification of f & g ×200). (h) A heterozygous T to G transversion (c.1673T>G) in exon 12 (arrow).

References

1. Weiss JS, Møller HU, Aldave AJ, et al. The IC3D classification of the corneal dystrophies – Edition 2. Cornea 2015;34:117–159.
2. Klintworth GK. Corneal dystrophies. Orphanet J Rare Dis 2009;4:7.
3. Munier FL, Frueh BE, Othenin-Girard P, et al. BIGH3 mutation spectrum in corneal dystrophies. Invest Ophthalmol Vis Sci 2002;43:949–954.
4. Kumar P, Henikoff S, Ng PC. Predicting the effects of coding non-synonymous variants on protein function using the SIFT algorithm. Nature Protocols 2009;4:1073–1081.
5. Adzhubei IA, Schmidt S, Peshkin L, et al. A method and server for predicting damaging missense mutations. Nature Methods 2010;7:248–249.
6. Li B, Krishnan VG, Mort ME, et al. Automated inference of molecular mechanisms of disease from amino acid substitutions. Bioinformatics 2009;25:2744–2750.
7. Calabrese R, Capriotti E, Fariselli P, et al. Functional annotations improve the predictive score of human disease-related mutations in proteins. Human Mutation 2009;30:1237–1244.
8. Edelstein SL, Huang AJ, Harocopos GJ, et al. Genotype of lattice corneal dystrophy (R124C mutation in TGFBI) in a patient presenting with features of Avellino corneal dystrophy. Cornea 2010;29:698–700.

Příloha 2. Schnyder corneal dystrophy and associated phenotypes caused by novel and recurrent mutations in the *UBIAD1* gene

Evans et al. BMC Ophthalmology (2018) 18:250
https://doi.org/10.1186/s12886-018-0918-8

BMC Ophthalmology

RESEARCH ARTICLE Open Access

Schnyder corneal dystrophy and associated phenotypes caused by novel and recurrent mutations in the *UBIAD1* gene

Cerys J. Evans[1†], Lubica Dudakova[2†], Pavlina Skalicka[2,3], Gabriela Mahelkova[4], Ales Horinek[5,6], Alison J. Hardcastle[1], Stephen J. Tuft[7] and Petra Liskova[2,3*]

Abstract

Background: The purpose of this study was to identify the genetic cause and describe the clinical phenotype of Schnyder corneal dystrophy (SCD) in six unrelated probands.

Methods: We identified two white Czech, two white British and two South Asian families with a clinical diagnosis of SCD. Ophthalmic assessment included spectral domain optical coherence tomography (SD-OCT) of one individual with advanced disease, and SD-OCT and confocal microscopy of a child with early stages of disease. *UBIAD1* coding exons were amplified and Sanger sequenced in each proband. A fasting serum lipid profile was measured in three probands. Paternity testing was performed in one family.

Results: A novel heterozygous c.527G>A; p.(Gly176Glu) mutation in *UBIAD1* was identified in one Czech proband. In the second Czech proband, aged 6 years when first examined, a previously described de novo heterozygous c.289G>A; p.(Ala97Thr) mutation was found. Two probands of South Asian descent carried a known c.305G>A; p.(Asn102Ser) mutation in the heterozygous state. Previously reported heterozygous c.361C>T; p.(Leu121Phe) and c.308C>T; p.(Thr103Ile) mutations were found in two white British families. Although crystalline deposits were present in all probands the affected area was small in some individuals. Corneal arcus and stromal haze were the most prominent phenotypical feature in two probands. In the Czech probands, SD-OCT confirmed accumulation of reflective material in the anterior stroma. Crystalline deposits were visualized by confocal microscopy. Mild dyslipidemia was found in all three individuals tested.

Conclusion: Although de novo occurrence of mutations in *UBIAD1* is extremely rare, SCD should be considered in the differential diagnosis of bilateral corneal haze and/or crystal deposition, especially in children.

Keywords: Schnyder corneal dystrophy, *UBIAD1*, Novel mutation, De novo, Crystalline deposits, Confocal microscopy, Spectral domain optical coherence tomography

Background

Schnyder corneal dystrophy (SCD; MIM #121800) is a rare autosomal dominant disorder characterized by bilateral corneal opacification due to an accumulation of unesterified cholesterol and phospholipids in the corneal stroma [1]. Approximately 50% of individuals have crystalline deposits [2]. An association with genu valgum and systemic hyperlipidemia has also been reported [3].

SCD is caused by mutations in the *UBIAD1* gene (MIM *611632), encoding a membrane-embedded UbiA prenyltransferase domain-containing protein which catalyses the Mg^{2+}-dependent transfer of a hydrophobic polyprenyl chain onto a variety of acceptor molecules, including vitamin K and coenzyme Q [1, 4, 5]. At least 26 mutations that cause SCD have been identified to date [6].

In this study we report the clinical and genetic investigation of six probands of white and South Asian origin.

* Correspondence: petra.liskova@lf1.cuni.cz
†Cerys J. Evans and Lubica Dudakova contributed equally to this work.
[2]Research Unit for Rare Diseases, Department of Paediatrics and Adolescent Medicine, First Faculty of Medicine, Charles University and General University Hospital in Prague, Ke Karlovu 2, 128 08 Prague 2, Czech Republic
[3]Department of Ophthalmology, First Faculty of Medicine, Charles University and General University Hospital in Prague, Prague, Czech Republic
Full list of author information is available at the end of the article

Methods

Clinical examination

The study was approved by the relevant research ethics committees and adhered to the tenets of the Helsinki Declaration. Previously unreported probands from six families with a clinical diagnosis of SCD were investigated; two were recruited in the Czech Republic and four in the UK (Table 1). Family history of SCD was documented and available family members were invited to participate.

Ophthalmic examination included best corrected Snellen visual acuity (BCVA) converted to decimal values, intraocular pressure, and fundal examination after pupil dilation. We performed corneal imaging of probands 1 and 2 using spectral domain optical coherence tomography (SD-OCT) (Spectralis; Heidelberg Engineering GmbH). Proband 2 also underwent scanning slit confocal microscopy equipped with a non-applanating 40× immersion objective lens (Confoscan 3.0; Nidek Technologies, Viconza, Italy) [7].

We measured the fasting serum lipid profile of three probands and recorded the levels of total cholesterol, high and low-density lipoproteins, and triglycerides. The presence of joint deformity, scoliosis or learning difficulty was based on self-reported symptoms.

Molecular genetic analysis

Genomic DNA from probands and any additional available family members was extracted from venous blood samples using a Gentra Puregene blood kit (Qiagen, Hilden, Germany) or from saliva using an Oragene kit (Oragene OG-300, DNA Genotek, Canada). We then performed PCR amplification and Sanger sequencing of the two *UBIAD1* coding exons and exon/intron boundaries (primer sequences and conditions are listed in Table 2). Variants were annotated against the reference sequence for transcript NM_013319.2. Mutation description followed standard nomenclature guidelines (http://varnomen.hgvs.org/) starting with nucleotide numbering c.1 at the A of the ATG translation initiation codon. Pathogenicity was evaluated in silico by six different algorithms (PROVEAN [8], SNPs&GO [9], MutPred [10], SIFT [11], PolyPhen-2 [12] and MutationTaster [13]). We also performed paternity testing in family 2, using a previously published set of markers [14]. The population frequency of variants was determined by the Genome Aggregation Database (gnomAD), which provides sequencing data from more than 123,136 exomes and 15,496 genomes from unrelated individuals of various ethnic backgrounds [15], and 2500 Czech control chromosomes available through the next generation sequencing projects of the Czech National Center for Medical Genomics (https://ncmg.cz/en).

Table 1 Demographic and clinical data of six probands with Schnyder corneal dystrophy

No	Ethnicity	Family history	*UBIAD1* mutation	Age (when recruited)/ gender	BCVA		Corneal phenotype	Chol (mmol/l)	HDL (mmol/l)	LDL (mmol/l)	TG (mmol/l)	Other relevant clinical data
					LE	RE						
1	White Czech	Y	c.527G>A p.(Gly176Glu)	36/M	0.6	0.7	Subepithelial central and mid-peripheral crystals in a ring pattern, minimal corneal arcus	**5.72**	1.58	**3.21**	1.51	
2	White Czech	N	c.289G>A p.(Ala97Thr)	6/F	0.6	0.5	Subepithelial mid-peripheral and mid-stromal crystals in a ring pattern	**4.89**	1.31	2.66	**2.05**	
3	White British	Not known	c.361C>T p.(Leu121Phe)	10/M	0.3	0.3	Mid-stromal central crystals	**5.00**	1.90	UA	1.80	Amblyopia in BE Lamellar keratoplasty in RE and LE at the age of 10 and 12 years
4	White British	Y	c.308C>T p.(Thr103Ile)	54/F	0.5	0.66	Central stromal haze, arcus, few mid-peripheral subepithelial crystals	**UA***	UA	UA	UA	
5	South Asian	Y	c.305G>A p.(Asn102Ser)	37/F	0.66	0.66	Diffuse stromal haze, few subepithelial mid-peripheral crystals	UA	UA	UA	UA	Knee deformities, scoliosis, learning difficulties
6	South Asian	Y	c.305G>A p.(Asn102Ser)	40/F	0.5	0.66	Central stromal haze, arcus, few subepithelial mid-peripheral crystals	UA	UA	UA	UA	

BCVA best corrected visual acuity, *LE* left eye, *RE* right eye, *BE* both eyes, *M* male, *F* female, *Chol* total cholesterol, *HDL* high density lipoprotein, *LDL* low density lipoprotein, *TG* triglycerides, *- elevated but value not known, *UA* unavailable data
Elevated values are shown in bold

Table 2 Primer sequences and condition used for PCR and Sanger sequencing of *UBIAD1* gene

Target	Forward primer	Reverse Primer	Size (bp)	Enzyme	Annealing Temp
exon 1	CCGTCCTTCCTCCTTCCC	AAGCCACCTTTGACATCCCT	700	GoTaqGreen	65 °C
exon 2	CCACCTGCACAGTCTAAGGA	CTGCCAAATCACATTCCTTCCT	689	GoTaqGreen	60 °C

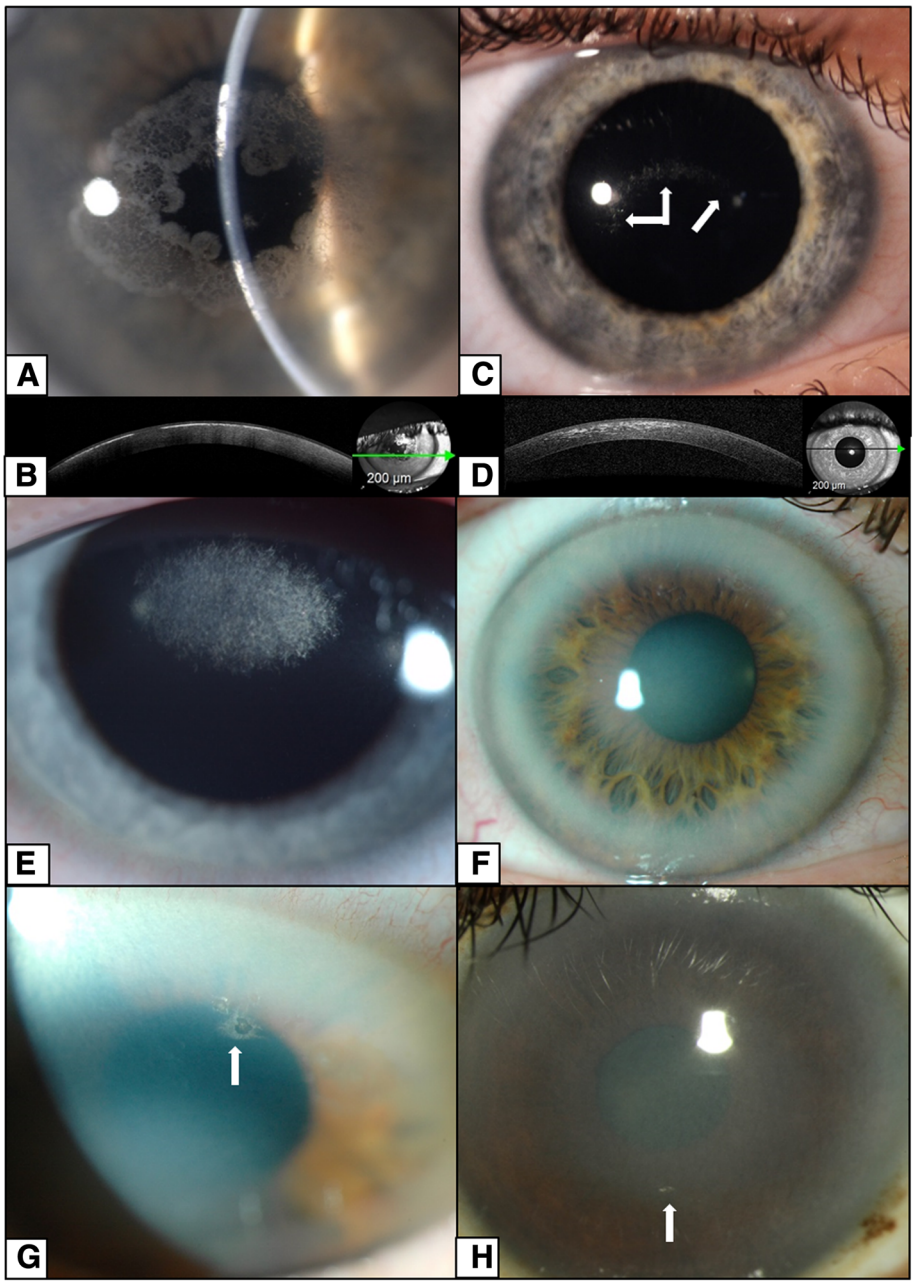

Fig. 1 Corneal phenotype observed in five probands with Schnyder corneal dystrophy. Ring of prominent superficial crystalline deposits in proband 1 aged 36 years (**a**), also documented by SD-OCT as a discontinuous hyper-reflective line beneath the epithelium and within the anterior corneal stroma (**b**). Discrete crystalline deposits in proband 2 aged 8 years (**c**) and more scattered opacities on SD-OCT (**d**). Central mid-stromal crystalline deposits in proband 3 aged 10 years (**e**). Diffuse stromal haze with prominent arcus in proband 4 aged 54 years (**f**, **g**) and proband 5 aged 37 years (**h**). Corneal crystals (arrows) were present in all probands, although in proband 2 they were a minor feature (**b**), corresponding to an early stage of the disease, and in probands 4 and 5 (**g**, **h**) they were present in only a very small area (arrows). All images show findings in the right eye

Results

Clinical, demographic and genotype data for all six probands are summarized in Table 1. There was no family history of SCD in two pedigrees; however, in family 3 the disease status of the proband's mother was unavailable. The corneal phenotypes were diverse and included anterior and mid-stromal crystalline deposits, diffuse stromal haze and arcus lipoides (Fig. 1). There was an incremental accumulation of corneal deposits with age, and the corneal changes were symmetric in all individuals. There were corneal crystals in all probands, although these deposits were minimal in some individuals (Fig. 1 g, h). Corneal crystals were present at slit lamp examination of proband 2 at age 6 years, but neither parent had signs of corneal disease. The patient was re-examined at the age 8 years, when an increase in the corneal crystals was noted (Fig. 1b), but the visual acuity had remained unchanged (Table 1).

Corneal imaging highlighted the presence of crystals. With SD-OCT there were highly reflective deposits in the anterior stroma of probands 1 and 2 (Fig. 1c, d), with confocal microscopy there were bright reflective crystalline deposits identified in the anterior stroma of proband 2 (Fig. 2e). On confocal microscopy small round deposits were also identified in the superficial epithelial cells (Fig. 2a), in and around anterior stromal keratocytes (Fig. 2d) and in mid-stroma (Fig. 2f). The basal epithelial cells, sub-epithelial nerves, posterior stroma and corneal endothelium all appeared normal (Fig. 2b, c, g, h).

Coexisting systemic disease was present in some probands. Proband 5 and her affected sister both had bilateral knee deformities, although their affected mother was normal (Fig. 3). In proband 1 a fasting lipid profile showed high levels of total cholesterol (5.72 mmol/l; normal values in adults < 5.17 mmol/l) [16] and in probands 2 and 3 there was a borderline elevation of total cholesterol to 4.89 mmol/l and 5.00 mmol/l, respectively (normal values in children < 4.40 mmol/l) [17].

A novel c.527G>A; p.(Gly176Glu) variant, predicted to be pathogenic or probably pathogenic by all six bioinformatic tools (Table 3), was identified in proband 1 of Czech origin. The amino acid residue Gly-176 is highly conserved and located in the transmembrane domain of *UBIAD1*, therefore a mutation is likely to disrupt the transmembrane helices and active site [18]. Czech proband 2 harboured a known *UBIAD1* c.289G>A; p.(Ala97Thr) mutation. This variant was absent in both parents, suggesting a de novo origin that was confirmed by paternity testing. The white British probands had previously reported mutations c.361C>T; p.(Leu121Phe) [19] and c.308C>T; p.(Thr103Ile) [6]. Two reportedly unrelated British families of South Asian origin, both harboured a known c.305G>A; p.(Asn102Ser) mutation [19–21]. Pedigrees and segregation of the respective

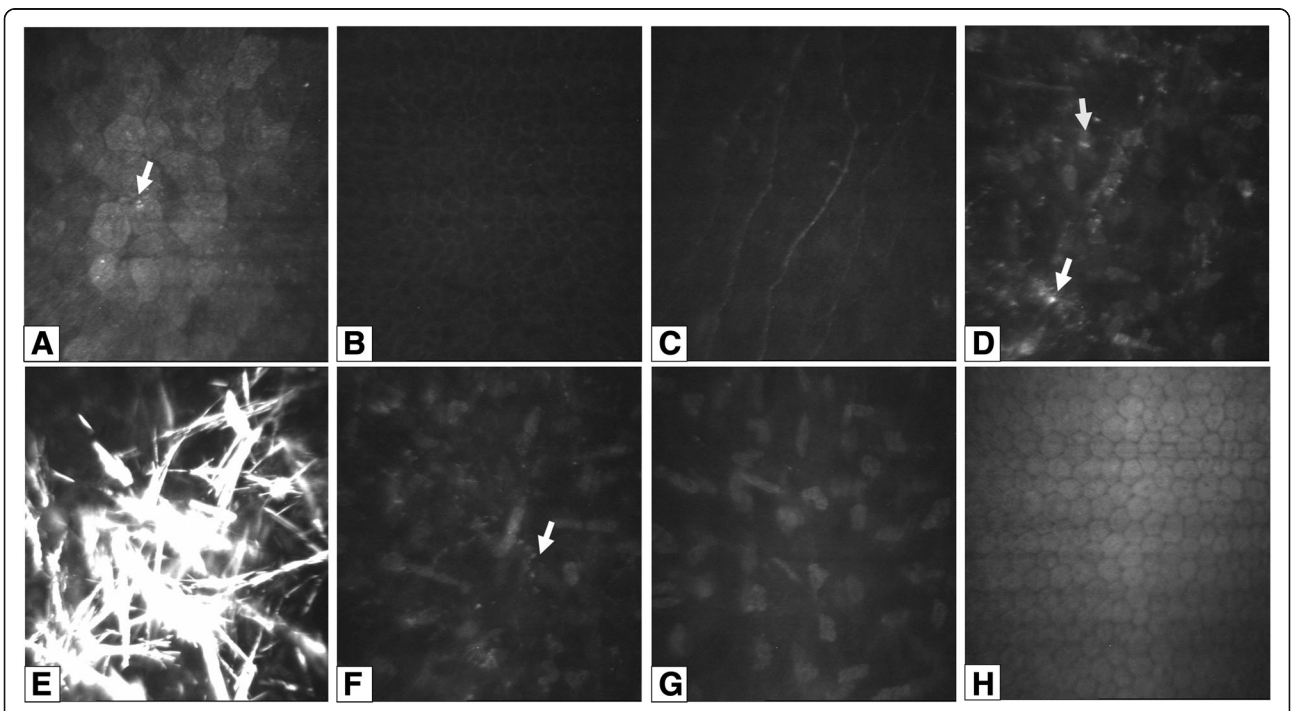

Fig. 2 Corneal confocal microscopy imaging in an 8-year old child with Schnyder corneal dystrophy. Superficial epithelial cells with small round hyperreflective deposits (arrows) in the left eye (**a**). Normal appearance of the basal epithelial cell layer (**b**), and subepithelial nerve plexus in the right eye (**c**). Hyper-reflective deposits within and around keratocytes (arrows) (**d**) and needle-shaped crystals in anterior stroma of the left eye (**e**). Hyper-reflective deposits in mid-stroma in the left eye (**f**), but with unaffected posterior stroma (**g**) and endothelium in the left eye (**h**)

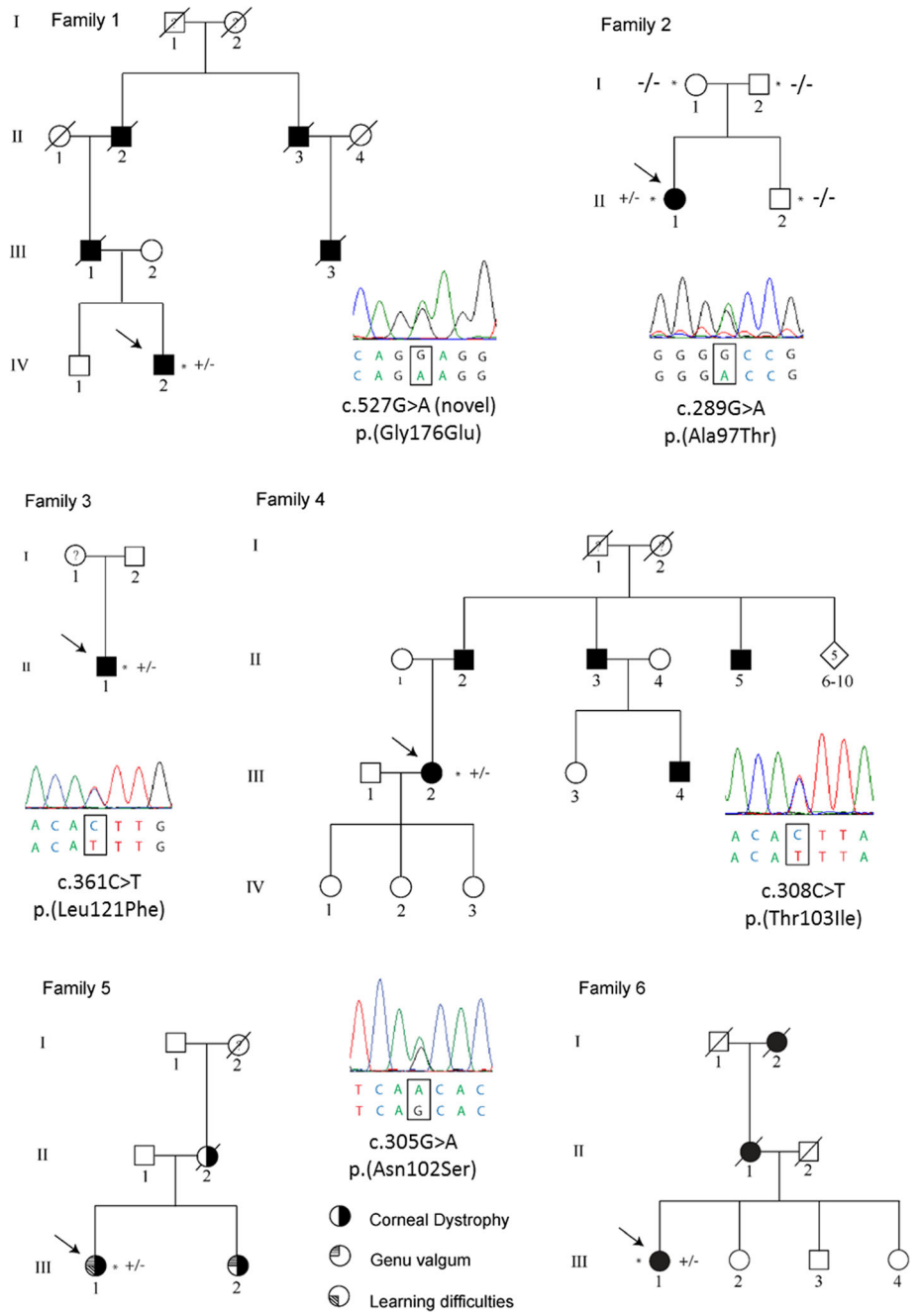

Fig. 3 Pedigrees of the six families with Schnyder corneal dystrophy. Sequence electropherograms of the identified heterozygous mutations in *UBIAD1* are also shown. The mutation arose de novo in family 2. Probands are indicated by an arrow and examined individuals by an asterisk. Mutation status in tested subjects is shown +/− for those who are heterozygous for a mutation in *UBIAD1* and −/− for those who do not carry the pathogenic variant. Individuals known to be affected by Schnyder corneal dystrophy are shown in black, whereas a question mark indicates that the disease status of the individual was unknown

heterozygous *UBIAD1* mutations are shown in Fig. 3. None of the *UBIAD1* pathogenic changes found in the current study were observed in the gnomAD dataset or in the Czech control population. All of the in silico algorithms predicted that the detected mutations were pathogenic or likely pathogenic, except for SNP&GO prediction for previously reported variant c.361C>T; p.(Leu121Phe) [19] (Table 3).

Discussion

In this study we report the phenotype and genotype of six families with SCD. Five different *UBIAD1* mutations were

Table 3 In silico analysis of *UBIAD1* missense variants identified in patients with Schnyder corneal dystrophy in the current study

	MutPred	Polyphen2	PROVEAN	SNP&GO	SIFT	MutationTaster
p.(Ala97Thr)	Disease	Probably damaging	Disease	Disease	Disease	Disease
p.(Leu121Phe)	Disease	Probably damaging	Disease	Benign	Disease	Disease
p.(Thr103Ile)	Possibly damaging	Probably damaging	Disease	Disease	Disease	Disease
p.(Asn102Ser)	Disease	Probably damaging	Disease	Disease	Disease	Disease
p.(Gly176Glu)	Possibly damaging	Probably damaging	Disease	Disease	Disease	Disease

Six different algorithms were used; tolerated and neutral scores are indicated in green as benign; yellow indicates a possibly damaging variant, and red was used for a probably damaging and disease-causing mutation
As for MutPred an overall probability score > 0.5 was considered as possibly damaging and a score > 0.75 was considered as disease-causing. NM_013319.2, NP_037451.1 and ENST00000376810.5 were used as reference sequences

identified in a heterozygous state, of which one, c.527G>A; p.(Gly176Glu), was novel. The youngest proband was found to harbour a de novo c.289G>A; p.(Ala97Thr) mutation, previously identified in an Irish-French family [18]. To the best of our knowledge, this is only the second observation of a spontaneously occurring mutation in an SCD patient [6]. The family history provided by proband 3 also indicated possible de novo occurrence of the identified mutation, but unfortunately this could not be confirmed as parental DNA samples were unavailable.

The c.305G>A; p.(Asn102Ser) mutation, identified in two South Asian probands, is the most frequently occurring *UBIAD1* mutation. It has been reported in several populations including the Czech Republic, Poland, Taiwan and China, supporting the hypothesis that it is a mutation hotspot [19–22]. One white British proband had a c.361C>T; p.(Leu121Phe) mutation, previously observed in three SCD families from the UK, America and Saudi Arabia [19, 23]. The c.308C>T; p.(Thr103Ile) mutation, detected in one white British individual, has previously been described in a proband of Japanese-European descent [6].

The clinical course of SCD is associated with characteristic corneal opacities that increase with age. Initially, central corneal haze and/or crystals are present; this was observed in our youngest proband, who was 6 years old when first examined. Arcus lipoides typically develops in the third decade, followed by mid-peripheral corneal haze in the late fourth decade [24], as documented in the current case series (probands 1, 4–5). Corneal crystals are present in approximately 50% of patients with SCD [2]. Interestingly, crystals were found in all six of our probands, although in two probands the area of crystal deposit was very small. However, the number of individuals we examined is relatively low compared with prior studies [2].

Confocal microscopy has previously been performed in two children with SCD, both at a similar age as our proband 2 [25]. Our findings corroborate observations of accumulation of crystal/reflective material in anterior stroma, both intra- and extracellularly. Interestingly, unlike the previous study, subepithelial nerves appeared normal and we were able to detect tiny reflective deposits in the corneal epithelium. Electron microscopy of corneas with SCD has also documented lipid accumulation inside epithelial cells [26, 27].

The differential diagnosis of crystalline corneal deposition includes monoclonal gammopathy and cystinosis. These conditions should be considered in any individual with corneal crystals who does not have a family history of SCD. Laboratory investigation should be guided by the presence of associated symptoms and patient age.

Dyslipidemia and genu valgum have been reported to be associated with SCD [3, 28]. Three of the six probands in this study had fasting serum lipid testing. Total cholesterol was elevated in one proband and borderline levels were found in the other two probands. Self-reported knee deformities were only present in proband 5 and her sister, although their mother was not affected, which may indicate that other genetic or environmental factors influence the expression of this trait.

Conclusions

SCD should be considered in the differential diagnosis of any unexplained corneal haze and/or crystal deposition, even in the absence of a family history of corneal disease.

Abbreviations

BCVA: Best corrected visual acuity; gnomAD: Genome Aggregation Database; MIM: Mendelian Inheritance in Man; SCD: Schnyder corneal dystrophy; *UBIAD1*: UbiA prenyltransferase domain-containing protein

Acknowledgements

We thank The Czech National Center for Medical Genomics (https://ncmg.cz/en) (LM2015091) for providing ethnically matched population frequency data (project CZ.02.1.01/0.0/0.0/16_013/0001634).

Funding

This work was supported by UNCE 204064 and PROGRES-Q26/LF1 programs of the Charles University, Fight for Sight, Moorfields Eye Charity, Rosetrees Trust, and the National Institute for Health Research Biomedical Research Centre based at Moorfields Eye Hospital NHS Foundation Trust and UCL Institute of Ophthalmology. PS was supported by GAUK 250361/2017, SVV 260367/2017 and PROGRES Q25/LF1/2. GM was supported by MH CZ – DRO, Motol University Hospital, Prague, Czech Republic 00064203. The views expressed are those of the authors and not necessarily those of the NHS, the NIHR or the Department of Health. This work was performed within the framework of ERN-EYE.

Availability of data and materials

The datasets used and/or analysed during the current study are available from the corresponding author on reasonable request.

Authors' contributions

CJE and LD provided molecular genetic analysis, paternity testing was done by AH. PS, GM, SJT and PL contributed in clinical data collection and analysis AJH, SJT and PL contributed to study design and writing. All authors read and approved the final manuscript.

Ethics approval and consent to participate

The study was approved by the Ethics committee of the General University Hospital in Prague (reference no. 151/11 S-IV) or Moorfields Eye Hospital (REC references 13/LO/1084 and 09/H0724/25). Written consent was obtained from all participants or their parents/legal guardians before inclusion.

Consent for publication

Not applicable.

Competing interests

The authors declare that they have no competing interests.

Publisher's Note

Author details

[1]UCL Institute of Ophthalmology, London, UK. [2]Research Unit for Rare Diseases, Department of Paediatrics and Adolescent Medicine, First Faculty of Medicine, Charles University and General University Hospital in Prague, Ke Karlovu 2, 128 08 Prague 2, Czech Republic. [3]Department of Ophthalmology, First Faculty of Medicine, Charles University and General University Hospital in Prague, Prague, Czech Republic. [4]Department of Ophthalmology, Second Faculty of Medicine, Charles University and Motol University Hospital, Prague, Czech Republic. [5]3rd Department of Medicine, Department of Endocrinology and Metabolism, First Faculty of Medicine, Charles University and General University Hospital in Prague, Prague, Czech Republic. [6]Institute of Biology and Human Genetics, First Faculty of Medicine, Charles University and General University Hospital in Prague, Prague, Czech Republic. [7]Moorfields Eye Hospital, London, UK.

Received: 22 January 2018 Accepted: 6 September 2018
Published online: 17 September 2018

References

1. Weiss JS, Kruth HS, Kuivaniemi H, Tromp G, White PS, Winters RS, et al. Mutations in the *UBIAD1* gene on chromosome short arm 1, region 36, cause Schnyder crystalline corneal dystrophy. Invest Ophthalmol Vis Sci. 2007;48:5007–12.
2. Weiss JS, Moller HU, Aldave AJ, Seitz B, Bredrup C, Kivelä T, et al. IC3D classification of corneal dystrophies--edition 2. Cornea. 2015;34:117–59.
3. Hoang-Xuan T, Pouliquen Y, Gasteau J. Schnyder's crystalline dystrophy. II. Association with genu valgum. J Fr Ophtalmol. 1985;8:743–7.
4. Orr A, Dube MP, Marcadier J, Jiang H, Federico A, George S, et al. Mutations in the *UBIAD1* gene, encoding a potential prenyltransferase, are causal for Schnyder crystalline corneal dystrophy. PLoS One. 2007;2:e685.
5. Li W. Bringing bioactive compounds into membranes: the UbiA superfamily of intramembrane aromatic prenyltransferases. Trends Biochem Sci. 2016;41:356–70.
6. Lin BR, Frausto RF, Vo RC, Chiu SY, Chen JL, Aldave AJ. Identification of the first de novo *UBIAD1* gene mutation associated with Schnyder corneal dystrophy. J Ophthalmol. 2016;2016:1968493.
7. Mahelkova G, Filous A, Odehnal M, Cendelin J. Corneal changes assessed using confocal microscopy in patient with unilateral buphthalmos. Invest Ophthalmol Vis Sci. 2013;54:4048–53.
8. Choi Y, Sims GE, Murphy S, Miller JR, Chan AP. Predicting the functional effect of amino acid substitutions and indels. PLoS One. 2012;7:e46688.
9. Calabrese R, Capriotti E, Fariselli P, Martelli PL, Casadio R. Functional annotations improve the predictive score of human disease-related mutations in proteins. Hum Mutat. 2009;30:1237–44.
10. Li B, Krishnan VG, Mort ME, Xin F, Kamati KK, Cooper DN, et al. Automated inference of molecular mechanisms of disease from amino acid substitutions. Bioinformatics. 2009;25:2744–50.
11. Kumar P, Henikoff S, Ng PC. Predicting the effects of coding non-synonymous variants on protein function using the SIFT algorithm. Nat Protoc. 2009;4:1073–81.
12. Adzhubei IA, Schmidt S, Peshkin L, Ramensky VE, Gerasimova A, Bork P, et al. A method and server for predicting damaging missense mutations. Nat Methods. 2010;7:248–9.
13. Schwarz JM, Rodelsperger C, Schuelke M, Seelow D. MutationTaster evaluates disease-causing potential of sequence alterations. Nat Methods. 2010;7:575–6.
14. Evans CJ, Liskova P, Dudakova L, Hrabcikova P, Horinek A, Jirsova K, et al. Identification of six novel mutation in *ZEB1* and description of the associated phenotypes in patients with posterior polymorphous corneal dystrophy 3. Ann Hum Genet. 2015;79:1–9.
15. Lek M, Karczewski KJ, Minikel EV, Samocha KE, Banks E, Fennell T, et al. Analysis of protein-coding genetic variation in 60,706 humans. Nature. 2016;536:285–91.
16. Expert panel on detection, evaluation, and treatment of high blood cholesterol in adults. Executive summary of the third report of the National Cholesterol Education Program (NCEP) expert panel on detection, evaluation, and treatment of high blood cholesterol in adults (adult treatment panel III). JAMA. 2001;285:2486–97.
17. American Academy of Pediatrics. Committee on nutrition. Cholesterol in childhood. Pediatrics. 1998;101:141–7.
18. Nickerson ML, Bosley AD, Weiss JS, Kostiha BN, Hirota Y, Brandt W, et al. The UBIAD1 prenyltransferase links menaquinone-4 [corrected] synthesis to cholesterol metabolic enzymes. Hum Mutat. 2013;34:317–29.
19. Weiss JS, Kruth HS, Kuivaniemi H, Tromp G, Karkera J, Mahurkar S, et al. Genetic analysis of 14 families with Schnyder crystalline corneal dystrophy reveals clues to UBIAD1 protein function. Am J Med Genet A. 2008;146A:271–83.
20. Du C, Li Y, Dai L, Gong L, Han C. A mutation in the *UBIAD1* gene in a Han Chinese family with Schnyder corneal dystrophy. Mol Vis. 2011;17:2685–92.
21. Nickerson ML, Kostiha BN, Brandt W, Fredericks W, Xu KP, Yu FS, et al. *UBIAD1* mutation alters a mitochondrial prenyltransferase to cause Schnyder corneal dystrophy. PLoS One. 2010;5:e10760.
22. Nowinska AK, Wylegala E, Teper S, Lyssek-Boron A, Aragona P, Roszkowska AM, et al. Phenotype-genotype correlation in patients with Schnyder corneal dystrophy. Cornea. 2014;33:497–503.
23. Al-Ghadeer H, Mohamed JY, Khan AO. Schnyder corneal dystrophy in a Saudi Arabian family with heterozygous *UBIAD1* mutation (p.L121F). Middle East Afr J Ophthalmol. 2011;18:61–4.
24. Weiss JS, Khemichian AJ. Differential diagnosis of Schnyder corneal dystrophy. Dev Ophthalmol. 2011;48:67–96.
25. Vesaluoma MH, Linna TU, Sankila EM, Weiss JS, Tervo TM. *In vivo* confocal microscopy of a family with Schnyder crystalline corneal dystrophy. Ophthalmology. 1999;106:944–51.
26. Rodrigues MM, Kruth HS, Krachmer JH, Willis R. Unesterified cholesterol in Schnyder's corneal crystalline dystrophy. Am J Ophthalmol. 1987;104:157–63.
27. Rodrigues MM, Kruth HS, Krachmer JH, et al. Cholesterol localization in ultrathin frozen sections in Schnyder's corneal crystalline dystrophy. Am J Ophthalmol. 1990;110:513–7.
28. Kohnen T, Pelton RW, Jones DB. Schnyder corneal dystrophy and juvenile, systemic hypercholesteremia. Klin Monatsbl Augenheilkd. 1997;211:135–7.

Příloha 3. Coincidental occurrence of Schnyder corneal dystrophy and posterior polymorphous corneal dystrophy type 3

Coincidental Occurrence of Schnyder Corneal Dystrophy and Posterior Polymorphous Corneal Dystrophy Type 3

Lubica Dudakova, PhD, Pavlina Skalicka, MD,*† Alice E. Davidson, PhD,‡ and Petra Liskova, MD, PhD*†‡*

Purpose: To report a simultaneous occurrence of 2 rare corneal dystrophies.

Methods: A 30-year-old man with a family history of posterior polymorphous corneal dystrophy type 3 (PPCD3) was invited for ophthalmic examination. Sanger sequencing of the coding regions and intron/exon boundaries of disease-associated genes, *ZEB1* and *UBIAD1*, was performed.

Results: The clinical findings suggested co-occurrence of PPCD3 and Schnyder corneal dystrophy in the proband. This dual diagnosis was supported by genetic findings. He was identified to carry a previously reported heterozygous nonsense mutation in *ZEB1*: c.2157C>G; p.(Tyr719*), and a novel heterozygous missense mutation in *UBIAD1*: c.569T>C; p.(Ile190Thr). The mother of the proband only carried c.2157C>G in *ZEB1*, and slit-lamp examination of her corneas showed endothelial lesions characteristic of PPCD3. The sister of the proband carried c.569T>C in *UBIAD1* and had corneal crystal deposition in her anterior stroma consistent with the diagnosis of Schnyder corneal dystrophy.

Conclusions: This case illustrates the coincidental occurrence of 2 rare and genetically distinct corneal dystrophies in a single patient. Furthermore, it highlights the need to perform comprehensive phenotyping in combination with appropriate genetic diagnostic testing to achieve an accurate diagnosis.

Received for publication December 17, 2018; revision received February 8, 2019; accepted February 8, 2019.

From the *Research Unit for Rare Diseases; First Faculty of Medicine, Charles University and General University Hospital in Prague, Prague, Czech Republic; First Faculty of Medicine, Charles University, Prague, Czech Republic; †Department of Ophthalmology, First Faculty of Medicine, Charles University and General University Hospital in Prague, Prague, Czech Republic; and ‡UCL Institute of Ophthalmology, London, United Kingdom.

Supported by GACR 17-12355S. Institutional support was provided by UNCE 204064 and PROGRES Q26 programs of Charles University. P. Skalicka was supported by GAUK 250361/2017 and SVV 260367/2017. A. E. Davidson is a Fight for Sight Early Career Investigator.

The authors have no conflicts of interest to disclose.

Supplemental digital content is available for this article. Direct URL citations appear in the printed text and are provided in the HTML and PDF versions of this article on the journal's Web site (www.corneajrnl.com).

Correspondence: Petra Liskova, MD, PhD, Research Unit for Rare Diseases, Department of Pediatrics and Adolescent Medicine, General University Hospital in Prague and First Faculty of Medicine, Charles University, Ke Karlovu 2, 128 08 Prague, Czech Republic (e-mail: petra.liskova@lf1.cuni.cz).

Key Words: posterior polymorphous corneal dystrophy, Schnyder corneal dystrophy, coincidental findings, *ZEB1*, *UBIAD1*

(*Cornea* 2019;00:1–3)

Corneal dystrophies comprise a group of rare phenotypically and genetically heterogeneous disorders. To date, mutations in 14 distinct genes have been reported to cause monogenic corneal dystrophies.[1–4]

Schnyder corneal dystrophy (SCD; OMIM #121800) is an autosomal dominant disease affecting the corneal stroma. Clinical findings include corneal crystals, stromal haze, and arcus.[5,6] In some patients, hyperlipidemia is present.[1] Posterior polymorphous corneal dystrophy (PPCD) is also an autosomal dominant disease manifesting predominantly as vesicles, bands, and opacities at the level of the corneal endothelium and Descemet membrane.[1] Three genes, *OVOL2*, *ZEB1*, and *GRHL2*, are known to be implicated in pathogenesis of PPCD1: PPCD type 1 (MIM #122000), type 3 (MIM #609141), and type 4 (MIM #618031), respectively.[1–3]

CASE REPORT

The study was approved by the Institutional Ethics Committee of the General University Hospital in Prague (reference no. 151/11 S-IV) and adhered to the Declaration of Helsinki. Informed consent was signed by the participants prior to the investigation being initiated. A 30-year-old man was invited for clinical ophthalmic review because of a family history of PPCD type 3 (PPCD3). His great-aunt had previously been shown to carry a heterozygous *ZEB1* nonsense mutation: c.2157C>G; p.(Tyr719*) (Fig. 1E).[7]

The patient reported poor vision in both eyes since childhood with no improvement on spectacle correction. His best-corrected visual acuity was 0.6 in the right eye and 0.9 in the left eye (Snellen charts). Because of a family history of PPCD3, the presence of corneal endothelial disease was expected. Slit-lamp examination revealed, however, not only mild changes of the posterior corneal layers but also stromal crystals in both eyes and partial arcus in the right eye (Figs. 1A–D) consistent with the diagnosis of SCD.

The patient was also found to have a borderline total cholesterol level (5.08 mmol/L, reference 2.9–5.0 mmol/L) and a slightly increased LDL cholesterol level (3.17 mmol/L, reference 1.2–3.0 mmol/L).

Direct sequencing confirmed the presence of the previously reported *ZEB1* nonsense mutation in the heterozygous state (Fig. 1E).[7] Screening of the *UBIAD1* gene identified a further novel heterozygous missense variant in the *UBIAD1* gene: c.569T>C; p.(Ile190Thr). This variant is predicted to be pathogenic by

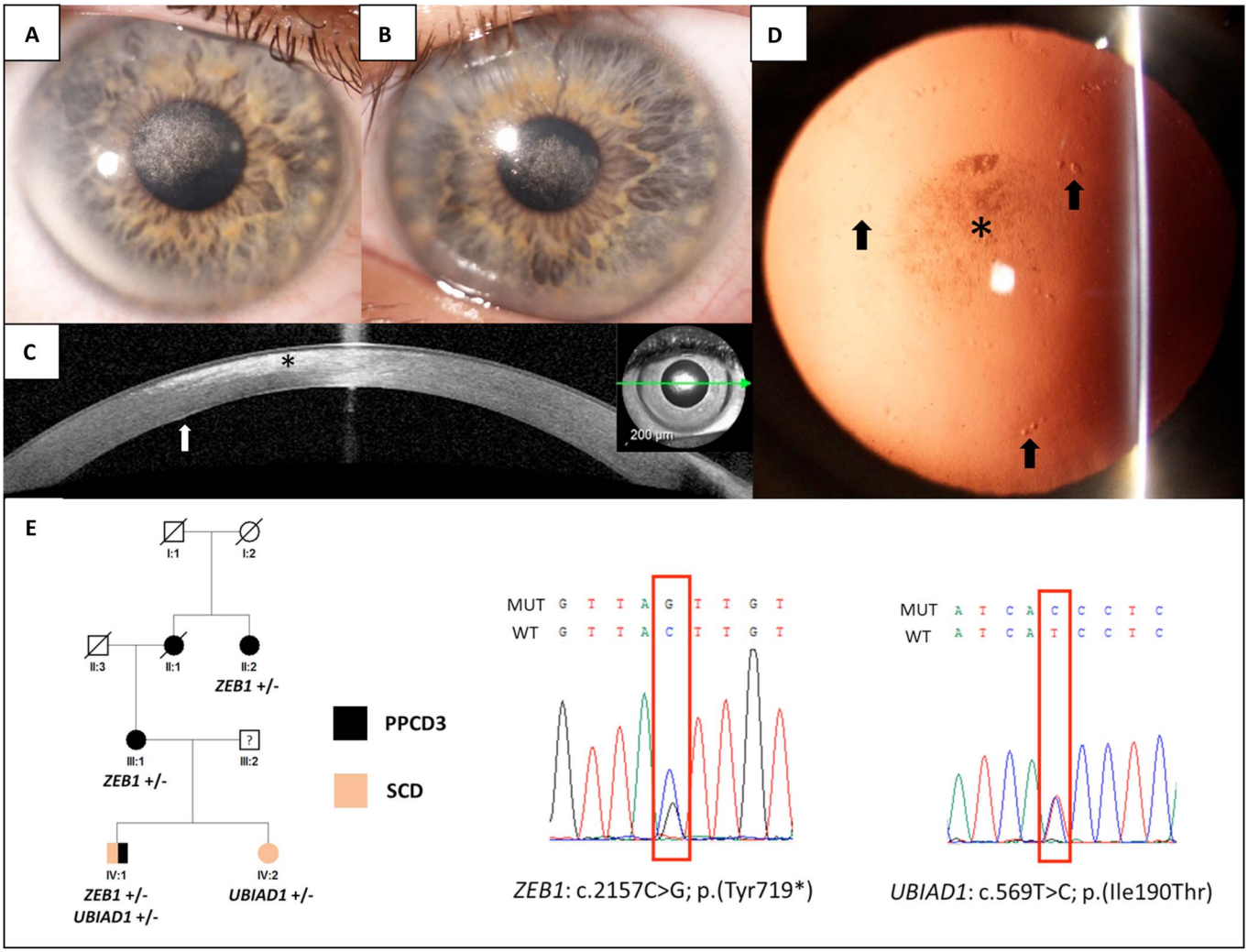

FIGURE 1. Results of genetic testing and corneal findings in an individual affected simultaneously with PPCD3 and SCD. Right (A) and (B) left corneal photographs under direct illumination, note bilateral crystalline deposits and partial arcus lipoides in the right eye. C, Spectral domain optical coherence imaging in the right eye (the position of the cross-section is indicated by the green arrow) showing stromal opacification due to crystals, very mild increased reflexivity, and unevenness of the posterior corneal surface (arrow). D, Right cornea in retroillumination. Lesions typical for PPCD3 are marked with arrows, and corneal deposits characteristic for SCD are indicated by an asterisk. E, Pedigree of the family showing mutational status of the tested subjects and sequence chromatograms of the mutations detected in *ZEB1* (reference sequence NM_030751.5) and *UBIAD1* (NM_013319.2).

PROVEAN, MutationTaster, MutPred2, and SIFT and absent from 141,456 unrelated individuals reported in gnomAD (see Supplemental Table 1, Supplemental Digital Content 1, http://links.lww.com/ICO/A771).

Clinical examination of the asymptomatic mother aged 53 years revealed bilateral opacities of the posterior corneal surface characteristic of PPCD3 (see Supplemental Figure 1A-1B, Supplemental Digital Content 1, http://links.lww.com/ICO/A771). Best corrected visual acuity (BVCA) was 1.0 bilaterally. The sister of the proband aged 29 years was also asymptomatic. Her BCVA was 0.9 and 1.0 in the right and left eyes, respectively. Discrete paracentral anterior stromal crystals and incipient arcus lipoides formation in the right eye were found to be consistent with a diagnosis of SCD (see Supplemental Figure 1C-1D, Supplemental Digital Content 1, http://links.lww.com/ICO/A771). The mother was identified to carry the same *ZEB1* nonsense mutation as her son p.(Tyr719*). The diagnosis of SCD in the sister was supported by the presence of the same heterozygous *UBIAD1* missense mutation as in her brother: p.(Ile190Thr) (Fig. 1E). Because the mother of the proband did not carry the *UBIAD1* variant, it was likely inherited from the sibling's father, who was unavailable for clinical examination and genetic testing.

DISCUSSION

In this report, we present a patient coincidentally affected by 2 distinct and rare corneal disorders, SCD and PPCD3. Both diagnoses are supported by molecular genetic investigation leading to identification of heterozygous pathogenic variants in *ZEB1* and *UBIAD1*. To the best or our

knowledge, this is the first report of these distinct and rare monogenic corneal dystrophies occurring in the same individual.

Including this study, in the Czech population, SCD has an estimated prevalence of at least 1 in 1,500,000[5,6] and PPCD3 of at least 1 in 340,000 (unpublished data).[7–10] The coincidental occurrence of these 2 rare and genetically distinct corneal dystrophies presenting in a single patient is therefore extremely low (i in 5.1×10^{11}).

Our case highlights the importance of considering a full family history in combination with accurate phenotyping information to guide the use of appropriate genetic diagnostic testing. We also expand the spectrum of disease-causing mutations associated with SCD.

REFERENCES

1. Weiss JS, Møller HU, Aldave AJ, et al. IC3D classification of corneal dystrophies: edition 2. *Cornea.* 2015;34:117–159.
2. Davidson AE, Liskova P, Evans CJ, et al. Autosomal-dominant corneal endothelial dystrophies CHED1 and PPCD1 are allelic disorders caused by non-coding mutations in the promoter of OVOL2. *Am J Hum Genet.* 2016;98:75–89.
3. Liskova P, Dudakova L, Evans CJ, et al. Ectopic GRHL2 expression due to non-coding mutations promotes cell state transition and causes posterior polymorphous corneal dystrophy 4. *Am J Hum Genet.* 2018;102:447–459.
4. Jonsson F, Byström B, Davidson AE, et al. Mutations in collagen, type XVII, alpha 1 (COL17A1) cause epithelial recurrent erosion dystrophy (ERED). *Hum Mutat.* 2015;36:463–473.
5. Evans CJ, Dudakova L, Skalicka P, et al. Schnyder corneal dystrophy and associated phenotypes caused by novel and recurrent mutations in the UBIAD1 gene. *BMC Ophthalmol.* 2018;18:250.
6. Weiss JS. Visual morbidity in thirty-four families with Schnyder crystalline corneal dystrophy (an American Ophthalmological Society thesis). *Trans Am Ophthalmol Soc.* 2007;105:616–648.
7. Liskova P, Tuft SJ, Gwilliam R, et al. Novel mutations in the ZEB1 gene identified in Czech and British patients with posterior polymorphous corneal dystrophy. *Hum Mutat.* 2007;28:638.
8. Evans CJ, Liskova P, Dudakova L, et al. Identification of six novel mutations in ZEB1 and description of the associated phenotypes in patients with posterior polymorphous corneal dystrophy 3. *Ann Hum Genet.* 2015;79:1–9.
9. Liskova P, Evans CJ, Davidson AE, et al. Heterozygous deletions at the ZEB1 locus verify haploinsufficiency as the mechanism of disease for posterior polymorphous corneal dystrophy type 3. *Eur J Hum Genet.* 2016;24:985–991.
10. Liskova P, Filipec M, Merjava S, et al. Variable ocular phenotypes of posterior polymorphous corneal dystrophy caused by mutations in the ZEB1 gene. *Ophthalmic Genet.* 2010;31:230–234.

Příloha 4: Antisense Therapy for a Common Corneal Dystrophy Ameliorates *TCF4* Repeat Expansion-Mediated Toxicity

ARTICLE

Antisense Therapy for a Common Corneal Dystrophy Ameliorates *TCF4* Repeat Expansion-Mediated Toxicity

Christina Zarouchlioti,[1,8] Beatriz Sanchez-Pintado,[1,8] Nathaniel J. Hafford Tear,[1,8] Pontus Klein,[2] Petra Liskova,[3,4] Kalyan Dulla,[2] Ma'ayan Semo,[1] Anthony A. Vugler,[1] Kirithika Muthusamy,[1,5] Lubica Dudakova,[3] Hannah J. Levis,[6] Pavlina Skalicka,[3,4] Pirro Hysi,[7] Michael E. Cheetham,[1] Stephen J. Tuft,[1,5] Peter Adamson,[2,9] Alison J. Hardcastle,[1,9] and Alice E. Davidson[1,9,*]

Fuchs endothelial corneal dystrophy (FECD) is a common disease for which corneal transplantation is the only treatment option in advanced stages, and alternative treatment strategies are urgently required. Expansion (≥50 copies) of a non-coding trinucleotide repeat in *TCF4* confers >76-fold risk for FECD in our large cohort of affected individuals. An FECD subject-derived corneal endothelial cell (CEC) model was developed to probe disease mechanism and investigate therapeutic approaches. The CEC model demonstrated that the repeat expansion leads to nuclear RNA foci, with the sequestration of splicing factor proteins (MBNL1 and MBNL2) to the foci and altered mRNA processing. Antisense oligonucleotide (ASO) treatment led to a significant reduction in the incidence of nuclear foci, MBNL1 recruitment to the foci, and downstream aberrant splicing events, suggesting functional rescue. This proof-of-concept study highlights the potential of a targeted ASO therapy to treat the accessible and tractable corneal tissue affected by this repeat expansion-mediated disease.

Introduction

Fuchs endothelial corneal dystrophy (FECD [MIM: 613267]) is a common, degenerative, age-related condition that usually presents during the fifth to sixth decade. The disease primarily affects the posterior cornea with the hallmark being the formation of focal excrescences of Descemet membrane (DM) termed "guttae." Isolated guttae are common in the elderly and a case definition for FECD usually requires that the guttae are confluent. When assessed with specular microscopy, the prevalence of guttae is higher in white (11.2% >55 years) than East Asian (5.5% >50 years) populations and higher in females (5.5%–11%) than males (1.5%–7%).[1,2] An estimate of the prevalence of confluent guttae in individuals of white or black ethnicity >50 years with assessment by slit-lamp biomicroscopy reported a figure of 4.5%.[3] Confluent guttae can be associated with a loss of corneal endothelial cell density to a critical stage when the remaining endothelium is unable to maintain appropriate stromal dehydration leading to fluid accumulation, painful epithelial bullae, and progressive corneal clouding reducing visual acuity.[4–6] Early-stage disease is typically managed with topical hypertonic saline to reduce symptoms, such as corneal swelling, but surgical intervention is currently the only treatment option available to individuals with advanced disease to restore bilateral vision and prevent blindness.[6] Full or partial keratoplasty are invasive procedures that rely upon specialist facilities and the availability of healthy donor material, of which there is a global shortage.[7] These issues, coupled with the global aging population, highlight the need for alternative and effective treatment strategies.

In 2010, a landmark FECD genome-wide association study (GWAS) identified a strong association with common non-coding variants located within the transcription factor encoding gene *TCF4* (MIM: 602272). The risk allele of the most highly associated SNP (rs613872) conferred a remarkably high odds ratio (OR) of 5.5 for individuals carrying one copy or an OR of 30 for individuals with two copies.[8] Subsequently, the SNP rs613872 was found to be in linkage disequilibrium with CTG18.1, a CTG repeat expansion situated within an intronic region of *TCF4*, connecting the initial GWAS signal with a putative functional variant.[9] This association has now been replicated in a range of ethnically distinct cohorts, supporting the hypothesis that expanded copies of the CTG18.1 repeat are associated with FECD.[10–14]

Transcripts containing expanded copies of the CUG repeat accumulate as discrete nuclear RNA foci within tissue derived from individuals affected with FECD;[15] similar to other repeat expansion-associated disorders, such as myotonic dystrophy type 1 (DM1 [MIM: 160900]), which is caused by an identical CTG repeat expansion located within the 3′ untranslated region (UTR) of *DMPK* (MIM: 605377).[16,17] DM1 pathogenesis has largely been attributed to these RNA aggregates sequestering RNA-splicing

[1]UCL Institute of Ophthalmology, London ECIV 9EL, UK; [2]ProQR Therapeutics, Zernikedreef 9, 2333 CK Leiden, the Netherlands; [3]Research Unit for Rare Diseases, Department of Paediatrics and Adolescent Medicine, First Faculty of Medicine, Charles University and General University Hospital in Prague, Ke Karlovu 2, Prague 128 08, Czech Republic; [4]Department of Ophthalmology, First Faculty of Medicine, Charles University and General University Hospital in Prague, U nemocnice 2, Prague, Czech Republic; [5]Moorfields Eye Hospital, London EC1V 2PD, UK; [6]Institute of Aging and Chronic Disease, University of Liverpool, Liverpool L7 8TX, UK; [7]Department of Ophthalmology and Twin Research, King's College London, London SE1 7EH, UK
[8]These authors contributed equally to this work
[9]These authors contributed equally to this work
*Correspondence: alice.davidson@ucl.ac.uk
https://doi.org/10.1016/j.ajhg.2018.02.010.

Table 1. Summary of CTG18.1 Genotyping Data in the FECD Cohort

	N	NE/NE	E/NE	E/E	≥1 E
Total FECD cohort (mean age = 69)	450	23.6% (106/450)	72.4% (326/450)	4.0% (18/450)	76.4% (344/450)
Females (mean age = 70)	265	27.2% (72/265)	69.1% (183/265)	3.8% (10/265)	72.8% (193/265)
Males (mean age = 68)	185	18.4% (34/185)	77.3% (143/185)	4.3% (8/185)	81.6% (151/185)
Subjects recruited at MEH	318	25.5% (81/318)	70.1% (223/318)	4.4% (14/318)	74.5% (237/318)
White (82.4%)	260	22.7% (59/260)	71.9% (187/260)	5.4% (14/260)	77.3% (201/260)
Other (17.6%)	58	37.9% (22/58)	62.1% (36/58)	0.0% (0/58)	62.1% (36/58)
Subjects recruited at GUH (white)	132	18.9% (25/132)	78.0% (103/132)	3.0% (4/132)	81.1% (107/132)
AMD cohort (mean age = 78)	550	95.8% (527/550)	4.2% (23/550)	0.0% (0/550)	4.2% (23/550)
Females (mean age = 78)	356	96.1% (342/356)	3.9% (14/356)	0.0% (0/356)	3.9% (14/356)
Males (mean age = 78)	194	95.4% (185/194)	4.6% (9/194)	0.0% (0/194)	4.6% (9/194)

Expanded alleles are defined as ≥50 CTG repeats. Abbreviations are as follows: NE, non-expanded CTG18.1 allele; E, expanded CTG18.1 allele; MEH, Moorfields Eye Hospital; GUH, General University Hospital in Prague.

factors, including MBNL1 and MBNL2,[18–20] leading to a functional deficiency of these proteins and subsequent global disruption of splicing.[21,22]

Studies using DM1 cell and animal models have shown that targeting the CTG expansion within *DMPK* using an antisense oligonucleotide (ASO) approach leads to a reduction in RNA foci and downstream markers of toxicity.[23,24] To determine whether similar strategies could be effective for CTG18.1-associated FECD and to translate FECD therapies into the clinic, appropriate FECD disease models are essential. Given the lack of animal models for FECD, coupled with the general poor association of animal model phenotypes with human complex disease, corneal endothelial cell (CEC) cultures derived from affected individuals offer an ideal opportunity to probe disease mechanism and investigate therapeutic approaches.

Here we demonstrate that the *TCF4* CTG18.1 expansion confers a highly significant disease risk in our large cohort of individuals affected by FECD. Our data define trinucleotide repeat size as a fundamental driver of RNA foci incidence in CECs. We identify downstream markers of RNA toxicity and assess the effectiveness of a targeted ASO treatment strategy for CTG18.1 expansion-associated FECD.

Material and Methods

Subject Recruitment and Phenotyping

The study followed the tenets of the Declaration of Helsinki and was approved by Moorfields Eye Hospital (MEH) ethics committee (REC reference 09/H0724/25) and the Ethics committee of the GUH, Czech Republic. Written informed consent was received from all participants included in this study. A total of 450 individuals (185 males and 265 females; mean cohort age, 69 years) were recruited to the study. Participants either had clinical signs of FECD (numerous corneal guttae on slit-lamp biomicroscopy) or had corneal transplantation surgery (either penetrating or endothelial keratoplasty) for FECD. The cohort was stratified based on gender and ethnicity (Table 1). For control purposes, DNA samples collected from 550 white European individuals with AMD were used in the study (194 males and 356 females; mean cohort age, 78 years) (Table 1). All risk calculations presented were performed using the white European samples only (392 FECD samples and 550 AMD samples).

TCF4 Expansion Genotyping

Genomic DNA was extracted from whole blood using conventional methodologies. A short tandem repeat (STR) assay was performed to genotype the CTG18.1 allele, in accordance with methods previously published by Wieben et al.[9] In brief, genomic DNA was amplified using a 5′FAM conjugated primer (5′-CAGATGAGTTTGGTGTAAGAT-3′) and an unlabeled reverse primer (5′-ACAAGCAGAAAGGGGGCTGCAA-3′). Post PCR product separation was performed on the ABI 3730 Electrophoresis 96 capillary DNA analyzer (Applied Biosystems). Data analysis was performed using GeneMarker software (SoftGenetics).

Collection of Endothelial Tissue Samples

Tissue derived from individuals affected by FECD was removed during endothelial keratoplasty surgery performed at MEH. As part of the procedure, 8 mm diameter discs of DM with attached endothelial cells were removed from the posterior surface of the central cornea. Control tissue, considered suitable for transplantation, was obtained from corneo-scleral rims stored in OptiSol-GS (Bausch & Lomb). All prepared tissue was stored in Lebovitz L15 Media (Life Technologies) supplemented with 1% antibiotic/antimycotic prior to being processed in the laboratory.

Primary CEC Culture

CECs retrieved from control tissue and from subjects diagnosed with FECD were cultured in accordance with a dual media approach described by Peh et al.[25] In brief, donated tissue comprising DM with attached endothelial cells was incubated in 0.2% collagenase type I powder in M5 media (Life Technologies) for 3 hr at 37°C to dislodge CECs from the DM. CECs were centrifuged and re-suspended again in M5 media to allow for cell adherence and stabilization. Media M5 contained Human Endothelial-SFM (Life Technologies) supplemented with 5% FBS,

1% antibiotic/antimycotic, and 0.1% selective ROCK inhibitor Y-27632 (AdooQ BioScience). Cells were seeded in cell culture ware pre-coated with FNC coating mixture (United States Biological). After 24 hr, to promote proliferation, culture media was replaced with M4 media containing Ham's F-12 Nutrient Mix GlutaMAX Supplement (Life Technologies)/Medium 199 GlutaMAX Supplement (Life Technologies), 20 μg/mL ascorbic acid, 1% insulin-transferrin-selenium (Life Technologies), 5% FBS, 1% antibiotic/antimycotic, 10 ng/mL bFGF (R&D Systems), and 0.1% selective ROCK inhibitor Y-27632 (AdooQ BioScience). Throughout culture, cells were kept in an incubator at 37°C, 5% CO_2 and medium was refreshed every 48 hr until the cells showed appropriate confluence for experimentation or passage. Cells were passaged a maximum of two times prior to any experiment being performed.

Generation of Fibroblast Cell Lines from Dermal Skin Biopsies

Primary fibroblast lines were generated as described by Carter et al.[26] Briefly, 5 mm skin biopsies were obtained under aseptic conditions and were shortly stored in DMEM/F-12, GlutaMAX (Life Technologies) supplemented with 10% FBS and 1% penicillin/streptomycin at 4°C until being processed. After the epidermal layer was removed, the biopsy samples were dissected into small pieces which were then immobilized under a glass coverslip for 24 hr (37°C, 5% CO_2). Fresh medium was added the following day and renewed every 2–3 days. At ~70% confluence, the cultures were passed through a cell strainer to remove pieces of tissue and finally seeded in T25 flasks.

Immunocytochemistry (ICC)

CECs grown on glass coverslips were fixed with 4% paraformaldehyde (PFA) in PBS for 10 min. After washing with PBS, cells were permeabilized with 0.1% Triton X-100 for 10 min and non-specific binding sites were blocked in PBS with 3% BSA and 10% donkey serum for 1 hr. The CECs were incubated with primary antibodies, diluted to the appropriate concentration (Table S1), in blocking solution overnight at 4°C. For MBNL1[27] and MBNL2 antibodies, 0.5% Triton X-100 was incorporated in the blocking solution instead, omitting the previous permeabilization step, and proceeding normally after. After washing with PBS, CECs were incubated in donkey fluorophore-bound secondary antibodies (Alexa Fluor 488, anti-mouse or anti-rabbit; Invitrogen) diluted 1:1,000 in 3% BSA PBS for 1 hr at room temperature. Cells were washed again and incubated in DAPI stain (1:5,000 dilution; Sigma) for 2 min. Finally, coverslips were mounted onto microscope slides using Fluorescent Mounting Medium (Dako). Appropriate negative controls were carried out by performing the same protocol without the addition of primary antibodies. Images were taken using a confocal Zeiss 700 microscope and processed with the Zeiss software.

ASO Transfections

CECs were transfected with ASOs complexed with DarmaFECT 4 transfection reagent (Dharmacon), in accordance with the manufacturer's instructions. The following ASOs were used; Control ASO: 5′-mG*mG*mU*mG*mG*mA*mU*mC*mA*mC*mG*mA*mG*mU*mU*mC*mA-3′, $(CAG)_7$ therapeutic oligo: 5′-mC*mA*mG*mC*mA*mG*mC*mA*mG*mC*mA*mG*mC*mA*mG*mC*mA*mG*mC*mA*mG*mC*mA*mG-3′. m denotes 2′-O-Methyl ribonucleotide, * denotes phosphthioate linkages.

A final oligo concentration of 200 nM was selected for all experiments based on optimization data presented in Figure S1. All ASO treatment experiments were performed 24 hr post transfection.

Fluorescence *In Situ* Hybridization (FISH)

CECs grown in chamber slides were washed once with PBS and fixed with 4% PFA in PBS for 10 min at room temperature. Once fixed, cells were washed twice with PBS and permeabilized with 70% ethanol for 15 min at room temperature. Cells were rehydrated using a 50% formamide and 2 × SSC buffer for 5 min at room temperature. Cells were incubated overnight at 37°C in hybridization solution containing 50% formamide, 2 × SSC, 10% dextran sulfate, 0.2% BSA, 1 mg/mL yeast tRNA, and 12 μg/mL of Cy3-$(CAG)_7$ probe. Cells were washed thoroughly using 50% formamide in 2 × SSC followed by 50% formamide in 0.1 × SSC before being stained with DAPI (1:5,000 dilution; Sigma) for 2 min at room temperature. Cells were washed with PBS and coverslips were mounted onto the microscope slide using fluorescent mounting medium (Dako). Images of foci were taken using a confocal Zeiss 700 microscope and processed with the Zeiss software.

Quantitative Foci Image Analysis

Z stack images of transfected and stained CECs were processed using Zeiss software. Images for each independent CEC line were taken using the same image acquisition parameters. Post capture, z stacks were processed as maximum intensity projection images. RNA foci were quantified by segmentation using CellProfiler (Broad Institute).[28] Nuclei were defined in the 405 nm (DAPI) channel, after a median filter was applied, by adaptive maximum correlation thresholding, followed by form-factor and eccentricity filtering. RNA foci were defined in the 561 nm (Cy3) channel, after a median filter was applied, as objects within the perimeter of a nucleus, using per-nucleus robust background thresholding, with parameters set per cell line, due to differences in staining intensity. Cells with high background in FISH staining, defined as mean intensity per nucleus, were discarded to reduce segmentation error. A minimum of 100 nuclei per independent condition and cell line were analyzed.

Dual FISH and ICC Assay

Following PFA fixation, cells were washed with PBS and then incubated in blocking solution containing 10% donkey serum, 0.5% Triton X-100, 3% BSA, and 0.4 U/μL RNase inhibitor in PBS for 1 hr at room temperature. Cells were subsequently incubated with mouse anti-MBNL1 antibody (1:1,000 in blocking solution; kindly provided by Thornton Lab, Chicago) overnight at 4°C. Following primary antibody incubation, cells were washed with PBS and incubated with secondary anti-mouse antibody conjugated with Alexa Fluor 488 (1:1,000 in 0.5% Triton X-100, 3% BSA) for 1 hr at room temperature. Cells were again washed with PBS and post-fixed in 4% PFA in PBS for 10 min. FISH was subsequently performed, in accordance with methods stated above.

Quantitative Image Analysis of MBNL1 Puncta

A minimum of ten images per condition for each transfected and stained CEC line were taken for analysis purposes, using a confocal Zeiss 700 microscope. In the same way as previously described, CellProfiler software was used to identify and quantify MBNL1 puncta, defined in the Cy2 channel. The percentage of objects found in a nucleus after treatment with both ASOs was plotted individually, per cell line investigated (Figure S2).

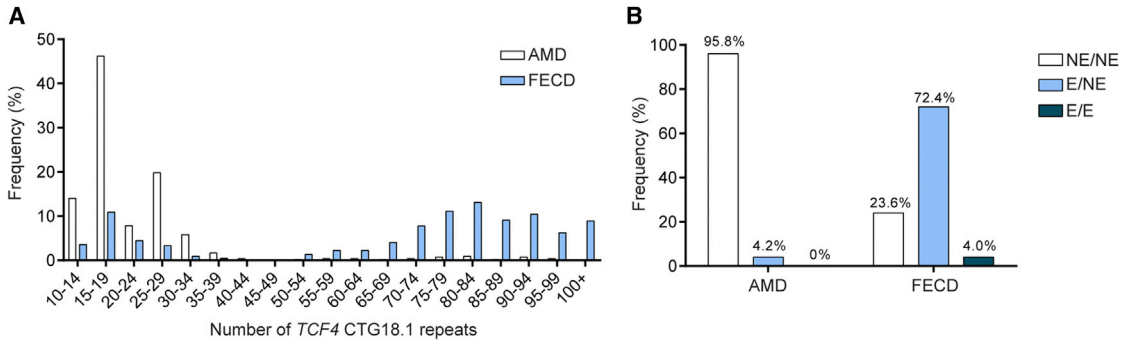

Figure 1. Expansion of CTG18.1 Is Associated with FECD in a British and Czech Cohort
(A) Frequency histogram comparing relative distribution of CTG repeat length in Fuchs endothelial corneal dystrophy (FECD) and age-related macular degeneration (AMD) cohorts. The longest allele detected, per individual tested, is shown. In total the FECD (blue) and AMD (white) cohorts comprised 450 and 550 individuals, respectively.
(B) Bar chart illustrating the relative frequency of individuals with both alleles non-expanded (NE/NE), one expanded allele (E/NE), or both alleles expanded (E/E) in both the FECD and AMD cohorts. Expanded alleles are defined as ≥50 CTG repeats.

Analysis of Pre-mRNA Splicing

Total RNA was extracted from primary CECs using NucleoSpin RNA XS kit according to manufacturer's guidelines (Macherey-Nagel). cDNA was reverse-transcribed using a Tetro cDNA synthesis kit (BIOLINE) with an oligo $(dT)_{18}$ primer mix in accordance with manufacturer's guidelines. Reverse transcription PCR was performed using intron spanning primers listed in Table S2 using GoTaq Green Master mix (Promega) and standard cycling parameters. The identities of all amplified products were confirmed by Sanger sequencing using standard methodologies. The relative intensities of PCR-amplified products resolved on agarose gels were calculated using Image Lab software package (BioRad).

Intraocular Administration of ASOs

C57BL/6 mice (n = 12) were given a single intravitreal administration into both eyes of Cy-3-labeled 2′Ome-PS-$(CAG)_7$ at doses of 0.025, 0.01, or 0.05 mg in 1 μL of PBS, PBS only, or a molar equivalent of free Cy3 label conjugated to the ASO. Mice were sacrificed at 48 hr following intravitreal injection (IVT). IVT injection method: Mice were anesthetized using ketamine hydrochloride/medetomidine hydrochloride i.p. Both eyes were dilated with 1% tropicamide and 2.5% phenylephrine drops. Injections of 1 μL were made below the limbus using a 32 g needle attached to a 2.5 μL Hamilton syringe, and animals were then recovered using antisedan.

Immunohistochemistry

Eyes were enucleated and immersion fixed in 4% PFA for 24 hr prior to rapid freezing in OCT imbedding compound. Eyes were removed and cryoprotected by overnight incubation (at 4°C) in 30% sucrose solution. Corneal tissue sections (16 μm) were cut on a cryostat and collected onto charged slides and viewed immediately on a confocal fluorescence microscope.

Statistical Analyses

To test for associations between FECD disease affection status and polymorphic markers, we built logistic regression models in the above described groups of affected subjects and control subjects. FECD diagnosis was the outcome and the number of alleles with 50 or more repeats was used as the independent variable. Three association models were built: the first model was run in both male and female participants and included adjustment for sex. The other two models were sex specific, restricted to strata of male and female participants only (therefore not adjusted for sex). All the models were tested for significance using the "glm" function from the R 3.4.1 statistical software base packages.

Statistical analyses of CECs were performed with GraphPad Prism 6 software. A chi-squared test was used to analyze differences in the distribution of foci incidence between the cells treated with the control and the $(CAG)_7$ ASO. Odds ratio tests were performed to analyze whether the likelihood of finding 0, 1, 2, 3, or 4 or more foci after treatment was increased or decreased. An unpaired two-tailed t test was used to calculate the difference in mean number of MBNL1-positive foci per nucleus between control and $(CAG)_7$ ASO treatments. A one-way analysis of variance (ANOVA) using Dunnett's multiple comparisons test with a single pooled variance was used to analyze differences between mean amplicon expression in expansion-negative and expansion-positive CEC lines compared with controls. Paired two-tailed t tests were conducted to analyze the effect of $(CAG)_7$ versus control ASO treatment on amplicon expression, for each respective transcript investigated. Data are represented as means ± 1 SD for bar graphs throughout the manuscript.

Results

Expansion of the CTG18.1 Trinucleotide Repeat Confers Significant Risk for FECD

A highly significant association between expansion of the CTG18.1 trinucleotide repeat (conservatively defined as ≥50 repeats) and FECD was identified (OR = 76.47; 95% CI: 47.45–123.2; $p = 5.69 \times 10^{-71}$) in the white European-only portion of the cohort (n = 392; Table 1). The distribution of the CTG18.1 expansion lengths among individuals affected by FECD and age-related macular degeneration (AMD), used as an ethnically matched control population for the purpose of this study, are summarized in Figures 1A and 1B and Table 1. For the AMD cohort, 4.2% (23/550) had one expanded copy (≥50 repeats) of the CTG18.1 allele, in line with reports from other unaffected populations screened for control purposes,[9,12–14] and none were found to have two expanded alleles. In contrast, 76.4% (344/450) of the FECD cohort

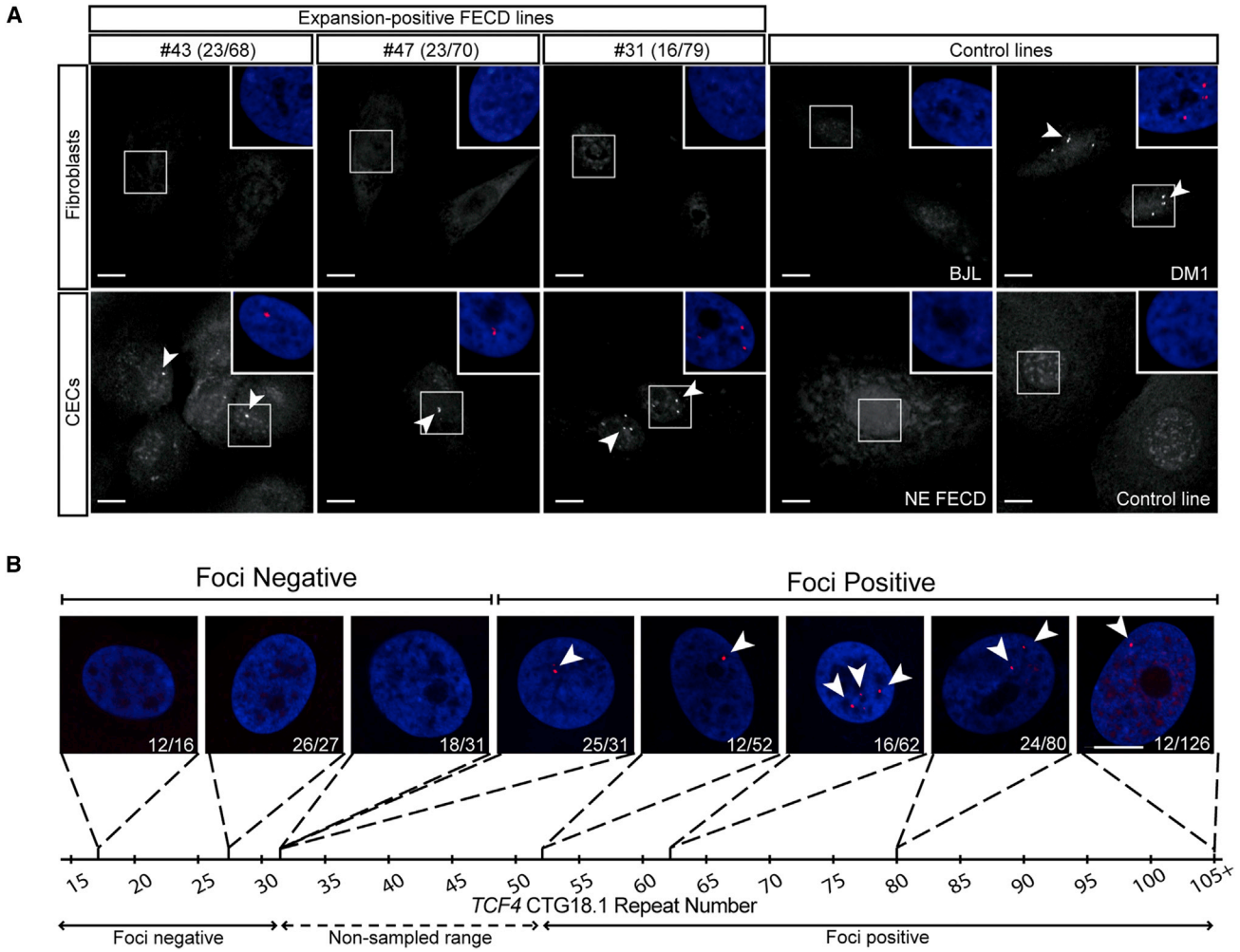

Figure 2. CTG18.1-Associated RNA Foci Occur in a Tissue-Specific Manner
(A) Fluorescence *in situ* hybridization (FISH) was used to detect CUG-specific RNA foci in fibroblast and corneal endothelial cells (CECs) lines derived from three individuals with FECD and expanded *TCF4* alleles. Fibroblast line BJL, non-expanded (NE) FECD, and healthy CECs were used as negative controls. Myotonic dystrophy 1 (DM1) fibroblasts were used as a positive control for foci detection (arrowheads). Each image is presented in greyscale and foci are indicated with arrowheads. Color insets (zoom panels) are presented. (B) Representative images of foci incidence among CECs derived from FECD-affected subjects with increasing CTG18.1 repeat lengths. Nuclei are stained with DAPI (blue). Foci detection was performed using Cy3-$(CAG)_7$ probe (red, arrowheads). Scale bars, 10 mm.

had one or more expanded copies of the CTG18.1 allele, of which 4.0% (18/450) had bi-allelic expansions. Interestingly, male subjects had a higher incidence of expanded CTG18.1 alleles (81.6% versus 72.8% with at least one expanded allele; Table 1) and the FECD risk associated with repeat expansion at this locus was higher in males (OR = 95.04, 95% CI: 43.08–209.70, $p = 1.62 \times 10^{-29}$) than in females (OR = 66.78, 95% CI: 36.79–121.20, $p = 2.06 \times 10^{-43}$), supporting the hypothesis that interaction of this locus with gender could be important.[29]

CEC Cultures as a Model of FECD

To investigate CTG18.1 expansion-associated pathology, the occurrence of stable sense-strand-derived CUG RNA foci in fibroblast primary cultures was investigated in six independent fibroblast lines (F#1–6) derived from FECD-affected subjects with expanded CTG18.1 genotypes (Table S3). For each line, FISH was performed using a Cy3-$(CAG)_7$ probe to determine the incidence of RNA-specific foci (Figure S3). Despite identifying multiple bright nuclear foci in a fibroblast line derived from a DM1 subject (positive control), none were detected in any of the FECD fibroblast lines investigated (Figure 2A).

On this basis, we tested the potential of using primary CECs, derived from tissue excised during endothelial keratoplasty, to investigate CTG18.1 expansion-associated pathology. The native "endothelial-like" properties of the CECs were confirmed by ICC and a variety of endothelial markers including sodium-potassium transporting adenosine triphosphatase (ATP1A1), zonula occludens 1 (ZO-1), N-cadherin, N-CAM, and CD166[30–32] (Figure S4). Furthermore, the cultured CECs displayed distinctive polygonal morphology.[25,33,34] FISH was performed, using the same Cy3-$(CAG)_7$ probe as described above, in three distinct

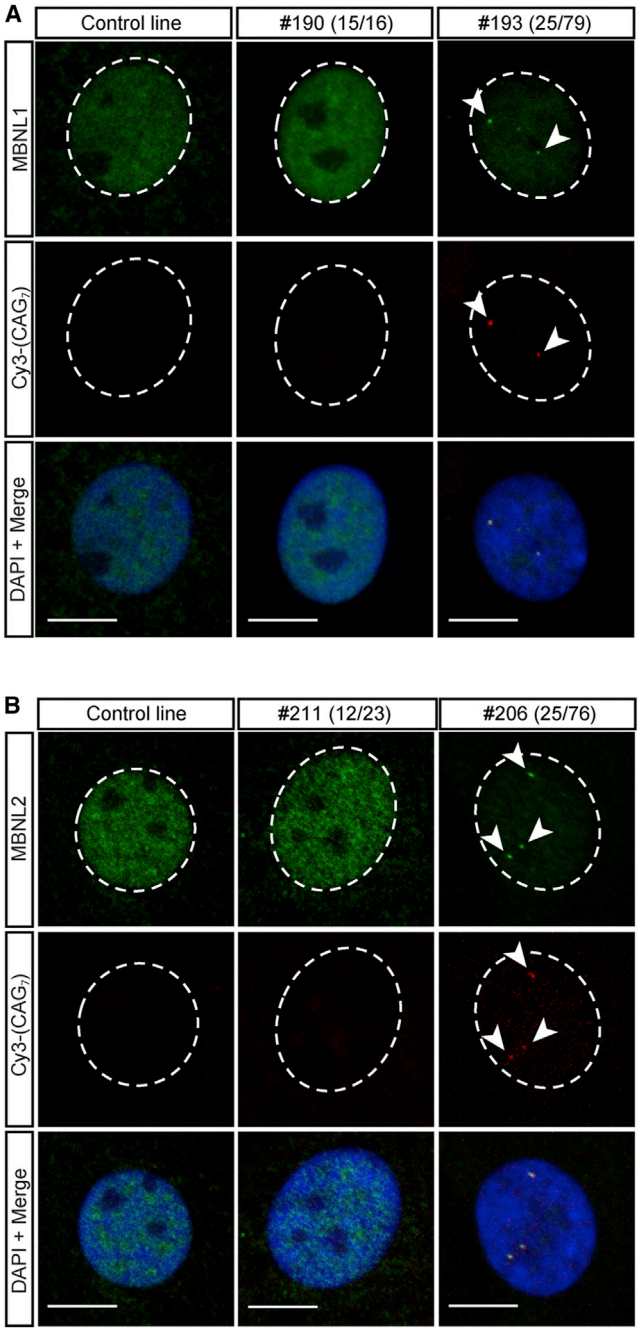

Figure 3. MBNL1 and MBNL2 Are Sequestered to RNA Foci in Corneal Endothelial Cells (CECs) Derived from FECD-Affected Subjects with CTG18.1 Expansions

Representative images of MBNL1 (A) and MBNL2 (B) protein nuclear localization in cell lines derived from expansion-positive FECD-affected subjects, expansion-negative FECD-affected subjects, and CECs derived from healthy individuals. RNA foci are labeled with a Cy3-$(CAG)_7$ FISH probe and DAPI is used to stain nuclei. Co-localization of the MBNL proteins and RNA foci is represented in the bottom row of both panels. Scale bars, 10 μm.

primary FECD CEC lines and corresponding individual-matched fibroblast lines (Figure 2A). In each instance, bright nuclear foci were detected in the FECD CECs, similar to those previously identified in corneal tissue,[15,35] whereas the corresponding fibroblasts were foci negative, suggesting that the endothelial-specific context is important and that the cultured primary CECs represent an ideal *ex vivo* system to investigate CTG18.1 expansion-associated corneal endothelial pathology (Figure 2A).

RNA Foci Are a Biomarker of CTG18.1-Associated Pathology in CECs

To further explore the incidence of RNA foci, we investigated a total of 36 independent CEC lines derived from FECD-affected subjects by FISH (Table S4; Figure 2B). In summary, no foci were detected in 9 CEC lines derived from FECD-affected subjects with CTG18.1 genotype status ranging from 12/12 to 18/31, in addition to a further 4 control lines. Bright nuclear foci were clearly detected in 27 CEC lines derived from individuals with alleles ranging from 25/31 to 12/126. Interestingly, CTG18.1 allele length of 31 repeats appears to represent a critical threshold for foci occurrence in CECs as individuals with genotypes of 18/31 and 25/31 were foci negative and positive, respectively. No samples were available with an expansion in the range between 32 and 52 repeats (Figure 2B; Table S4). On this basis, we classified CEC lines selected for further experimental investigation as non-expanded (NE) if both CTG alleles contained <31 repeats, whereas those with at least one allele ≥ 53 repeats were considered expanded (Tables S3–S9).

RNA Splicing Factors MBNL1 and MBNL2 Are Sequestered by Nuclear RNA Foci

To determine whether RNA binding proteins were being sequestered by the RNA foci, in the cultured FECD CECs, we employed a dual FISH and ICC approach. The nuclear distribution of MBNL1 and MBNL2 was investigated in multiple CEC lines derived from individuals with and without expanded copies of the repeat (Table S5). MBNL1 displayed a diffuse nuclear localization in three non-expanded (NE) CEC lines and no foci were detected, as anticipated (Figure 3A). Striking co-localization was observed between MBNL1 and the CUG-specific RNA foci in all three independent CTG18.1 expansion-positive lines examined (Figure 3A), concordant with a previous observation made in FECD-diseased tissue.[15] Similarly, the recruitment of MBNL2 to CUG-specific nuclear RNA foci was also detected in expansion-positive CECs ($n = 3$) and MBNL2 displayed diffuse nuclear localization in expansion-negative and control CEC lines ($n = 4$) (Figure 3B). These data demonstrate that RNA splicing factors are recruited to CUG RNA foci and suggest that this recruitment may induce a functional deficiency of proteins that would be predicted to alter alternative splicing events, in a similar downstream pathway to what has been established for DM1.[18–22,36]

Expansion of CTG18.1 Is Associated with Altered mRNA Processing

Transcriptomic analysis of endothelial tissue derived from individuals affected with FECD has previously suggested

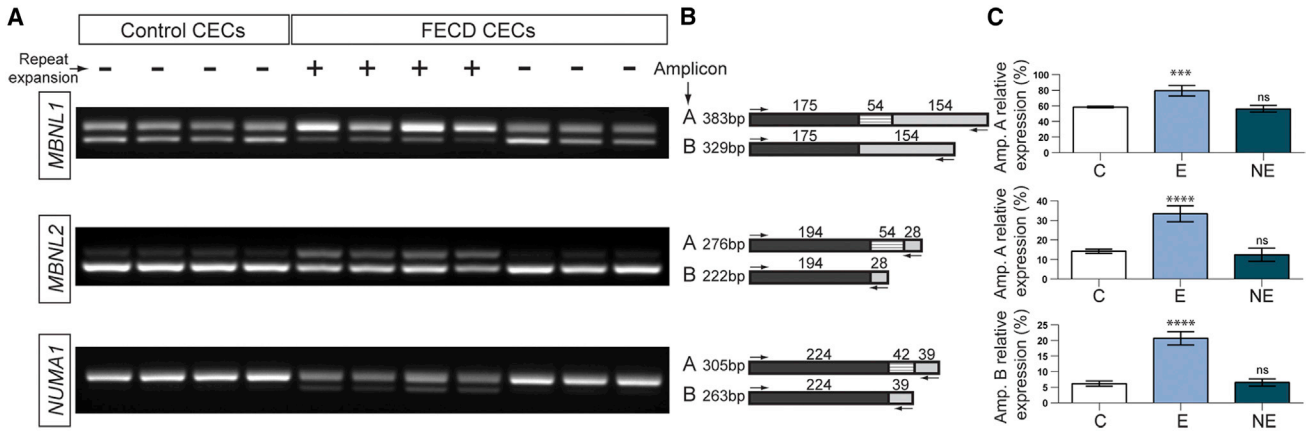

Figure 4. Altered Pre-mRNA Splicing Events Are Specific to CTG18.1 Expanded Corneal Endothelial Cells (CECs) Derived from FECD-Affected Subjects

(A) Reverse transcriptase (RT)-PCRs reactions are shown for three selected alternative splicing events investigated for the following transcripts: *MBNL1*, *MBNL2*, and *NUMA1*. Samples are grouped in the following categories; controls (lanes 1–4), FECD CTG18.1 expansion positive (lanes 5–8), and FECD CTG18.1 expansion negative (lanes 9–11).

(B) Schematic representations of RT-PCR-generated amplicons are provided for each transcript-specific reaction. Primer locations are denoted with arrows. The respective sizes of all amplified products are given.

(C) Percentage expression of amplicons of interest (A or B) relative to total amplified products, per reaction, are presented as a mean for each respective group (C, E, and NE). Error bars represent ±1 standard deviation. p values were calculated by one-way analysis of variance (ANOVA); ****$p < 0.0001$, ***$p < 0.001$, ns, non-significant.

abnormal regulation of alternative pre-mRNA splicing in CTG18.1 expansion-positive tissue.[15,37] Therefore, we investigated whether signatures of differential splicing were present in cultured primary CECs. Total RNA was isolated from four FECD CTG18.1 expansion-positive and three FECD CTG18.1 expansion-negative CEC lines (CTG18.1 genotype listed in Table S6), in addition to four CEC lines derived from healthy control subjects. RT-PCR analysis was performed to investigate differential splicing of the three most robustly detected aberrant events observed in tissue derived from affected subjects: *MBNL1* (MIM: 606516), *MBNL2* (MIM: 607327), and *NUMA1* (MIM: 164009).[37] For each transcript analyzed, significantly different ($p < 0.001$) patterns of splicing were observed only in the FECD expansion-positive lines compared to FECD expansion-negative and unaffected control lines, supporting the hypothesis that abnormal regulation of mRNA processing is specific to CTG18.1-related pathology (Figure 4).

ASO Treatment Reduces the Incidence of Nuclear RNA Foci

A fully 2′-O-methyl-phosohorothioate(2′-O-Me-PS) modified $(CAG)_7$ ASO complimentary to $(CUG)_n$ repeats has previously been shown to effectively silence *DMPK1* trinucleotide repeat expansion transcripts in a DM1 humanized animal model and human DM1 cell system and to reduce the number of DM1-associated RNA foci in a repeat-length-dependent manner.[23,24] We therefore tested whether transfecting with 2′-O-Me-PS-$(CAG)_7$ ASOs, complimentary to *TCF4* CTG18.1-derived transcripts, could induce a similar reduction in CUG-specific RNA foci, a biomarker of CTG18.1-related pathology, in the CEC cultures.

A series of six FECD CEC lines, with confirmed expanded CTG18.1 genotypes (Table S7), were selected for ASO treatment. Each independent line was transfected with 200 nM of either $(CAG)_7$ or a control ASO of identical chemical structure and of comparable length but specific to a completely unrelated sequence. A final oligo concentration of 200 nM was selected for all experiments based on optimization data (Figure S1). All lines analyzed showed a striking reduction in foci number in response to $(CAG)_7$ ASO treatment (Figures 5 and S5). Violin plots summarize the shift in distribution of RNA foci-positive nuclei observed comparing the control ASO-treated CECs versus $(CAG)_7$ ASO treatment ($n = 6$) (chi square test, $\chi^2 = 160.78$, $df = 4$, $p = 0.001$; Figure 5B). The percentage of nuclei containing zero, one, two, three, and four or more foci was analyzed, and odds ratio (OR) test confirmed that the likelihood of finding zero foci was significantly increased in cells treated with the $(CAG)_7$ ASO compared to cells treated with the control ASO ($OR = 6.2024$, 95% CI, $p < 0.0001$).

ASO Treatment Rescues MBNL1 Nuclear Localization

To determine the effect of $(CAG)_7$ ASO treatment on MBNL1 distribution, four independent expansion-positive CEC lines (Table S8) were selected and ICC was performed, following treatment with either the $(CAG)_7$ or control ASO. In all four lines treated with the $(CAG)_7$ ASO, there was an obvious redistribution of MBNL1 and a significant reduction in MBNL1-positive puncta ($p < 0.0001$), demonstrating that ASOs can rescue aberrant MBNL1 nuclear localization associated with the CTG18.1 expansion-related pathology (Figures 3A, 5D, 5E, and S2).

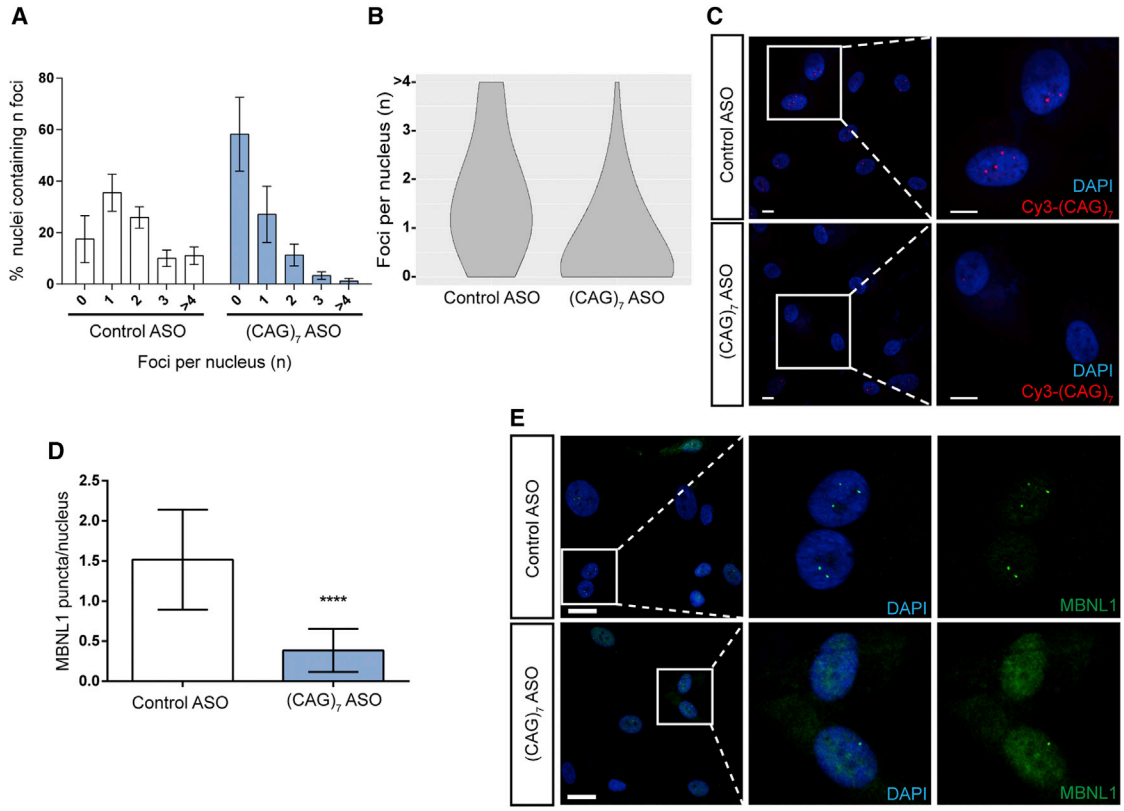

Figure 5. ASO-Mediated Treatment of Corneal Endothelial Cells (CECs) Significantly Reduces Foci Number and Rescues MBNL1 Nuclear Localization

(A) Foci incidence for control and $(CAG)_7$ antisense oligonucleotide (ASO)-treated FECD-affected subject-derived CECs. The graph shows percentages of nuclei that contain 0, 1, 2, 3, and 4 or more foci after treatment with the different ASOs. Mean ± SD are represented in each case (n = 6).

(B) Violin plots representing the distribution of the frequencies of each group of nuclei (containing 0, 1, 2, 3, and 4 or more foci) in cells treated with control and $(CAG)_7$ ASOs (n = 6).

(C) Representative images of ASO treatment on foci incidence. Sense RNA foci detection using Cy3-$(CAG)_7$ probe (red). Scale bars, 10 μm.

(D) Number of MBNL1 puncta present per nucleus when cells were treated with either a control ASO or with the $(CAG)_7$ ASO. The mean ± SD from 4 independent expansion-positive CEC lines, where a minimum of 95 nuclei were evaluated per line. p values were calculated using an unpaired two tailed t test; ****$p < 0.0001$.

(E) Representative example illustrating the reduction of MBNL1 puncta and the changes in MBNL1 localization when cells were treated with control and $(CAG)_7$ ASOs. In all cases CECs were treated with 200 nM $(CAG)_7$ or control ASO for 24 hr. Scale bars, 25 μm.

ASO Treatment Reduces Aberrant mRNA Processing

We investigated the potential of $(CAG)_7$ ASO treatment to reverse the shift in alternative splicing events previously observed in expansion-positive CEC lines (Figure 4). Ten FECD expansion-positive CEC lines (Table S9) were treated with either the $(CAG)_7$ or control ASO. Following treatment, RNA was extracted and RT-PCR was performed. For both *MBNL1* and *MBNL2* there was a highly significant ($p < 0.0001$) shift in the relative proportions of alternatively spliced transcripts after $(CAG)_7$ ASO treatment (n = 10) toward the control CEC spliceoform distribution (Figure 6). Furthermore, a significant ($p \leq 0.05$) shift in the relative proportions of alternatively spliced transcripts was also demonstrated for *NUMA1* (n = 10) (Figure 6). These data therefore demonstrate that the $(CAG)_7$ ASO is effective at rescuing the differential splicing events associated with CTG18.1 expansion-related pathology (Figures 4 and 6).

Intraocular Injections Enable Effective *In Vivo* Delivery of ASOs to the Corneal Endothelium

To assess the likely accessibility of ASOs to the corneal endothelium, C57B16 mice were injected intravitreally with varying concentrations (0.025, 0.01, and 0.005 mg) of Cy-3-labeled 2′Ome-PS-$(CAG)_7$. Confocal fluorescence microscopy revealed that the ASO was present in corneal endothelium, keratocytes, and stroma, specifically accumulating in both the nuclear and perinuclear region of both the endothelial and stromal cells. This localization increased in a dose-dependent manner, showing stronger accumulation in cell layers at 48 hr post-dosing (Figure S6). ASOs with identical chemistry, following intraocular injection, have previously been shown *in vivo* to display a similar peri-nuclear and nuclear localization in other cell types in conjunction with effective molecular activity.[38] These data highlight the potential for the $(CAG)_7$ ASO to target CECs *in vivo*, an essential prerequisite for the effective delivery of an ASO-mediated FECD therapy.

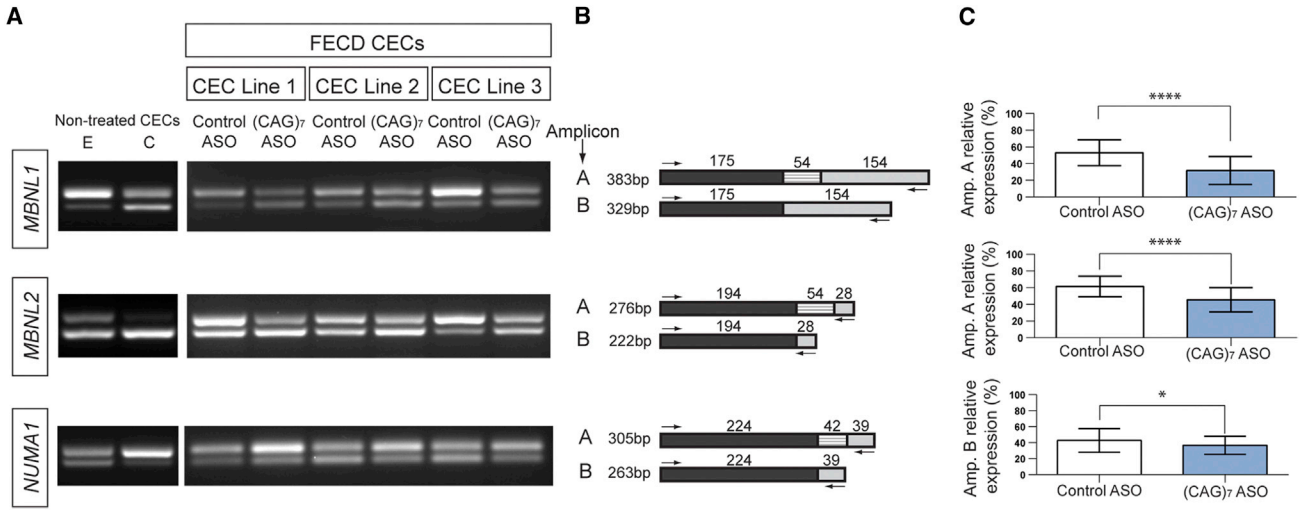

Figure 6. ASO Treatment Rescues Differential Splicing Events Underlying CTG18.1-Associated Pathology
(A) Representative RT-PCR images for non-treated samples with either expanded (E) or control (C) (non-expanded CTG18.1 genotypes) are shown on the far left, for reference purposes. Representative RT-PCRs are shown for three independent ASO-treated CEC lines.
(B) Schematic representations are provided for each respective reaction. Primer locations are denoted with arrows. The respective sizes of all amplified products are given.
(C) Percentage expression of amplicons of interest (A or B) relative to total amplified products, per reaction, are presented as a mean for control-ASO versus $(CAG)_7$ ASO-treated groups. The mean from 10 independent CEC lines ± SD. In all cases CECs were treated with 200 nM $(CAG)_7$ or control ASO for 24 hr. p values were calculated using a paired two tailed t test for each event investigated; ****$p < 0.0001$, *$p < 0.05$.

Discussion

ASOs have recently emerged as a powerful therapeutic option for disease intervention, including those caused by trinucleotide repeat expansions.[10,39–42] Here we show that a non-coding CTG trinucleotide repeat expansion in *TCF4* (CTG18.1) confers greater than 76-fold risk for FECD in a large white British and Czech cohort. We demonstrate that primary CECs derived from FECD-affected subjects display the predicted hallmarks of primary and downstream repeat-expansion-associated pathology, and subsequently show that these changes are reversed by an ASO treatment specifically targeted at the CTG18.1 trinucleotide repeat expansion. An ASO-based treatment could therefore offer an innovative therapeutic approach that could benefit a substantial number of individuals affected by this common and sight-threatening condition.[43]

The data presented here suggest that the *TCF4* repeat expansion leads to CEC-specific dysfunction, as unlike other trinucleotide expansion diseases, nuclear RNA foci are not observed in case-matched fibroblasts. These data, at least in part, explain the corneal-specific phenotype resulting from repeat expansions in this widely expressed gene and highlight the importance of investigating the trinucleotide expansion in primary human CECs. *TCF4* haploinsufficiency causes the systemic condition Pitt-Hopkins syndrome, but the noncoding repeat expansion exclusively affects the cornea.[44,45] Interestingly, a recent study has reported that FECD is a common ocular finding in DM1-affected case subjects.[46] Combined with our data, this suggests that the corneal endothelium is susceptible to toxicity induced by these genetically distinct repeat expansions, driven by RNA foci.

It is well established for a wide range of repeat expansion disorders that disease onset and incidence of RNA foci manifest only above a critical level of nucleotide repeats.[47] A threshold for CTG18.1 repeat length and FECD association is yet to be fully defined. Performing FISH with 36 distinct CEC lines derived from FECD-affected subjects has enabled us to identify the threshold for the number of repeats required to produce nuclear RNA foci in our model (Figure 2B; Table S4). Nine CEC lines with CTG18.1 genotypes ranging from 12/12 to 18/31 were found to lack RNA foci. A further 27 lines with CTG18.1 genotypes ranging from 25/31 to 12/126 were all found to exhibit punctate nuclear RNA foci. These data allow us to correlate CTG18.1 genotype status with CUG RNA foci incidence and indicate that a repeat size of more than 31 trinucleotide repeats is sufficient to drive the accumulation of stable CUG RNA foci in primary CECs (Figure 2B; Table S4). This identified threshold also correlates notably with the binominal distribution of CTG18.1 repeat length observed in our FECD cohort (Figure 1A), which is likely attributed to the instability of the repeat above approximately 30 copies. Interestingly, RNAs containing more than 30 CUG repeats have recently been demonstrated to undergo phase separation to form nuclear foci.[47] The threshold for this repeat length-dependent process (30 CUG repeats) is remarkably similar to what we have observed with respect to CTG18.1-related foci occurrence in CECs (Figure 2B). These phase separation data further support the use of agents that disrupt RNA-RNA base-pairing, such as ASOs,

as viable treatment options for RNA foci-induced cellular toxicity.[47] Taken together, these data suggest that a CTG18.1 length ≥ 32 should, in future, be considered as FECD risk associated. We repeated the tests for association with FECD defining the expanded repeats as ≥ 32, instead of the previously used more conservative threshold of ≥ 50. The association model became more significant ($p = 3.79 \times 10^{-74}$), although the disease risk conferred by this locus was lower (OR = 34.14; 95% CI: 23.35–49.91). Future analysis of CECs from individuals affected by FECD with repeat lengths in the unidentified range of 31–53 could further refine this important threshold.

We investigated the downstream consequences of RNA foci and have identified that sequestration of RNA splicing factors, MBNL1 and MBNL2 (Figure 3), in addition to abnormal patterns of alternative splicing were detectable in a repeat expansion-specific manner (Figure 4). These observations reinforce the notion that such RNA structures induce toxic gain-of-function effects that are likely to be disrupting overall cellular homeostasis, implicating aberrant RNA metabolism in the pathogenesis of CTG18.1-associated FECD.[15,37] Furthermore, these data demonstrate that these events are specific to CTG18.1-mediated FECD and are not a general downstream consequence of the disease, given that CECs derived from FECD-affected case subjects without expanded copies of the repeat did not display features of aberrant RNA metabolism.

Importantly, we demonstrate here that an ASO targeted to the CTG trinucleotide *TCF4* expansion can ameliorate disease-associated markers of RNA toxicity in CECs derived from FECD-affected subjects, specifically reducing RNA foci formation (Figures 5A–5C), prompting MBNL1 nuclear redistribution (Figures 5D and 5E) and partially suppressing differential splicing events (Figure 6). We additionally demonstrate that the ASO can access the corneal endothelium when injected intravitreally in mice (Figure S6). Entry of fluorescently labeled ASO to the corneal endothelial cells is an endogenous property of naked 2′Ome-PS-ASOs oligo and no other excipients are required to induce entry into these cells. Access to the CECs is also both dose and time dependent, suggesting that ASOs are rapidly taken up by cells after dosing. While it may be desirable to consider a topical eye drop therapy for FECD using an ASO approach, this is highly unlikely to be effective using naked ASOs given the structure of the corneal epithelium and the size and charge of ASOs; an adjunctive delivery technology would likely have to be considered in this case.

Future studies using CECs from affected individuals will be helpful in defining an effective ASO concentration, which can lead to a good clinical dose estimate when considering introduction to the anterior ocular chamber, which has a small fixed but rapidly exchanging volume. Detailed pharmacokinetic studies will be required to define the optimal dosing time interval, which is expected to be months, based on the rapid cellular uptake and the tissue/cellular longevity of similar 2′Ome-PS-ASOs in studies that have examined intraocular dosing of ASOs.[48] It is important to note that in the final stages of FECD there is significant endothelial cell loss, and consequently ASO-specific treatment is intended to prevent further cell loss. The most likely group of affected individuals to benefit from such a therapeutic intervention will be those individuals who are in the early stages of disease and have not yet experienced significant endothelial cell loss. Importantly, these at-risk individuals can be effectively identified by a CTG18.1 genotyping test.

In summary, we demonstrate proof-of-concept data that a targeted $(CAG)_7$ ASO treatment reduces gain-of-function RNA toxicity induced by *TCF4* CTG18.1 expansion, in a cellular and human genomic context. With the absence of FECD animal models, human *ex vivo* models are vital, both to provide a validation of the therapeutic approach for FECD and to continue the translation of ASO therapies into the clinic. ASO therapies are already in clinical trials for a variety of repeat expansion disorders including DM1[41] and Huntington disease (MIM: 143100), and additionally, intraocular ASO therapies are proposed for retinitis pigmentosa (RP [MIM: 268000]), RP associated with Usher syndrome (MIM: 608400), and Leber congenital amaurosis (MIM: 610142).[49–52] We propose that our proof-of-concept study provides evidence to translate this therapeutic approach to FECD given the accessibility of the diseased tissue and the relatively delayed onset of disease, which provides a window of opportunity to identify at risk individuals with *TCF4* repeat expansions and prevent disease progression in pre-symptomatic individuals.

Supplemental Data

Supplemental Data include six figures and nine tables and can be found with this article online at https://doi.org/10.1016/j.ajhg.2018.02.010.

Acknowledgments

We would like to thank all affected individuals for participating in this research. We would also like to acknowledge Dr. Charles A. Thornton for generously providing the MBNL1 (A2764) antibody used in this study and Miracles for Sight Eye bank for providing control corneal tissue. We thank Prof. Andrew Webster and Dr. Valentina Cipriani for granting access to AMD DNA samples and Prof. Veronica van Heyningen for providing a critical appraisal of the manuscript. This work was funded by Fight for Sight Early Career Investigator Award (A.E.D.), Academy of Medical Sciences (A.E.D.), The National Institute for Health Research Biomedical Research Centre at Moorfields Eye Hospital National Health Service Foundation Trust and UCL Institute of Ophthalmology, Rosetrees Trust (A.E.D. and A.J.H.), Wellcome Trust (M.E.C.), and ProQR Therapeutics. L.D., P.S., and P.L. were supported by PROGRES-Q26/LF1 and GACR 17-12355S. L.D. and P.L. were further supported by UNCE 204064 and P.S. by GA UK 250361/2017 and SVV 260367/2017. A patent has been filed by ProQR with UK and European patent offices (1517565) describing a method of treating FECD. P.A. is a listed inventor on this patent. P.K., K.D., and P.A. are all employees of ProQR Therapeutics. This work was supported in part by a grant from ProQR Therapeutics.

Received: January 3, 2018
Accepted: February 14, 2018
Published: March 8, 2018

Web Resources

CellProfiler (Broad Institute), http://cellprofiler.org/
GeneMarker Software (SoftGenetics), https://softgenetics.com/GeneMarker.php
GraphPad Prism 6 software, https://www.graphpad.com/scientific-software/prism/
OMIM, http://www.omim.org/
R 3.4.1 statistical software base packages, https://cran.r-project.org/

References

1. Zoega, G.M., Fujisawa, A., Sasaki, H., Kubota, A., Sasaki, K., Kitagawa, K., and Jonasson, F. (2006). Prevalence and risk factors for cornea guttata in the Reykjavik Eye Study. Ophthalmology *113*, 565–569.
2. Kitagawa, K., Kojima, M., Sasaki, H., Shui, Y.B., Chew, S.J., Cheng, H.M., Ono, M., Morikawa, Y., and Sasaki, K. (2002). Prevalence of primary cornea guttata and morphology of corneal endothelium in aging Japanese and Singaporean subjects. Ophthalmic Res. *34*, 135–138.
3. Lorenzetti, D.W., Uotila, M.H., Parikh, N., and Kaufman, H.E. (1967). Central cornea guttata. Incidence in the general population. Am. J. Ophthalmol. *64*, 1155–1158.
4. Vedana, G., Villarreal, G., Jr., and Jun, A.S. (2016). Fuchs endothelial corneal dystrophy: current perspectives. Clin. Ophthalmol. *10*, 321–330.
5. Eghrari, A.O., Riazuddin, S.A., and Gottsch, J.D. (2015). Fuchs corneal dystrophy. Prog. Mol. Biol. Transl. Sci. *134*, 79–97.
6. Goldberg, R.A., Raza, S., Walford, E., Feuer, W.J., and Goldberg, J.L. (2014). Fuchs endothelial corneal dystrophy: clinical characteristics of surgical and nonsurgical patients. Clin. Ophthalmol. *8*, 1761–1766.
7. Golchet, G., Carr, J., and Harris, M.G. (2000). Why don't we have enough cornea donors? A literature review and survey. Optometry *71*, 318–328.
8. Baratz, K.H., Tosakulwong, N., Ryu, E., Brown, W.L., Branham, K., Chen, W., Tran, K.D., Schmid-Kubista, K.E., Heckenlively, J.R., Swaroop, A., et al. (2010). E2-2 protein and Fuchs's corneal dystrophy. N. Engl. J. Med. *363*, 1016–1024.
9. Wieben, E.D., Aleff, R.A., Tosakulwong, N., Butz, M.L., Highsmith, W.E., Edwards, A.O., and Baratz, K.H. (2012). A common trinucleotide repeat expansion within the transcription factor 4 (TCF4, E2-2) gene predicts Fuchs corneal dystrophy. PLoS ONE *7*, e49083.
10. Scoles, D.R., Meera, P., Schneider, M.D., Paul, S., Dansithong, W., Figueroa, K.P., Hung, G., Rigo, F., Bennett, C.F., Otis, T.S., and Pulst, S.M. (2017). Antisense oligonucleotide therapy for spinocerebellar ataxia type 2. Nature *544*, 362–366.
11. Soliman, A.Z., Xing, C., Radwan, S.H., Gong, X., and Mootha, V.V. (2015). Correlation of severity of Fuchs endothelial corneal dystrophy with triplet repeat e'xpansion in TCF4. JAMA Ophthalmol. *133*, 1386–1391.
12. Vasanth, S., Eghrari, A.O., Gapsis, B.C., Wang, J., Haller, N.F., Stark, W.J., Katsanis, N., Riazuddin, S.A., and Gottsch, J.D. (2015). Expansion of CTG18.1 trinucleotide repeat in TCF4 is a potent driver of Fuchs' corneal dystrophy. Invest. Ophthalmol. Vis. Sci. *56*, 4531–4536.
13. Xing, C., Gong, X., Hussain, I., Khor, C.C., Tan, D.T., Aung, T., Mehta, J.S., Vithana, E.N., and Mootha, V.V. (2014). Transethnic replication of association of CTG18.1 repeat expansion of TCF4 gene with Fuchs' corneal dystrophy in Chinese implies common causal variant. Invest. Ophthalmol. Vis. Sci. *55*, 7073–7078.
14. Mootha, V.V., Gong, X., Ku, H.C., and Xing, C. (2014). Association and familial segregation of CTG18.1 trinucleotide repeat expansion of TCF4 gene in Fuchs' endothelial corneal dystrophy. Invest. Ophthalmol. Vis. Sci. *55*, 33–42.
15. Du, J., Aleff, R.A., Soragni, E., Kalari, K., Nie, J., Tang, X., Davila, J., Kocher, J.P., Patel, S.V., Gottesfeld, J.M., et al. (2015). RNA toxicity and missplicing in the common eye disease fuchs endothelial corneal dystrophy. J. Biol. Chem. *290*, 5979–5990.
16. Mahadevan, M., Tsilfidis, C., Sabourin, L., Shutler, G., Amemiya, C., Jansen, G., Neville, C., Narang, M., Barceló, J., O'Hoy, K., et al. (1992). Myotonic dystrophy mutation: an unstable CTG repeat in the 3′ untranslated region of the gene. Science *255*, 1253–1255.
17. Taneja, K.L., McCurrach, M., Schalling, M., Housman, D., and Singer, R.H. (1995). Foci of trinucleotide repeat transcripts in nuclei of myotonic dystrophy cells and tissues. J. Cell Biol. *128*, 995–1002.
18. Miller, J.W., Urbinati, C.R., Teng-Umnuay, P., Stenberg, M.G., Byrne, B.J., Thornton, C.A., and Swanson, M.S. (2000). Recruitment of human muscleblind proteins to (CUG)(n) expansions associated with myotonic dystrophy. EMBO J. *19*, 4439–4448.
19. Holt, I., Jacquemin, V., Fardaei, M., Sewry, C.A., Butler-Browne, G.S., Furling, D., Brook, J.D., and Morris, G.E. (2009). Muscleblind-like proteins: similarities and differences in normal and myotonic dystrophy muscle. Am. J. Pathol. *174*, 216–227.
20. Ciesiolka, A., Jazurek, M., Drazkowska, K., and Krzyzosiak, W.J. (2017). Structural characteristics of simple RNA repeats associated with disease and their deleterious protein interactions. Front. Cell. Neurosci. *11*, 97.
21. Charizanis, K., Lee, K.Y., Batra, R., Goodwin, M., Zhang, C., Yuan, Y., Shiue, L., Cline, M., Scotti, M.M., Xia, G., et al. (2012). Muscleblind-like 2-mediated alternative splicing in the developing brain and dysregulation in myotonic dystrophy. Neuron *75*, 437–450.
22. Du, H., Cline, M.S., Osborne, R.J., Tuttle, D.L., Clark, T.A., Donohue, J.P., Hall, M.P., Shiue, L., Swanson, M.S., Thornton, C.A., and Ares, M., Jr. (2010). Aberrant alternative splicing and extracellular matrix gene expression in mouse models of -myotonic dystrophy. Nat. Struct. Mol. Biol. *17*, 187–193.
23. Mulders, S.A., van den Broek, W.J., Wheeler, T.M., Croes, H.J., van Kuik-Romeijn, P., de Kimpe, S.J., Furling, D., Platenburg, G.J., Gourdon, G., Thornton, C.A., et al. (2009). Triplet-repeat oligonucleotide-mediated reversal of RNA toxicity in myotonic dystrophy. Proc. Natl. Acad. Sci. USA *106*, 13915–13920.
24. González-Barriga, A., Mulders, S.A., van de Giessen, J., Hooijer, J.D., Bijl, S., van Kessel, I.D., van Beers, J., van Deutekom, J.C., Fransen, J.A., Wieringa, B., and Wansink, D.G. (2013). Design and analysis of effects of triplet repeat oligonucleotides in cell models for myotonic dystrophy. Mol. Ther. Nucleic Acids *2*, e81.
25. Peh, G.S., Chng, Z., Ang, H.P., Cheng, T.Y., Adnan, K., Seah, X.Y., George, B.L., Toh, K.P., Tan, D.T., Yam, G.H., et al. (2015). Propagation of human corneal endothelial cells: a novel dual media approach. Cell Transplant. *24*, 287–304.

26. Carter, D.A., Nommiste, B., Coffey, P.J., and Carr, A.-J.F. (2016). Spontaneous generation of patient-specific retinal pigment epithelial cells using induced pluripotent stem cell technology. In Working with Stem Cells (Cham: Springer International Publishing), pp. 143–161.
27. Lin, X., Miller, J.W., Mankodi, A., Kanadia, R.N., Yuan, Y., Moxley, R.T., Swanson, M.S., and Thornton, C.A. (2006). Failure of MBNL1-dependent post-natal splicing transitions in myotonic dystrophy. Hum. Mol. Genet. *15*, 2087–2097.
28. Carpenter, A.E., Jones, T.R., Lamprecht, M.R., Clarke, C., Kang, I.H., Friman, O., Guertin, D.A., Chang, J.H., Lindquist, R.A., Moffat, J., et al. (2006). CellProfiler: image analysis software for identifying and quantifying cell phenotypes. Genome Biol. *7*, R100.
29. Afshari, N.A., Igo, R.P., Jr., Morris, N.J., Stambolian, D., Sharma, S., Pulagam, V.L., Dunn, S., Stamler, J.F., Truitt, B.J., Rimmler, J., et al. (2017). Genome-wide association study identifies three novel loci in Fuchs endothelial corneal dystrophy. Nat. Commun. *8*, 14898.
30. He, Z., Forest, F., Gain, P., Rageade, D., Bernard, A., Acquart, S., Peoc'h, M., Defoe, D.M., and Thuret, G. (2016). 3D map of the human corneal endothelial cell. Sci. Rep. *6*, 29047.
31. Bartakova, A., Alvarez-Delfin, K., Weisman, A.D., Salero, E., Raffa, G.A., Merkhofer, R.M., Jr., Kunzevitzky, N.J., and Goldberg, J.L. (2016). Novel identity and functional markers for human corneal endothelial cells. Invest. Ophthalmol. Vis. Sci. *57*, 2749–2762.
32. Ding, V., Chin, A., Peh, G., Mehta, J.S., and Choo, A. (2014). Generation of novel monoclonal antibodies for the enrichment and characterization of human corneal endothelial cells (hCENC) necessary for the treatment of corneal endothelial blindness. MAbs *6*, 1439–1452.
33. Peh, G.S., Toh, K.P., Ang, H.P., Seah, X.Y., George, B.L., and Mehta, J.S. (2013). Optimization of human corneal endothelial cell culture: density dependency of successful cultures in vitro. BMC Res. Notes *6*, 176.
34. Peh, G.S., Toh, K.P., Wu, F.Y., Tan, D.T., and Mehta, J.S. (2011). Cultivation of human corneal endothelial cells isolated from paired donor corneas. PLoS ONE *6*, e28310.
35. Mootha, V.V., Hussain, I., Cunnusamy, K., Graham, E., Gong, X., Neelam, S., Xing, C., Kittler, R., and Petroll, W.M. (2015). TCF4 triplet repeat expansion and nuclear RNA foci in Fuchs' endothelial corneal dystrophy. Invest. Ophthalmol. Vis. Sci. *56*, 2003–2011.
36. Konieczny, P., Stepniak-Konieczna, E., and Sobczak, K. (2017). MBNL expression in autoregulatory feedback loops. RNA Biol. *15*, 1–8.
37. Wieben, E.D., Aleff, R.A., Tang, X., Butz, M.L., Kalari, K.R., Highsmith, E.W., Jen, J., Vasmatzis, G., Patel, S.V., Maguire, L.J., et al. (2017). Trinucleotide repeat expansion in the transcription factor 4 (TCF4) gene leads to widespread mRNA splicing changes in Fuchs' endothelial corneal dystrophy. Invest. Ophthalmol. Vis. Sci. *58*, 343–352.
38. Gérard, X., Perrault, I., Munnich, A., Kaplan, J., and Rozet, J.M. (2015). Intravitreal injection of splice-switching oligonucleotides to manipulate splicing in retinal cells. Mol. Ther. Nucleic Acids *4*, e250.
39. Schoch, K.M., and Miller, T.M. (2017). Antisense oligonucleotides: translation from mouse models to human neurodegenerative diseases. Neuron *94*, 1056–1070.
40. Jiang, J., Zhu, Q., Gendron, T.F., Saberi, S., McAlonis-Downes, M., Seelman, A., Stauffer, J.E., Jafar-Nejad, P., Drenner, K., Schulte, D., et al. (2016). Gain of toxicity from ALS/FTD-linked repeat expansions in C9ORF72 is alleviated by antisense oligonucleotides targeting GGGGCC-containing RNAs. Neuron *90*, 535–550.
41. Wheeler, T.M., Leger, A.J., Pandey, S.K., MacLeod, A.R., Nakamori, M., Cheng, S.H., Wentworth, B.M., Bennett, C.F., and Thornton, C.A. (2012). Targeting nuclear RNA for in vivo correction of myotonic dystrophy. Nature *488*, 111–115.
42. Kordasiewicz, H.B., Stanek, L.M., Wancewicz, E.V., Mazur, C., McAlonis, M.M., Pytel, K.A., Artates, J.W., Weiss, A., Cheng, S.H., Shihabuddin, L.S., et al. (2012). Sustained therapeutic reversal of Huntington's disease by transient repression of huntingtin synthesis. Neuron *74*, 1031–1044.
43. Gipson, I.K. (2013). Age-related changes and diseases of the ocular surface and cornea. Invest. Ophthalmol. Vis. Sci. *54*, ORSF48-53.
44. Amiel, J., Rio, M., de Pontual, L., Redon, R., Malan, V., Boddaert, N., Plouin, P., Carter, N.P., Lyonnet, S., Munnich, A., and Colleaux, L. (2007). Mutations in TCF4, encoding a class I basic helix-loop-helix transcription factor, are responsible for Pitt-Hopkins syndrome, a severe epileptic encephalopathy associated with autonomic dysfunction. Am. J. Hum. Genet. *80*, 988–993.
45. Zweier, C., Peippo, M.M., Hoyer, J., Sousa, S., Bottani, A., Clayton-Smith, J., Reardon, W., Saraiva, J., Cabral, A., Gohring, I., et al. (2007). Haploinsufficiency of TCF4 causes syndromal mental retardation with intermittent hyperventilation (Pitt-Hopkins syndrome). Am. J. Hum. Genet. *80*, 994–1001.
46. Mootha, V.V., Hansen, B., Rong, Z., Mammen, P.P., Zhou, Z., Xing, C., and Gong, X. (2017). Fuchs' endothelial corneal dystrophy and RNA foci in patients with myotonic dystrophy. Invest. Ophthalmol. Vis. Sci. *58*, 4579–4585.
47. Jain, A., and Vale, R.D. (2017). RNA phase transitions in repeat expansion disorders. Nature *546*, 243–247.
48. Henry, S.P., Miner, R.C., Drew, W.L., Fitchett, J., York-Defalco, C., Rapp, L.M., and Levin, A.A. (2001). Antiviral activity and ocular kinetics of antisense oligonucleotides designed to inhibit CMV replication. Invest. Ophthalmol. Vis. Sci. *42*, 2646–2651.
49. Murray, S.F., Jazayeri, A., Matthes, M.T., Yasumura, D., Yang, H., Peralta, R., Watt, A., Freier, S., Hung, G., Adamson, P.S., et al. (2015). Allele-specific inhibition of rhodopsin with an antisense oligonucleotide slows photoreceptor cell degeneration. Invest. Ophthalmol. Vis. Sci. *56*, 6362–6375.
50. Lentz, J.J., Jodelka, F.M., Hinrich, A.J., McCaffrey, K.E., Farris, H.E., Spalitta, M.J., Bazan, N.G., Duelli, D.M., Rigo, F., and Hastings, M.L. (2013). Rescue of hearing and vestibular function by antisense oligonucleotides in a mouse model of human deafness. Nat. Med. *19*, 345–350.
51. Garanto, A., Chung, D.C., Duijkers, L., Corral-Serrano, J.C., Messchaert, M., Xiao, R., Bennett, J., Vandenberghe, L.H., and Collin, R.W. (2016). In vitro and in vivo rescue of aberrant splicing in CEP290-associated LCA by antisense oligonucleotide delivery. Hum. Mol. Genet. *25*, 2552–2563.
52. Parfitt, D.A., Lane, A., Ramsden, C.M., Carr, A.J., Munro, P.M., Jovanovic, K., Schwarz, N., Kanuga, N., Muthiah, M.N., Hull, S., et al. (2016). Identification and correction of mechanisms underlying inherited blindness in human iPSC-derived optic cups. Cell Stem Cell *18*, 769–781.

Příloha 5: Ectopic *GRHL2* Expression Due to Non-coding Mutations Promotes Cell State Transition and Causes Posterior Polymorphous Corneal Dystrophy 4

Ectopic *GRHL2* Expression Due to Non-coding Mutations Promotes Cell State Transition and Causes Posterior Polymorphous Corneal Dystrophy 4

Petra Liskova,[1,2,3,6,*] Lubica Dudakova,[1,6] Cerys J. Evans,[3,6] Karla E. Rojas Lopez,[3,6] Nikolas Pontikos,[3,6] Dimitra Athanasiou,[3] Hodan Jama,[3] Josef Sach,[4] Pavlina Skalicka,[1,2] Viktor Stranecky,[1] Stanislav Kmoch,[1] Caroline Thaung,[3,5] Martin Filipec,[2] Michael E. Cheetham,[3] Alice E. Davidson,[3,7] Stephen J. Tuft,[5,7] and Alison J. Hardcastle[3,5,7,*]

In a large family of Czech origin, we mapped a locus for an autosomal-dominant corneal endothelial dystrophy, posterior polymorphous corneal dystrophy 4 (PPCD4), to 8q22.3–q24.12. Whole-genome sequencing identified a unique variant (c.20+544G>T) in this locus, within an intronic regulatory region of *GRHL2*. Targeted sequencing identified the same variant in three additional previously unsolved PPCD-affected families, including a *de novo* occurrence that suggests this is a recurrent mutation. Two further unique variants were identified in intron 1 of *GRHL2* (c.20+257delT and c.20+133delA) in unrelated PPCD-affected families. GRHL2 is a transcription factor that suppresses epithelial-to-mesenchymal transition (EMT) and is a direct transcriptional repressor of *ZEB1*. *ZEB1* mutations leading to haploinsufficiency cause PPCD3. We previously identified promoter mutations in *OVOL2*, a gene not normally expressed in the corneal endothelium, as the cause of PPCD1. OVOL2 drives mesenchymal-to-epithelial transition (MET) by directly inhibiting EMT-inducing transcription factors, such as *ZEB1*. Here, we demonstrate that the *GRHL2* regulatory variants identified in PPCD4-affected individuals induce increased transcriptional activity *in vitro*. Furthermore, although *GRHL2* is not expressed in corneal endothelial cells in control tissue, we detected GRHL2 in the corneal "endothelium" in PPCD4 tissue. These cells were also positive for epithelial markers E-Cadherin and Cytokeratin 7, indicating they have transitioned to an epithelial-like cell type. We suggest that mutations inducing MET within the corneal endothelium are a convergent pathogenic mechanism leading to dysfunction of the endothelial barrier and disease.

Introduction

Posterior polymorphous corneal dystrophy (PPCD) is a rare autosomal-dominant disorder, primarily affecting the corneal endothelium and Descemet membrane. The severity and phenotype of PPCD is variable.[1] Mild manifestations of the disease include asymptomatic corneal endothelial changes such as vesicular, band-like, and geographic lesions. In severe cases, corneal endothelial failure may occur and corneal transplantation is required to restore vision.[1–4] Aberrant corneal endothelial cells have been shown to proliferate and migrate onto the trabecular meshwork and iris acquiring an epithelial-like morphology.[1,5–8] Secondary complications are common and include corneal edema, glaucoma, iris adherence to the cornea, and corectopia.[1,2]

PPCD is a genetically heterogeneous condition, with approximately a third of cases attributed to heterozygous mutations in the transcription factor encoding gene *ZEB1* (MIM: 189909) (PPCD3 [MIM: 609141]).[3,9–11] Recently, we and others have established that heterozygous regulatory mutations in the promoter of *OVOL2* (MIM: 616441) cause PPCD1 (MIM: 122000).[2,12] ZEB1 and OVOL2 control cell state, through regulation of epithelial-to-mesenchymal transition (EMT) and the converse process of mesenchymal-to-epithelial transition (MET), through a mutually inhibitory pathway.[13,14] EMT and MET are central processes in development, and these finely tuned and reversible cell state transition pathways also support the maintenance of cellular identity and function.[15,16] Aberrant regulation of MET and EMT underpins tumor progression and malignant transformation processes, as well as playing an important role in other disease conditions including fibrosis, wound repair, and inflammation.[17,18]

Corneal endothelial cells are embryonically derived from the neural crest and form a monolayer of post-mitotic hexagonal cells on the inner surface of the cornea. They are specialized cells that have a barrier-pump function, governing fluid and solute transport across the posterior surface of the cornea and maintaining the cornea in a relatively dehydrated state that is essential for optical transparency.[19,20] Haploinsufficiency and subsequent reduced expression of *ZEB1* in the corneal endothelium is thought to underlie the pathology of PPCD3,[10] whereas inappropriate ectopic expression of *OVOL2* in corneal endothelial cells is the proposed mechanism for PPCD1.[2,12] The

[1]Research Unit for Rare Diseases, Department of Paediatrics and Adolescent Medicine, First Faculty of Medicine, Charles University and General University Hospital in Prague, Ke Karlovu 2, Prague 128 08, Czech Republic; [2]Department of Ophthalmology, First Faculty of Medicine, Charles University and General University Hospital in Prague, U Nemocnice 2, Prague 128 08, Czech Republic; [3]UCL Institute of Ophthalmology, University College London, London EC1V 9EL, UK; [4]Institute of Pathology, Third Faculty of Medicine, Charles University, Faculty Hospital Kralovske Vinohrady, Srobarova 50, Prague 100 34, Czech Republic; [5]Moorfields Eye Hospital, London EC1V 2PD, UK
[6]These authors contributed equally to this work
[7]These authors contributed equally to this work
*Correspondence: petra.liskova@lf1.cuni.cz (P.L.), a.hardcastle@ucl.ac.uk (A.J.H.)
https://doi.org/10.1016/j.ajhg.2018.02.002.

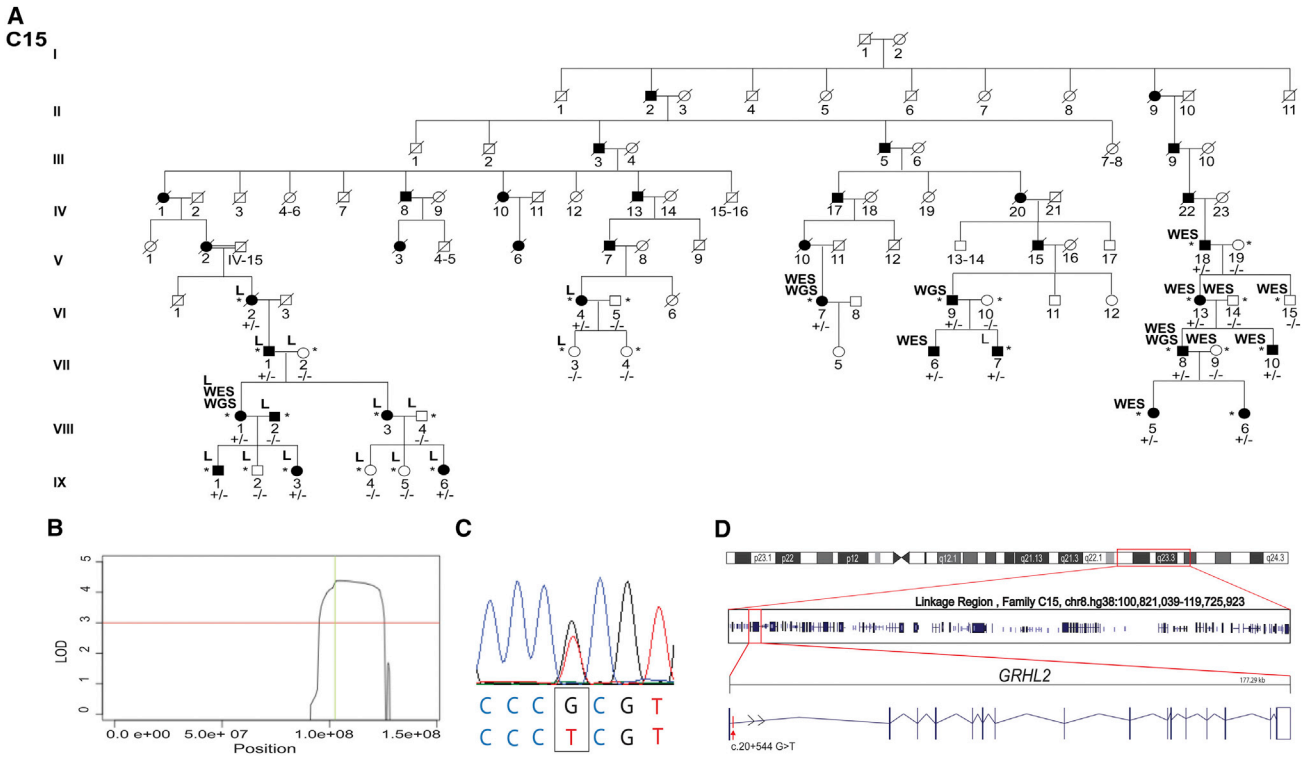

Figure 1. Identification of a Locus for Autosomal-Dominant PPCD on 8q22.3–q24.12 and a Unique Variant in Intron 1 of *GRHL2*
(A) Abridged pedigree structure of PPCD-affected family C15 of Czech origin. L indicates samples used for SNP genotyping and linkage analysis. WES and WGS indicate DNA samples analyzed by whole-exome and whole-genome sequencing, respectively. Individuals who were heterozygous for the *GRHL2* c.20+544G>T mutation are indicated by +/−, and those lacking the mutation are indicated by −/−.
(B) Linkage analysis identified a single locus with a significant LOD score (>3, red line) spanning chromosome 8q22.3–q24.12 from chr8.hg38:100,821,039–119,725,923 with a maximum LOD score of 4.38 (green line).
(C) Heterozygous variant c.20+544G>T (chr8.hg38:101,493,333G>T) identified by WGS, located in intron 1 of *GRHL2* (GenBank: NM_024915; Ensembl: ENST00000251808.7), was confirmed by Sanger sequencing.
(D) Boxed region on chr8 depicts the PPCD4 linked interval, and the position and exon structure of the *GRHL2* gene (5′ to 3′) and intronic mutation are shown.

disrupted balance of cell state transition regulators OVOL2 and ZEB1 within the diseased corneal endothelial cells could result in cellular *trans*-differentiation of the corneal endothelial cells into an epithelial-like state through the MET pathway.[2,10,14,21,22] This hypothesis is supported by multiple studies demonstrating the epithelial-like phenotype of endothelial cells in PPCD, including histopathological and transcriptomic studies,[1,5,6,21,22] and is likely a consequence of gene mutations specifically affecting corneal endothelial cells.

Despite these recent advances in our understanding of the molecular basis of PPCD, there is evidence for further genetic heterogeneity of PPCD.[12,21,23] Here, we describe an additional PPCD locus, PPCD4, which was mapped to 8q22.3–q24.12, and the subsequent identification of causative non-coding variants in *GRHL2* with further evidence for the importance of MET in PPCD.

Material and Methods

Study Subjects and Clinical Examination

All participants signed informed consent approved by the ethics committee of the General University Hospital in Prague (reference no. 151/11 S-IV) or Moorfields Eye Hospital (REC references 13/LO/1084 and 09/H0724/25) before inclusion in the study. Ophthalmic examination included best corrected distance Snellen visual acuity (BCVA) converted to decimal values, intraocular pressure, slit-lamp biomicroscopy and specular microscopy (Noncon ROBO Pachy SP-9000; Konan Medical Inc.) and spectral-domain optical coherence tomography (SD-OCT) (Spectralis; Heidelberg Engineering GmbH). Genomic DNA was extracted from venous blood samples using a Gentra Puregene blood kit (QIAGEN) or from saliva using a Oragene kit (Oragene OG-300, DNA Genotek).

Linkage Analysis

Linkage analysis was performed using selected individuals from family C15 (Figure 1A). Nine affected (VI:2, VI:4, VII:1, VIII:1, VIII:3, VII:7, IX:1, IX:3, IX:6) and seven unaffected samples (VII:2, VII:3, VIII:2, VIII:4, IX:2, IX:4, IX:5) were genotyped using an Illumina Omni2.5 Exome-8 array. Parametric linkage analysis, assuming dominant inheritance of a fully penetrant rare allele (disease allele frequency 0.00001) was performed using MERLIN.[24] The following criteria were applied to select markers for linkage: only polymorphic SNPs with annotated rs numbers were analyzed, Mendelian inconsistent SNPs or SNPs with missing alleles were discarded, a SNP density of 0.1 cM was maintained.

Whole-Exome Sequencing (WES)

WES was performed using a TruSeq exome enrichment kit (Illumina) and Illumina HiSeq2000 sequence platform on DNA samples of affected individuals VIII:1, VI:7, VII:6, and VII:10 from family C15, and using a SureSelect Human All Exon 50Mb Kit (Agilent) and Illumina HiSeq2000 sequence platform for individuals V:18, VI:13, VI:14. VI:15, VII:8, VII:9, and VIII:5. Reads were aligned to the GRCh38/hg38 human reference sequence with Novoalign v.2.05 (Novocraft). The WES data were analyzed using the Phenopolis platform.[25] ExomeDepth was used to identify copy-number variants (CNVs).[26] Aligned data were visualized with the Integrated Genomics Viewer (IGV, Broad Institute). On the basis that PPCD is a rare dominant disease, WES data were filtered for rare variants with a minor allele frequency (MAF $\leq$ 0.005 according to ExAC) in family C15 and a control WES dataset generated from 20 unrelated individuals of Czech origin (National Centre for Medical Genomics).

Whole-Genome Sequencing (WGS)

Four distantly related affected individuals (VI:7, VI:9, VII:8, and VIII:1) from C15 were analyzed by WGS using a TruSeq Nano DNA library preparation kit and a HiSeq X Ten sequencer (Illumina). Reads were aligned to the GRCh38/hg38 human reference sequence with Novoalign v.2.05 (Novocraft). Variant calling was performed with GATK HaplotypeCaller[27] and annotated using the Variant Effect Predictor (VEP)[28] which provides allele frequency annotation in various control datasets, predicts the effects of variants on nearby transcripts, and reports the potential regulatory role for non-coding regions.

Sanger Sequencing of Potential Regulatory Regions of *GRHL2*

For unsolved PPCD-affected case subjects, a region of 2,728 bp (chr8 hg38:101,491,361–101,494,128) encompassing potential regulatory regions of *GRHL2*, including the 5′ untranslated region (UTR), exon 1, and partial intron 1 (Figure S1), was amplified by PCR (GoTaqGreen, Promega, primers and conditions available on request) and Sanger sequenced using BigDye terminator sequencing on an ABI PRISM 3100 Genetic Analyzer (Applied Biosystems). *GRHL2* variants associated with disease have been submitted to ClinVar.

In Silico Analysis of Variants

In addition to the annotation data provided by the VEP, variants of interest were also analyzed by splice site prediction tools Human Splicing Finder,[29] NNSPLICE,[30] MaxEntScan,[31] and NetGene2.[32] ENCODE (Encyclopedia of DNA elements) data were manually interrogated using IGV for transcription factor binding in the genomic region of interest containing candidate variants.[33] The effect of variant on transcription factor binding was predicted by Alibaba 2.1[34] and MatInspector.[35] Alibaba 2.1 predicts transcription factor binding sites in an input nucleotide sequence using binding sites collected from TRANSFAC.[36] MatInspector predicts transcription factor binding sites using a library of weight matrices.

Cell Culture, RNA Extraction, and RT-PCR

RNA was extracted from whole corneal buttons donated after enucleation surgery for posterior segment melanoma and cell cultures, using an RNeasy Extraction Kit (QIAGEN). Primary endothelial cells were expanded and cultured as previously described.[2] An immortalized human corneal endothelial cell line, B4G12, was cultured according to published protocols.[37] Normal donor corneoscleral rims stored in Optisol (Chrion Ophthalmics) were obtained from Moorfields Lions Eye Bank, and limbal epithelial stem cells (HLEC/HLE-S) and stromal fibroblasts (SF) were isolated and cultured as previously described.[38] HEK293 cells were cultured with standard reagents and conditions. cDNA was reverse transcribed using oligo(dT) priming with a Tetro cDNA synthesis kit (Bioline). *GRHL2* was amplified with intron-spanning primers from exon 4 to exon 8 forward 5′-GCGCC TATCTCAAAGACGAC-3′ and reverse 5′-CGTCCCAGGTAAAGGA AACA-3′ and beta actin was amplified using primers forward 5′-CTGGGACGACATGGAGAAAA-3′ and reverse 5′-AAGGAAG GCTGGAAGAGTGC-3′.

Histology and Immunostaining

Cornea tissue from individual III:1 (age 8.5 years) from family C23 removed during penetrating keratoplasty was fixed in 10% neutral-buffered formalin. The sample was then processed into paraffin wax and 5-μm sections were cut. Sections were stained with tinctorial haematoxylin and eosin (H&E) using conventional methods.

A second cornea removed from individual II:1 (age 41 years) from family C23, also during penetrating keratoplasty, and a control cornea (Miracles In Sight Inc.) were embedded in optimal cutting temperature compound and snap frozen. Tissue sections were then cut to 4-μm thickness using a cryostat, thaw-mounted onto histological slides, and air-dried for 30 min. Immunostaining was performed manually using the Bond Polymer Refine Detection kit (DS9800, Leica). Sections were fixed for 10 min in acetone followed by 10 min in methanol. After washing with distilled water, a peroxidase block was used for 30 min to quench any endogenous peroxidase activity, followed by three washes with Tris-based saline 0.1% (v/v) Tween (TBS-T). Immunodetection of proteins of interest was carried out with the following primary antibodies: rabbit anti-GRHL2 (1:100, HPA004820, Sigma Aldrich), rabbit anti-N-cadherin (1:300, ab18203, Abcam), mouse anti-E-Cadherin (1:200, M3612, Dako), and human anti-Cytokeratin 7 (CK7, 1:2,000, M7018, Dako) for 1 hr at 37°C. Subsequently tissue sections were washed three times with TBS-T and incubated with post-primary linker IgG for 15 min for localization of mouse antibodies followed by three washes with TBS-T and incubation with poly-HRP IgG for 30 min for localization of rabbit antibodies. After three washes with TBS-T and distilled water, staining was visualized with 3,3′-diaminobenzidine tetrahydrochloride hydrate (DAB), washed, and counterstained with Mayer's Haematoxylin to allow the visualization of nuclei. Tissue sections were then dehydrated in graded ethanol and in xylene prior to mounting with DPX mounting medium.

H&E staining was performed using a Leica Autostainer XL with integrated coverlipper (CV5030). Staining was visualized using a Nikon Eclipse 80i microscope equipped with a DXM1200C digital camera. Images of corneal sections were taken using the same magnification between the control and diseased tissue.

Luciferase Assay

Primers were designed to amplify a genomic region that encompasses potential *GRHL2* regulatory regions, spanning all variants of interest. A 2,728-bp product (chr8:101,491,361–101,494,128) containing upstream sequence, exon 1, and partial intron 1 of

Table 1. Unique Variants within the PPCD4 Locus, chr8.hg38:100,821,039–119,725,923, Identified by WGS in Family C15

Variant No.	Coordinates (hg19)	Coordinates (hg38)	Reference Allele	Observed Allele	Location	Closest Transcript	CADD score	Allele Count/Total Alleles Screened				
								Kaviar	gnomAD	1000G	UK10K	GoNL
1	102,121,864	101,109,636	C	T	intergenic	–	7.875	0/26,378	0/30,978	0/5,007	0/7,562	0/998
2	102,505,561	101,493,333	G	T	intronic	*GRHL2*	10.76	0/26,378	0/30,978	0/5,007	0/7,562	0/998
3	115,648,021	114,635,792	A	T	intergenic	–	6.33	0/26,378	0/30,978	0/5,007	0/7,562	0/998

Three novel variants were identified within the mapped PPCD4 locus from four WGS datasets (C15; VI:7, VI:9, VII:8, VIII:1) filtered by (1) removal of all variants located outside refined locus, (2) all variants with a MAF ≥ 0.005 in publicly available Kaviar, gnomAD, 1000G, UK10K, GoNL datasets, and (3) that were shared between the four affected individuals. Abbreviations are as follows: Kaviar, Kaviar Genomic Variant database; gnomAD, The Genome Aggregation Database; 1000G, 1000 Genomes Project; UK10K, UK10K Rare Genetic Variants in Health and Disease; GoNL, Genomes of the Netherlands. One variant (G>T) is within the *GRHL2* gene (intronic) whereas the remaining two were intergenic.

the *GRHL2* gene (Figure S1) was amplified from control genomic DNA, cloned into pGEM-TEasy (Promega) and sub-cloned into the promoter-less firefly luciferase reporter vector pGL3-Basic (Promega). Primers used for cloning incorporated KpnI and *Nhe*I restriction site to facilitate subcloning (forward 5′-GGTACCCA AGCTTTCCACGTCCTCC-3′ and reverse 5′-GCTAGCCAAAGTTA CCGGGGAAAGCAA-3′). Variants identified in PPCD4-affected individuals were introduced by site-directed mutagenesis using a Q5 Site-Directed Mutagenesis Kit (New England Biolabs) and all constructs were verified by Sanger sequencing. Wild-type or mutant *GRHL2* promoter pGL3-Basic plasmids (90 ng) were used to co-transfect HEK293 cells with 10 ng of pRL-CMV (CMV-promoter driven *Renilla* luciferase reporter, Promega) using TransIT-LT1 transfection reagent (Mirus). At 24 hr post-transfection, luciferase activity was measured using an Orion L Microplate Luminometer (Titertek Berthol) and a dual-luciferase reporter assay system (Dual-Glo Luciferase Assay System, Promega).

Results

Defining a New Locus for Autosomal-Dominant Posterior Polymorphous Corneal Dystrophy (PPCD4)

In a large autosomal-dominant PPCD-affected family of Czech origin (C15, Figure 1A), targeted Sanger sequencing did not identify any likely disease-associated variants within established PPCD-associated genes, including the *OVOL2* promoter region.[11,23] Furthermore, quantitative real-time PCR and Illumina HumanOmniExpress BeadChip SNP array analysis did not detect CNVs encompassing known PPCD-associated genes.[10] Therefore, we performed WES using DNA samples from affected (VIII:1, VI:7, VII:6, VII:10, V:18, VI:13, VII:8, VIII:5) and unaffected (VI:14, VII:9, VI:15) individuals from family C15. WES data were filtered for rare variants in affected individuals that were absent from unaffected individuals; no potential mutations were identified. We therefore considered that an additional PPCD locus and/or a variant not captured by WES might be causative in this family.

We therefore defined the locus segregating with disease in family C15 through linkage analysis by genotyping nine affected and seven unaffected individuals from a large branch of family C15 (Figure 1A). A single locus was identified, chr8. hg38:100,821,039–119,725,923, spanning chromosome 8q22.3–q24.12, with a maximum LOD score of 4.38 (Figure 1B), thereby delineating a locus for PPCD (PPCD4).

Identification of a Rare Non-coding *GRHL2* Variant in the Index PPCD4-Affected Family

Next, we performed WGS in four distantly related affected individuals from family C15 (Figure 1A) and filtered for variants located within the PPCD4 locus (chr8.hg38:100,821,039–119,725,923) that were shared between all four affected individuals. We filtered our WGS datasets to exclude all variants that have a MAF ≥ 0.005 in the gnomAD, Kaviar, 1000G, GoNL, and UK10X datasets. Using this approach, three unique variants were identified in the linkage region that were confirmed by Sanger sequencing (Table 1). Two variants were intergenic, and one variant occurred within intron 1 of *GRHL2*. We found no bioinformatic evidence to implicate the intergenic variants in regions of active promoters or enhancers. In contrast, c.20+544G>T (chr8.hg38:101,493,333G>T), located in intron 1 of *GRHL2*, maps to a promoter region for this gene (ENSR00000228091), reflected in the CADD score (Figures 1C and 1D; Table 1).

To further delineate the PPCD4 locus in family C15, rare variants filtered from WGS data, including the c.20+544G>T variant in intron 1 of *GRHL2*, were genotyped and assessed for segregation in the extended pedigree by Sanger sequencing. Importantly, additional recombination events were identified in family C15 that further refined the PPCD4 locus to between chr8.hg38:101,411,163 and 109,214,442 excluding the two intergenic variants as candidates (Figure S1).

Interrogation of ENCODE data to identify potential enhancer and promoter regions of *GRHL2* revealed a cluster of transcription factor binding sites upstream of *GRHL2*, and spanning the 5′ UTR, first exon, and partial region of intron 1. The transcription factor binding prediction tools MatInspector and AliBaba 2.1 predict that the c.20+544G>T variant disrupts binding sites, leading to loss, or gain, of multiple transcription factors that are expressed in the corneal endothelium (Table 2 and Figure S1). Further analysis of c.20+544G>T in ENCODE data (Ensembl) identified this precise base location in intron 1 as a bivalent histone modification site, with

Table 2. Three *GRHL2* Intron 1 Variants Associated with PPCD4

							Open Chromatin/Methylation Marks		
Coordinates (hg19)	**Coordinates (hg38)**	**HGVS**	**CADD Score**	**Family**	**TF Gained**	**TF Lost**	**H1ESC**	**NHDF-AD**	**NHEK**
102,505,274	101,493,046	c.20+257delT	6.62	B4	POC/Zinc finger proteins, STAT6	EBF1	CTCF DNase1 H3K4me1	DNaseI H3K36me3H3K9ac	CTCF DNaseI H3K4me1 H3K9ac
102,505,150	101,492,922	c.20+133delA	13.23	B5	GLI3, ZBTBZA	ZNF354C	DNaseI H3K4me1 H3K4me3 H3K9ac	DNaseI H3K9ac	CTCF H3K4me1 H3K9ac
102,505,561	101,493,333	c.20+544G>T	10.76	C15 C23 C26 C33	ESRRA GLIS1 E2F3	SP1 NRF1 MYC E2F2 AHR	CTCF DNaseI H3K4me1	CTCF H3K4me1	CTCF DNaseI H3K4me3 H3K9ac

Three novel regulatory region variants in *GRHL2* identified in British and Czech families. Variants were located in intron 1 of *GRHL2*, identified by WGS (C15, C23, C33, C26) or targeted sequencing (B4, B5). All three variants are absent from public databases (Kaviar, gnomAD, 1000G, UK10K, GoNL datasets), have high CADD scores, are predicted to gain or lose binding sites for TFs expressed in corneal endothelium, and fall in peaks for open chromatin or methylation marks associated with gene regulation for different cell lines. Abbreviations are as follows: H1ESC, human embryonic stem cells; NHDF-AD, adult dermal fibroblasts; NHEK, normal human epidermal keratinocytes; CTCF, CCCTC-binding factor; DNaseI, deoxyribonuclease I; H3K9ac, H3 lysine 9 acetylation; H3K4me, H3 lysine4 monomethylation; H3K4me3, H3 lysine 4 trimethylation; H3K36me3, H3 lysine 36 trimethylation.

histone H3 lysine 4 trimethylation (H3K4me3) and histone H3 lysine 27 trimethylation (H3K27me3) modifications in different cell types, which are associated with gene activation and repression, respectively[39,40] (Table 2 and Figure S2). In addition, this location marks a DNase I hypersensitive site and CTCF binding site, commonly associated with accessible chromatin and transcription factor binding and for forming local chromatin loops necessary for the tethering of promoters with associated regulatory elements, respectively[41,42] (Table 2 and Figure S2).

GRHL2 is a member of a highly conserved family of transcription factors, with an essential role during epithelial differentiation and suppression of EMT.[14,43] GRHL2 acts as a direct transcriptional repressor of *ZEB1*.[44] Furthermore, GRHL2 is also thought to *trans*-activate *OVOL2* expression, forming a signaling network that regulates EMT and stabilizes epithelial specific gene expression.[45] Given the role of *ZEB1* haploinsufficiency and potential inappropriate ectopic expression of *OVOL2* in the pathogenesis of PPCD, the c.20+544G>T variant in *GRHL2* represented an outstanding candidate disease-causing variant in family C15.

Targeted Screening of *GRHL2* Regulatory Regions in Unsolved PPCD-Affected Families

Given that the c.20+544G>T variant lies within a regulatory region of *GRHL2*, a 2,728-bp region encompassing the 5′ UTR, exon 1, and partial intron 1 of *GRHL2* containing predicted regulatory regions and transcription factor binding sites (Figure S2), was therefore PCR amplified and Sanger sequenced in unsolved PPCD cases. The same variant, c.20+544G>T, was identified in three additional families of Czech origin (C23, C26, and C33, Figure 2). None of the probands were knowingly related to the original pedigree or to each other. In two families (C23 and C26), the variant was shown to segregate with disease; however, in family C33 the proband was the only affected individual, and the variant was absent in both parents (Figure 2). Paternity testing[3] confirmed the identity of the proband's biological father, thereby suggesting that the variant occurred *de novo* in this individual.

To investigate potential ancestral haplotypes in families of Czech origin, rare variants identified in the WGS data from family C15 that refined the PPCD4 locus were genotyped by Sanger sequencing. The same mini-haplotype was identified in families C23 and C26, with an additional recombination event refining the haplotype (chr8.hg38:101,411,163–102,437,115), suggesting that the *GRHL2* variant in these families arose in a common ancestor (Figure S1). This analysis also confirmed the lack of an ancestral haplotype in family C33, further supporting the finding that this variant arose independently.

Screening the 2,728-bp *GRHL2* region in 19 genetically unsolved, unrelated PPCD-affected case subjects from the UK cohort identified two further variants. A single-nucleotide deletion c.20+257delT (chr8.hg38:101,493,046del; Figure 2) in intron 1 of *GRHL2* was identified in a proband from family B4 (Table 2). In family B5, a 1-bp deletion, also situated within the first intron of *GRHL2*, c.20+133delA (chr8.hg38:101,492,922del), was identified in the proband (II:4) and her affected brother (II:1) and was absent in her unaffected sister (II:6) (Figure 2 and Table 2). Both variants were absent from the control databases gnomAD, Kaviar, 1000G, GoNL, and UK10X (Figure 2 and Table 2).

To further verify the pathogenicity of the *GRHL2* variants (Table 2), a genomic region encompassing the Czech c.20+544G>T variant and the two other variants identified in individuals with PPCD, was Sanger sequenced in 210 Czech control samples (420 alleles). None of the PPCD-associated variants were detected in the control cohort. Interestingly, only a single heterozygous variant (rs548346355) was identified in a single individual in the control cohort, suggesting that this region is a highly conserved region. Similar to the variant identified in the Czech families, the c.20+257delT and c.20+133delA variants occur within regions rich in transcription factor

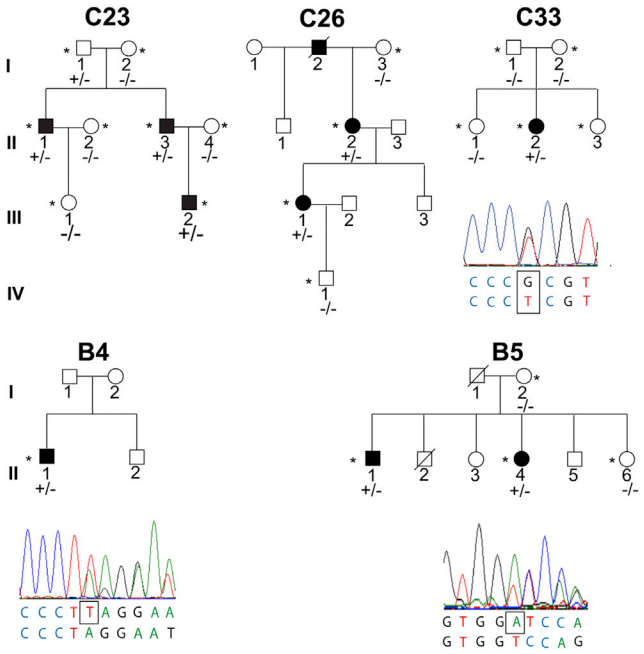

Figure 2. Additional PPCD-Affected Families with *GRHL2* Regulatory Region Mutations

Presence of a *GRHL2* variant, shown in the electropherograms, is indicated by +/− in each family and absence by −/−. The heterozygous variant in intron 1 of *GRHL2*, c.20+544G>T, was found to segregate with disease in families C23 and C26 of Czech origin who share an ancestral haplotype with C15. The same mutation was identified in an affected individual in family C33 that occurred *de novo*. Two other mutations in intron 1 of *GRHL2* were identified; a 1-bp deletion, c.20+257delT (chr8.hg38:101,493,046delT), was identified in the proband in family B4, and a 1-bp deletion, c.20+133delA (chr8.hg38: 101,492,922delA), in affected individuals in family B5. *GRHL2* variants are annotated according to transcript GenBank: NM_024915 and Ensembl ENST00000251808.7.

binding sites, DNase I, CTCF sites, and histone modification domains identified by interrogating ENCODE data (Table 2 and Figure S3). All PPCD4-associated variants are predicted (MatInspector and AliBaba 2.1) to result in the gain, or loss, of binding of at least one transcription factor expressed in the corneal endothelium (Tables 2 and S1, Figure S3).

Clinical Characterization of PPCD4

In this cohort, PPCD4 was found to display both inter- and intra-familial phenotypic variation. In the 27 affected individuals from families of Czech origin, harboring the same *GRHL2* mutation, 26 had typical corneal signs of PPCD, with an irregular posterior corneal surface and occasional opacities of variable size and shape clinically described as bands or geographic or vesicular lesions (Figures 3A, 3B, and 3G). The disease presented subjectively as blurred vision due to corneal edema in four individuals (Figure 3D). In two children, corneal edema and associated irritation of the eye was noted at 2 and 3 months after birth. Five individuals initially presented with a diagnosis of secondary glaucoma, either during a regular check-up, familial screening, or due to the development of corectopia (Figure 3C), prompting a visit to an eye specialist. Five individuals had low vision in one or both eyes since childhood and have not reported subsequent major changes of their visual function. One subject noticed decrease in visual acuity in the second decade of life. Nine individuals were asymptomatic at their last examination, and in one individual, information about the subjective onset was not available.

At the last follow-up, best corrected visual acuity ranged from 1.0 bilaterally in five individuals to light perception in a 55-year-old male with secondary glaucoma and bullous keratopathy. Corneal transplantation was performed in 7 out of 27 (25.9%) individuals, and of these, 3 had bilateral surgery. The mean age of the first surgery was 34.9 ± 17.9 years (range 8.5 to 59 years). Glaucoma was diagnosed in seven individuals (25.9%), unilaterally in one male. The mean age of a diagnosis of glaucoma was 46.4 ± 17.1 years (range 20 to 63 years), but two subjects developed glaucoma after penetrating keratoplasty, and in these individuals, glaucoma may have been precipitated by surgery. Two subjects had an enucleation of a painful blind eye, one at the age of 25 years and the second at 70 years. Corectopia was noted in four eyes of three individuals and was associated with secondary glaucoma in all case subjects. Secondary corneal calcification (band keratopathy) developed bilaterally in two individuals (Figure 4C).

Specular microscopy and SD-OCT imaging documented a reduced endothelial cell density, with both normal and abnormal morphology and irregularities of the posterior corneal surface (Figures 3I–3K). In a 79-year-old individual, the disease status was unknown because the corneal periphery was obscured by age-related stromal haze. Although the corneal center was clear, the endothelial cell density count was 1,295 cells/mm^2 in the right eye and 1,309 cells/mm^2 in the left eye (normal range 2,400–2,600 cells/mm^2).[46] H&E staining of a full-thickness corneal sample (individual III:2, family C23) revealed an oedematous cornea with variation in endothelial cell size and shape and focal multilayering of the cells (Figure 3H).

The proband of B4 had an unusually prominent fold of Descemet membrane (Figure 3E). There was no family history of eye disease and the other family members were unavailable for examination.

Proband B5 (II:4) had markedly asymmetric disease with diffuse geographic endothelial changes restricted to her left eye (Figures 3A and 3F). She also had left amblyopia and a decompensated left exotropia. Intraocular pressures were normal in both eyes and there were no iris abnormalities. The endothelial cell density was markedly reduced in her affected eye (871 cells/mm^2) compared to 3,165 cells/mm^2 in her right eye. Her brother (II:1) carried the same *GRHL2* variant but had a significantly different phenotype. Although the endothelial cell count was lower than expected (1,900 cells/mm^2 both eyes), there were no changes in cell morphology. Notably, numerous elevated

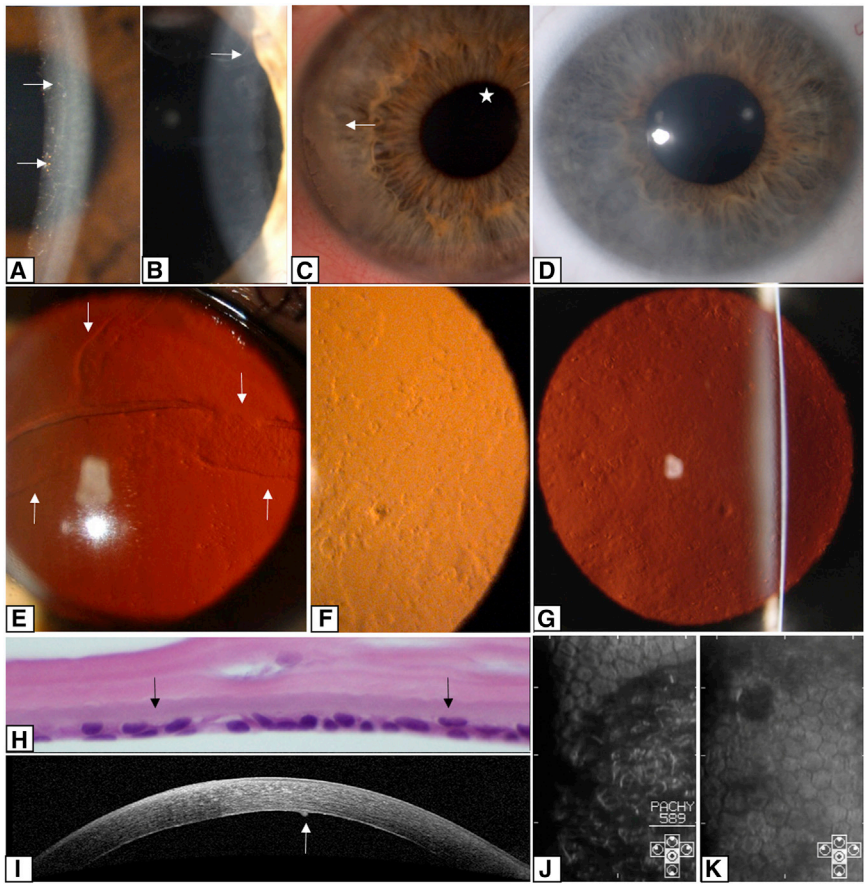

Figure 3. Corneal Disease Associated with Regulatory Region Mutations in *GRHL2*

(A) Lines and vesicules (arrows) seen on oblique illumination in the left cornea of individual II:4 from family B5 (age 30 years).

(B) A prominent posterior corneal line (arrow) seen on oblique broad-beam illumination of individual II:3 from family C23 (age 46 years).

(C) Subepithelial calcium deposition (arrow) and corectopia (asterisk) in the right eye of individual VII:6 from family C15 (age 29 years).

(D) Diffuse corneal stromal haze seen on direct illumination in individual III:2 from family C23 (age 11 years).

(E–G) Retroillumination of the cornea to show bands (arrows) and vesicular and geographic shaped lesions. Shown are (E) right cornea of individual II:1 from family B4 (age 53 years), (F) left cornea of individual II:4 from family B5 (age 30 years) showing irregularity of reflex from scattered lesions at the posterior corneal surface, and (G) left cornea of individual VI:9 from family C15 (age 58 years).

(H) Histological specimen of central corneal section from individual III:2 from family C23 (age 8.5 years) (H&E, magnification 600×); endothelial cells have formed a double layer (arrows).

(I) SD-OCT cross-section of the right cornea of individual VI:9 from family C15 (age 58 years) shows increased reflectivity of the posterior corneal layers with a protrusion of Descemet membrane (arrow).

(J and K) Specular microscopy images showing regional variation in the size and shape of the endothelial cells: (J) right eye of individual VIII:3 from family C15 (age 37 years) and (K) left eye of individual II:2 from family C33 (age 5.5 years). The dark areas correspond to areas displaced from the plane of specular reflection, presumably caused by protrusions and irregularities of the posterior corneal surface.

Hassal-Henle bodies were present in the far periphery of the cornea.

Expression of *GRHL2* in Healthy and Diseased Corneal Endothelium

Our interrogation of publicly available RNA-seq data from healthy adult and fetal human corneal endothelial tissue revealed no evidence of *GRHL2* expression[47] (Figure S4A). Examination of additional publicly available RNA-seq data also confirmed lack of *GRHL2* expression in corneal stromal cells, whereas high levels of expression were detected in the corneal epithelium[48] (Figure S4A). We therefore further defined corneal expression of *GRHL2* in cultured cells by RT-PCR and the distribution of GRHL2 in corneal tissue by immunohistochemistry (IHC).

GRHL2 expression was detected in cultured human corneal epithelial cells derived from limbal epithelial stem cells and in a spontaneously immortalized human corneal epithelial cell line with progenitor-like characteristics, but was absent in corneal endothelial tissue, an immortalized cell line of human corneal endothelial origin, and stromal fibroblasts by RT-PCR (Figure S4B).

GRHL2 encodes a transcription factor that is a direct transcriptional repressor of *ZEB1*.[49] Given this role, in addition to the lack of *GRHL2* expression in the corneal endothelium, we hypothesized that the putative regulatory mutations could lead to inappropriate transcriptional activation and ectopic expression of *GRHL2* in the corneal endothelium, similar to the mechanism we proposed for the variants in *OVOL2*.[2] To explore this hypothesis further, a full-thickness corneal sample from individual II:1 from family C23, with the *GRHL2* c.20+544G>T variant, was analyzed by IHC and compared to control tissue. First, we tested for presence of GRHL2 in different cell layers. GRHL2 was detected in the nuclei of epithelial cells in control tissue, consistent with its role as a transcription factor, and was absent from the stroma and endothelium, concordant with the transcriptomic data (Figure 4A). Strikingly, in the diseased cornea, endothelial cell nuclei were positive for GRHL2, suggesting that the c.20+544G>T *GRHL2* variant induces ectopic expression of *GRHL2* resulting in detection of GRHL2 protein in the corneal endothelium.

Differences in the levels of epithelial, mesenchymal, and endothelial markers were also observed between the diseased and control endothelial cells (Figure 4C). N-Cadherin, which is normally detected in corneal endothelial and epithelium cells,[50,51] was detected in the control endothelium and the diseased tissue (Figure 4C). In contrast,

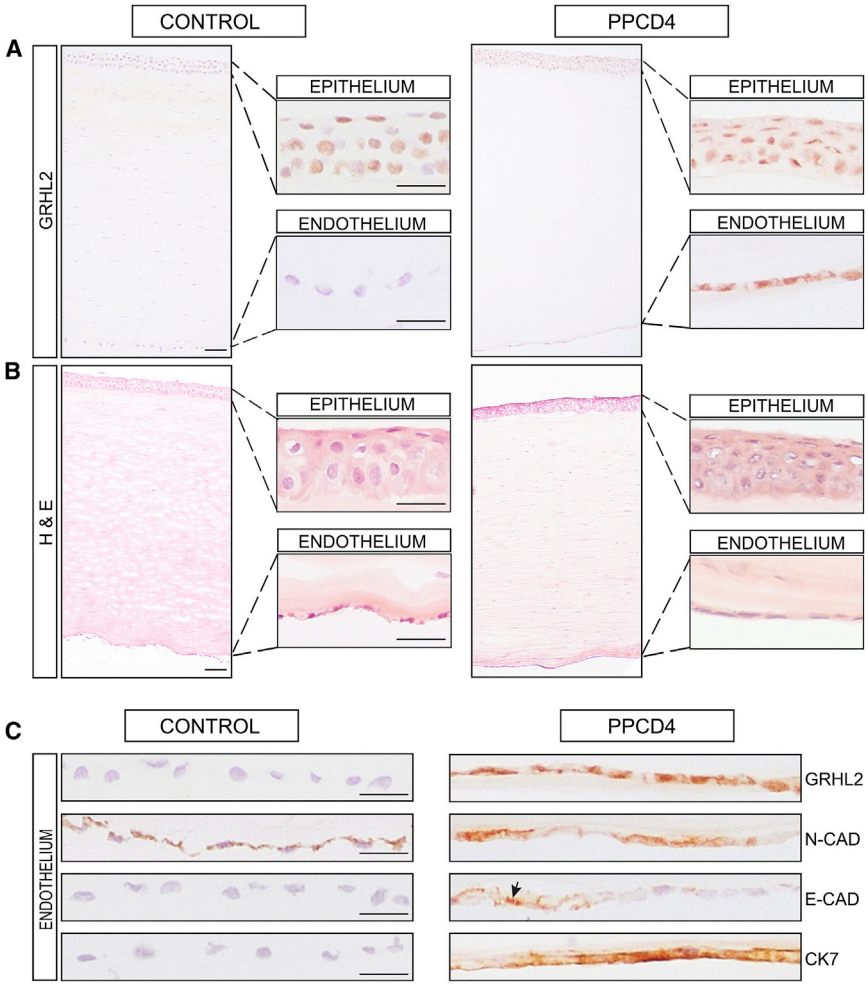

Figure 4. Immunohistochemistry of a PPCD4 Diseased Cornea Reveals GRHL2 Immunoreactivity and Cell State Transition in the Corneal Endothelium

(A) Full thickness corneal tissue from control (left) and affected (right) individual with a c.20+544G>T *GRHL2* mutation (II:1 family C23) were stained with anti-GRHL2. Magnified images of the epithelium and endothelium are shown in insets. GRHL2 is detected in the nuclei of control and PPCD4 corneal epithelial cells but is absent in the control endothelium. In contrast, GRHL2 is also detected in the nuclei of the PPCD4 endothelial cells.

(B) H&E staining showing integrity of full-thickness corneal sections for the diseased and control samples.

(C) Magnified images of control and PPCD4 endothelial cells stained for GRHL2 and corneal epithelial and endothelial markers N-Cadherin (N-CAD), E-Cadherin (E-CAD), and Cytokeratin 7 (CK7). GRHL2 is localized in the nuclei in diseased endothelial cells. N-Cadherin was detected in control endothelial tissue and in the diseased endothelium. E-cadherin was negative in control endothelium but is expressed in the diseased endothelial tissue (arrowhead) with some areas of negative staining. CK7 was positive in the diseased endothelium and negative in the control sample. All sections were counterstained with Mayer's hematoxylin to identify nuclei. Scale bar 50 μm.

E-Cadherin, a component of adherens junctions and marker of epithelial cell status, is not detected in healthy corneal endothelium;[47,50] however, regions of positive staining for E-Cadherin were evident in the PPCD4 endothelium, which was negative in the control, indicating that the cells had diverged from their normal identity (Figure 4C). This upregulation of E-Cadherin is consistent with cells undergoing MET.

Previous IHC studies of PPCD1 and PPCD3 samples have shown inappropriate positive staining for keratins in diseased tissue.[5] CK7, a marker of corneal epithelial cells, was positive in the diseased endothelium and negative in the control sample (Figure 4C). Collectively, these data indicate that the PPCD4 endothelial cells were in transition to an epithelial-like cell type or had already diverged. We hypothesize that this diseased cell state transition is due to ectopic expression of *GRHL2* in the corneal endothelium, induced by the c.20+544G>T variant.

Promoter Mutations Result in Increased Expression of *GRHL2*

Given the striking ectopic detection of GRHL2 in diseased PPCD4 corneal endothelial cells (Figure 4), and that *in silico* analysis of all three PPCD4 variants identified are predicted to alter transcriptional activity (Table 2 and Figure S3), we experimentally tested how each of these variants alter *GRHL2* promoter activity *in vitro*. A 2,728-bp fragment encompassing the position of all three variants and predicted surrounding regulatory regions was cloned into a promoter-less firefly luciferase reporter vector. The PPCD4-associated variants were independently introduced by site-directed mutagenesis. HEK293 cells were co-transfected with each of the *GRHL2* promoter constructs to test promoter activity, in combination with *Renilla* luciferase for normalization purposes. The wild-type *GRHL2* construct was an active promoter region driving expression of firefly luciferase (Figure 5). Each of the three *GRHL2* PPCD4-associated mutations were found to significantly ($p \leq 0.001$) increase the promoter activity of the region compared to the wild-type sequence (Figure 5).

Discussion

In this study we identified a locus for autosomal-dominant PPCD, PPCD4, on chromosome 8q22.3–q24.12. WGS

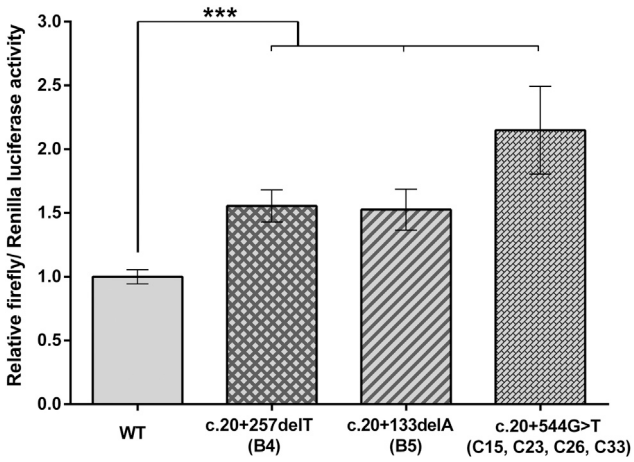

Figure 5. Intron 1 of *GRHL2* Is Transcriptionally Active and PPCD4 Mutations Cause Increased Promoter Activity *In Vitro*
A dual-luciferase reporter assay was used to determine whether intron 1 of *GRHL2* had promoter activity and the effect of PPCD4 mutations. HEK293 cells were co-transfected with pRL-CMV (*Renilla* luciferase) and pGL3-basic (firefly luciferase) containing 2,728 bp of the wild-type or respective *GRHL2* promoter sequence mutants. Wild-type activity was normalized to 1, and the relative luciferase activity of all mutants was expressed with respect to the wild-type. All PPCD4-associated *GRHL2* variants significantly increased the relative luciferase activity. Data represent a minimum of three independent biological replicates in triplicate. Error bars represent ±1 SD. p values were calculated by one-way ANOVA (***$p \leq 0.001$).

revealed three unique non-coding variants within the linked region in the index family (C15), one of which, c.20+544G>T, mapped within a potential regulatory region of *GRHL2*. Additional recombination events were identified by genotyping in the extended family, that refined the PPCD4 locus (chr8.hg38:101,411,163–109,214,442) and excluded two of the variants, leaving c.20+544G>T as the outstanding candidate disease-causing variant.

The same variant was found in two additional unsolved PPCD-affected families of Czech origin that shared an ancestral haplotype with family C15. A *de novo* occurrence of this variant was identified in another PPCD-affected individual, suggesting that this is a recurrent mutation. Two further unique variants were found in intron 1 of *GRHL2* (c.20+257delT and c.20+133delA) in additional unrelated individuals affected with PPCD.

All three *GRHL2* mutations were located in a conserved uncharacterized regulatory region. We hypothesize that the mechanism of disease is similar to the mechanism we and others proposed for *OVOL2* promoter mutations that cause PPCD1, whereby mutations lead to an overactive promoter that drives inappropriate ectopic expression of *OVOL2* in the corneal endothelium.[2,12] To understand further how the promoter mutations affect expression of *GRHL2* in corneal endothelial cells and contribute to the pathogenesis of PPCD4, we performed IHC on a corneal sample from a PPCD4-affected individual. *GRHL2* is not normally expressed in the corneal endothelium *in vivo*; however, in PPCD4-diseased corneal tissue, we detect GRHL2 in the corneal "endothelium" supporting the hypothesis that the PPCD4 variants result in inappropriate activation and ectopic expression of *GRHL2*. Furthermore, we demonstrate that this putative regulatory region of *GRHL2* is transcriptionally active and that all PPCD4-associated variants significantly increased *GRHL2* promoter activity compared to wild-type.

Interestingly, mutations leading to presumed haploinsufficiency of *GRHL2* cause autosomal-dominant non-syndromic hearing impairment (DNFA28 [MIM: 608641])[52–54] and homozygous missense mutations have been associated with autosomal-recessive ectodermal dysplasia syndrome with hearing loss (ECTDS [MIM: 616029]).[55] None of the PPCD-affected individuals with *GRHL2* promoter mutations in our study reported hearing loss or other features of ectodermal dysplasia syndrome. This is not unexpected given that neither of the previously described *GRHL2*-associated disease mechanisms are predicted to result in the aberrant upregulation and ectoptic expression of *GRHL2*.

In addition to *GRHL2* in the PPCD4 corneal "endothelium," we also detected E-Cadherin and Cytokeratin 7, consistent with cellular state transition as the mechanism of disease for PPCD4, through the MET pathway. This is also consistent with the abnormal "endothelial" cell morphology detected in PPCD4-affected case subjects using specular microscopy and examination of histological sections.

GRHL2 has an important role in epithelial morphogenesis through *trans*-activation of genes required for the formation of the apical junctional complex and repression of EMT. In duct cells of the kidney, GRHL2 regulates lumen expansion and epithelial barrier formation by *trans*-activating *OVOL2* expression, which in turn activates the expression of E-Cadherin, claudin 4 (epidermal tight junctions), and Rab25 (apical trafficking).[56] OVOL2 maintains the transcriptional program of human corneal epithelium cells by repressing expression of mesenchymal genes such as *ZEB1*.[14,49] Similarly, GRHL2 is known to be a direct transcriptional repressor of *ZEB1*.[44] Importantly, haploinsufficiency of *ZEB1* causes PPCD3, and ectopic expression of *OVOL2* in the corneal endothelium caused by promoter mutations, leading to repression of *ZEB1* transcription, is the mechanism proposed for PPCD1[2,10,12,21] (Figure 6). Therefore, we propose that ZEB1, OVOL2, and GRHL2 form a finely balanced mutually inhibitory EMT/MET pathway that controls specific cell characteristics and intermediate cell states[13,14,49] (Figure 6).

In support of this proposed mechanism, a transcriptomic profile of PPCD corneal endothelial cells derived from a subject with PPCD3 harboring a pathogenic *ZEB1* mutation and a PPCD-affected individual with unknown molecular cause, with no potentially pathogenic variant detected in *ZEB1* or the *OVOL2* promoter using the

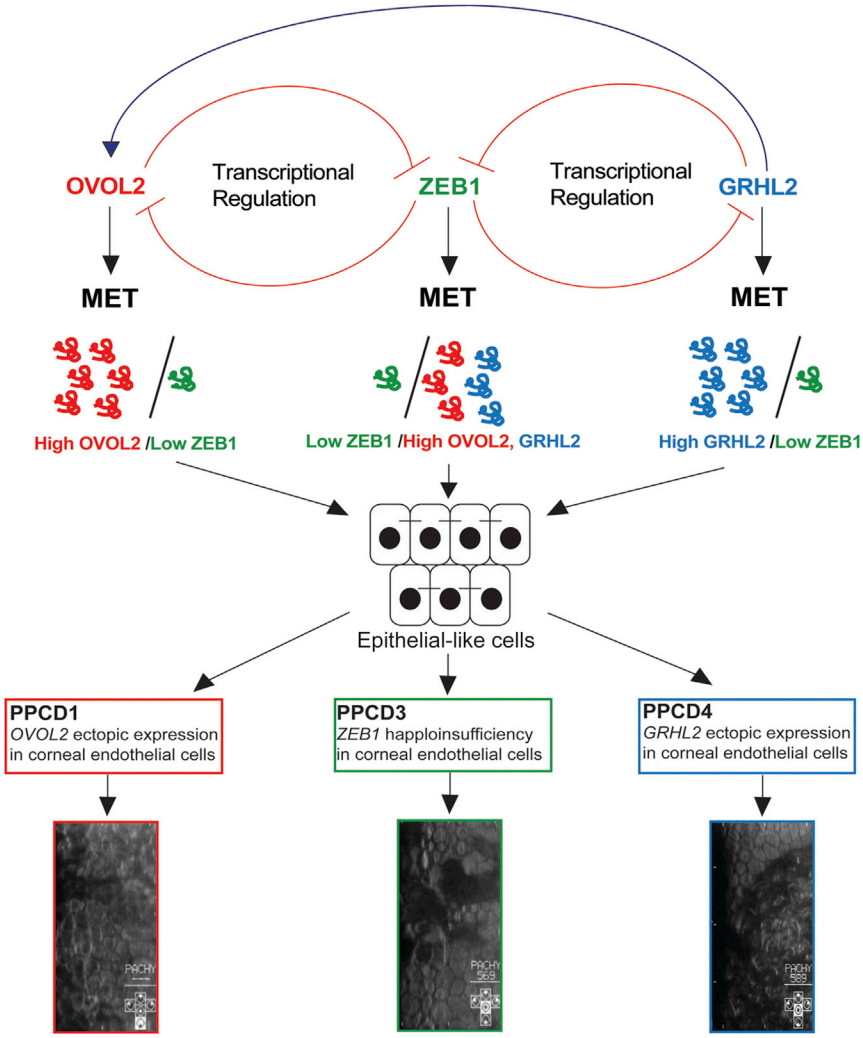

Figure 6. Schematic of Proposed Model of PPCD Pathogenicity

Epithelial-to-mesenchymal transition (EMT) and mesenchymal-to-epithelial transition (MET) are mediated by a precise regulation of transcription factors. ZEB1 promotes EMT and maintains the normal state of human corneal endothelial cells. OVOL2 and GRHL2 are direct transcriptional repressors of *ZEB1*. ZEB1 can also repress the expression of both of these genes, and this mechanism may maintain the cellular state of healthy corneal endothelial cells. In PPCD, mutations that cause haploinsufficiency and reduced expression of *ZEB1* and promoter mutations that drive ectopic expression of *GRHL2* or *OVOL2* in corneal endothelial cells are the proposed mechanisms that result in cell state transition through the MET pathway. GRHL2 activates the expression of *OVOL2*, so ectopic expression is predicted to also result in ectopic expression of OVOL2 and repression of ZEB1, driving corneal endothelium cells to transition to epithelial-like cells, presenting as stratified and irregularly shaped cells.

methods employed, revealed a significant decrease in *ZEB1* expression compared to controls.[21] Furthermore, transcriptomic data of the corneal endothelium of an individual with PPCD of undefined genetic cause identified *GRHL2* as the most differentially expressed gene (upregulated) compared to controls.[21]

Collectively, these data support the disease mechanism of ectopic expression of *GRHL2* in PPCD4 endothelial cells as a result of mutations in a regulatory region and that MET is a convergent pathogenic mechanism leading to intermediate cell states and dysfunction of the endothelial barrier and disease in PPCD (Figure 6).

Accession Numbers

GRHL2 variants associated with disease have been submitted to ClinVar.

Supplemental Data

Supplemental Data include four figures and one table and can be found with this article online at https://doi.org/10.1016/j.ajhg.2018.02.002.

Acknowledgments

We thank all the families for participating in this research. This work was funded by awards from GACR 17-12355S (P.L., L.D., P.S.), Fight for Sight, the Rosetrees Trust, Moorfields Eye Charity (A.J.H., S.J.T., A.E.D., K.E.R.L., and C.J.E.), The Academy of Medical Sciences (A.E.D.), and the Wellcome Trust (M.E.C.). S.J.T., N.P., and A.J.H. were supported by the National Institute for Health Research Biomedical Research Centre based at Moorfields Eye Hospital NHS Foundation Trust and UCL Institute of Ophthalmology. Institutional support was provided by UNCE 204064 (P.L., L.D., S.K., V.S.) and Progres-Q26/LF1. P.S. was also funded by GAUK 250361/2017 and SVV 260367/2017 and S.K. and V.S. by grant 15-28208A from the Ministry of Health of the Czech Republic and the project LQ1604 NPU II from the Ministry of Education, Youth, and Sports of the Czech Republic.

We thank The National Center for Medical Genomics (LM2015091) for providing allele frequencies in an ethnically matched population (project CZ.02.1.01/0.0/0.0/16_013/0001634). This study was performed within the framework of ERN-EYE. The pGL3-Control vector was a kind gift from Dr. Stephanie Halford. We would like to thank Ales Horinek for paternity testing and Erik Kykal for basic bioinformatic analysis.

Received: December 15, 2017
Accepted: February 2, 2018
Published: February 22, 2018

Web Resources

1000 Genomes, http://www.internationalgenome.org/
Alibaba 2.1, http://gene-regulation.com/pub/programs/alibaba2/index.html
ClinVar, https://www.ncbi.nlm.nih.gov/clinvar/
dbSNP, https://www.ncbi.nlm.nih.gov/projects/SNP/
ENCODE, https://genome.ucsc.edu/ENCODE/
Ensembl Genome Browser, http://www.ensembl.org/index.html
ExAC Browser, http://exac.broadinstitute.org/
ExomeDepth, http://cran.r-project.org/web/packages/ExomeDepth/index.html
GATK, https://software.broadinstitute.org/gatk/
gnomAD Browser, http://gnomad.broadinstitute.org/
GoNL (Genomes of the Netherlands), http://www.nlgenome.nl/search/
IGV, http://www.broadinstitute.org/igv/
Kaviar Browser, http://db.systemsbiology.net/kaviar/
MatInspector, http://www.genomatix.de/index.html
NCBI Genome build GRCh38, https://www.ncbi.nlm.nih.gov/assembly?term=GRCh38&cmd=DetailsSearch
NHLBI Exome Sequencing Project (ESP) Exome Variant Server, http://evs.gs.washington.edu/EVS/
Novoalign, http://www.novocraft.com/products/novoalign/
OMIM, http://www.omim.org/
RefSeq, http://www.ncbi.nlm.nih.gov/RefSeq
SAMtools, http://www.htslib.org/
SeattleSeq Annotation, http://snp.gs.washington.edu/SeattleSeqAnnotation150/
Sequence Variant Nomenclature, http://varnomen.hgvs.org/
UCSC Genome Browser, http://genome.ucsc.edu
UK10K Consortium, http://www.uk10k.org/
Variant Effect Predictor, http://useast.ensembl.org/Homo_sapiens/Tools/VEP

References

1. Krachmer, J.H. (1985). Posterior polymorphous corneal dystrophy: a disease characterized by epithelial-like endothelial cells which influence management and prognosis. Trans. Am. Ophthalmol. Soc. *83*, 413–475.
2. Davidson, A.E., Liskova, P., Evans, C.J., Dudakova, L., Noskova, L., Pontikos, N., Hartmannová, H., Hodaňová, K., Stránecký, V., Kozmík, Z., et al. (2016). Autosomal-dominant corneal endothelial dystrophies CHED1 and PPCD1 are allelic disorders caused by non-coding mutations in the promoter of *OVOL2*. Am. J. Hum. Genet. *98*, 75–89.
3. Evans, C.J., Liskova, P., Dudakova, L., Hrabcikova, P., Horinek, A., Jirsova, K., Filipec, M., Hardcastle, A.J., Davidson, A.E., and Tuft, S.J. (2015). Identification of six novel mutations in *ZEB1* and description of the associated phenotypes in patients with posterior polymorphous corneal dystrophy 3. Ann. Hum. Genet. *79*, 1–9.
4. Weiss, J.S., Møller, H.U., Aldave, A.J., Seitz, B., Bredrup, C., Kivelä, T., Munier, F.L., Rapuano, C.J., Nischal, K.K., Kim, E.K., et al. (2015). IC3D classification of corneal dystrophies–edition 2. Cornea *34*, 117–159.
5. Jirsova, K., Merjava, S., Martincova, R., Gwilliam, R., Ebenezer, N.D., Liskova, P., and Filipec, M. (2007). Immunohistochemical characterization of cytokeratins in the abnormal corneal endothelium of posterior polymorphous corneal dystrophy patients. Exp. Eye Res. *84*, 680–686.
6. Rodrigues, M.M., Sun, T.T., Krachmer, J., and Newsome, D. (1980). Epithelialization of the corneal endothelium in posterior polymorphous dystrophy. Invest. Ophthalmol. Vis. Sci. *19*, 832–835.
7. Henriquez, A.S., Kenyon, K.R., Dohlman, C.H., Boruchoff, S.A., Forstot, S.L., Meyer, R.F., and Hanninen, L.A. (1984). Morphologic characteristics of posterior polymorphous dystrophy. A study of nine corneas and review of the literature. Surv. Ophthalmol. *29*, 139–147.
8. Merjava, S., Malinova, E., Liskova, P., Filipec, M., Zemanova, Z., Michalova, K., and Jirsova, K. (2011). Recurrence of posterior polymorphous corneal dystrophy is caused by the overgrowth of the original diseased host endothelium. Histochem. Cell Biol. *136*, 93–101.
9. Krafchak, C.M., Pawar, H., Moroi, S.E., Sugar, A., Lichter, P.R., Mackey, D.A., Mian, S., Nairus, T., Elner, V., Schteingart, M.T., et al. (2005). Mutations in *TCF8* cause posterior polymorphous corneal dystrophy and ectopic expression of COL4A3 by corneal endothelial cells. Am. J. Hum. Genet. *77*, 694–708.
10. Liskova, P., Evans, C.J., Davidson, A.E., Zaliova, M., Dudakova, L., Trkova, M., Stranecky, V., Carnt, N., Plagnol, V., Vincent, A.L., et al. (2016). Heterozygous deletions at the *ZEB1* locus verify haploinsufficiency as the mechanism of disease for posterior polymorphous corneal dystrophy type 3. Eur. J. Hum. Genet. *24*, 985–991.
11. Liskova, P., Tuft, S.J., Gwilliam, R., Ebenezer, N.D., Jirsova, K., Prescott, Q., Martincova, R., Pretorius, M., Sinclair, N., Boase, D.L., et al. (2007). Novel mutations in the *ZEB1* gene identified in Czech and British patients with posterior polymorphous corneal dystrophy. Hum. Mutat. *28*, 638.
12. Chung, D.D., Frausto, R.F., Cervantes, A.E., Gee, K.M., Zakharevich, M., Hanser, E.M., Stone, E.M., Heon, E., and Aldave, A.J. (2017). Confirmation of the *OVOL2* promoter mutation c.-307T>C in posterior polymorphous corneal dystrophy 1. PLoS ONE *12*, e0169215.
13. Hong, T., Watanabe, K., Ta, C.H., Villarreal-Ponce, A., Nie, Q., and Dai, X. (2015). An Ovol2-Zeb1 mutual inhibitory circuit governs bidirectional and multi-step transition between epithelial and mesenchymal states. PLoS Comput. Biol. *11*, e1004569.
14. Kitazawa, K., Hikichi, T., Nakamura, T., Mitsunaga, K., Tanaka, A., Nakamura, M., Yamakawa, T., Furukawa, S., Takasaka, M., Goshima, N., et al. (2016). OVOL2 maintains the transcriptional program of human corneal epithelium by suppressing epithelial-to-mesenchymal transition. Cell Rep. *15*, 1359–1368.
15. Kalluri, R., and Weinberg, R.A. (2009). The basics of epithelial-mesenchymal transition. J. Clin. Invest. *119*, 1420–1428.
16. Chen, T., You, Y., Jiang, H., and Wang, Z.Z. (2017). Epithelial-mesenchymal transition (EMT): A biological process in the development, stem cell differentiation, and tumorigenesis. J. Cell. Physiol. *232*, 3261–3272.
17. Pradella, D., Naro, C., Sette, C., and Ghigna, C. (2017). EMT and stemness: flexible processes tuned by alternative

splicing in development and cancer progression. Mol. Cancer *16*, 8.
18. Singh, A.J., Ramsey, S.A., Filtz, T.M., and Kioussi, C. (2017). Differential gene regulatory networks in development and disease. Cell. Mol. Life Sci. Published online October 10, 2017. https://doi.org/10.1007/s00018-017-2679-6.
19. Eghrari, A.O., Riazuddin, S.A., and Gottsch, J.D. (2015). Overview of the cornea: structure, function, and development. Prog. Mol. Biol. Transl. Sci. *134*, 7–23.
20. Srinivas, S.P. (2012). Cell signaling in regulation of the barrier integrity of the corneal endothelium. Exp. Eye Res. *95*, 8–15.
21. Chung, D.D., Frausto, R.F., Lin, B.R., Hanser, E.M., Cohen, Z., and Aldave, A.J. (2017). Transcriptomic profiling of posterior polymorphous corneal dystrophy. Invest. Ophthalmol. Vis. Sci. *58*, 3202–3214.
22. Zakharevich, M., Kattan, J.M., Chen, J.L., Lin, B.R., Cervantes, A.E., Chung, D.D., Frausto, R.F., and Aldave, A.J. (2017). Elucidating the molecular basis of PPCD: Effects of decreased ZEB1 expression on corneal endothelial cell function. Mol. Vis. *23*, 740–752.
23. Liskova, P., Gwilliam, R., Filipec, M., Jirsova, K., Reinstein Merjava, S., Deloukas, P., Webb, T.R., Bhattacharya, S.S., Ebenezer, N.D., Morris, A.G., and Hardcastle, A.J. (2012). High prevalence of posterior polymorphous corneal dystrophy in the Czech Republic; linkage disequilibrium mapping and dating an ancestral mutation. PLoS ONE *7*, e45495.
24. Abecasis, G.R., Cherny, S.S., Cookson, W.O., and Cardon, L.R. (2002). Merlin–rapid analysis of dense genetic maps using sparse gene flow trees. Nat. Genet. *30*, 97–101.
25. Pontikos, N., Yu, J., Moghul, I., Withington, L., Blanco-Kelly, F., Vulliamy, T., Wong, T.L.E., Murphy, C., Cipriani, V., Fiorentino, A., et al.; UKIRDC (2017). Phenopolis: an open platform for harmonization and analysis of genetic and phenotypic data. Bioinformatics *33*, 2421–2423.
26. Plagnol, V., Curtis, J., Epstein, M., Mok, K.Y., Stebbings, E., Grigoriadou, S., Wood, N.W., Hambleton, S., Burns, S.O., Thrasher, A.J., et al. (2012). A robust model for read count data in exome sequencing experiments and implications for copy number variant calling. Bioinformatics *28*, 2747–2754.
27. McKenna, A., Hanna, M., Banks, E., Sivachenko, A., Cibulskis, K., Kernytsky, A., Garimella, K., Altshuler, D., Gabriel, S., Daly, M., and DePristo, M.A. (2010). The Genome Analysis Toolkit: a MapReduce framework for analyzing next-generation DNA sequencing data. Genome Res. *20*, 1297–1303.
28. McLaren, W., Gil, L., Hunt, S.E., Riat, H.S., Ritchie, G.R., Thormann, A., Flicek, P., and Cunningham, F. (2016). The Ensembl variant effect predictor. Genome Biol. *17*, 122.
29. Desmet, F.O., Hamroun, D., Lalande, M., Collod-Béroud, G., Claustres, M., and Béroud, C. (2009). Human Splicing Finder: an online bioinformatics tool to predict splicing signals. Nucleic Acids Res. *37*, e67.
30. Reese, M.G., Eeckman, F.H., Kulp, D., and Haussler, D. (1997). Improved splice site detection in Genie. J. Comput. Biol. *4*, 311–323.
31. Eng, L., Coutinho, G., Nahas, S., Yeo, G., Tanouye, R., Babaei, M., Dörk, T., Burge, C., and Gatti, R.A. (2004). Nonclassical splicing mutations in the coding and noncoding regions of the ATM Gene: maximum entropy estimates of splice junction strengths. Hum. Mutat. *23*, 67–76.
32. Brunak, S., Engelbrecht, J., and Knudsen, S. (1991). Prediction of human mRNA donor and acceptor sites from the DNA sequence. J. Mol. Biol. *220*, 49–65.
33. ENCODE Project Consortium (2004). The ENCODE (ENCyclopedia Of DNA Elements) Project. Science *306*, 636–640.
34. Grabe, N. (2002). AliBaba2: context specific identification of transcription factor binding sites. In Silico Biol. (Gedrukt) *2*, S1–S15.
35. Cartharius, K., Frech, K., Grote, K., Klocke, B., Haltmeier, M., Klingenhoff, A., Frisch, M., Bayerlein, M., and Werner, T. (2005). MatInspector and beyond: promoter analysis based on transcription factor binding sites. Bioinformatics *21*, 2933–2942.
36. Wingender, E. (2008). The TRANSFAC project as an example of framework technology that supports the analysis of genomic regulation. Brief. Bioinform. *9*, 326–332.
37. Valtink, M., Gruschwitz, R., Funk, R.H., and Engelmann, K. (2008). Two clonal cell lines of immortalized human corneal endothelial cells show either differentiated or precursor cell characteristics. Cells Tissues Organs (Print) *187*, 286–294.
38. Massie, I., Dziasko, M., Kureshi, A., Levis, H.J., Morgan, L., Neale, M., Sheth, R., Tovell, V.E., Vernon, A.J., Funderburgh, J.L., and Daniels, J.T. (2015). Advanced imaging and tissue engineering of the human limbal epithelial stem cell niche. Methods Mol. Biol. *1235*, 179–202.
39. Harikumar, A., and Meshorer, E. (2015). Chromatin remodeling and bivalent histone modifications in embryonic stem cells. EMBO Rep. *16*, 1609–1619.
40. Vastenhouw, N.L., Zhang, Y., Woods, I.G., Imam, F., Regev, A., Liu, X.S., Rinn, J., and Schier, A.F. (2010). Chromatin signature of embryonic pluripotency is established during genome activation. Nature *464*, 922–926.
41. Kundaje, A., Meuleman, W., Ernst, J., Bilenky, M., Yen, A., Heravi-Moussavi, A., Kheradpour, P., Zhang, Z., Wang, J., Ziller, M.J., et al.; Roadmap Epigenomics Consortium (2015). Integrative analysis of 111 reference human epigenomes. Nature *518*, 317–330.
42. Nakahashi, H., Kieffer Kwon, K.R., Resch, W., Vian, L., Dose, M., Stavreva, D., Hakim, O., Pruett, N., Nelson, S., Yamane, A., et al. (2013). A genome-wide map of CTCF multivalency redefines the CTCF code. Cell Rep. *3*, 1678–1689.
43. Xiang, J., Fu, X., Ran, W., and Wang, Z. (2017). Grhl2 reduces invasion and migration through inhibition of TGFβ-induced EMT in gastric cancer. Oncogenesis *6*, e284.
44. Frisch, S.M., Farris, J.C., and Pifer, P.M. (2017). Roles of Grainyhead-like transcription factors in cancer. Oncogene *36*, 6067–6073.
45. Aue, A., Hinze, C., Walentin, K., Ruffert, J., Yurtdas, Y., Werth, M., Chen, W., Rabien, A., Kilic, E., Schulzke, J.D., et al. (2015). A grainyhead-like 2/Ovo-like 2 pathway regulates renal epithelial barrier function and lumen expansion. J. Am. Soc. Nephrol. *26*, 2704–2715.
46. McCarey, B.E., Edelhauser, H.F., and Lynn, M.J. (2008). Review of corneal endothelial specular microscopy for FDA clinical trials of refractive procedures, surgical devices, and new intraocular drugs and solutions. Cornea *27*, 1–16.
47. Chen, Y., Huang, K., Nakatsu, M.N., Xue, Z., Deng, S.X., and Fan, G. (2013). Identification of novel molecular markers through transcriptomic analysis in human fetal and adult corneal endothelial cells. Hum. Mol. Genet. *22*, 1271–1279.

48. Bath, C., Muttuvelu, D., Emmersen, J., Vorum, H., Hjortdal, J., and Zachar, V. (2013). Transcriptional dissection of human limbal niche compartments by massive parallel sequencing. PLoS ONE *8*, e64244.
49. Cieply, B., Riley, P., 4th, Pifer, P.M., Widmeyer, J., Addison, J.B., Ivanov, A.V., Denvir, J., and Frisch, S.M. (2012). Suppression of the epithelial-mesenchymal transition by Grainyhead-like-2. Cancer Res. *72*, 2440–2453.
50. He, Z., Forest, F., Gain, P., Rageade, D., Bernard, A., Acquart, S., Peoc'h, M., Defoe, D.M., and Thuret, G. (2016). 3D map of the human corneal endothelial cell. Sci. Rep. *6*, 29047.
51. Wang, H.S., Hung, S.C., Peng, S.T., Huang, C.C., Wei, H.M., Guo, Y.J., Fu, Y.S., Lai, M.C., and Chen, C.C. (2004). Mesenchymal stem cells in the Wharton's jelly of the human umbilical cord. Stem Cells *22*, 1330–1337.
52. Kim, Y.R., Kim, M.A., Sagong, B., Bae, S.H., Lee, H.J., Kim, H.J., Choi, J.Y., Lee, K.Y., and Kim, U.K. (2015). Evaluation of the contribution of the EYA4 and GRHL2 genes in Korean patients with autosomal dominant non-syndromic hearing loss. PLoS ONE *10*, e0119443.
53. Van Laer, L., Van Eyken, E., Fransen, E., Huyghe, J.R., Topsakal, V., Hendrickx, J.J., Hannula, S., Mäki-Torkko, E., Jensen, M., Demeester, K., et al. (2008). The grainyhead like 2 gene (GRHL2), alias TFCP2L3, is associated with age-related hearing impairment. Hum. Mol. Genet. *17*, 159–169.
54. Vona, B., Nanda, I., Neuner, C., Müller, T., and Haaf, T. (2013). Confirmation of GRHL2 as the gene for the DFNA28 locus. Am. J. Med. Genet. A. *161A*, 2060–2065.
55. Petrof, G., Nanda, A., Howden, J., Takeichi, T., McMillan, J.R., Aristodemou, S., Ozoemena, L., Liu, L., South, A.P., Pourreyron, C., et al. (2014). Mutations in GRHL2 result in an autosomal-recessive ectodermal Dysplasia syndrome. Am. J. Hum. Genet. *95*, 308–314.
56. Boivin, F.J., and Schmidt-Ott, K.M. (2017). Transcriptional mechanisms coordinating tight junction assembly during epithelial differentiation. Ann. N Y Acad. Sci. *1397*, 80–99.

Příloha 6: The utility of massively parallel sequencing for posterior polymorphous corneal dystrophy type 3 molecular diagnosis

Experimental Eye Research 182 (2019) 160–166

Contents lists available at ScienceDirect

Experimental Eye Research

journal homepage: www.elsevier.com/locate/yexer

The utility of massively parallel sequencing for posterior polymorphous corneal dystrophy type 3 molecular diagnosis

Lubica Dudakova[a], Cerys J. Evans[b], Nikolas Pontikos[b], Nathaniel J. Hafford-Tear[b], Frantisek Malinka[a,c], Pavlina Skalicka[a,d], Ales Horinek[e,f], Francis L. Munier[g], Nathalie Voide[g], Pavel Studeny[h], Lucia Vanikova[i], Tomas Kubena[j], Karla E. Rojas Lopez[b], Alice E. Davidson[b], Alison J. Hardcastle[b], Stephen J. Tuft[k], Petra Liskova[a,b,d,*]

[a] Research Unit for Rare Diseases, Department of Paediatrics and Adolescent Medicine, First Faculty of Medicine, Charles University and General University Hospital in Prague, Ke Karlovu 2, 128 08, Prague 2, Czech Republic
[b] UCL Institute of Ophthalmology, 11-43 Bath Street, EC1V 9EL, London, United Kingdom
[c] Department of Computer Science, Czech Technical University in Prague, Karlovo Namesti 13, 128 08, Prague, Czech Republic
[d] Department of Ophthalmology, First Faculty of Medicine, Charles University and General University Hospital in Prague, U Nemocnice 2, 128 08, Prague, Czech Republic
[e] 3rd Department of Medicine - Department of Endocrinology and Metabolism, First Faculty of Medicine, Charles University and General University Hospital in Prague, U Nemocnice 1, 128 08, Prague 2, Czech Republic
[f] Institute of Biology and Human Genetics, First Faculty of Medicine, Charles University and General University Hospital in Prague, Albertov 4, 128 00, Prague, Czech Republic
[g] Jules-Gonin Eye Hospital, Fondation Asile des Aveugles, University of Lausanne, Avenue de France 15, 1004, Lausanne, Switzerland
[h] Ophthalmology Department, Third Faculty of Medicine, Charles University and Teaching Hospital Kralovske Vinohrady, Srobarova 1150/50, 100 34, Prague, Czech Republic
[i] Center for Eye Microsurgery, Gagarinova 7/B, 821 03, Bratislava, Slovakia
[j] Ophthalmology Clinic of Dr. Tomas Kubena, U Zimniho Stadionu 1759, 760 00, Zlin, Czech Republic
[k] Moorfields Eye Hospital, 162 City Road, EC1V 2PD, London, United Kingdom

ARTICLE INFO

Keywords:
ZEB1
Posterior polymorphous corneal dystrophy type 3
Massively parallel sequencing
Exome
Genome
Aberrant splicing
Breakpoint mapping

ABSTRACT

The aim of this study was to identify the molecular genetic cause of disease in posterior polymorphous corneal dystrophy (PPCD) probands of diverse origin and to assess the utility of massively parallel sequencing in the detection of *ZEB1* mutations. We investigated a total of 12 families (five British, four Czech, one Slovak and two Swiss). Ten novel and two recurrent disease-causing mutations in *ZEB1*, were identified in probands by Sanger (n = 5), exome (n = 4) and genome (n = 3) sequencing. Sanger sequencing was used to confirm the mutations detected by massively parallel sequencing, and to perform segregation analysis. Genome sequencing revealed that one proband harboured a novel ~0.34 Mb heterozygous *de novo* deletion spanning exons 1–7 and part of exon 8. Transcript analysis confirmed that the *ZEB1* transcript is detectable in blood-derived RNA samples and that the disease-associated variant c.482-2A > G leads to aberrant pre-mRNA splicing. *De novo* mutations, which are a feature of PPCD3, were found in the current study with an incidence rate of at least 16.6%. In general, massively parallel sequencing is a time-efficient way to detect PPCD3-associated mutations and, importantly, genome sequencing enables the identification of full or partial heterozygous *ZEB1* deletions that can evade detection by both Sanger and exome sequencing. These findings contribute to our understanding of PPCD3, for which currently, 49 pathogenic variants have been identified, all of which are predicted to be null alleles.

1. Introduction

Posterior polymorphous corneal dystrophy (PPCD) is a genetically heterogeneous, autosomal dominant disorder, characterised by vesicular lesions, bands and opacities at the level of Descemet membrane and the corneal endothelium (Cibis et al., 1977). Decreased visual acuity can result from amblyopia, irregular astigmatism from corneal steepening, secondary glaucoma and/or corneal edema (Krachmer, 1985; Liskova et al., 2010, 2013). To date, variants within three genes *ZEB1*, *OVOL2* and *GRHL2* have been identified to be disease-causing

* Corresponding author. Research Unit for Rare Diseases, Department of Paediatrics and Adolescent Medicine, First Faculty of Medicine, Charles University and General University Hospital in Prague, Ke Karlovu 2, 128 08, Prague 2, Czech Republic.
E-mail address: petra.liskova@lf1.cuni.cz (P. Liskova).

https://doi.org/10.1016/j.exer.2019.03.002
Received 31 October 2018; Received in revised form 5 February 2019; Accepted 2 March 2019
Available online 07 March 2019
0014-4835/

(Krafchak et al., 2005; Davidson et al., 2016; Le et al., 2016; Liskova et al., 2018).

Mutations in the zinc finger E-box binding homeobox 1 (*ZEB1)* cause PPCD type 3 (PPCD3; OMIM #609141) (Krafchak et al., 2005). In addition to ocular features, it has been reported that patients with PPCD3 have an increased incidence of hernia and hydrocele (Krafchak et al., 2005; Liskova et al., 2013). Three cases with agenesis or hypoplasia of the corpus callosum have also been documented (Jang et al., 2014; Chaudhry et al., 2017). Individuals with PPCD3 can be asymptomatic, and there are rare reports of incomplete penetrance (Krafchak et al., 2005; Liskova et al., 2013).

ZEB1 encodes a zinc finger transcription factor. The protein plays a role in epithelial-mesenchymal transition (EMT) by activating the transcription of mesenchymal genes while repressing epithelial genes (Park et al., 2008). EMT is important for embryonic development, wound healing, fibrosis and cancer progression (Chen et al., 2017). Importantly, it is hypothesised that dysregulation of this pathway underpins the pathophysiology of PPCD (Davidson et al., 2016; Liskova et al., 2018). PPCD3 is attributed to ZEB1 haploinsufficiency (Liskova et al., 2016; Chung et al., 2017), and the reduced levels of ZEB1 induce an altered cellular response to apoptotic stimuli and cell barrier function (Zakharevich et al., 2017).

In this study, we demonstrate the utility of massively parallel sequencing for the identification of *ZEB1* mutations. Furthermore, we establish that it is possible to determine the effects of *ZEB1* variants on pre-mRNA splicing using blood-derived RNA. Finally, we present a comprehensive summary of *ZEB1* mutations that have been reported to cause PPCD3 to date.

2. Methods

2.1. Participants, clinical examination and samples

The study was approved by the Ethics committee of the General University Hospital in Prague (reference no. 151/11 S-IV) or Moorfields Eye Hospital (REC references 13/LO/1084 and 09/H0724/25) and adhered to the tenets of the Helsinki Declaration. All participants signed informed consent. Twelve families were investigated; four white Czech (C31, C32, C34, C36), four white British (B9, B10, B11 and B12), one South Asian British (B13), one white Slovak (SK1) and two white Swiss (SW1, SW2). A diagnosis of PPCD was based on established clinical criteria (Cibis et al., 1977; Liskova et al., 2010, 2013). Best corrected visual acuity (BCVA) was measured using Snellen charts and converted to decimal values. Participating individuals were asked to provide information on their general health status.

Genomic DNA from probands and any additional available family members was extracted from venous blood using a Gentra Puregene blood kit (Qiagen, Hilden, Germany) or from saliva using an Oragene kit (Oragene OG-300, DNA Genotek, Canada). In one affected individual total RNA was isolated from venous blood using a QIAamp RNA Blood Mini Kit (Qiagen), and transcribed into cDNA with the SuperScript III Reverse Transcriptase (Thermo Fisher, Waltham, Massachusetts).

2.2. Sanger sequencing

We first excluded the presence of pathogenic variants in regulatory regions of *OVOL2* and *GRHL2* in all probands by conventional Sanger sequencing (Davidson et al., 2016; Liskova et al., 2018). In probands from families C31, C32, C34 and B9-B11 (Fig. 1) the entire *ZEB1* coding region and flanking intronic sequences (NM_030751.5, NG_017048.1) were amplified by PCR and directly sequenced (Evans et al., 2015). Sequence variants were described according to the Human Genome Variation Society guidelines (http://varnomen.hgvs.org/) (den Dunnen et al., 2016). Direct sequencing was also used to confirm the likely disease-causing variants found by massively parallel sequencing which included a large deletion. Furthermore, direct sequencing was also used for segregation analysis within the families.

2.3. Massively parallel sequencing

DNA from the probands from families C31, B12, B13, SW1 and SW2 (Fig. 1) were subjected to exome sequencing. Sequencing libraries were generated using a SureSelect Human All Exome V6 capture kit (Agilent, Santa Clara, California). Libraries were sequenced on HiSeq4000 sequencer (Illumina). Probands from families C31, C36 and SK1 (Figs. 1–3) were analysed by genome sequencing using a TruSeq Nano DNA library preparation kit and a HiSeq X Ten sequencer (Illumina, San Diego, California). Reads were aligned to the GRCh37/hg19 human reference sequence with NovoAlign V3.02.08 (Novocraft, Malaysia). Variant calling was performed with Genome Analysis Tool Kit (GATK) HaplotypeCaller (version 4.0.1.2) (McKenna et al., 2010). Variants were annotated using the Variant Effect Predictor (McLaren et al., 2016).

Both coding and non-coding rare variants with a minor allele frequency (MAF) ≤ 0.005 as per gnomAD (Lek et al., 2016) in genes known to be implicated in the pathogenesis of corneal endothelial dystrophies (*ZEB1*, *GRHL2*, *OVOL2*, *COL8A2*, *SLC4A11*, *TCF4*) (Biswas et al., 2001; Krafchak et al., 2005; Vithana et al., 2006; Baratz et al., 2010; Davidson et al., 2016; Le et al., 2016; Liskova et al., 2018) were further investigated for potential pathogenicity. The frequency of detected variants was also determined in 2,430 exomes generated from Czech individuals available through projects of the National Centre for Medical Genomics (http://ncmg.cz/en). Larger structural variations were compared to entries in the Database of Genomic Variants (http://dgv.tcag.ca/dgv/app/home; accessed December 2018) (MacDonald et al., 2014). The exome and genome sequencing data, aligned to the human reference GRCh37/hg19, were visualized with the Integrated Genomics Viewer (IGV) (Broad institute, California, USA) (Thorvaldsdottir et al., 2013).

In one patient we did not detect a pathogenic variant and we therefore manually searched aligned genome sequencing reads for stretches of homozygosity around the *ZEB1* locus indicative of a heterozygous deletion. Importantly, we used the soft clip function of the IGV software to visualise the likely breakpoints. Primers were designed at each end (forward 5′- CTTTCTGCTGAGGCCATTTC-3′ and reverse 5′-TGGGTGACTAGAGCCAGACC-3′ primer) and the PCR product was Sanger sequenced to confirm the breakpoints.

A schematic diagram of the pipeline used to process genomic DNA samples in our study is shown in Supplementary Fig. S1.

2.4. Paternity testing

Paternity testing was performed in families C31 and C32 to prove *de novo* origin of the detected mutations using an established set of 16 forensic markers (Ensenberger et al., 2010).

2.5. Functional assessment of pre-mRNA splicing

To assess the effect of a selected variant on pre-mRNA splicing, cDNA of an affected individual II:2 from family C36 was amplified and analysed by direct sequencing, spanning a region of *ZEB1* exons 4–7 using forward 5′-CTGAGGCACCTGAAGAGGAC-3′ and reverse 5′-TTG CAGTTTGGGCATTCATA-3′ primer.

2.6. Review of mutations associated with PPCD3

We performed a comprehensive and manually curated review of all publicly available literature reporting *ZEB1* PPCD3-associated mutations. All variants listed in this article are annotated in accordance with transcript NM_030751.5 and GRCh37/hg19 human genome assembly.

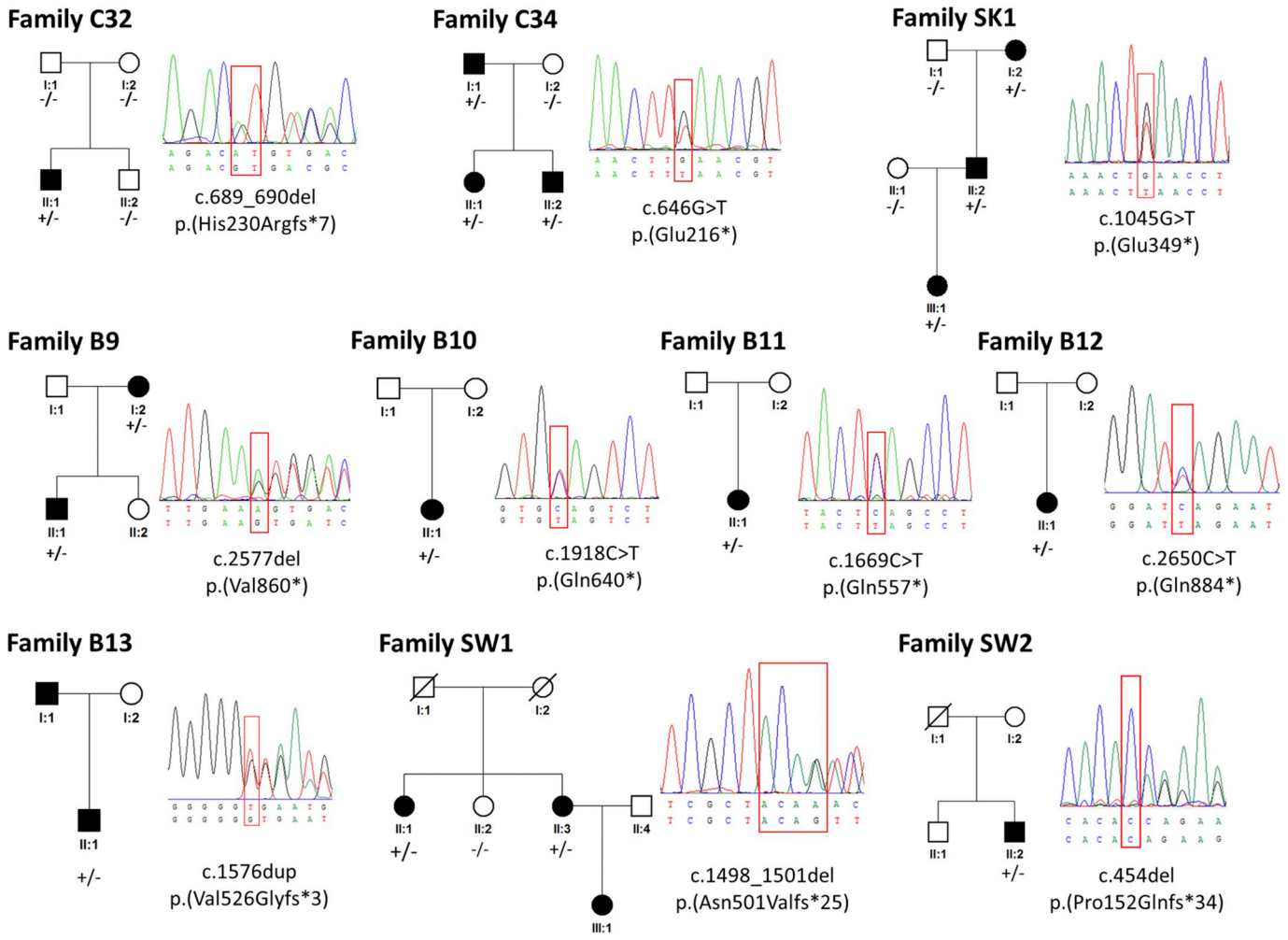

Fig. 1. Disease-causing *ZEB1* point mutations and small heterozygous deletions identified in ten families. Affected individuals are shown as black symbols. Individuals who tested positive for a particular mutation in each family are labelled with +/− and those who were negative with −/−. The proband from family C32 harboured a known mutation c.689_690del which arose *de novo*; three affected individuals from family C34 carried a novel mutation c.646G > T; in family SK1 three individuals had novel mutation c.1045G > T; in family B9 two affected individuals had a novel mutation c.2577del and in families B10, B11 and B12 the probands were found to each harbour a different novel mutation c.1918C > T, c.1669C > T and c.2650C > T, respectively. The proband from family B13 carried a recurrent mutation c.1576dup. Two Swiss families SW1 and SW2 carried novel c.1498_1501del and c.454del, respectively.

3. Results

The clinical, demographic and sequencing data of 19 affected individuals from 12 families with PPCD3 are summarized in Table 1.

Slit-lamp examination showed characteristic bilateral corneal signs in all affected subjects. Only 9 eyes of 5 individuals (26.3%) (mean age 27 ± 11.9; range 8–40) had a BCVA of 1.0, while moderate or severe visual impairment (i. e. BCVA < 0.33) was present in 10 eyes of 7 individuals (36.8%) (mean age 39 ± 16,5, range 20–59). Two individuals had nystagmus, including subject II:2 from family C34 who was noted to have cloudy corneas from 6 weeks of age. Four individuals (21%) had a keratoplasty in at least one eye. None of the participants in this study had been diagnosed with glaucoma. Two individuals out of 19 reported that they had undergone surgery for hernia and one for hydrocele. None of the probands had signs of cognitive deficiency consistent with agenesis or hypoplasia of corpus callosum (Jang et al., 2014; Chaudhry et al., 2017).

In total, we identified ten novel heterozygous variants in *ZEB1* that were evaluated as pathogenic; c.454del, c.482-2A > G, c.646G > T, c.1045G > T, c.1498_1501del, c.1669C > T, c.1918C > T, c.2577del, c.2650C > T (Figs. 1 and 2) and a large ~0.34 Mb deletion (Fig. 3). Two known *ZEB1* mutations were also found; c.689_690del and c.1576dup (Fig. 1). In concordance with previous observations (Krafchak et al., 2005; Evans et al., 2015; Liskova et al., 2016) all affected individuals had a heterozygous loss-of-function allele. The c.1576dup mutation was observed in an individual who also had a unique c.469C > G; p.(His157Asp) variant, predicted to be benign by four out of the five software tools we used (Supplementary Table 1). Unfortunately, familial samples were not able available to determine the phase of these variants in the affected proband. In samples analysed by massively parallel sequencing no potentially disease-associated variants were found in other genes known to be associated with corneal endothelial dystrophies.

Of note, the proband from family C31 with sporadic disease underwent screening by Sanger sequencing, followed by exome and genome sequencing. Visualising the aligned genome sequencing reads in IGV using a soft clip function enabled us to identify likely deletion breakpoints (Supplementary Fig. S2). Sanger sequencing across the region confirmed the presence of the deletion encompassing *ZEB1* exons 1–7 and part of exon 8 (chr10.hg19:g.31,476,838_31,812,958del) (Fig. 3).

In samples that underwent exome sequencing, the sequencing depth of the *ZEB1* gene (NM_030751.5) exceeded 20x in at least 97.7% of the coding region across all samples analysed (n = 5). In samples subjected to genome sequencing, the sequencing depth of the entire *ZEB1* region (NG_017048.1) exceeded 20x in at least 97.9% of the region across all

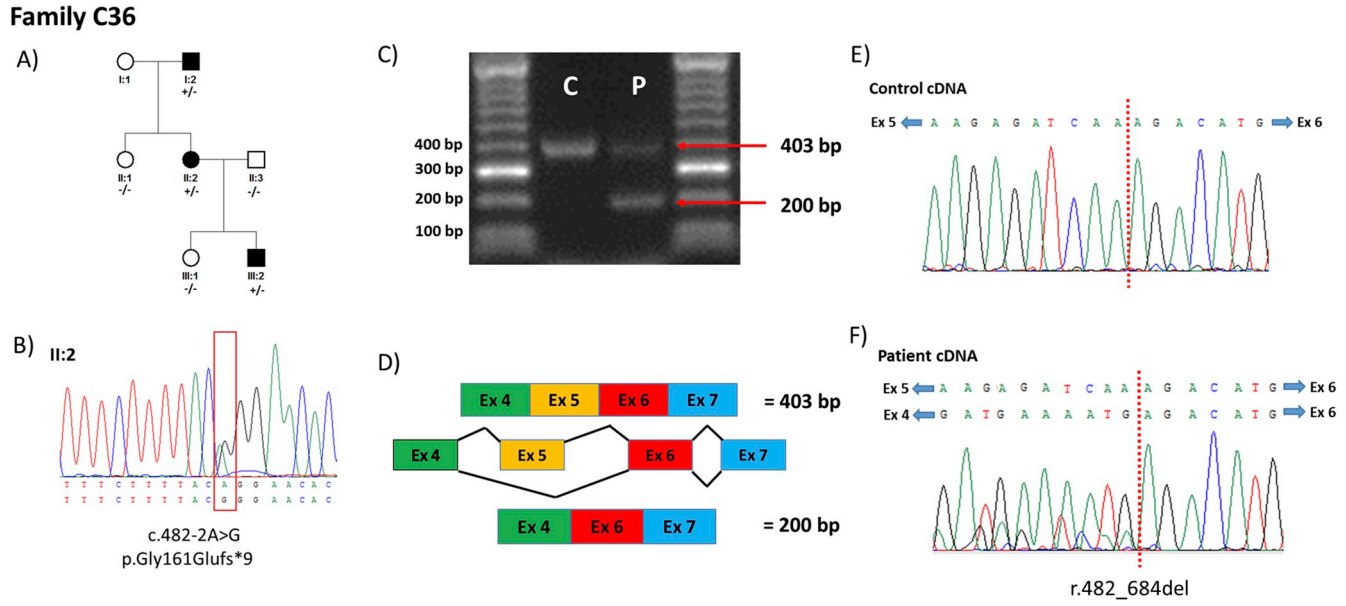

Fig. 2. Assessment of the c.482-2A > G *ZEB1* variant on pre-mRNA splicing in family C36. Pedigree (A), a novel heterozygous mutation located in a canonical splice site (B). PCR of blood derived cDNA (C) from a control individual (lane 1 marked as C) and the patient sample (Lane 2, marked as P) showing two different products. The smaller fragment was found to represent skipping of exon 5 (D) due to aberrant pre-mRNA splicing (r.482_684del) (NM_030751.5, NG_017048.1). Direct sequencing of the PCR amplified products confirming expected splicing patterns in the control sample (E) and one wild type and one aberrant transcript resulting in exon 5 skipping in the patient sample (F).

samples analysed (n = 3).

In family C36, analysis of the *ZEB1* transcript in the blood of an individual who had a splice site variant, c.482-2A > G, demonstrated that the mutation alters pre-mRNA splicing, resulting in exon 5 skipping and insertion of a premature termination codon, described as r.482_684del, p.Gly161Glufs*9 (Fig. 2).

None of the novel pathogenic mutations located in *ZEB1* coding region or the unique variant p.(His157Asp) were found in gnomAD, Database of Genomic Variants or in data specific to the Czech population. Segregation analysis within the families also supported their pathogenicity (Figs. 1–3). As parents in families C31 and C32 were clinically unaffected and did not carry *ZEB1* mutations detected in their children, we suspected *de novo* origin of the mutations, which was subsequently confirmed by paternity testing (Figs. 1 and 3).

A schematic representation of all PPCD3-associated *ZEB1* variants that have been reported to date, including this study, is provided in Fig. 4. In total, 49 mutations have been identified in 54 families of various ethnic backgrounds. All are predicted to be null alleles and hence support the hypothesis that PPCD3 arises due to *ZEB1* haploinsufficiency. Further details on the identified mutations are shown in Supplementary Table 2.

4. Discussion

In this study we report ten novel and two recurrent mutations in *ZEB1*, as well as the first genetic study of PPCD3 patients from Slovakia and Switzerland. Importantly, we show that massively parallel sequencing is a useful tool, particularly genome sequencing, to genetically diagnose the condition. We also demonstrate for the first time that it is possible to experimentally determine the effect of *ZEB1* variants on pre-mRNA splicing using whole-blood derived RNA. In addition, we put our work in context by providing a comprehensive review of all disease-

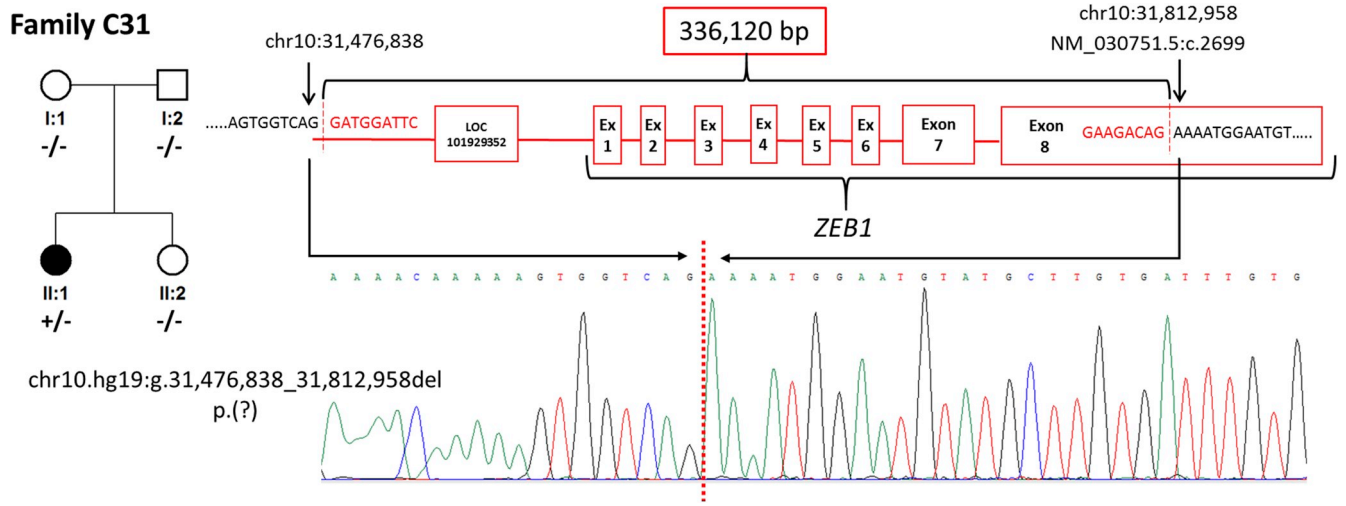

Fig. 3. A schematic representation of the *de novo* partial heterozygous *ZEB1* deletion found in family C31. The breakpoints of the deletion were identified, and the corresponding sequence chromatogram is shown.

Table 1
Clinical, demographical and molecular genetic findings in 19 individuals with posterior polymorphous corneal dystrophy type 3.

Family	Patient ID	Gender	Age (y)†	Ethnicity	BCVA*		Other		Systemic findings
					RE	LE	RE	LE	
C31	II:1	F	30	White Czech	0.4	0.1	Ambylopia	Ambylopia	Nil
C32	II:1	M	8	White Czech	1.0	1.0	Nil	Nil	Nil
C34	I:1	M	52	White Czech	CF*	0.2	Nystagmus Amblyopia PK at 41 y PCVA 0.16	Nystagmus Amblyopia	Hypertension, impaired glucose tolerance
	II:1	F	25		1.0	0.7	Nil	Nil	Nil
	II:2	M	23		0.2	0.1	Nystagmus Amblyopia Esotropia	Nystagmus Amblyopia	Hydrocele
C36	I:2	M	67	White Czech	0.9	0.9	Nil	Nil	Inguinal hernias Atrial fibrillation constrictive pericarditis
	II:2	F	40		1.0	1.0	Nil	Nil	Nil
	III:2	M	5.5		0.7	0.8	Nil	Nil	Nil
SK1	II:2	M	38	White Slovak	0.7	0.8	Nil	Nil	Hydrocele
	III:1	F	20		0.2*	0.5	Corneal edema DMEK at 19 y PCVA 0.3	Nil	Nil
B9	I:2	F	59	White British	0.63	0.025	Anterior synechiae Corectopia	Anterior synechiae Corectopia	Nil
	II:1	M	27		0.5	0.5	Nil	Nil	Nil
B10	II:1	F	57	White British	0.32*	0.32*	Nil DMEK at 55 y PCVA 0.63	Nil DMEK at 56 y PCVA 0.63	Nil
B11	II:1	F	13	White British	0.5	0.5	Nil	Nil	Nil
B12	II:1	F	36	White British	0.63	NA	Nil	PK at 20 y PCVA 0.1	Nil
B13	II:1	M	33	South Asian	0.25	0.5	Nil	Nil	Nil
SW1	II:1	F	33	White Swiss	1.0	1.0	Nil	Nil	Nil
	II:3	F	29		1.0	1.0	Nil	Nil	Nil
SW2	II:2	M	36	White Swiss	0.5	0.6	Nil	Nil	Umbilical and inguinal hernia Varices Spontaneous luxation of the left patella

BCVA: best corrected visual acuity; **CF**: counting fingers; **DMEK:** Descemet membrane endothelial keratoplasty; **F**: female; **LE:** left eye; **M**: male; **PCVA**: postoperative corrected visual acuity; **PK**: penetrating keratoplasty; **RE:** right eye; **Y**: years; *decimal notation, before keratoplasty, †at most recent examination.

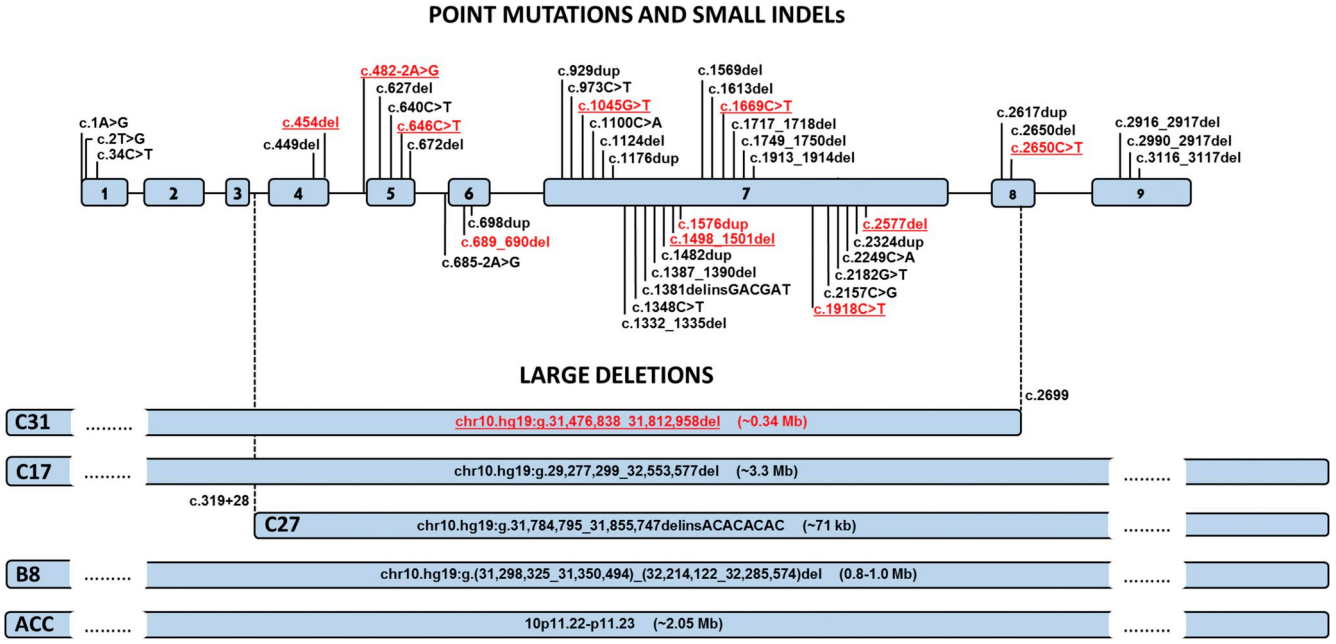

Fig. 4. Schematic diagram of the *ZEB1* gene showing 49 heterozygous pathogenic mutations identified to date in patients with posterior polymorphous corneal dystrophy type 3. Larger deletions are shown as a bar with coordinates of the deleted region (GRCh37/hg19). Mutations identified in the current study are highlighted in red, novel variants are underlined. Description of coding and splicing mutations are based on reference sequence NM_030751.5, NG_017048.1 and numbering starts at the translation initiation site. (For interpretation of the references to colour in this figure legend, the reader is referred to the Web version of this article.)

associated *ZEB1* variants reported to date.

All *ZEB1* reported pathogenic variants either introduce premature termination codons or comprise large deletions predicted to completely disrupt the gene transcription (Krafchak et al., 2005; Aldave et al., 2007; Liskova et al., 2007, 2010, 2013, 2016; Vincent et al., 2009; Nguyen et al., 2010; Bakhtiari et al., 2013; Lechner et al., 2013; Jang et al., 2014; Evans et al., 2015). Although it has been anticipated that aberrant *ZEB1* transcripts are likely eliminated by the mRNA nonsense mediated decay surveillance pathway, cellular studies have shown that *ZEB1* disease-causing variants may, in addition to the reduced protein production, also result in impaired nuclear localization of the encoded protein (Chung et al., 2014).

Of the 49 *ZEB1* pathogenic variants that have been described, five (10%) were large deletions (Liskova et al., 2016; Chaudhry et al., 2017). Their size varies considerably (0.071–3.3 Mb), and importantly they can evade detection by exome sequencing, qPCR or SNP arrays, depending on primer or SNP locations. Genome sequencing overcomes these limitations. In proband from family 31 it has allowed us to detect the fifth unique deletion in association with PPCD3 and to precisely visualise and map its breakpoints. On this basis we decided to use genome sequencing as the first line approach in two other probands. Massively parallel sequencing also enabled us to screen multiple genes associated with corneal endothelial disease, which could be useful in determining the genetic cause in cases of bilateral corneal edema of uncertain aetiology (Bakhtiari et al., 2013; Evans et al., 2015). We also conducted transcript analysis using blood-derived RNA to show for the first time that a novel splicing mutation c.482-2A > G causes aberrant pre-mRNA splicing.

There have only been two recurrent *ZEB1* mutations reported. In this study we have documented the *de novo* origin of c.689_690del; p.(His230Arg*7), previously found in an American family (Bakhtiari et al., 2013). We have also identified c.1576dup; p.(Val526Glyfs*3) in a patient of South Asian ethnicity, previously reported in three families from North America (Krafchak et al., 2005; Bakhtiari et al., 2013; Lechner et al., 2013) and one British family (Evans et al., 2015). Interestingly, this patient (B13-II:1) also harboured an additional unique missense variant in *ZEB1* p.(His157Asp). Unfortunately, we were not able to determine the phase of this variant with respect to c.1576dup to assess its contribution to the phenotype. However, *in silico* analysis suggests that it is likely benign and, if not, we hypothesise that it is located on the same allele as the c.1576dup mutation variant given that bi-allelic loss-of-function *ZEB1* alleles are embryonic lethal (Takagi et al., 1998; Liu et al., 2008).

The *de novo* mutation rate amongst PPCD3 probands is unknown, partly because individuals with PPCD3 can be asymptomatic, and some subjects even show incomplete penetrance for the disease, and thus a reported family history can be unreliable (Krafchak et al., 2005; Liskova et al., 2007, 2010; Bakhtiari et al., 2013; Evans et al., 2015). Herein, we identified *de novo* mutations in two of 12 families studied, resulting in an incidence rate of 16.6% in this study. However, this figure may be an underestimate because although there was no family history reported in families B10-B12 and SW2, the parents of the probands were unavailable for examination or testing.

ZEB1 null alleles are found at an extremely low frequency in large-scale public databases such as gnomAD and the Database of Genomic Variants. As they lack individual-level data without details of ophthalmic examination, the presence of such variants in these datasets does not exclude their potential pathogenic role (Cooper et al., 2011; Coe et al., 2014).

In summary, given that *ZEB1* deletions of various sizes as well as non-coding pathogenic variants in *GRHL2* and *OVOL2* are present in a significant number of PPCD cases, we consider genome sequencing to be a time and cost-effective approach to identify the molecular genetic cause of PPCD.

Funding

This work was supported by GACR 17-12355S. Institutional support was provided by UNCE 204064 and PROGRES Q26 programs of the Charles University. FM was supported by the OP VVV MEYS project CZ.02.1.01/0.0/0.0/16_019/0000765 “Research Center for Informatics”. PS was supported by GAUK 250361/2017 and SVV 260367/2017. AH was supported by the grant no. RVO-VFN 64165 of the Ministry of Health of the Czech Republic. We thank The National Center for Medical Genomics (LM2015091) providing ethnically matched population frequency data (project CZ.02.1.01/0.0/0.0/16_013/0001634). We further thank Fight for Sight, Academy of Medical Sciences, the National Institute for Health Research, Rosetrees Trust, and Moorfields Eye Charity for supporting this research program. The research was also supported by the National Institute for Health Research Biomedical Research Centre based at Moorfields Eye Hospital NHS Foundation Trust and UCL Institute of Ophthalmology. The views expressed are those of the authors and not necessarily those of the NHS, the NIHR or the Department of Health.

Acknowledgements

We thank Marie Trková for description of deletions according to current nomenclature and to Petra Brunclíková and Marika Hakenová for patient recruitment. This work was performed within the framework of ERN-EYE.

Appendix A. Supplementary data

Supplementary data to this article can be found online at https://doi.org/10.1016/j.exer.2019.03.002.

References

Aldave, A.J., Yellore, V.S., Yu, F., Bourla, N., Sonmez, B., Salem, A.K., Rayner, S.A., Sampat, K.M., Krafchak, C.M., Richards, J.E., 2007. Posterior polymorphous corneal dystrophy is associated with *TCF8* gene mutations and abdominal hernia. Am. J. Med. Genet. 143A, 2549–2556.

Bakhtiari, P., Frausto, R.F., Roldan, A.N., Wang, C., Yu, F., Aldave, A.J., 2013. Exclusion of pathogenic promoter region variants and identification of novel nonsense mutations in the zinc finger E-box binding homeobox 1 gene in posterior polymorphous corneal dystrophy. Mol. Vis. 19, 575–580.

Baratz, K.H., Tosakulwong, N., Ryu, E., Brown, W.L., Branham, K., Chen, W., Tran, K.D., Schmid-Kubista, K.E., Heckenlively, J.R., Swaroop, A., Abecasis, G., Bailey, K.R., Edwards, A.O., 2010. E2-2 protein and Fuchs's corneal dystrophy. N. Engl. J. Med. 363, 1016–1024.

Biswas, S., Munier, F.L., Yardley, J., Hart-Holden, N., Perveen, R., Cousin, P., Sutphin, J.E., Noble, B., Batterbury, M., Kielty, C., Hackett, A., Bonshek, R., Ridgway, A., McLeod, D., Sheffield, V.C., Stone, E.M., Schorderet, D.F., Black, G.C., 2001. Missense mutations in COL8A2, the gene encoding the alpha2 chain of type VIII collagen, cause two forms of corneal endothelial dystrophy. Hum. Mol. Genet. 10, 2415–2423.

Cibis, G.W., Krachmer, J.A., Phelps, C.D., Weingeist, T.A., 1977. The clinical spectrum of posterior polymorphous dystrophy. Arch. Ophthalmol. 95, 1529–1537.

Coe, B.P., Witherspoon, K., Rosenfeld, J.A., van Bon, B.W., Vulto-van Silfhout, A.T., Bosco, P., Friend, K.L., Baker, C., Buono, S., Vissers, L.E., Schuurs-Hoeijmakers, J.H., Hoischen, A., Pfundt, R., Krumm, N., Carvill, G.L., Li, D., Amaral, D., Brown, N., Lockhart, P.J., Scheffer, I.E., Alberti, A., Shaw, M., Pettinato, R., Tervo, R., de Leeuw, N., Reijnders, M.R., Torchia, B.S., Peeters, H., O'Roak, B.J., Fichera, M., Hehir-Kwa, J.Y., Shendure, J., Mefford, H.C., Haan, E., Gécz, J., de Vries, B.B., Romano, C., Eichler, E.E., 2014. Refining analyses of copy number variations identifies specific genes associated with developmental delay. Nat. Genet. 46, 1063–1071.

Cooper, G.M., Coe, B.P., Girirajan, S., Rosenfeld, J.A., Vu, T.H., Baker, C., Williams, C., Stalker, H., Hamid, R., Hannig, V., Abdel-Hamid, H., Bader, P., McCracken, E., Niyazov, D., Leppig, K., Thiese, H., Hummel, M., Alexander, N., Gorski, J., Kussmann, J., Shashi, V., Johnson, K., Rehder, C., Ballif, B.C., Shaffer, L.G., Eichler, E.E., 2011. A copy number variation morbidity map of developmental delay. Nat. Genet. 43, 838–846.

Chaudhry, A., Chung, B.H., Stavropoulos, D.J., Araya, M.P., Ali, A., Heuon, E., Chitayat, D., 2017. Agenesis of the corpus callosum, developmental delay, autism spectrum disorder, facial dysmorphism, and posterior polymorphous corneal dystrophy associated with *ZEB1* gene deletion. Am. J. Med. Genet. 173, 2467–2471.

Chen, T., You, Y., Jiang, H., Wang, Z.Z., 2017. Epithelial-mesenchymal transition (EMT): a biological process in the development, stem cell differentiation, and tumorigenesis. J. Cell. Physiol. 232, 3261–3272.

Chung, D.W., Frausto, R.F., Ann, L.B., Jang, M.S., Aldave, A.J., 2014. Functional impact

of *ZEB1* mutations associated with posterior polymorphous and Fuchs' endothelial dystrophies. Investig. Ophthalmol. Vis. Sci. 55, 6159–6166.
Chung, D.D., Frausto, R.F., Lin, B.R., Hanser, E.M., Cohen, Z., Aldave, A.J., 2017. Transcriptomic profiling of posterior polymorphous corneal dystrophy. Investig. Ophthalmol. Vis. Sci. 58, 3202–3214.
Davidson, A.E., Liskova, P., Evans, C.J., Dudakova, L., Noskova, L., Pontikos, N., Hartmannova, H., Hodanova, K., Stranecky, V., Kozmik, Z., Levis, H.J., Idigo, N., Sasai, N., Mahler, G.J., Bellingham, J., Veli, N., Ebenzer, N.D., Cheetham, M.E., Daniels, J.T., Thaung, C.M., Jirsova, K., Plagnol, V., Filipec, M., Kmoch, S., Tuft, S.J., Hardastle, A.J., 2016. Autosomal-dominant corneal endothelial dystrophies CHED1 and PPCD1 are allelic disorders caused by non-coding mutations in the promoter of *OVOL2*. Am. J. Hum. Genet. 98, 75–89.
den Dunnen, J.T., Dalgleish, R., Maglott, D.R., Hart, R.K., Greenblatt, M.S., McGowan-Jordan, J., Roux, A.F., Smith, T., Antonarakis, S.E., Taschner, P.E., 2016. HGVS recommendations for the description of sequence variants: 2016 update. Hum. Mutat. 37, 564–569.
Ensenberger, M.G., Thompson, J., Hill, B., Homick, K., Kearney, V., Mayntz-Press, K.A., Mazur, P., McGuckian, A., Myers, J., Raley, K., Raley, S.G., Rothove, R., Wilson, J., Wieczorek, D., Fulmer, P.M., Storts, D.R., Krenke, B.E., 2010. Developmental validation of the PowerPlex 16 HS System: an improved 16-locus fluorescent STR multiplex. Forensic Sci. Int. Genet. 4, 257–264.
Evans, C.J., Liskova, P., Dudakova, L., Hrabcikova, P., Horinek, A., Jirsova, K., Filipec, M., Hardcastle, A.J., Davidson, A.E., Tuft, S.J., 2015. Identification of six novel mutations in *ZEB1* and description of the associated phenotypes in patients with posterior polymorphous corneal dystrophy 3. Ann. Hum. Genet. 79, 1–9.
Jang, M.S., Roldan, A.N., Frausto, R.F., Aldave, A.J., 2014. Posterior polymorphous corneal dystrophy 3 is associated with agenesis and hypoplasia of the corpus callosum. Vis. Res. 100, 88–92.
Krachmer, J.H., 1985. Posterior polymorphous corneal dystrophy: a disease characterized by epithelial-like endothelial cells which influence management and prognosis. Trans. Am. Ophthalmol. Soc. 83, 413–475.
Krafchak, C.M., Pawar, H., Moroi, S.E., Sugar, A., Lichter, P.R., Mackey, D.A., Mian, S., Nairus, T., Elner, V., Schteingart, M.T., Downs, C.A., Kijek, T.G., Johnson, J.M., Trager, E.H., Rozsa, F.W., Mandal, M.N., Epstein, M.P., Vollrath, D., Ayyagari, R., Boehnke, M., Richards, J.E., 2005. Mutations in *TCF8* cause posterior polymorphous corneal dystrophy and ectopic expression of *COL4A3* by corneal endothelial cells. Am. J. Hum. Genet. 77, 694–708.
Le, D.J., Chung, D.W., Frausto, R.F., Kim, M.J., Aldave, A.J., 2016. Identification of potentially pathogenic variants in the posterior polymorphous corneal dystrophy 1 locus. PLoS One 11 (6), e0158467.
Lechner, J., Dash, D.P., Muszynska, D., Hosseini, M., Segev, F., George, S., Frazer, D.G., Moore, J.E., Kaye, S.B., Young, T., Simpson, D.A., Churchill, A.J., Heon, E., Willoughby, C.E., 2013. Mutational spectrum of the *ZEB1* gene in corneal dystrophies supports a genotype-phenotype correlation. Investig. Ophthalmol. Vis. Sci. 54, 3215–3223.
Lek, M., Karczewski, K.J., Minikel, E.V., Samocha, K.E., Banks, E., Fennell, T., O'Donnell-Luria, A.H., Ware, J.S., Hill, A.J., Cummings, B.B., Tukiainen, T., Birnbaum, D.P., Kosmicki, J.A., Duncan, L.E., Estrada, K., Zhao, F., Zou, J., Pierce-Hoffman, E., Berghout, J., Cooper, D.N., Deflaux, N., DePristo, M., Do, R., Flannick, J., Fromer, M., Gauthier, L., Goldstein, J., Gupta, N., Howrigan, D., Kiezun, A., Kurki, M.I., Moonshine, A.L., Natarajan, P., Orozco, L., Peloso, G.M., Poplin, R., Rivas, M.A., Ruano-Rubio, V., Rose, S.A., Ruderfer, D.M., Shakir, K., Stenson, P.D., Stevens, C., Thomas, B.P., Tiao, G., Tusie-Luna, M.T., Weisburd, B., Won, H.H., Yu, D., Altshuler, D.M., Ardissino, D., Boehnke, M., Danesh, J., Donnelly, S., Elosua, R., Florez, J.C., Gabriel, S.B., Getz, G., Glatt, S.J., Hultman, C.M., Kathiresan, S., Laakso, M., McCarroll, S., McCarthy, M.I., McGovern, D., McPherson, R., Neale, B.M., Palotie, A., Purcell, S.M., Saleheen, D., Scharf, J.M., Sklar, P., Sullivan, P.F., Tuomilehto, J., Tsuang, M.T., Watkins, H.C., Wilson, J.G., Daly, M.J., MacArthur, D.G., Exome Aggregation Consortium, 2016. Analysis of protein-coding genetic variation in 60,706 humans. Nature 536, 285–291.
Liskova, P., Tuft, S.J., Gwilliam, R., Ebenezer, N.D., Jirsova, K., Prescott, Q., Martincova, R., Pretorius, M., Sinclair, N., Boase, D.L., Jeffrey, M.J., Deloukas, P., Hardcastle, A.J., Filipec, M., Bhattacharya, S.S., 2007. Novel mutations in the *ZEB1* gene identified in Czech and British patients with posterior polymorphous corneal dystrophy. Hum. Mutat. 28, 638.
Liskova, P., Filipec, M., Merjava, S., Jirsova, K., Tuft, S.J., 2010. Variable ocular phenotypes of posterior polymorphous corneal dystrophy caused by mutations in the *ZEB1* gene. Ophthalmic Genet. 31, 230–234.
Liskova, P., Palos, M., Hardcastle, A.J., Vincent, A.L., 2013. Further genetic and clinical insights of posterior polymorphous corneal dystrophy 3. JAMA Ophthalmol. 131, 1296–1303.
Liskova, P., Evans, C.J., Davidson, A.E., Zaliova, M., Dudakova, L., Trkova, M., Stranecky, V., Carnt, N., Plagnol, V., Vincent, A.L., Tuft, S.J., Hardcastle, A.J., 2016. Heterozygous deletions at the *ZEB1* locus verify haploinsufficiency as the mechanism of disease for posterior polymorphous corneal dystrophy type 3. Eur. J. Hum. Genet. 24, 985–991.
Liskova, P., Dudakova, L., Evans, C.J., Rojas Lopez, K.E., Pontikos, N., Athanasiou, D., Jama, H., Sach, J., Skalicka, P., Stranecky, V., Kmoch, S., Thaung, C., Filipec, M., Cheetham, M.E., Davidson, A.E., Tuft, S.J., Hardcastle, A.J., 2018. Ectopic *GRHL2* expression due to non-coding mutations promotes cell state transition and causes posterior polymorphous corneal dystrophy 4. Am. J. Hum. Genet. 102, 447–459.
Liu, Y., Peng, X., Tan, J., Darling, D.S., Kaplan, H.J., Dean, D.C., 2008. Zeb1 mutant mice as a model of posterior corneal dystrophy. Investig. Ophthalmol. Vis. Sci. 49, 1843–1849.
MacDonald, J.R., Ziman, R., Yuen, R.K., Feuk, L., Scherer, S.W., 2014. The Database of Genomic Variants: a curated collection of structural variation in the human genome. Nucleic Acids Res. 42, D986–D992.
McKenna, A., Hanna, M., Banks, E., Sivachenko, A., Cibulskis, K., Kernytsky, A., Garimella, K., Altshuler, D., Gabriel, S., Daly, M., DePristo, M.A., 2010. The Genome Analysis Toolkit: a MapReduce framework for analyzing next-generation DNA sequencing data. Genome Res. 20, 1297–1303.
McLaren, W., Gil, L., Hunt, S.E., Riat, H.S., Ritchie, G.R., Thormann, A., Flicek, P., Cunningham, F., 2016. The ensembl variant effect predictor. Genome Biol. 17, 122.
Nguyen, D.Q., Hosseini, M., Billingsley, G., Heon, E., Churchill, A.J., 2010. Clinical phenotype of posterior polymorphous corneal dystrophy in a family with a novel *ZEB1* mutation. Acta Ophthalmol. 88, 695–699.
Park, S.M., Gaur, A.B., Lengyel, E., Peter, M.E., 2008. The miR-200 family determines the epithelial phenotype of cancer cells by targeting the E-cadherin repressors *ZEB1* and *ZEB2*. Genes Dev. 22, 894–907.
Takagi, T., Moribe, H., Kondoh, H., Higashi, Y., 1998. DeltaEF1, a zinc finger and homeodomain transcription factor, is required for skeleton patterning in multiple lineages. Development 125, 21–31.
Thorvaldsdottir, H., Robinson, J.T., Mesirov, J.P., 2013. Integrative Genomics Viewer (IGV): high-performance genomics data visualization and exploration. Briefings Bioinf. 14, 178–192.
Vincent, A.L., Niederer, R.L., Richards, A., Karolyi, B., Patel, D.V., McGhee, C.N., 2009. Phenotypic characterisation and *ZEB1* mutational analysis in posterior polymorphous corneal dystrophy in a New Zealand population. Mol. Vis. 15, 2544–2553.
Vithana, E.N., Morgan, P., Sundaresan, P., Ebenezer, N.D., Tan, D.T., Mohamed, M.D., Anand, S., Khine, K.O., Venkataraman, D., Yong, V.H., Salto-Tellez, M., Venkatraman, A., Guo, K., Hemadevi, B., Srinivasan, M., Prajna, V., Khine, M., Casey, J.R., Inglehearn, C.F., Aung, T., 2006. Mutations in sodium-borate cotransporter SLC4A11 cause recessive congenital hereditary endothelial dystrophy (CHED2). Nat. Genet. 38, 755–757.
Zakharevich, M., Kattan, J.M., Chen, J.L., Lin, B.R., Cervantes, A.E., Chung, D.D., Frausto, R.F., Alvade, A.J., 2017. Elucidating the molecular basis of PPCD: effects of decreased *ZEB1* expression on conreal endothelial cell function. Mol. Vis. 23, 740–752.

Příloha 7: IPSC-derived corneal endothelial-like cells act as an appropriate model system to assess the impact of *SLC4A11* variants on pre-mRNA splicing

IPSC-Derived Corneal Endothelial-like Cells Act as an Appropriate Model System to Assess the Impact of *SLC4A11* Variants on Pre-mRNA Splicing

Kristyna Brejchova,[1] Lubica Dudakova,[1] Pavlina Skalicka,[1,2] Robert Dobrovolny,[1] Petr Masek,[3,4] Martina Putzova,[5] Mariya Moosajee,[6–8] Stephen J. Tuft,[6,7] Alice E. Davidson,[6] and Petra Liskova[1,2,6]

[1]Research Unit for Rare Diseases, Department of Pediatrics and Adolescent Medicine, First Faculty of Medicine, Charles University and General University Hospital in Prague, Czech Republic
[2]Department of Ophthalmology, First Faculty of Medicine, Charles University and General University Hospital in Prague, Prague, Czech Republic
[3]Clinic of Ophthalmology, University Hospital Ostrava, Ostrava, Czech Republic
[4]Department of Craniofacial Surgery, University of Ostrava, Ostrava, Czech Republic
[5]Biopticka laborator s.r.o., Pilsen, Czech Republic
[6]UCL Institute of Ophthalmology, London, United Kingdom
[7]Moorfields Eye Hospital NHS Foundation Trust, London, United Kingdom
[8]Great Ormond Street Hospital for Children, London, United Kingdom

Correspondence: Petra Liskova, Research Unit for Rare Diseases, Department of Pediatrics and Adolescent Medicine, First Faculty of Medicine and General Teaching Hospital, Charles University, Ke Karlovu 2, Praha 2, Prague 12808, Czech Republic;
petra.liskova@lf1.cuni.cz.

KB and LD contributed equally to the work presented here and should therefore be regarded as equivalent authors.

Submitted: February 21, 2019
Accepted: June 15, 2019

Citation: Brejchova K, Dudakova L, Skalicka P, et al. IPSC-derived corneal endothelial-like cells act as an appropriate model system to assess the impact of SLC4A11 variants on pre-mRNA splicing. *Invest Ophthalmol Vis Sci*. 2019;60:3084–3090. https://doi.org/10.1167/iovs.19-26930

Purpose. To report molecular genetic findings in six probands with congenital hereditary endothelial dystrophy (CHED) variably associated with hearing loss (also known as Harboyan syndrome). Furthermore, we developed a cellular model to determine if disease-associated variants induce aberrant *SLC4A11* pre-mRNA splicing.

Methods. Direct sequencing of the entire *SLC4A11* coding region was performed in five probands. In one individual, whole genome sequencing was undertaken. The effect of c.2240+5G>A on pre-mRNA splicing was evaluated in a corneal endothelial-like (CE-like) cell model expressing *SLC4A11*. CE-like cells were derived from autologous induced pluripotent stem cells (iPSCs) via neural crest cells exposed to B27, PDGF-BB, and DKK-2. Total RNA was extracted, and RT-PCR was performed followed by Sanger and a targeted next generation sequencing (NGS) approach to identify and quantify the relative abundance of alternatively spliced transcripts.

Results. In total, 11 different mutations in *SLC4A11* evaluated as pathogenic were identified; of these, c.1237G>A, c.2003T>C, c.1216+1G>A, and c.2240+5G>A were novel. The c.2240+5G>A variant was demonstrated to result in aberrant pre-mRNA splicing. A targeted NGS approach confirmed that the variant introduces a leaky cryptic splice donor site leading to the production of a transcript containing an insertion of six base pairs with the subsequent introduction of a premature stop codon (p.Thr747*). Furthermore, a subset of transcripts comprising full retention of intron 16 also were observed, leading to the same functionally null allele.

Conclusions. This proof-of-concept study highlights the potential of using CE-like cells to investigate the pathogenic consequences of *SLC4A11* disease–associated variants.

Keywords: congenital hereditary endothelial dystrophy, SLC4A11, corneal endothelial-like cells model, induced pluripotent stem cells

Congenital hereditary endothelial dystrophy (CHED, MIM #217700) is a rare autosomal recessive disorder typically presenting as corneal edema leading to severe visual impairment from birth. A subset of patients with CHED suffers from progressive, postlingual sensorineural hearing loss,[1] in which case the condition is referred to as Harboyan syndrome (MIM #217400).

Both CHED and Harboyan syndrome are caused by bi-allelic pathogenic variants in the solute carrier family 4 member 11, *SLC4A11* (MIM *610206) gene.[2] SLC4A11 is a transmembrane protein carrier facilitating Na^+-coupled OH^- (or H^+) transport, H^+-NH_3 cotransport, as well as H^+ (OH^-) flux.[3–5] The protein also promotes transmembrane water flux regulated by the osmolarity of the extracellular environment.[6] Studies in *Slc4a11* null mice and human corneal endothelial (CE) cell cultures depleted of *SLC4A11* using targeted small interfering RNA have shown that impairment of SLC4A11 function increased oxidative stress and decreased endothelial cell viability.[7,8]

In humans, the *SLC4A11* gene is expressed only in tissues that are not readily amenable to biopsy, including the corneal endothelium, salivary and thyroid gland, trachea, inner ear,

kidney, and testis.[9,10] Hence, the differentiation of induced pluripotent stem cells (iPSCs) into various relevant cell types represents an attractive option to characterize disease-associated variants.[11] To date, there are only three studies differentiating human iPSCs into CE-like cells.[12–14] However, iPSC-derived CE-like cells have not yet been used to investigate the pathogenic consequences of any disease-associated *SLC4A11* variants.

In this study, we report the disease-causing mutations in six families with CHED and demonstrate that in some instances the onset of disease may be delayed until after the first few years of life. Furthermore, using CE-like cells differentiated from iPSCs, we have assessed the effect of a novel intronic mutation on pre-mRNA splicing of *SLC4A11*.

Methods

Editorial Policies and Ethical Considerations

The study adhered to the tenets set out in the Declaration of Helsinki and was approved by the ethics committee of the General University Hospital in Prague (151/11 S-IV) and Moorfields Eye Hospital (13/LO/1084 and 09/H0724/25). All participants or their legal representatives signed informed consent before inclusion in the study.

Clinical Assessment

Ophthalmic assessment included distant Snellen best-corrected visual acuity (BCVA) or V2000 Linear kays in children younger than 4 years extrapolated to decimal values, Jaeger cards for near vision, slit-lamp biomicroscopy, IOP, and keratometry. Central corneal thickness was measured with ultrasonic pachymetry (Pachmate 2; DGH Technology, Exton, PA, USA) or by spectral-domain optical coherence tomography (SD-OCT), (Spectralis; Heidelberg Engineering GmbH, Heidelberg, Germany), which was also used for retinal imaging.

SLC4A11 Screening

DNA was isolated from peripheral venous blood according to the manufacturer's protocols with the Gentra Puregene TM Blood Kit (Qiagen, Hilden, Germany) or from saliva using an Oragene DNA kit OG-500 (DNA Genotek, Inc., Ottawa, Ontario, Canada). All *SLC4A11* coding exons (RefSeq NM_032034.3) including intron/exon boundaries were sequenced by conventional Sanger sequencing using primers listed in Supplementary Table S1. One proband was analyzed by genome sequencing performed using a TruSeq Nano DNA library preparation kit and a HiSeq X Ten sequencer (Illumina, Inc., San Diego, CA, USA). The reads were aligned with the SeqMan NGen version 11 (DNAStar, Madison, WI, USA) using the default parameters. Mutation description followed recommendations of the Human Genome Variation Society (http://varnomen.hgvs.org/).[15] The frequency of the detected *SLC4A11* variants was established from the Genome Aggregation Database (gnomAD; http://gnomad.broadinstitute.org/)[16] providing data on more than 120,000 individuals and in 4528 Czech chromosomes available through the NGS projects of the National Centre for Medical Genomics (https://ncmg.cz/en).

The effect of missense variants was evaluated in silico by using six software tools (Supplementary Table S2). Four tools were used to assess variants potentially affecting pre-mRNA splicing (Supplementary Table S3).

Identified novel variants were submitted to the Locus Specific Database (https://databases.lovd.nl/shared/genes/SLC4A11).

iPSCs Generation

Peripheral blood mononuclear cells (PBMCs) obtained from a heterozygous carrier with an intronic *SLC4A11* variant c.2240+5G>A, and a healthy control were isolated with Histopaque (Sigma-Aldrich, St. Louis, MO, USA) according to the manufacturer's instructions. They were then frozen in 10% dimethyl sulfoxide (Sigma-Aldrich) and inactivated fetal bovine serum (BenchMark Fetal Bovine Serum; Gemini Bio-Products, West Sacramento, CA, USA) and stored in liquid nitrogen.

Reprogramming of PBMCs into iPSC line was performed using the Cyto Tune-iPS 2.0 Sendai Reprogramming Kit (Invitrogen, Carlsbad, CA, USA) as previously described.[17] Briefly, the cells were transduced at an appropriate multiplicity of infection (MOI) with each of the three reprogramming vectors MOI = 5:5:3 (hKOS:hc-Myc:hKlf4). Colonies of iPSCs were grown in the presence of feeder cells (irradiated mouse embryonic fibroblasts) in human embryonic stem cell (HES) medium containing Dulbecco's modified Eagle's medium-F12, 20% knockout serum replacement, 1% nonessential amino acids (all from Thermo Fisher Scientific, Waltham, MA, USA), 100 U/mL penicillin–100 μg/mL streptomycin (Merck, Darmstadt, Germany), 0.1 mM 2-mercaptoethanol (Sigma-Aldrich), and with 8 ng/mL bFGF (PeproTech, Rocky Hill, NJ, USA).

iPSCs Differentiation into CE-like Cells

To achieve differentiation of iPSCs into CE-like cells, we modified a previously published protocol originally devised to differentiate human embryonal stem cells into CE-like cells.[18] The iPSCs were seeded onto Geltrex coated plates (Life Technologies, Grand Island, NY, USA), grown in mTeSR1 medium (STEMCELL Technologies, Inc., Vancouver, Canada) and cultured for at least one passage to adapt to feeder-free culture conditions. Once the cells reached approximately 80% confluency, they were cultured with HES medium supplemented with dual Smad inhibitors, 500 ng/mL Noggin (PeproTech), and 10 mM SB431542 (Sigma-Aldrich), starting on day 0 for 2 days with daily media changes. On day 2, the media was replaced with "cornea medium" containing HES medium with the addition of 0.1X B27 supplement (Thermo Fisher Scientific), 10 ng/mL human recombinant platelet-derived growth factor-BB (PeproTech), and 10 ng/mL recombinant mouse Dkk-2 (PeproTech). The iPSC-derived CE-like cells were then maintained in cornea media for additional 8 days with daily changes. In addition to showing expression of *SLC4A11* by RT-PCR (as described below), the presence of CE cell status was evaluated after 10 days with primary antibodies against commonly used markers ZO-1 (Invitrogen), N-cadherin (Abcam, Cambridge, UK), and CD166 (BD Pharmingen, San Jose, CA, USA).[19,20]

Transcript Analysis

RNA was extracted from iPSC-derived CE-like cells and tissue obtained from a patient with Fuchs endothelial corneal dystrophy who underwent Descemet membrane endothelial keratoplasty using standard phenol-chloroform extraction.[21] cDNA was reverse transcribed using SuperScript III kit (Thermo Fisher Scientific). *GAPDH* was used as positive control (using primers Forward 5′-GCCAAGGTCATCCATGACAAC-3′, Reverse 5′- GTCCACCACCCTGTTGCTGTA-3′). Primers spanning *SLC4A11* exons 16 to 19 were designed (Forward 5′-CACAGGGCTGTCTCTGTTTG-3′, Reverse 5′-CAGAGCAGTCACCCACACAC-3′) and cDNA-derived PCR products were sequenced by conventional Sanger sequencing using Big Dye terminator chemistry on an ABI PRISM 3100 genetic analyzer (Applied Biosystems, Forester City, CA, USA).

Table 1. Clinical and Demographic Data Including Longitudinal Observations in Six Probands With CHED Variably Associated With Hearing Impairment

Family/ ID	Age, y*	BCVA		CCT, µm		Other Information	Hearing Impairment
		RE	LE	RE	LE		
C2/II:1	5	0.5	0.4	1098	1078	LE convergent strabismus	Y - onset at 5 y, mild
C3/II:1	70	0.01	0	UA	PK	LE PK at 10 y, vision lost after injury at 36 y	Y
C4/II:2	7	0.02†	0.03†	UA	UA	Horizontal nystagmus	Y - onset at 14 y, mild
	35	HM	0.05	PK	PK	RE PK at 7 y LE PK at 8.5 y, rePK	
C5/II:2	10	0.4	0.4	1032	1032	Visual impairment noticed at 5 y Good near vision	Y - onset at 6 y, perceptive, mild nonprogressive, hearing aid since 8.5 y
B1/II:1	3	0.54	0.64	1046	1036	Nil	N
B2/II:1	6	0.25†	0.25†	UA	UA	RE exotropia	N
	10	0.05†	0.66	UA	PK	RE PK at 10 y, rePK, rePK+cataract	
	47	0.66	0.66	PK	PK+ DMEK	LE PK at 7 y, DMEK+cataract	

CCT, central corneal thickness; DMEK, Descemet membrane endothelial keratoplasty; HM, hand movement; LE, left eye; N, no; PK, penetrating keratoplasty; RE, right eye; rePK, repeated penetrating keratoplasty; UA, unavailable data; Y, yes.

* At examination.

† Prior to PK.

A targeted next generation sequencing (NGS) approach was subsequently used to verify and quantify the identity of alternatively spliced transcripts present within the iPSC-derived CE-like cells originating from a control individual and a heterozygous carrier of the c.2240+5G>A *SLC4A11* variant. Library was prepared by KAPA HyperPlus Kit (Roche, Pleasanton, CA, USA) using RT-PCR primers spanning exons 16 to 19 (see above) and standard adaptors (KAPA Dual-Indexed Adapter Kit; Roche) according to the manufacturer instructions and sequenced on Illumina sequencing platform (NextSeq 550). Reads were then aligned to GRCh37 using STAR software[22] and visualized with the Integrated Genomics Viewer (Broad Institute, Berkeley, CA, USA).[23]

Results

Six probands with CHED were investigated. None of the affected families reported a history for corneal disease or consanguinity. In four individuals, the disease was associated with hearing loss (Table 1). Five of the six patients were noted to have cloudy corneas since birth (Figs. 1A, 1B). The BCVA in eyes that had not had corneal transplantation ranged from 0.64 in the proband from family B1 aged 3 years to 0.01 in a 70-year-old proband from family C3 (Fig. 1E). Corneal thickness measurements were available for six eyes and ranged from 1032 µm to 1098 µm. Probands from families C2 and C5 had an SD-OCT examination of the posterior pole, which confirmed a normal macula architecture and no retinal pathology. A summary of clinical findings is provided in Table 1.

Of note, the reduced visual acuity in the proband from family C5 was only detected at routine review at the age of 5 years. Retrospectively, the parents admitted noticing mild corneal clouding of variable intensity; however, this did not prompt them to have the child examined by an ophthalmologist. At the age of 10 years, the distance visual acuity was 0.4 in both eyes, but with normal near vision of J1 with Jaeger cards. At age 10, both corneas were hazy and markedly thickened (Figs. 1C, 1D; Table 1).

In total, 11 different *SLC4A11* variants evaluated as pathogenic were identified, including four novel mutations (Table 2; Fig. 2). Segregation analysis confirmed that four of the affected probands harbored compound heterozygous *SLC4A11* variants (Fig. 2). DNA samples from families C3 and B2 were not available for segregation analysis. The evidence to support pathogenicity of each variant is listed in Table 2,[24–30] including a summary of previously performed functional studies in cellular models. Novel missense mutations c.1237G>A,

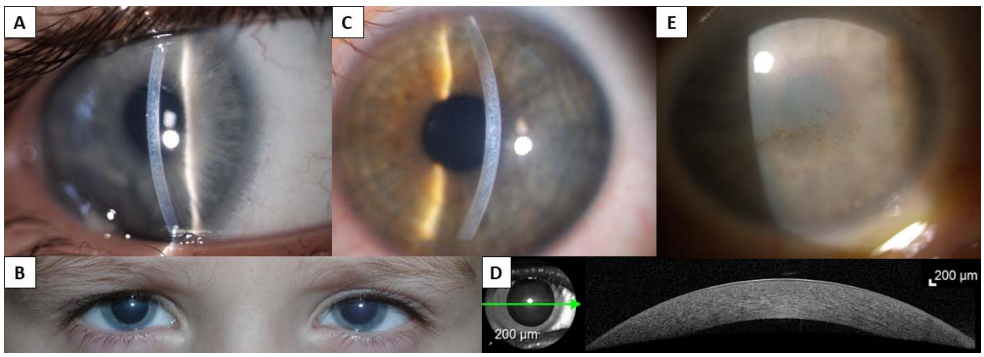

Figure 1. Clinical findings in individuals with CHED. Slit-lamp photograph in a narrow beam of the right cornea of proband from family C2, aged 5 years (**A**) and readily visible bilateral corneal clouding in the same individual (**B**). Left corneal photograph of proband from family C5, aged 10 years (**C**), and SD-OCT imaging documenting abnormal thickness and diffuse mild loss of transparency. *Green arrow* indicates where the cross-section image was taken (**D**). Slit-lamp photograph of the right eye of proband from family C3, aged 70 years; note diffuse opacity and spheroidal degeneration (**E**).

Table 2. Summary of *SLC4A11* Mutations Identified in Six Families with CHED

Family	Population	Mutation		Zygosity	GnomAD*	Czech Alleles	Pathogenicity Evidence	References
		DNA	Protein					
C2	European Czech	c.1216+1G>A	"p.?"	HET	0	0	Predicted pathogenic	Novel
		c.2411G>A	p.(Arg804His)	HET	3/245,612	0	Decreased level of matured mutant protein compared with wild type	24, 25
C3	European Czech	c.2263C>T	p.(Arg755Trp)	HOM†	2/244,792	0	Endoplasmic reticulum retained, misfolded protein	24, 26–28
C4	European Czech	c.2527_2529del	p.(Leu843del)	HET	0	0	Predicted pathogenic	29
		c.1237G>A	p.(Gly413Arg)	HET	0	1/4,528	Predicted pathogenic	Novel
C5	European Czech	c.625C>T	p.(Arg209Trp)	HET	3/246,062	0	Endoplasmic reticulum retained, misfolded protein	24, 28
		c.2240+5G>A	p.Thr747*	HET	0	0	Splicing defect verified by cDNA analysis (current study)	Novel
B1	European British	c.2240+1G>A	"p.?"	HET	6/276,692	0	Predicted pathogenic	27, 29
		c.427G>A	p.(Glu143Lys)	HET	1/246,144	0	Endoplasmic reticulum retained, misfolded protein	24, 27, 30
B2	European British	c.2003T>C	p.(Leu668Pro)	HET†	4/244,724	0	Predicted pathogenic	Novel
		c.2528T>C	p.(Leu843Pro)	HET†	6/276,968	0	Endoplasmic reticulum retained, misfolded protein	1, 24

p.? refers to unknown effect on protein structure. HET, heterozygous; HOM, homozygous.

* Heterozygous allele count/total number of alleles.

† Segregation analysis not performed, hence possibility of a deletion or existence of a possibly pathogenic intronic variant in a trans configuration exists.

p.(Gly413Arg), and c.2003T>C, p.(Leu668Pro) were predicted to have a pathogenic effect using all six tools (Supplementary Table S2). One novel mutation identified in the current study, c.1216+1G>A, was located in a canonical splice site and another mutation near to an intron-exon boundary c.2240+5G>A. Their effect on pre-mRNA splicing was assessed in silico using four different tools. All algorithms predicted that both variants abolish splice donor sites (Supplementary Table S3).

However, because the c.2240+5G>A variant was not located within the canonical splice site, we wanted to generate experimental evidence to support its potential pathogenicity. *SLC4A11* is not expressed in accessible tissue, hence we decided to generate CE-like cells from patient-derived iPSCs to investigate if the variant alters splicing. We deliberately selected a heterozygous carrier of the c.2240+5G>A *SLC4A11* variant to generate iPSCs given that bi-allelic *SLC4A11* mutations have previously been suggested to decrease cell viability.[31,32]

Importantly, the iPSC-derived CE-like cells were demonstrated to express not only *SLC4A11,* but also additional CE cell markers (ZO-1, N-Cadherin, and CD166) by immunocytochemistry, confirming their endothelial cell-like status (Fig. 3A). RT-PCR primers binding exons surrounding the variant of interest were used to amplify the iPSC-derived CE-like cells cDNA (Fig. 3B). Although PCR products generated from the c.2240+5G>A-positive and control CE-like cells appeared to be the same size (Fig. 3C), Sanger sequencing revealed that at least two distinct products were amplified in the c.2240+5G>A-positive sample: the wild-type product and an alternatively spliced product. Examination of the Sanger sequencing trace confirmed that the c.2240+5G>A variant introduced a cryptic donor site 7 base pairs (bp) downstream of the wild-type site, resulting in the insertion of six nucleotides leading to a premature stop codon p.Thr747* (Fig. 3D).

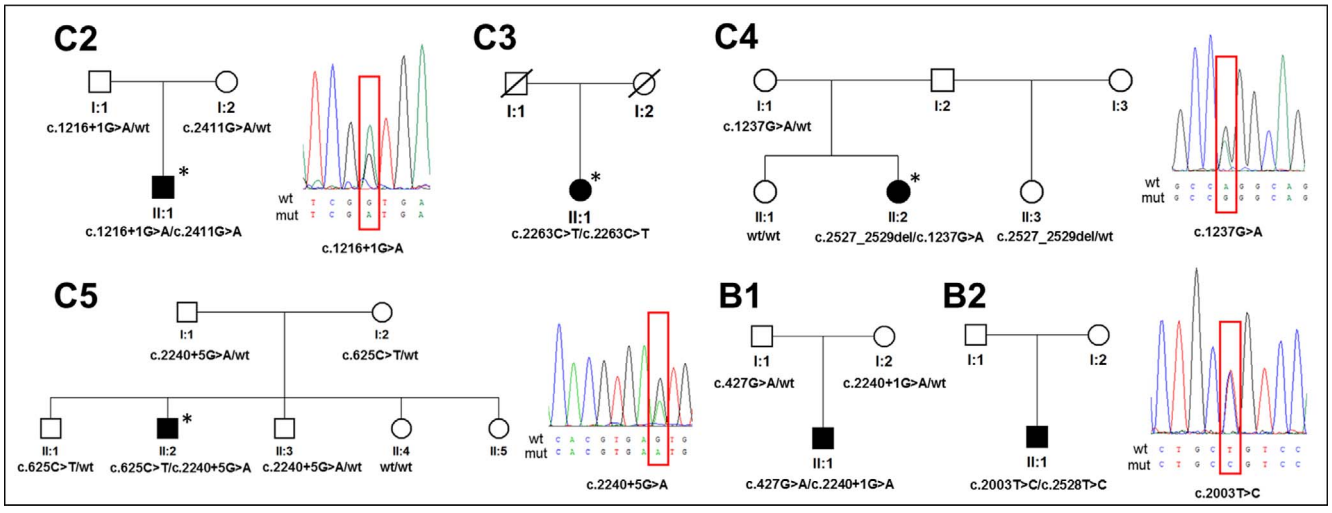

Figure 2. Detected *SLC4A11* mutations and their segregation within six families with CHED. Sequence chromatograms of novel mutations (within *red boxes*) are also shown. Individuals with hearing impairment are indicated by an asterisk.

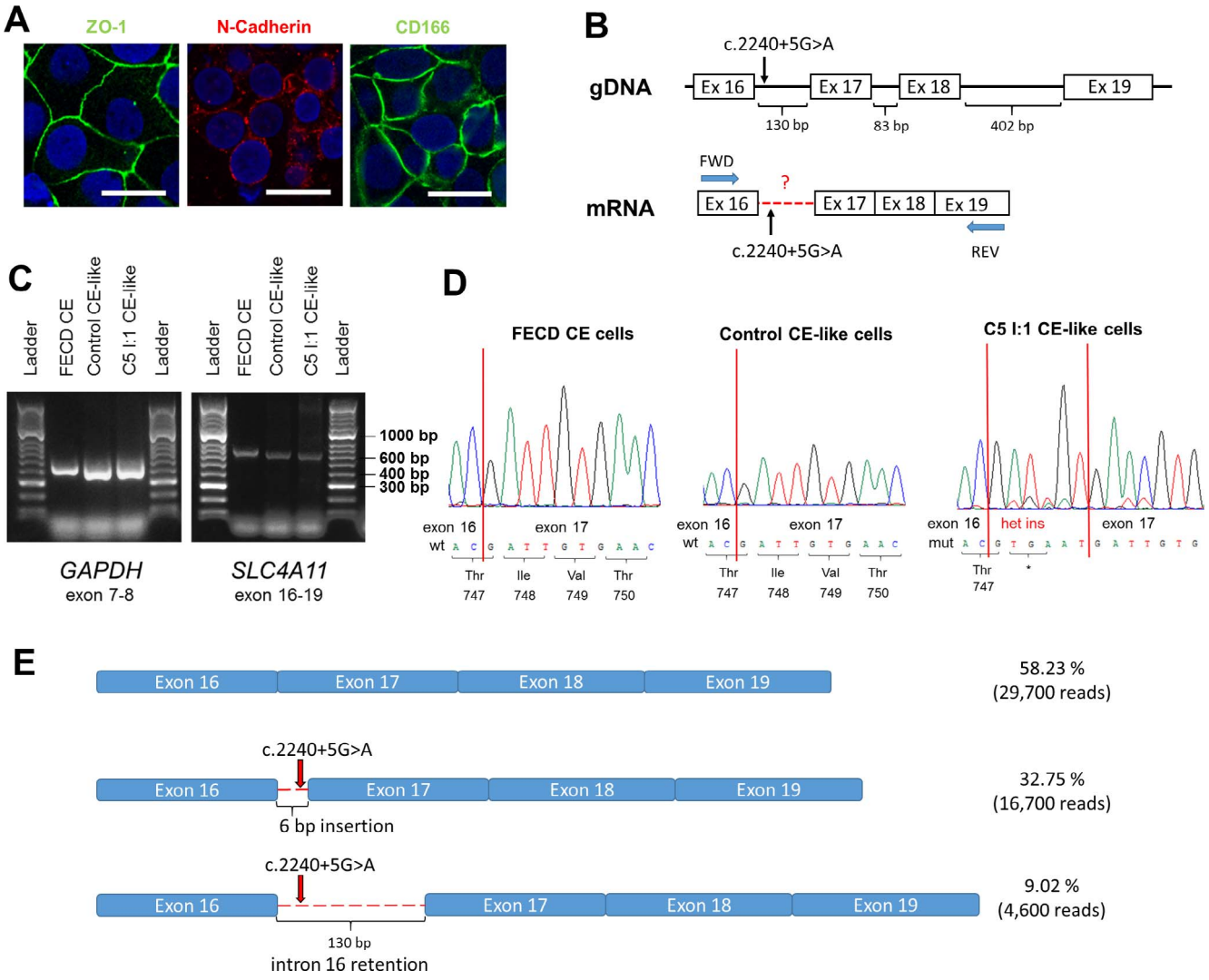

Figure 3. Functional analysis of the effect of a novel mutation c.2240+5G>A in *SLC4A11* using cDNA derived from CE-like cells. (**A**) Immunocytochemical staining of CE-like cells derived from iPSCs of a healthy heterozygous carrier of c.2240+5G>A variant (individual I:1 from family C5). The *scale bar* represents 20 µm. (**B**) Schematic representation of *SLC4A11* transcript with marked variant functionally assessed and primer annealing positions. (**C**) Electrophoresis of PCR product derived from different sources of cDNA; CE cells gained from a patient with Fuchs endothelial corneal dystrophy (FECD CE), control iPSC CE-like cells and iPSC CE-like cells from subject C5 I:1. (**D**) Sequence chromatograms of a PCR product spanning *SLC4A11* exons 16 to 19 derived from cDNA from CE cells gained from a patient with FECD, CE-like cells from a healthy control individual and from a healthy heterozygous carrier of c.2240+5G>A variant. (**E**) Schematic representation of results obtained by targeted NGS of cDNA from a heterozygous carrier of c.2240+5G>A (individual I:1 from family C5) showing the precise number of different reads obtained for each of the three transcript variants.

Targeted NGS sequencing was next performed to verify the identity of the alternatively spliced product(s) and quantify their relative abundance (Fig. 3E; Supplementary Fig. S1). In summary, 32.75% (16,700/51,000 reads) of total generated and mapped reads were identified to encompass the same 6-bp insertion that had previously been characterized by Sanger sequencing. Interestingly, a further 9.02% of reads (4600) contained the entire sequence of intron 16 (Fig. 3E; Supplementary Fig. S1). If translated, this transcript is predicted to lead to insertion of 130 bp and subsequent a premature stop codon p.Thr747*, as the first 6 bp are common for both aberrant transcripts. Importantly, all reads comprising intron 16 retention were noted to contain the c.2240+5A variant and are hence transcribed exclusively from the mutant allele (Supplementary Fig. S1). Given the heterozygous status of the sample, a minimum of 50% of total reads were hypothesized to correspond to the wild-type transcript. Interestingly, 58.23% of the total reads mapped to the wild-type transcript, suggesting that some wild-type transcripts may be transcribed from the mutant allele and/or that the mutant transcripts are degraded by nonsense-mediated decay, resulting in a shorter half-life than the wild-type transcript, and hence potentially explaining their collective relatively lower abundance (43.75%). However, it also must be acknowledged that the relative difference observed also may be influenced by different amplification efficiencies of the PCR products generated from the alternatively spliced transcripts.

Discussion

In this study, we report on clinical findings and molecular genetic investigation in six probands with CHED. Furthermore, we also have developed an iPSC-derived CE-like model system

to enable us to assess the effect of c.2240+5G>A on *SLC4A11* pre-mRNA splicing.

Because of the relative inaccessibility of tissues expressing *SLC4A11* in vivo, previous functional studies of *SLC4A11* mutations have been performed using transiently transfected human embryonic kidney cell lines (HEK293), involving the overexpression of the transcript in its non-native cellular context.[24,33,34] Our use of a CE-like cells model importantly enabled us to assess the variant of interest effect on pre-mRNA splicing within its native genomic and cellular context. We were able to verify the CE-like status of the model system by demonstrating that endothelial markers *SLC4A11*, ZO-1, N-Cadherin, and CD166 were all detected.[19] This system could be readily adopted in future to investigate not only the consequence of other *SLC4A11* variants on pre-RNA splicing, but also other functional outcomes, such as SLC4A11 transport function, protein stability, and localization. Likewise, mutations altering the expression and/or function of other CE cell–specific transcripts and proteins also could be investigated using the same approach.

Two novel missense mutations p.(Gly413Arg) and p.(Leu668Pro), found in a compound heterozygote state with previously reported mutations,[29,35] were predicted to be pathogenic by our in silico analysis. The effect of other missense mutations except for p.(Leu843del) has been previously studied in transiently co-transfected HEK293 cellular model.[24,30] The overall predicted effect of all three splicing mutations identified in this study c.1216+1G>A, c.2240+5G>A, and c.2240+1G>A is degradation of the transcript due to mRNA nonsense-mediated decay mechanism. Although c.1216+1G>A and c.2240+1G>A were not studied functionally, they are likely to cause aberrant pre-mRNA splicing because of their location in canonical splice sites.

The proband from family C5 (compound heterozygote for c.2240+5G>A, p.Thr747* and c.625C>T, p.[Arg209Trp]) is the only individual lacking clear congenital signs of CHED in this series. Interestingly, p.(Arg209Trp) has previously been observed in the homozygous state in a patient with a severe and congenital disease onset.[28] We therefore hypothesize that the milder phenotypic presentation in our proband could be attributed to the c.2240+5G>A resulting in the introduction of a "leaky" donor splice site, producing a mix of aberrantly spliced transcripts and some residual wild-type product as suggested by quantification of targeted NGS sequencing reads. Alternatively, the notably reduced levels of mutant versus wild-type transcripts may be attributed to nonsense-mediated decay; both identified aberrantly spliced transcripts contain premature termination codon. Unfortunately, no informative heterozygous polymorphism was present within the amplified coding region to enable us to infer the phase of wild-type reads generated.

Four of the six patients in our study had hearing impairment and should therefore be classified as Harboyan syndrome. However, a recent review has confirmed that premature deafness is a feature of most, if not all, cases with CHED, supporting the concept that Harboyan syndrome and CHED should not be considered distinct clinical entities.[36] At a minimum, periodic audiometry is recommended for all individuals with CHED.

Our study further highlights the usefulness of molecular genetic testing to decipher the diagnosis in patients with bilateral corneal opacity as demonstrated in proband from family C3 with advanced corneal changes and no past clinical notes. Genetic testing also enables CHED to be distinguished from other causes of early-onset corneal edema, such as posterior polymorphous corneal dystrophy type 3, which in contrast to CHED is inherited in an autosomal dominant fashion. Thus, identification of disease-causing mutations has direct implications for clinical management.[37,38]

In summary, we anticipate that the use of iPSC-derived CE-like cells will be a useful tool to access the effects of variants of unknown significance on pre-mRNA splicing of corneal endothelial–specific proteins and other functional outcomes, such as protein function, stability, and localization.

Acknowledgments

The authors thank The National Center for Medical Genomics (LM2015091) for providing ethnically matched population frequency data (project CZ.02.1.01/0.0/0.0/16_013/0001634) and Marcela Michalickova and Ivana Kaincova for ophthalmic examination of proband from family C2. The authors declare they have no conflicts of interest with the contents of this article.

Supported by GACR 17-12355S. Institutional support was provided by UNCE 204064 and PROGRES Q26 programs of the Charles University. Also supported by grants GAUK 250361/2017 and SVV 260367/2017 (PS), Fight for Sight and Moorfields Eye Charity (AED), the National Institute for Health Research (NIHR) Biomedical Research Centre based at Moorfields Eye Hospital NHS Foundation Trust and UCL Institute of Ophthalmology (AED, ST, and MM), and the Wellcome Trust, London (MM).

Disclosure: **K. Brejchova**, None; **L. Dudakova**, None; **P. Skalicka**, None; **R. Dobrovolny**, None; **P. Masek**, None; **M. Putzova**, None; **M. Moosajee**, None; **S.J. Tuft**, None; **A.E. Davidson**, None; **P. Liskova**, None

References

1. Desir J, Abramowicz M. Congenital hereditary endothelial dystrophy with progressive sensorineural deafness (Harboyan syndrome). *Orphanet J Rare Dis*. 2008;3:28.
2. Kodaganur SG, Kapoor S, Veerappa AM, et al. Mutation analysis of the *SLC4A11* gene in Indian families with congenital hereditary endothelial dystrophy 2 and a review of the literature. *Mol Vis*. 2013;19:1694–1706.
3. Kao L, Azimov R, Abuladze N, Newman D, Kurtz I. Human SLC4A11-C functions as a DIDS-stimulatable $H(^+)(OH(^-))$ permeation pathway: partial correction of R109H mutant transport. *Am J Physiol Cell Physiol*. 2015;308:C176–C188.
4. Ogando DG, Jalimarada SS, Zhang W, Vithana EN, Bonanno JA. SLC4A11 is an EIPA-sensitive Na(+) permeable pHi regulator. *Am J Physiol Cell Physiol*. 2013;305:C716–C727.
5. Zhang W, Ogando DG, Bonanno JA, Obukhov AG. Human SLC4A11 is a novel NH_3/H^+ co-transporter. *J Biol Chem*. 2015; 290:16894–16905.
6. Vilas GL, Loganathan SK, Liu J, et al. Transmembrane water-flux through SLC4A11: a route defective in genetic corneal diseases. *Hum Mol Genet*. 2013;22:4579–4590.
7. Guha S, Chaurasia S, Ramachandran C, Roy S. SLC4A11 depletion impairs NRF2 mediated antioxidant signaling and increases reactive oxygen species in human corneal endothelial cells during oxidative stress. *Sci Rep*. 2017;7:4074.
8. Han SB, Ang HP, Poh R, et al. Mice with a targeted disruption of Slc4a11 model the progressive corneal changes of congenital hereditary endothelial dystrophy. *Invest Ophthalmol Vis Sci*. 2013;54:6179–6189.
9. Groger N, Frohlich H, Maier H, et al. SLC4A11 prevents osmotic imbalance leading to corneal endothelial dystrophy, deafness, and polyuria. *J Biol Chem*. 2010;285:14467–14474.
10. Parker MD, Ourmozdi EP, Tanner MJ. Human BTR1, a new bicarbonate transporter superfamily member and human AE4 from kidney. *Biochem Biophys Res Commun*. 2001;282: 1103–1109.
11. Ebert AD, Liang P, Wu JC. Induced pluripotent stem cells as a disease modeling and drug screening platform. *J Cardiovasc Pharmacol*. 2012;60:408–416.

12. Ali M, Khan SY, Vasanth S, et al. Generation and proteome profiling of PBMC-originated, iPSC-derived corneal endothelial cells. *Invest Ophthalmol Vis Sci*. 2018;59:2437–2444.
13. Wagoner MD, Bohrer LR, Aldrich BT, et al. Feeder-free differentiation of cells exhibiting characteristics of corneal endothelium from human induced pluripotent stem cells. *Biol Open*. 2018;7:bio032102.
14. Zhao JJ, Afshari NA. Generation of human corneal endothelial cells via in vitro ocular lineage restriction of pluripotent stem cells. *Invest Ophthalmol Vis Sci*. 2016;57:6878–6884.
15. den Dunnen JT, Dalgleish R, Maglott DR, et al. HGVS recommendations for the description of sequence variants: 2016 update. *Hum Mutat*. 2016;37:564–569.
16. Lek M, Karczewski KJ, Minikel EV, et al. Analysis of protein-coding genetic variation in 60,706 humans. *Nature*. 2016; 536:285–291.
17. Reboun M, Rybova J, Dobrovolny R, et al. X-chromosome inactivation analysis in different cell types and induced pluripotent stem cells elucidates the disease mechanism in a rare case of mucopolysaccharidosis type II in a female. *Folia Biol (Praha)*. 2016;62:82–89.
18. McCabe KL, Kunzevitzky NJ, Chiswell BP, Xia X, Goldberg JL, Lanza R. Efficient generation of human embryonic stem cell-derived corneal endothelial cells by directed differentiation. *PLoS One*. 2015;10:e0145266.
19. Zarouchlioti C, Sanchez-Pintado B, Hafford Tear NJ, et al. Antisense therapy for a common corneal dystrophy ameliorates TCF4 repeat expansion-mediated toxicity. *Am J Hum Genet*. 2018;102:528–539.
20. He Z, Forest F, Gain P, et al. 3D map of the human corneal endothelial cell. *Sci Rep*. 2016;6:29047.
21. Chomczynski P, Sacchi N. Single-step method of RNA isolation by acid guanidinium thiocyanate-phenol-chloroform extraction. *Anal Biochem*. 1987;162:156–159.
22. Dobin A, Davis CA, Schlesinger F, et al. STAR: ultrafast universal RNA-seq aligner. *Bioinformatics*. 2013;29:15–21.
23. Thorvaldsdottir H, Robinson JT, Mesirov JP. Integrative Genomics Viewer (IGV): high-performance genomics data visualization and exploration. *Brief Bioinform*. 2013;14:178–192.
24. Alka K, Casey JR. Molecular phenotype of *SLC4A11* missense mutants: setting the stage for personalized medicine in corneal dystrophies. *Hum Mutat*. 2018;39:676–690.
25. Jiao X, Sultana A, Garg P, et al. Autosomal recessive corneal endothelial dystrophy (CHED2) is associated with mutations in *SLC4A11*. *J Med Genet*. 2007;44:64–68.
26. Hemadevi B, Veitia RA, Srinivasan M, et al. Identification of mutations in the *SLC4A11* gene in patients with recessive congenital hereditary endothelial dystrophy. *Arch Ophthalmol*. 2008;126:700–708.
27. Ramprasad VL, Ebenezer ND, Aung T, et al. Novel *SLC4A11* mutations in patients with recessive congenital hereditary endothelial dystrophy (CHED2). *Hum Mutat*. 2007;28:522–523.
28. Sultana A, Garg P, Ramamurthy B, Vemuganti GK, Kannabiran C. Mutational spectrum of the *SLC4A11* gene in autosomal recessive congenital hereditary endothelial dystrophy. *Mol Vis*. 2007;13:1327–1332.
29. Paliwal P, Sharma A, Tandon R, et al. Congenital hereditary endothelial dystrophy—mutation analysis of *SLC4A11* and genotype-phenotype correlation in a North Indian patient cohort. *Mol Vis*. 2010;16:2955–2963.
30. Chiu AM, Mandziuk JJ, Loganathan SK, Alka K, Casey JR. High throughput assay identifies glafenine as a corrector for the folding defect in corneal dystrophy-causing mutants of *SLC4A11*. *Invest Ophthalmol Vis Sci*. 2015;56:7739–7753.
31. Liu J, Seet LF, Koh LW, et al. Depletion of SLC4A11 causes cell death by apoptosis in an immortalized human corneal endothelial cell line. *Invest Ophthalmol Vis Sci*. 2012;53: 3270–3279.
32. Roy S, Praneetha DC, Vendra VP. Mutations in the corneal endothelial dystrophy-associated gene *SLC4A11* render the cells more vulnerable to oxidative insults. *Cornea*. 2015;34: 668–674.
33. Badior KE, Alka K, Casey JR. SLC4A11 three-dimensional homology model rationalizes corneal dystrophy-causing mutations. *Hum Mutat*. 2017;38:279–288.
34. Vilas GL, Morgan PE, Loganathan SK, Quon A, Casey JR. A biochemical framework for SLC4A11, the plasma membrane protein defective in corneal dystrophies. *Biochemistry*. 2011; 50:2157–2169.
35. Desir J, Moya G, Reish O, et al. Borate transporter *SLC4A11* mutations cause both Harboyan syndrome and non-syndromic corneal endothelial dystrophy. *J Med Genet*. 2007;44:322–326.
36. Siddiqui S, Zenteno JC, Rice A, et al. Congenital hereditary endothelial dystrophy caused by *SLC4A11* mutations progresses to Harboyan syndrome. *Cornea*. 2014;33:247–251.
37. Cunnusamy K, Bowman CB, Beebe W, Gong X, Hogan RN, Mootha VV. Congenital corneal endothelial dystrophies resulting from novel de novo mutations. *Cornea*. 2016;35: 281–285.
38. Evans CJ, Liskova P, Dudakova L, et al. Identification of six novel mutations in *ZEB1* and description of the associated phenotypes in patients with posterior polymorphous corneal dystrophy 3. *Ann Hum Genet*. 2015;79:1–9.

Investigative Ophthalmology & Visual Science

Příloha 8: Paraproteinemic keratopathy associated with monoclonal gammopathy of undetermined significance (MGUS): clinical findings in twelve patients including recurrence after keratoplasty)

Acta Ophthalmologica

Paraproteinemic keratopathy associated with monoclonal gammopathy of undetermined significance (MGUS): clinical findings in twelve patients including recurrence after keratoplasty

Pavlina Skalicka,[1,2] Lubica Dudakova,[1] Michalis Palos,[2] Lukas J. Huna,[2] Cerys J. Evans,[3] Gabriela Mahelkova,[4] Martin Meliska,[2] Tomas Stopka,[5] Stephen Tuft[6] and Petra Liskova[1,2]

[1]Research Unit for Rare Diseases, Department of Pediatrics and Adolescent Medicine, First Faculty of Medicine, Charles University and General University Hospital, Prague, Czech Republic
[2]Department of Ophthalmology, First Faculty of Medicine, Charles University and General University Hospital, Prague, Czech Republic
[3]UCL Institute of Ophthalmology, London, UK
[4]Department of Ophthalmology, Second Faculty of Medicine, Charles University and Motol University Hospital, Prague, Czech Republic
[5]BIOCEV, First Faculty of Medicine, Charles University, Prague, Czech Republic
[6]Moorfields Eye Hospital, London, UK

ABSTRACT.

Purpose: **To describe the ocular findings of 12 subjects with paraproteinemic keratopathy associated with monoclonal gammopathy of undetermined significance (MGUS).**

Methods: **Ocular examination included corneal spectral domain optical coherence tomography. In three individuals with an initial diagnosis of a lattice or Thiel–Behnke corneal dystrophy, the *TGFBI* gene was screened by conventional Sanger sequencing.**

Results: **We confirmed a diagnosis of MGUS by systemic examination and serum protein electrophoresis in 12 individuals (9 males and 3 females), with a mean age at presentation of 52.2 years (range 24–63 years) and mean follow-up 6.4 years (range 0–17 years). The best-corrected visual acuity (BCVA) at presentation ranged from 1.25 to 0.32. In all individuals, the corneal opacities were bilateral. The appearances were diverse and included superficial reticular opacities and nummular lesions, diffuse posterior stromal opacity, stromal lattice lines, superficial and stromal crystalline deposits, superficial haze and a superficial ring of hypertrophic tissue. In one individual, with opacities first recorded at 24 years of age, we documented the progression of corneal disease over the subsequent 17 years. In another individual, despite systemic treatment for MGUS, recurrence of deposits was noted following bilateral penetrating keratoplasties. The three individuals initially diagnosed with inherited corneal dystrophy were negative for *TGFBI* mutations by direct sequencing.**

Conclusion: **A diagnosis of MGUS should be considered in patients with bilateral corneal opacities. The appearance can mimic corneal dystrophies or cystinosis. In our experience, systemic treatment of MGUS did not prevent recurrence of paraproteinemic keratopathy following keratoplasty.**

Key words: corneal deposits – corneal dystrophy – cystinosis – monoclonal gammopathy of undetermined significance – paraproteinemic keratopathy – *TGFBI*

Acta Ophthalmol.

doi: 10.1111/aos.14123

Introduction

Monoclonal gammopathy of undetermined significance (MGUS) is a common haematological condition that is the result of an abnormal proliferation of a B-lymphocyte clone that secretes immunoglobulin. The prevalence of MGUS increases with age from 1.7% in individuals 50–59 years of age to 6.6% in individuals >80 years (Kyle et al. 2006). It is usually a benign condition that does not require treatment, although patients should be monitored because of a conversion rate of 1% per year to multiple myeloma or another plasma-cell or lymphoid disorder (Kyle et al. 2018). Secondary organ damage from immunoglobulin deposition can also occur, with the kidneys, eye and skin the most commonly affected (Glavey & Leung 2016; Fermand et al. 2018). To raise awareness of the potential for systemic disease in this patient group, the concept of monoclonal gammopathy of clinical significance (MGCS) has recently been introduced (Fermand et al. 2018).

Ocular disease associated with MGUS includes keratopathy, sub-conjunctival histiocytosis, infiltration of the orbit and extraocular muscles, maculopathy and uveal effusion (Glavey &

Leung 2016). Corneal disease only develops in approximately 1% of individuals with MGUS (Bourne et al. 1989). The pattern of the corneal opacities is very varied, and the appearance can mimic various degenerative changes and inherited diseases, including corneal dystrophies and cystinosis. Iridescent crystalline deposits throughout the stroma are the most common sign, but nummular subepithelial lesions, stromal lattice lines and granular deposits, diffuse stromal opacity, and a peripheral corneal ring have also been described (Lisch et al. 2012, 2016; Milman et al. 2015). Deposition of copper at the level of Descemet membrane can occur as well (Lewis et al. 1976; Hawkins et al. 2001). Recently, a new clinical classification of MGUS-induced paraproteinemic keratopathies has been proposed that describes 17 distinct phenotypes (Lisch et al. 2016).

Vision is often unaffected, but a minority require surgical intervention (e.g. superficial keratectomy or keratoplasty), although there is a high risk of disease recurrence after surgery (Milman et al. 2015).

In this study, we report 12 further cases of paraproteinemic keratopathy associated with MGUS and describe the outcome of four individuals who had surgery. We confirm the broad spectrum of clinical appearances, the potential for early onset of disease and we highlight the significant delay that can occur before the correct diagnosis is confirmed.

Materials and Methods

The Ethics committees of the General University Hospital in Prague and Moorfields Eye Hospital approved the study. A diagnosis of MGUS was based on a monoclonal component <30 g/l on serum protein electrophoresis with differentiation by immunofixation, and the absence of significant relevant disease on systemic investigation. Systemic investigation was under the care of a haematologist and was directed towards the detection of multiple myeloma, amyloid light-chain amyloidosis, Waldenström macroglobulinemia, plasmacytoma or non-Hodgkin lymphoma. Investigations included a full blood test with differential cell count, renal and liver function, urinalysis for Bence Jones proteins, echocardiography, chest X-ray, abdominal ultrasonography and a bone marrow analysis including flow cytometry and histology.

Ocular examination included Snellen best-corrected visual acuity (BCVA) extrapolated to decimal values, slit-lamp biomicroscopy, intraocular pressure and corneal spectral domain optical coherence tomography (SD-OCT) (Ophthalmic Technologies Inc., Toronto, Canada and Spectralis; Heidelberg Engineering GmbH, Heidelberg, Germany). We also performed confocal microscopy on one individual (Confoscan 3, NIDEK Technologies, Italy). In three individuals, initially diagnosed with epithelial-stromal corneal dystrophy, we extracted DNA from venous blood and performed standard Sanger sequencing of *TGFBI* coding exons 4, 11-14 (reference sequence NM_0003 58.2) (Liskova et al. 2008).

Results

We identified 12 individuals (9 males and 3 females) who matched the inclusion criteria of MGUS-associated keratopathy with a mean age at presentation of 52.2 years (range 24–63 years) (Table 1). The paraprotein band (M component) was an IgG kappa light (IgGκ) chain in 10 individuals, IgG lambda (IgGλ) in one case and IgA lambda (IgAλ) in one case (Table 1). Free light chains were only detected in the urine of individual #8. Sequencing of *TGFBI* exons for pathogenic mutations was negative in cases #1, #2 and #3. No systemic abnormalities were identified. None of the individuals reported a family history of corneal disease.

The corneal signs were bilateral in all cases. The clinical findings are summarized in Table 1, and the corneal features are illustrated in Figures 1–3. Visual acuity was reduced (<0.66) by corneal opacity in at least one eye of five individuals (#1, #2, #7, #10 and #12). In case #1 the vision deteriorated during follow-up (from 1.0 in both eyes to 0.5 in the right and 0.3 in the left eye) due to an increase in deposits. Associated ocular disease was uncommon. Case #5 had several episodes of episcleritis and keratoconjunctivitis that rapidly responded to topical corticosteroid. Three individuals (#3, #4 and #6) were asymptomatic, with opacities only identified at routine ophthalmic review. An abnormally high value for central corneal thickness [normal mean 555.50 $\pm$ 29.64 μm, range 510–624 (Lopez de la Fuente et al. 2016)] was observed in the left eye of case #10 and #9.

There was no evidence for increasing levels of serum immunoglobulins during follow-up (data not shown).

Five individuals with notable features of their disease are described in more detail. Case #1 first developed signs at an unusually early age. He was diagnosed with lattice corneal dystrophy at the age of 24 years, when his BCVA 1.0 in both eyes. MGUS was not suspected until, at the age of 40 years when *TGFBI* screening for disease-causing mutations was negative (Figure 1A,B). At his latest follow-up visit (age 41 years), his BCVA had decreased to 0.5 right eye and 0.3 left eye.

Case #2 was initially suspected to have lattice corneal dystrophy but was subsequently confirmed to have paraproteinemia. He had a combined right penetrating keratoplasty (PK) with cataract extraction, with no evidence of a recurrence of corneal opacity after 2.5 years.

Case #10 presented at the age of 60 years with bilateral superficial corneal opacities and reduced vision of unknown aetiology (Figure 1L). He then had an anterior lamellar keratoplasty in the left eye. Paraproteinemia was first suspected as a cause for his disease 2 years after surgery, when it was noted that there was recurrence of haze at the graft interface, although there was no recurrence of the superficial opacity (Figure 1M).

Case #11 had diffuse corneal stromal crystals with bilateral raised peripheral corneal rings associated with ocular surface inflammation and photophobia (Figure 1N–O). The peripheral tissue was excised on five occasions from the left eye and once from the right eye over a period of 10 years, with symptomatic relief but a rapid recurrence on each occasion. To reduce the risk of further recurrences, she was offered treatment with lenalidomide but declined.

Case #12 presented at the age of 61 years with granular and arborizing linear stromal deposits (Figure 2A–D). Because of poor vision (0.33), he had a left PK at the age of 61 years but with recurrence of corneal opacity 9 months after the surgery (Figure 2G). A right PK was planned at age 64 years and,

Table 1. Table 1. Characteristics of 12 cases with monoclonal gammopathy of unknown significance (MGUS) prior to corneal surgery.

Case	Age* gender	M-type	Serum M-type (g/l)**	BCVA***		Initial clinical diagnosis	Clinical Description	Location	CCT*** (μm)		Corneal surgery	Follow-up (years)
				RE	LE				RE	LE		
1	24 M	IgGκ	5.1	0.5	0.3	Lattice corneal dystrophy	Linear opacities with intervening haze and nummular lesions	Entire stroma (linear opacities) and superficial stroma (nummular lesions)	530	525	Nil	17
2	63 M	IgGκ	6.9	0.32[$]	0.5	Lattice corneal dystrophy	Linear and reticular opacities with intervening haze	Predominantly superficial stroma	515	501	RE PK	5
3	53 M	IgGκ	1.5	1.0	1.0	Thiel–Behnke corneal dystrophy	Reticular opacities, dots and nummular lesions	Predominantly superficial central stroma	543	535	Nil	2
4	47 F	IgGλ	0.7	1.0	1.0	Central cloudy corneal dystrophy	Diffuse opacity	Deep central stroma	UA	UA	Nil	0
5	48 M	IgAλ	13.3	1.0	1.0	Paraproteinemic keratopathy	Circular band with patches of crystalline deposits and conjunctival inflammation	Deep peripheral stroma (ring), temporal and nasal stromal edge (crystals)	514	535	Nil	15
6	45 M	IgGκ	10.6	1.25	1.25	Cystinosis	Crystalline deposits	Entire stroma	UA	UA	Nil	1
7	57 M	IgGκ	9.0	0.63	1.0	Paraproteinemic keratopathy	Crystalline deposits	Patches within superficial stroma	530	528	Nil	9
8	59 F	IgGκ	12.9	0.05[#]	0.05[#]	Cystinosis	Crystalline deposits	Entire stroma	536	528	Nil	3
9	61 M	IgGκ	8.89	0.66	1.0	Cystinosis	Crystalline deposits	Epithelium and entire stroma	552	664	Nil	1
10	60 M	IgGκ	4.0	0.16[#]	0.1[$#]	Unknown cause	Haze limited to a thin layer	Superficial stroma	615	625	LE ALK	2
11	48 F	IgGk	10.0	0.66	1.0	Paraproteinemic keratopathy	Hypertrophic peripheral corneal ring and crystalline deposits	Superficial stroma (ring) and entire stroma (crystals)	487	470	BE peripheral keratectomies	12
12	61 M	IgGκ	6.5	0.33[$]	0.33[$]	Paraproteinemic keratopathy	Arborizing linear and granular opacities	Deep central stroma	UA	UA	BE PK	10

Normal values for M-protein <0.4 g/l.
ALK = anterior lamellar keratoplasty, BCVA = best-corrected visual acuity, BE = both eyes, CCT = central corneal thickness, F = female, Ig = immunoglobulin, LE = left eye, M = male, PK = penetrating keratoplasty, RE = right eye, UA = data unavailable, κ = kappa, λ = lambda.
* Age in years when corneal deposits were first noted.
** Maximum recorded level.
*** At most recent visit.
[#] Decrease of vision attributed to cataract.
[$] Prior to keratoplasty.

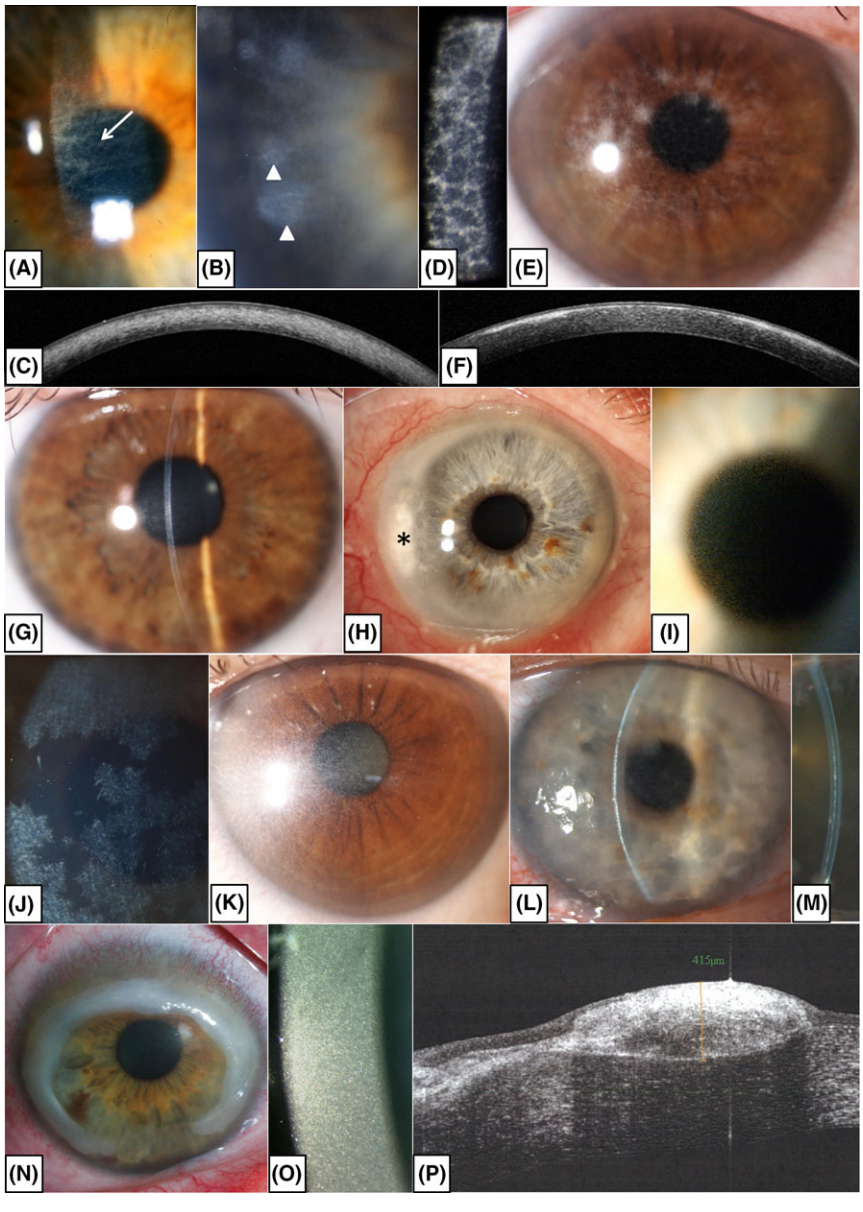

Fig. 1. Diverse corneal findings in eight patients with monoclonal paraproteinemic keratopathy. (A) Linear opacities located in the corneal stroma (arrow) and (B) peripheral subepithelial nummular lesions (arrowheads) in broad slit-lamp view (case #1 at age of 26 years); (C) SD-OCT demonstrating that the entire stromal depth can be involved (case # 1 at age 40 years). (D, E) Reticular opacities and nummular lesions in case #3 and (F) their predominantly anterior stromal location on SD-OCT. (G) Diffuse deep central stromal haze in case #4. (H) Peripheral corneal ring infiltrate in case #5 with crystalline deposits at inner temporal edge (asterisk). (I) Myriads of tiny stromal crystals in case #6. (J) Patches of superficial stromal crystalline deposits in case #7. (K) Diffuse illumination of stromal crystalline deposits in case #8. (L) Superficial haze and uneven corneal surface in case #10, and (M) recurrence of haze at the graft interface 2 years following surgery. (N) Hypertrophic superficial peripheral ring in case #11, with punctiform crystals located in the entire stroma (O), SD-OCT showing subepithelial localization of the ring and its thickness (415 μm) (P).

following haematological consultation, he had six cycles of systemic R-CHOP treatment (rituximab, cyclophosphamide, doxorubicin, vincristine and prednisone) over 4 months, with the first cycle starting 5 weeks after the corneal surgery. Despite this treatment, paraproteinemic keratopathy recurred in the right eye after 3 years (Figure 2E,F). A repeat left PK with cataract extraction was performed 5 years after the initial surgery, and this graft has remained clear after 5 years without further systemic treatment (Figure 2I). A repeat right PK has not been performed.

We were able to perform confocal microscopy in two individuals with crystalline deposits. In case #8, this demonstrated predominantly extracellular needle-shaped deposits in the stroma (Figure 3A). Deposits were also noted in the epithelial layer but the corneal endothelium was not involved. Case #10 had much denser crystalline deposits located both within the epithelial cells and keratocytes (Figure 3B,E), which precluded visualization of the endothelium.

Discussion

In this report, we describe the clinical features of a further 12 individuals with paraproteinemic keratopathy secondary to MGUS and we confirm the remarkable diversity of the clinical appearances. Although this variation in phenotype is recognized to be characteristic of paraproteinemic keratopathy, there is still the potential for novel combinations of features and diagnostic confusion, particularly with an inherited corneal dystrophy or cystinosis (Kamal et al. 2009; Lisch et al. 2012).

In one individual (#1), the onset of clinical signs was documented at 24 years of age, which, to the best of our knowledge, is the earliest reported age of manifestation. In this patient, further investigation was only prompted when a screen for *TGFBI* mutations was negative, with a delay of 16 years before the correct diagnosis was made.

Individuals with paraproteinemic keratopathy can be visually asymptomatic, and corneal opacity may only be noted during routine ophthalmic review (Milman et al. 2015; Lisch et al. 2016). Progression of the opacity is usually very slow, with a documented deterioration of vision in only one individual (#1) in this series, while in six the visual acuity remained at 1.0 in at least one eye during follow-up. However, paraproteinemic keratopathy can also cause significant visual loss. Three individuals in this series had at least one keratoplasty: individual #12 had bilateral PKs, individual #2 had a PK in one eye, while individual #10 had an anterior lamellar keratoplasty for superficial stromal opacity, but with an early recurrence in three of

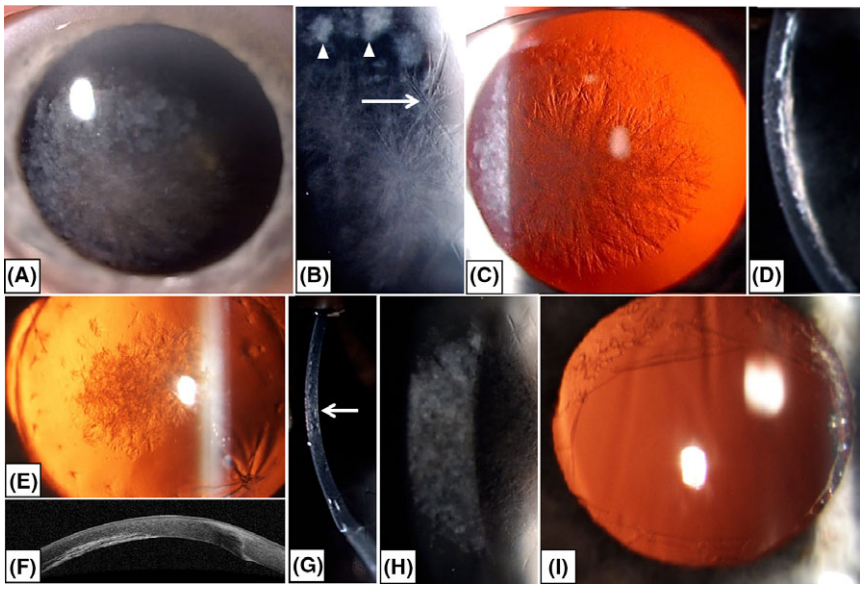

Fig. 2. Paraproteinemic keratopathy and recurrence of the disease after keratoplasty in case #12. (A) Slit-lamp photograph of the right eye prior to penetrating keratoplasty (PK) (age 64 years) demonstrating branching linear (arrows) and granular deposits (arrowheads) predominantly affecting the central cornea (B). These changes are seen in higher magnification (C), and they are clearly visualized by retroillumination (D). A narrow slit-beam view shows that the deposits are predominantly limited to the posterior corneal stroma. (E) Recurrence of the posterior deposits in the right eye 3 years after penetrating keratoplasty (PK) (age 67 years), also documented by SD-OCT (F). (G) Narrow slit-beam view showing first signs of disease recurrence in the left cornea (arrows) 9 months after PK (age 61 years). (H) Broad slit-beam view documenting increase in deposits 2 years after left PK (age 63 years). (I) Clear graft 5 years after repeated PK in the left eye in retroillumination (age 71 years).

the eyes. Other symptoms, such as conjunctival inflammation, are rare and was only seen in individual #5 with IgAλ paraproteinemia and individual #11 with IgGκ paraproteinemia, who both had a peripheral corneal stromal ring infiltrate – an appearance previously reported with IgGκ light chain MGUS (Lisch et al. 2012). Case #11 experienced a rapid recurrence of these peripheral ring infiltrates on several occasions following excision.

The effect of systemic treatment for paraproteinemic keratopathy on the risk of recurrence of corneal opacity after keratoplasty is unpredictable (Milman et al. 2015; Lisch et al. 2016). Individual #12 in our series illustrates this point. He had bilateral PKs for reduced vision from corneal opacity, with a recurrence of disease in the first eye after 9 months. Therefore, soon after the PK was performed in the second eye, systemic R-CHOP therapy was introduced to reduce the risk of recurrence. Despite this treatment, there was continued opacification in the first eye as well as the onset of opacity in the contralateral keratoplasty after 3 years. However, following a repeat keratoplasty in the first eye, and without additional systemic treatment, there was no further recurrence in the subsequent 5 years.

Previous ultrastructural studies of paraproteinemic keratopathy have demonstrated deposition of immunoglobulin in all layers of the cornea, both intracellularly and extra-cellularly. Immunohistochemistry has identified light or heavy chains, or both (Garibaldi et al. 2005). Confocal microscopy performed in two individuals corroborated these findings. The mechanism for the deposition of paraprotein in the cornea and the variety of clinical appearances remains unknown, as is the reason that only a small proportion of individuals with MGUS are affected. Interestingly, in two eyes out of 18 (11.1%) there appeared to be an increase in corneal thickness associated with paraprotein deposition.

In conclusion, a diagnosis of paraproteinemic keratopathy should trigger a referral to a haematologist to exclude the presence of a malignant monoclonal gammopathy. However, in the majority of cases systemic investigation will be negative, leading to a diagnosis of MGUS. Although MGUS was previously considered to be a benign

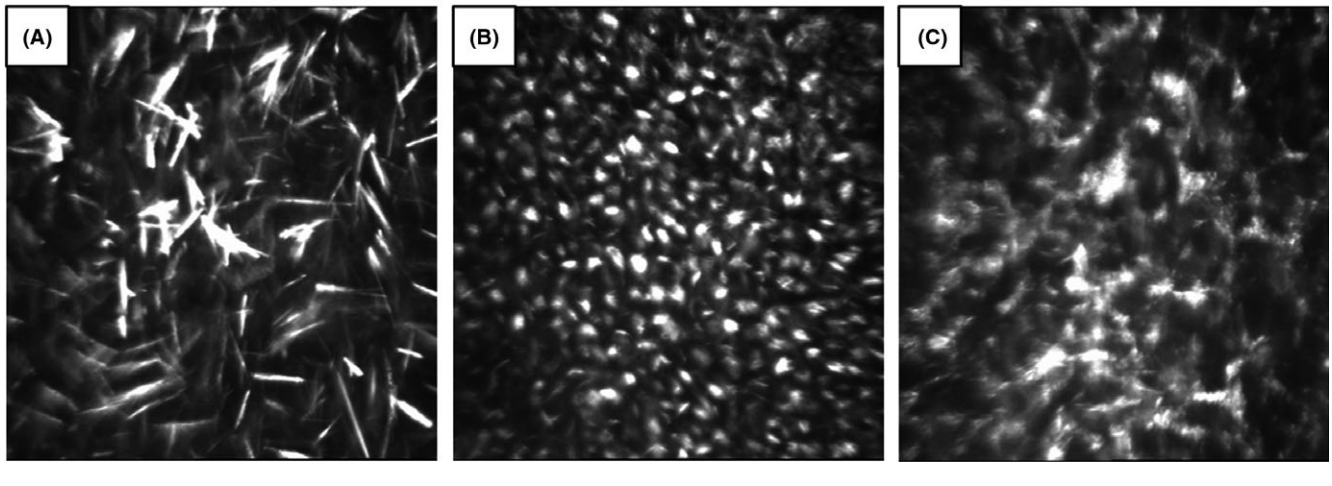

Fig. 3. Confocal microscopic images of two individuals with paraproteinemic crystalline keratopathy. (A) Needle-shaped deposits in mid-stroma of case #8. (B) Hyper-reflective material within epithelial cells and (C) keratocytes in the anterior stroma of case #11.

condition, the cumulative probability of progression to malignancy is estimated to be 12% at 10 years, increasing to 30% at 25 years (Kyle et al. 2002). Therefore, long-term monitoring of individuals with MGUS by a haematologist is necessary. To prevent unwarranted delay in making the diagnosis of MGUS, we believe that plasma protein electrophoresis should be part of the investigation for bilateral corneal opacities of unknown aetiology, especially in individuals with no family history for corneal disease. Because individuals with a MGUS may require specific treatment for systemic disease, and because the associated corneal opacity may affect vision and require surgery, the presence of paraproteinemic keratopathy is certainly a clinically significant finding. Therefore, we agree that the concept of MGCS is a more appropriate term (Fermand et al. 2018). Genetic confirmation of corneal dystrophy, even if there are characteristic features, should be also sought. In our experience, familiarity with the varied clinical signs that characterize paraproteinemic keratopathy will reduce the time to making a correct diagnosis.

References

Bourne WM, Kyle RA, Brubaker RF & Greipp PR (1989): Incidence of corneal crystals in the monoclonal gammopathies. Am J Ophthalmol **107**: 192–193.

Fermand JP, Bridoux F, Dispenzieri A, Jaccard A, Kyle RA, Leung N & Merlini G (2018): Monoclonal gammopathy of clinical significance: a novel concept with therapeutic implications. Blood **132**: 1478–1485.

Garibaldi DC, Gottsch J, de la Cruz Z, Haas M & Green WR (2005): Immunotactoid keratopathy: a clinicopathologic case report and a review of reports of corneal involvement in systemic paraproteinemias. Surv Ophthalmol **50**: 61–80.

Glavey SV & Leung N (2016): Monoclonal gammopathy: The good, the bad and the ugly. Blood Rev **30**: 223–231.

Hawkins AS, Stein RM, Gaines BI & Deutsch TA (2001): Ocular deposition of copper associated with multiple myeloma. Am J Ophthalmol **131**: 257–259.

Kamal KM, Rayner SA, Chen MC & Aldave AJ (2009): Classic lattice corneal dystrophy associated with monoclonal gammopathy after exclusion of a TGFBI mutation. Cornea **28**: 97–98.

Kyle RA, Therneau TM, Rajkumar SV, Offord JR, Larson DR, Plevak MF, Melton LJ 3rd (2002): A long-term study of prognosis in monoclonal gammopathy of undetermined significance. N Engl J Med **346**: 564–569.

Kyle RA, Therneau TM, Rajkumar SV et al. (2006): Prevalence of monoclonal gammopathy of undetermined significance. N Engl J Med **354**: 1362–1369.

Kyle RA, Larson DR, Therneau TM, Dispenzieri A, Kumar S, Cerhan JR & Rajkumar SV (2018): Long-term follow-up of monoclonal gammopathy of undetermined significance. N Engl J Med **378**: 241–249.

Lewis RA, Hultquist DE, Baker BL, Falls HF, Gershowitz H & Penner JA (1976): Hypercupremia associated with a monoclonal immunoglobulin. J Lab Clin Med **88**: 375–388.

Lisch W, Saikia P, Pitz S, Pleyer U, Lisch C, Jaeger M & Rohrbach JM (2012): Chameleon-like appearance of immunotactoid keratopathy. Cornea **31**: 55–58.

Lisch W, Wasielica-Poslednik J, Kivela T et al. (2016): The hematologic definition of monoclonal gammopathy of undetermined significance in relation to paraproteinemic keratopathy (An American Ophthalmological Society Thesis). Trans Am Ophthalmol Soc **114**: T7.

Liskova P, Klintworth GK, Bowling BL et al. (2008): Phenotype associated with the H626P mutation and other changes in the TGFBI gene in Czech families. Ophthalmic Res **40**: 105–108.

Lopez de la Fuente C, Sanchez-Cano A, Segura F, Hospital EO & Pinilla I (2016): Evaluation of total corneal thickness and corneal layers with spectral-domain optical coherence tomography. J Refract Surg **32**: 27–32.

Milman T, Kao AA, Chu D et al. (2015): Paraproteinemic keratopathy: the expanding diversity of clinical and pathologic manifestations. Ophthalmology **122**: 1748–1756.

Received on September 17th, 2018.
Accepted on April 3rd, 2019.

Correspondence:
Petra Liskova
Research Unit for Rare Diseases
Department of Pediatrics and Adolescent Medicine
First Faculty of Medicine
Charles University and General University Hospital in Prague
Ke Karlovu 2, Praha 2
128 08
Prague
Czech Republic
Tel: +420 22 496 7139
Fax: +420 22 469 7139
Email: petra.liskova@lf1.cuni.cz

This work was supported by UNCE 204064 and PROGRES-Q26/LF1 programs of the Charles University, Fight for Sight, Moorfields Eye Charity, Rosetrees Trust, and the National Institute for Health Research Biomedical Research Centre based at Moorfields Eye Hospital NHS Foundation Trust and UCL Institute of Ophthalmology. PS was supported by GAUK 250361/2017 and SVV 260367/2017. GM was supported by MH CZ – DRO, Motol University Hospital, Prague, Czech Republic 00064203. The views expressed are those of the authors and not necessarily those of the NHS, the NIHR or the Department of Health. This work was performed within the framework of ERN-EYE.

Příloha 9: Analysis of *KERA* in four families with cornea plana identifies two novel mutations

Acta Ophthalmologica

Acta Ophthalmologica 2017

Case Series

Analysis of *KERA* in four families with cornea plana identifies two novel mutations

Lubica Dudakova,[1,*] Jang Hee J. Vercruyssen,[2,*] Irina Balikova,[2,3] Lavina Postolache,[3] Bart P. Leroy,[2,4,5] Pavlina Skalicka[1,6] and Petra Liskova[1,6]

[1]Institute of Inherited Metabolic Disorders, First Faculty of Medicine, Charles University and General University Hospital in Prague, Praha, Czech Republic; [2]Department of Ophthalmology, Ghent University Hospital, Ghent, Belgium; [3]Department of Ophthalmology, Queen Fabiola Children's University Hospital, Brussels, Belgium; [4]Center for Medical Genetics, Ghent University Hospital and Ghent University, Ghent, Belgium; [5]Division of Ophthalmology and Center for Cellular and Molecular Therapeutics, The Children's Hospital of Philadelphia, Philadelphia, PA, USA; [6]Department of Ophthalmology, First Faculty of Medicine, Charles University and General University Hospital in Prague, Prague, Czech Republic

ABSTRACT.

Purpose: **To identify the molecular genetic cause in four families of various ethnic backgrounds with cornea plana.**

Methods: **Detailed ophthalmological examination and direct sequencing of the *KERA* coding region in five patients of Czech and Turkish origin and their available family members.**

Results: **Compound heterozygosity for a novel missense mutation c.209C>T; p.(Pro70Leu) and a novel splice site mutation c.887-1G>A in *KERA* were detected in two affected siblings of Czech origin. *In silico* analysis supported the pathogenicity of both variants. The second proband of Czech origin harboured c.835C>T; p.(Arg279*) in a homozygous state. Homozygous mutations c.740A>G; p.(Asn247-Ser) and c.674C>T; p.(Ile225Thr) were identified in the Turkish probands, both born out of consanguineous marriages. Observed ocular phenotypes were typical of cornea plana with the exception of one Czech patient who also had marked thinning and protrusion in the superior part of the left cornea (mean keratometry 47.2 D). No corneal endothelial cell pathology was found by specular microscopy in seven eyes, in three eyes visualization of the posterior corneal surface was unsuccessful.**

Conclusion: ***KERA*** **mutation c.740A>G has been identified to date in three different populations, which makes it the most frequently occurring mutation in patients with cornea plana. Marked corneal thinning and ectasia are a very rare finding in this disorder and longitudinal follow-up needs to be performed to determine its potential progressive nature.**

Key words: cornea plana – *KERA* – novel mutation – phenotype

Acta Ophthalmol.

doi: 10.1111/aos.13484

Introduction

Autosomal recessive cornea plana (OMIM #217300) is a rare disorder without systemic abnormalities, characterized by the presence of small, flat corneas resulting in high hyperopia and a shallow anterior chamber, widened limbal zone and is variably associated with a centrally located stromal opacity (plaque) and iris abnormalities (Pellegata et al. 2000; Khan et al. 2006a,b; Khan 2007). Unusual, rare features include corneal ectasia, potentially leading to hydrops and idiopathic corneal decompensation (Khan et al. 2005, 2006a,b; Liskova et al. 2007; AlBakri & Khan 2016).

The disorder is caused by bi-allelic mutations in *KERA* gene. This gene encodes keratocan, a small leucine-rich proteoglycan, required to generate the proper diameter and spacing of corneal stromal fibres (Kao & Liu 2002; Liu et al. 2003).

Herein, we report on the results of molecular genetic analysis of *KERA* in four families with cornea plana of different ethnic backgrounds. All but one patient with corneal ectasia presented with an ocular phenotype characteristic of this disorder.

Materials and Methods

Clinical examination

The study was approved by the relevant research ethics committees and adhered to the tenets set out in the Helsinki Declaration. All participants signed informed consent prior to inclusion into the study.

Four families with the occurrence of cornea plana were investigated in total; two affected siblings born to unrelated Czech parents, another previously unreported Czech proband and two probands of Turkish origin, both living in Belgium. Unlike the Czech families, the latter two patients reported parental consanguinity.

Best-corrected visual acuity (BCVA) was established either using Snellen or

LogMAR charts, all converted to decimal values. Intraocular pressure was measured by ICare tonometer (Iolat Ov, Helsinki, Finland) or Goldmann applanation tonometry. In the Czech patients keratometry, anterior chamber depth (ACD) and axial length were measured with the IOLMaster V.5 (Carl Zeiss Meditec AG, Jena, Germany). In patients from Belgium, these measurements were made with the Lenstar (Haag-Streit AG, Koeniz, Switzerland). In the Czech patients corneal endothelium including cell density (ECD) was evaluated by specular microscope Noncon ROBO Pachy SP-9000 (Konan Medical Inc., Tokyo, Japan) and in the other probands by Topcon SP-2000P (Topcon, Europe Medical BV, Capelle a/d IJssel, the Netherlands). Anterior segment spectral domain optical coherence tomography (SD-OCT) (Ophthalmic Technologies Inc., Toronto, ON, Canada and Spectralis, Heidelberg Engineering GmbH, Heidelberg, Germany) was used to visualize the stromal plaque and to measure the thickness of corneal cross sections. Corneal topography using Pentacam (Oculus Inc., Wetzlar, Germany) failed to pass the internal quality check in all patients despite repeated examinations.

Molecular genetic analysis

Direct sequencing of the *KERA* coding region was performed as previously described (Liskova et al. 2007). NM_007035.3 and NG_021223.1 were taken as the reference sequences. Mutation description followed the HGVS guidelines (http://www.hgvs.org/mutnomen/). Missense changes were scored for disease effect using a range of prediction tools; PROVEAN (Choi et al. 2012), SNPs&GO (Calabrese et al. 2009), MutPred (Li et al. 2009), SIFT (Kumar et al. 2009), PolyPhen-2 (Adzhubei et al. 2010) and MutationTaster (Schwarz et al. 2010). As cDNA was not available to experimentally evaluate the effect of one mutation located at the intron–exon boundary on pre-mRNA splicing, splice site prediction tools Human Splicing Finder (Desmet et al. 2009), NNSPLICE (Reese et al. 1997), MaxEntScan (Yeo & Burge 2004) and NetGene2 were applied (Brunak et al. 1991).

Evolutionary amino acid conservation of affected residues was visualized by multiple sequence alignment using T-Coffee (Di Tommaso et al. 2011). Public variant database ExAc (Exome Aggregation Consortium, http://exac.broadinstitute.org) was searched for the frequency of the detected sequence changes (accessed 8 February 2017). Population frequency specific to the Czech population was further checked in 1732 chromosomes available in house through the next-generation sequencing projects of The National Centre for Medical Genomics (http://ncmg.cz/en).

Results

Two affected male siblings aged 20 and 13 years were examined in the Department of Ophthalmology, First Faculty of Medicine, Charles University and General University Hospital in Prague.

The older brother had in the right eye abnormally low keratometry readings, shallow anterior chamber, hyperopic refractive values, indistinct limbus and central corneal opacity (Table 1 and Fig. 1A,B). Spectral domain optical coherence tomography (SD-OCT) imaging showed previously described flattened posterior surface bordered by a circle of thinning in the midperipheral cornea (Rantala & Majander 2015) (Fig. 1C). In the left eye, however, abnormally steep keratometry readings (K1/K2 44.47/49.93 D) were found (Table 1). Available medical records documented reduction of BCVA in the left eye from 0.5 to 0.3 and change in cycloplegic refraction from +3.00/−4.50 × 90° to −4.75/−6.75 × 53° between 18 and 20 years of age. Superior corneal thinning and ectasia were clearly distinguishable biomicroscopically and on anterior segment SD-OCT (Fig. 1D–F). Only one image could be captured paracentrally by specular microscopy in the right eye, but normal corneal endothelial cell morphology was found (Fig. S1A).

In the younger brother both eyes exhibited findings consistent with cornea plana diagnosis (Table 1), including the presence of an indistinct limbus and incipient central corneal opacity surrounded by a thinner rim (Fig. S1B, C). Normal corneal endothelial cell density and morphology were found bilaterally.

The second proband of Czech origin was a 70-year-old female, who

Table 1. Results of measurements taken in five patients with cornea plana. Pedigrees of individual families are shown in Fig. 1.

Family/ Origin	ID	Gender/ age (y)	Central corneal haze		BCVA		Refraction (DS, DC)		CCT (μm)		ACD (mm)		IOP (mmHg)		ECD (mm^2)		Axial length (mm)		K1/K2 (D)	
			RE	LE	RE	LE	RE	LE	RE	LE	RE	LE	RE	LE	RE	LE	RE	LE	RE	LE
1/Czech	II:1	M/20	Y	Y	0.5	0.3	+3.75/−5.75 × 90°	−4.75/−6.75 × 53°	456	427	2.55	3.19	16	16	3571*	UA	24.21	24.72	35.87/40.23	44.47/49.93
	II:2	M/13	Y	Y	0.9	0.9	+12.0	+11.0	518	511	1.88	2.04	20	20	3333	3508	24.16	24.05	24.83/26.22	25.41/26.79
2/Czech	I:1	F/70	Y	Y	0.2	0.3	+2.75	+1.5	402	418	1.94	2.07	20	18	UA	UA	25.77	26.26	27.37/30.24	29.25/30.11
3/Turkish	II:2	M/18	Y	Y	0.6	0.6	+7.0/−2.5 × 40°	+6.0/−2.0 × 50°	547	550	2.72	2.65	10	13	3882	3967	23.18	23.40	31.40/33.50	30.90/32.80
4/Turkish	II:1	F/5	N	N	0.7	0.7	+7.75	+7.75	517	495	UA	UA	20.5	21.5	3600	3103	20.84	20.95	31.25/33.00	30.25/33.25

ACD = anterior chamber depth, BCVA = best-corrected visual acuity, CCT = central corneal thickness, D = dioptre, DS = dioptre sphere, DC = dioptre cylinder, ECD = endothelial cell density, IOP = intraocular pressure, K1 = flat keratometry, K2 = steep keratometry, LE = left eye, RE = right eye, UA = unavailable data, y = years.
Normal values of ACD using IOLMaster 3.36 ± 0.41 mm (Frisch et al. 2007).
Normal values of ACD using Lenstar 2.93 ± 0.30 mm (O'Donnell et al. 2012).
* Paracentral.

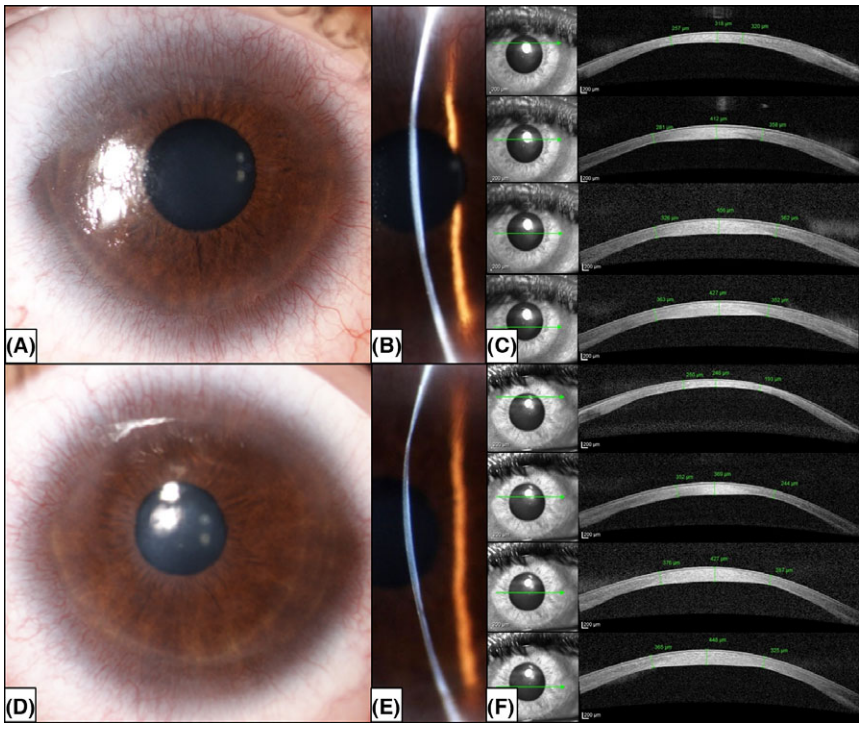

Fig. 1. Anterior segment findings in a 20-year-old Czech proband with cornea plana. Slit-lamp photograph of the right (A) and left eye (D). Narrow slit-beam view of the right (B) and left eye (E) reveals thinning at the edge of the central corneal plaque with marked protrusion in the superior part of the left eye. Cross sectional SD-OCT images confirm thinning at the edges of the stromal plaque in the right (C) and left cornea (F) and marked superotemporal thinning, especially prominent in the left eye. Values of the thickest and the thinnest measurements are shown in green.

presented with typical corneal findings indicative of cornea plana, including an arcus senilis (Fig. S1D, E). In addition, she also had bilateral rotatory nystagmus. Spectral domain optical coherence tomography (SD-OCT) also confirmed the presence of flattened posterior corneal surface in the area of central opacity and thinning at the edge (Table 1, Fig. S1E, F).

A Turkish male and an unrelated Turkish girl, both living in Belgium, were examined in the Department of Ophthalmology at the Ghent University Hospital and the Queen Fabiola Children's University Hospital in Brussels, respectively. In both patients, a diagnosis of cornea plana was made, based on the typical clinical findings described above (see Table 1). In the 18-year-old male, slit lamp examination revealed central corneal plaque with thinning at its borders (Fig. S1G). These findings were also discernible on SD-OCT. Specular microscopy was normal with an endothelial cell density of more than 3500 cells/mm^2 in both eyes (Table 1, Fig. S1H). In the 5-year-old Turkish female, the corneal endothelium did not show any pathology either, although a difference in cell density of 497 cells/mm^2 between the two eyes was found (see Table 1), which was considered to be non-significant, related to examination difficulties due to her young age.

None of the patients had additional anomalies of the iris**.**

All measurements taken in patients with cornea plana who took part in our study are summarized in Table 1.

Sequencing of *KERA* revealed two novel compound heterozygous mutations; c.209C>T; p.(Pro70Leu) and c.887-1G>A in the first Czech family (Fig. 2A); c.835C>T; p.(Arg279*) in a homozygous state in the second Czech family (Fig. 2B) and two previously reported homozygous pathogenic mutations; c.740A>G; p.(Asn247Ser) in the first family of Turkish origin (Fig. 2C) and c.674C>T; p.(Ile225Thr) in the second family of Turkish origin (Fig. 2D). All missense mutations identified in this study are located in leucine-rich repeats domains (Roos et al. 2015). ExAC data set shows that c.740A>G and c.209C>T have been detected in the general population, albeit with a low frequency (Table S1) which is consistent with recessive inheritance. None of the identified mutations was found in 866 unrelated Czech individuals without cornea plana. Prediction algorithms as well as high conservation across species supported pathogenic nature of all variants detected (Table S2 and S3 and Fig. S2).

Discussion

Cornea plana is a very rare trait. So far only 11 *KERA* mutations in patients from seven different ethnic backgrounds have been reported (Pellegata et al. 2000; Khan et al. 2004; Ebenezer et al. 2005; Liskova et al. 2007; Dudakova et al. 2014; Roos et al. 2015; Kumari et al. 2016). Herein, we report on the phenotype and identification of disease-causing mutations in five previously unreported patients from two Turkish families, both living in Belgium, and two families of Czech origin with cornea plana, with compound heterozygosity for two novel *KERA* mutations in one of them.

Available literature suggests that the ocular phenotype of cornea plana does not vary significantly with different mutations in *KERA* (Khan et al. 2006a,b, 2009; Liskova et al. 2007).

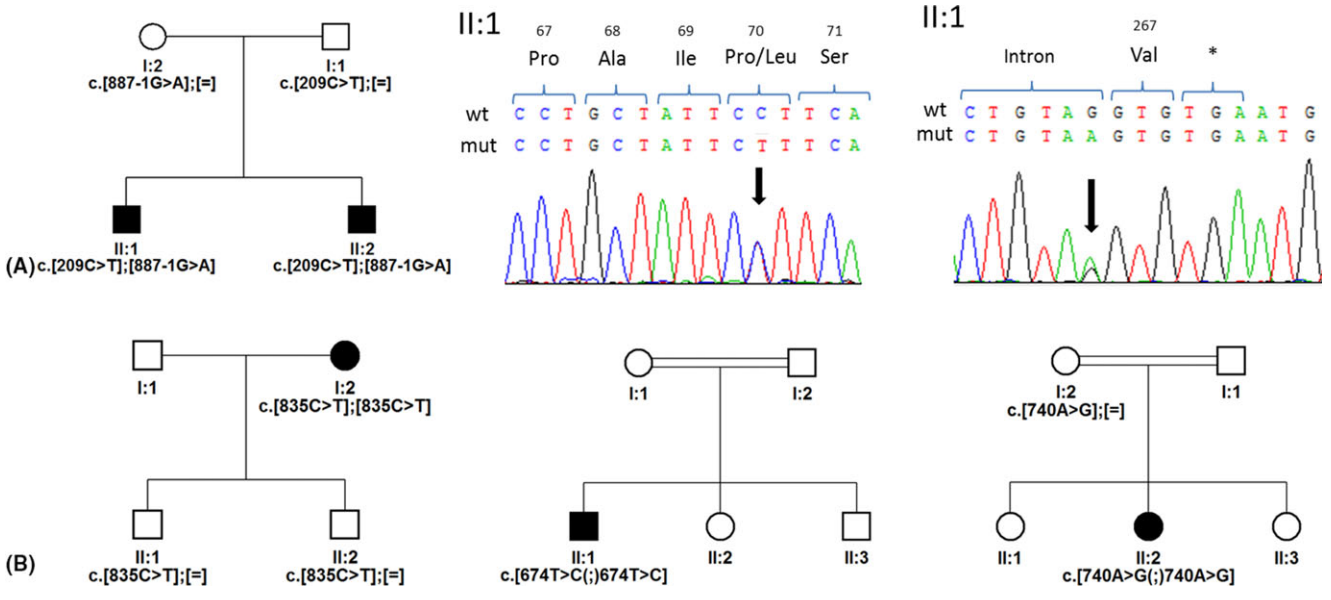

Fig. 2. Pedigrees with probands and sequence chromatograms of detected novel mutations. Czech family I, novel mutation c.209C>T and novel mutation c.887-1G>A (A), Czech family II (B), Turkish family I (C), Turkish family II (D). Mutational status is only shown in individuals available for genetic testing.

Consistent with that, all but one patient in our cohort exhibited a typical corneal phenotype without endothelial abnormalities. The only rare phenotypical finding in the current study was in a 20-year-old Czech male. His clinical records indicated high hyperopic and astigmatic correction for both eyes evolving towards myopic astigmatism in the left eye over 2 years, presumably due to thinning and protrusion of the superotemporal corneal quadrant.

Two novel mutations c.209C>T and c.887-1G>A were identified in a compound heterozygous state in one of the Czech families. The proband of the second Czech family was homozygous for c.835C>T; p.(Arg279*). This mutation has been previously found in a compound heterozygous state in another Czech patient and in a homozygous state in one Saudi family with cornea plana (Khan et al. 2005; Dudakova et al. 2014). A known *KERA* mutation c.674C>T; p.(Ile225Thr) in a homozygous state was found in one of the Turkish probands. This pathogenic variant was previously reported in another family of Turkish origin (Roos et al. 2015). The other Turkish proband was homozygous for c.740A>G; p.(Asn247-Ser) previously observed in a large cohort of Finnish families and one British family with cornea plana (Pellegata et al. 2000; Liskova et al. 2007). ExAC data set shows that it was found in a heterozygous state in 66 individuals of European descent of 36,488 corresponding to an allele frequency of 0.0005468; while it was not present in 23,860 individuals of African, East Asian, Latino and South Asian populations. This supports a hypothesis that c.740A>G is a founder mutation specific to the European population (Liskova et al. 2007). Also, an earlier study investigating haplotype of single nucleotide polymorphisms around *KERA* in one Finnish patient and two UK patients homozygous for this particular mutation showed sharing of an extended haplotype (Pellegata et al. 2000; Liskova et al. 2007).

To date the c.674C > T; p.(Ile225Thr) in *KERA* has been only observed in Turkish population suggesting a common founder. All three missense mutations found in our study were located within the leucine-rich repeat domain, which is essential for binding between keratocan and the collagen fibrils in the corneal stroma during development (Roos et al. 2015).

Both parents of the Belgian Turkish probands were not available for mutation segregation analysis. Although a gene deletion on one allele, leading to pseudo-homozygosity therefore cannot entirely be excluded, we consider this scenario as unlikely because of parental consanguinity in both sets of parents. However, in the Czech proband who is homozygous for c.835C>T; p.(Arg279*) pseudo-homozygosity remains an option even though both her sons were tested to be heterozygous for this change.

In the first report on *KERA* mutations in the Czech population (Dudakova et al. 2014), a hypothesis was proposed that a founder effect may be present as previously several patients with cornea plana were described in this particular geographical area (Forsius 1961). The identification of two novel *KERA* mutations as well as a previously reported pathogenic variant c.835C>T; p.(Arg279*) does not exclude a possible founder effect. Alternatively, the condition may be just underdiagnosed and/or unreported in many countries.

References

Adzhubei IA, Schmidt S, Peshkin L, Ramensky VE, Gerasimova A, Bork P, Kondrashov AS & Sunyaev SR (2010): A method and server for predicting damaging missense mutations. Nat Methods **7**: 248–249.

AlBakri A & Khan AO (2016): Regarding corneal decompensation in recessive cornea plana. Ophthalmic Genet **37**: 350–351.

Brunak S, Engelbrecht J & Knudsen S (1991): Prediction of human mRNA donor and acceptor sites from the DNA sequence. J Mol Biol **220**: 49–65.

Calabrese R, Capriotti E, Fariselli P, Martelli PL & Casadio R (2009): Functional annotations improve the predictive score of

human disease-related mutations in proteins. Hum Mutat **30**: 1237–1244.

Choi Y, Sims GE, Murphy S, Miller JR & Chan AP (2012): Predicting the functional effect of amino acid substitutions and indels. PLoS ONE **7**: e46688.

Desmet FO, Hamroun D, Lalande M, Collod-Beroud G, Claustres M & Beroud C (2009): Human Splicing Finder: an online bioinformatics tool to predict splicing signals. Nucleic Acids Res **37**: e67.

Di Tommaso P, Moretti S, Xenarios I, Orobitg M, Montanyola A, Chang JM, Taly JF & Notredame C (2011): T-Coffee: a web server for the multiple sequence alignment of protein and RNA sequences using structural information and homology extension. Nucleic Acids Res **39**: W13–W17.

Dudakova L, Palos M, Hardcastle AJ & Liskova P (2014): Corneal endothelial findings in a Czech patient with compound heterozygous mutations in KERA. Ophthalmic Genet **35**: 252–254.

Ebenezer ND, Patel CB, Hariprasad SM, Chen LL, Patel RJ, Hardcastle AJ & Allen RC (2005): Clinical and molecular characterization of a family with autosomal recessive cornea plana. Arch Ophthalmol **123**: 1248–1253.

Forsius H (1961): Studien uber Cornea plana congenita bei 19 Kranken in 9 Familien. Acta Ophthalmol **39**: 203–221.

Frisch IB, Rabsilber TM, Becker KA, Reuland AJ & Auffarth GU (2007): Comparison of anterior chamber depth measurements using Orbscan II and IOLMaster. Eur J Ophthalmol **17**: 327–331.

Kao WW & Liu CY (2002): Roles of lumican and keratocan on corneal transparency. Glycoconj J **19**: 275–285.

Khan AO (2007): Sclerocornea and cornea plana are distinct entities. Surv Ophthalmol **52**: 325; author reply 325–326.

Khan A, Al-Saif A & Kambouris M (2004): A novel KERA mutation associated with autosomal recessive cornea plana. Ophthalmic Genet **25**: 147–152.

Khan AO, Aldahmesh M, Al-Saif A & Meyer B (2005): Pellucid marginal degeneration coexistent with cornea plana in one member of a family exhibiting a novel KERA mutation. Br J Ophthalmol **89**: 1538–1540.

Khan AO, Aldahmesh M & Meyer B (2006a): Corneal ectasia and hydrops in a patient with autosomal recessive cornea plana. Ophthalmic Genet **27**: 99–101.

Khan AO, Aldahmesh M & Meyer B (2006b): Recessive cornea plana in the Kingdom of Saudi Arabia. Ophthalmology **113**: 1773–1778.

Khan AO, Aldahmesh MA, Al-Gehedan S, Meyer BF & Alkuraya FS (2009): Corneal decompensation in recessive cornea plana. Ophthalmic Genet **30**: 142–145.

Kumar P, Henikoff S & Ng PC (2009): Predicting the effects of coding non-synonymous variants on protein function using the SIFT algorithm. Nat Protoc **4**: 1073–1081.

Kumari D, Tiwari A, Choudhury M, Kumar A, Rao A & Dixit M (2016): A Novel KERA Mutation in a Case of Autosomal Recessive Cornea Plana With Primary Angle-Closure Glaucoma. J Glaucoma **25**: e106–e109.

Li B, VG Krishnan, Mort ME, Xin F, Kamati KK, Cooper DN, Mooney SD & Radivojac P (2009): Automated inference of molecular mechanisms of disease from amino acid substitutions. Bioinformatics **25**: 2744–2750.

Liskova P, Hysi PG, Williams D, Ainsworth JR, Shah S, de la Chapelle A, Tuft SJ & Bhattacharya SS (2007): Study of p.N247S KERA mutation in a British family with cornea plana. Mol Vis **13**: 1339–1347.

Liu CY, Birk DE, Hassell JR, Kane B & Kao WW (2003): Keratocan-deficient mice display alterations in corneal structure. J Biol Chem **278**: 21672–21677.

O'Donnell C, Hartwig A & Radhakrishnan H (2012): Comparison of central corneal thickness and anterior chamber depth measured using LenStar LS900, Pentacam, and Visante AS-OCT. Cornea **31**: 983–988.

Pellegata NS, Dieguez-Lucena JL, Joensuu T et al. (2000): Mutations in KERA, encoding keratocan, cause cornea plana. Nat Genet **25**: 91–95.

Rantala E & Majander A (2015): Anterior segment optical coherence tomography in autosomal recessive cornea plana. Acta Ophthalmol **93**: e232–e233.

Reese MG, Eeckman FH, Kulp D & Haussler D (1997): Improved splice site detection in Genie. J Comput Biol **4**: 311–323.

Roos L, Bertelsen B, Harris P, Bygum A, Jensen H, Gronskov K & Tumer Z (2015): Case report: a novel KERA mutation associated with cornea plana and its predicted effect on protein function. BMC Med Genet **16**: 40.

Schwarz JM, Rodelsperger C, Schuelke M & Seelow D (2010): MutationTaster evaluates disease-causing potential of sequence alterations. Nat Methods **7**: 575–576.

Yeo G & Burge CB (2004): Maximum entropy modeling of short sequence motifs with applications to RNA splicing signals. J Comput Biol **11**: 377–394.

Received on February 10th, 2017.
Accepted on April 18th, 2017.

Correspondence:
Petra Liskova, MD, PhD
Institute of Inherited Metabolic Disorders
General University Hospital in Prague and
First Faculty of Medicine
Charles University
Ke Karlovu 2, 128 08 Prague
Czech Republic
Tel/Fax: +420 224 967 139
Email: petra.liskova@lf1.cuni.cz

*Contributed equally to the study

This work was supported by UNCE 204011 and PROGRES-Q26/LF1 programs of the Charles University. We thank The National Centre for Medical Genomics (LM2015091) for providing ethnically matched population frequency data. PS was supported by GAUK 227015/2017. The authors would like to thank Martin Meliška for his technical assistance with SD-OCT data generation and analysis. BPL is a Senior Clinical Investigator of the Research Foundation–Flanders (Belgium) (FWO). This study was performed within the framework of ERN-EYE.

Supporting Information

Additional Supporting Information may be found in the online version of this article:

Figure S1. Corneal imaging in patients with cornea plana.
Figure S2. Evolutionary conservation of the KERA protein.
Table S1. Mutations in *KERA* coding region and intron-exon boundaries identified in four families with cornea plana.
Table S2. *In silico* analysis of rare *KERA* missense variants detected in the current study.
Table S3. *In silico* analysis of *KERA* mutation potentially affecting splicing identified in the current study.

Příloha 10: Brittle cornea syndrome: A systemic review of disease-causing mutations in *ZNF469* and two novel variants identified in a patient followed for 26 years

Brittle cornea syndrome: A systemic review of disease-causing mutations in *ZNF469* and two novel variants identified in a patient followed for 26 years

Pavlina Skalicka[a,b], Louise F. Porter[c,d], Kristyna Brejchova[a], Frantisek Malinka[a,e], Lubica Dudakova[a], Petra Liskova[a,b]

Aims. Brittle cornea syndrome (BCS) is a rare autosomal recessive disorder. The aim of this study was to review *ZNF469* mutations associated with BCS type 1 to date and to describe an additional case of Czech/Polish background.
Methods. Whole genome sequencing was undertaken to identify the molecular genetic cause of disease in the proband. Sequence variants in *ZNF469* previously reported as BCS type 1-causing were searched in the literature, manually curated and aligned to the reference sequence NM_001127464.2.
Results. The proband has been reviewed since childhood with progressive myopia and hearing loss. Aged 13 years had been diagnosed with Stickler syndrome. Aged 16.5 years, he developed acute hydrops in the left eye managed by corneal transplantation. At the age of 26, he experienced right corneal rupture after blunt trauma, also managed by grafting. He had a number of secondary complications and despite regular follow-up and timely management, the right eye became totally blind and the left eye had light perception at the last follow-up visit, aged 42. He was found to be a compound heterozygote for two novel mutations c.1705C>T; p.(Gln569*) and c.1402_1411del; p.(Pro468Alafs*31) in *ZNF469*. In total 22 disease-causing variants in *ZNF469* have been identified, mainly in consanguineous families or endogamous populations. Only four probands, including the case described in the current study, harboured compound heterozygous mutations.
Conclusion. BCS occurs very rarely in outbred populations which may cause diagnostic errors due to poor awareness of the disease. Investigation into the underlying molecular genetic cause in patients with connective tissue disorders may lead to a re-evaluation of their clinical diagnosis.

Key words: *ZNF469*, deafness, brittle cornea syndrome, blindness, corneal rupture, penetrating keratoplasty

Received: January 25, 2019; Accepted: April 5, 2019; Available online: April 17, 2019
https://doi.org/10.5507/bp.2019.017

[a]Research Unit for Rare Diseases, Department of Paediatrics and Adolescent Medicine, First Faculty of Medicine, Charles University and General University Hospital in Prague, Prague, Czech Republic
[b]Department of Ophthalmology, First Faculty of Medicine, Charles University and General University Hospital in Prague, Prague, Czech Republic
[c]St Paul's Eye Unit, The Royal Liverpool University Hospital, Prescot St, Liverpool, UK
[d]Department of Eye and Vision Science, Institute of Ageing and Chronic Disease, University of Liverpool, Liverpool, UK
[e]Department of Computer Science, Czech Technical University in Prague, Prague, Czech Republic
Corresponding author: Petra Liskova, e-mail: petra.liskova@lf1.cuni.cz

INTRODUCTION

Brittle cornea syndrome (BCS) is a rare generalized connective tissue disorder inherited as an autosomal recessive trait. Clinical ocular features include fragile thin ectatic corneas and blue sclerae. Variable commonly associated extraocular manifestations comprise skeletal and/or connective tissue abnormalities, such as joint hypermobility with occasional dislocations, kyphoscoliosis, hyperlaxity of the skin, dental abnormalities and hearing loss which develops in around one third of cases[1,2].

Mutations within two genes *ZNF469* (ref.[2,3]) and *PRDM5* (ref.[4,5]) are known to be associated with BCS type 1 (BCS1; MIM #229200) and type 2 (BCS2; MIM #614170), respectively. The disease mechanism remains unclear. Both encoded proteins ZNF469 and PRDM5 are transcription factors regulating extracellular matrix components, particularly fibrillar collagens suggesting involvement in the same pathway[3,5,6].

In this review we summarize and evaluate for pathogenicity using recent bioinformatics tools all variants in *ZNF469* previously reported as BCS1-causing including two novel *ZNF469* mutations identified in a case of Czech/Polish descent under ophthalmic review for 26 years.

MATERIALS AND METHODS

The study was approved by the Ethics committee of General University in Prague and adhered to the Declaration of Helsinki. Informed consents were signed prior to the start of all investigations.

DNA from the proband and participating family members was extracted from a venous blood sample using the Gentra Puregene blood kit (Qiagen, Hilden, Germany) and analysed by genome sequencing using a TruSeq Nano DNA library preparation kit and a HiSeq X Ten sequencer

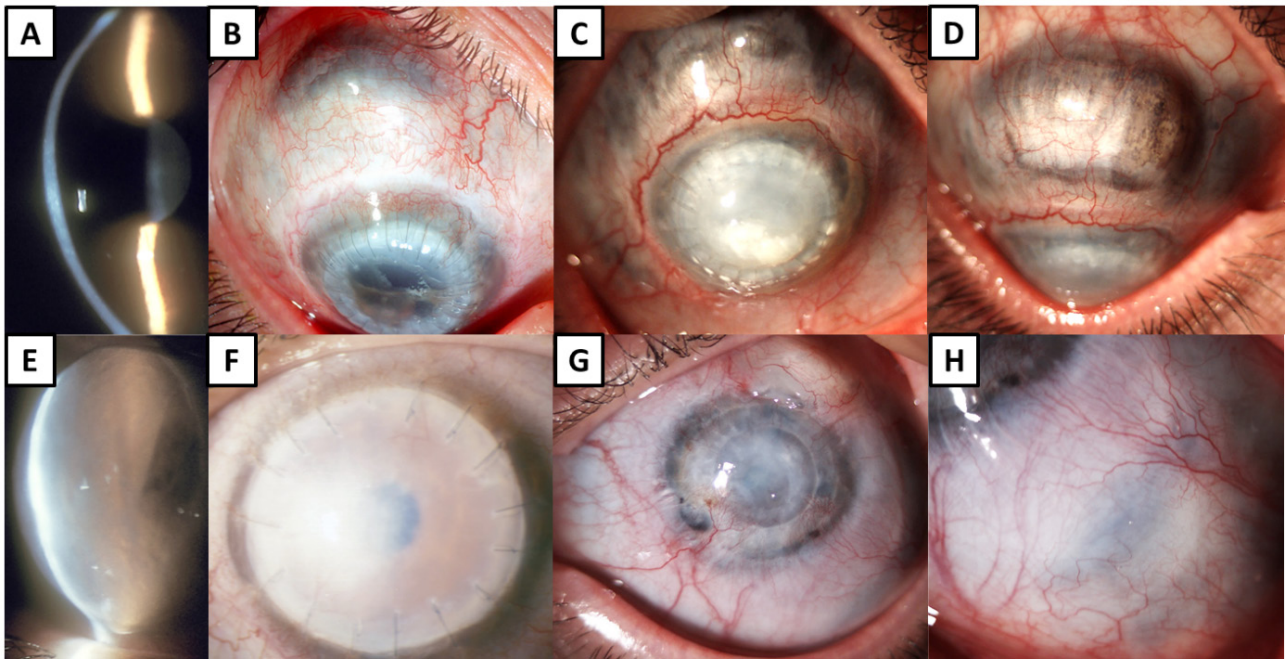

Fig. 1. Ocular findings in a patient with brittle cornea syndrome. (A) Narrow slit-beam view of the right cornea with ectasia (age 16.5 years), (B) right eye after tectonic penetrating keratoplasty, note blue sclerae superior from the corneal limbus (age 26.5), (C) opaque right graft with lipoid keratopathy and progression of scleral thinning, (D) in detail (age 42). (E) Acute hydrops in the left eye (age 16.5); (F) left graft failure (age 17.5), (G) left eye with a vascularized graft (age 42), (H) detail of blue sclerae (age 42).

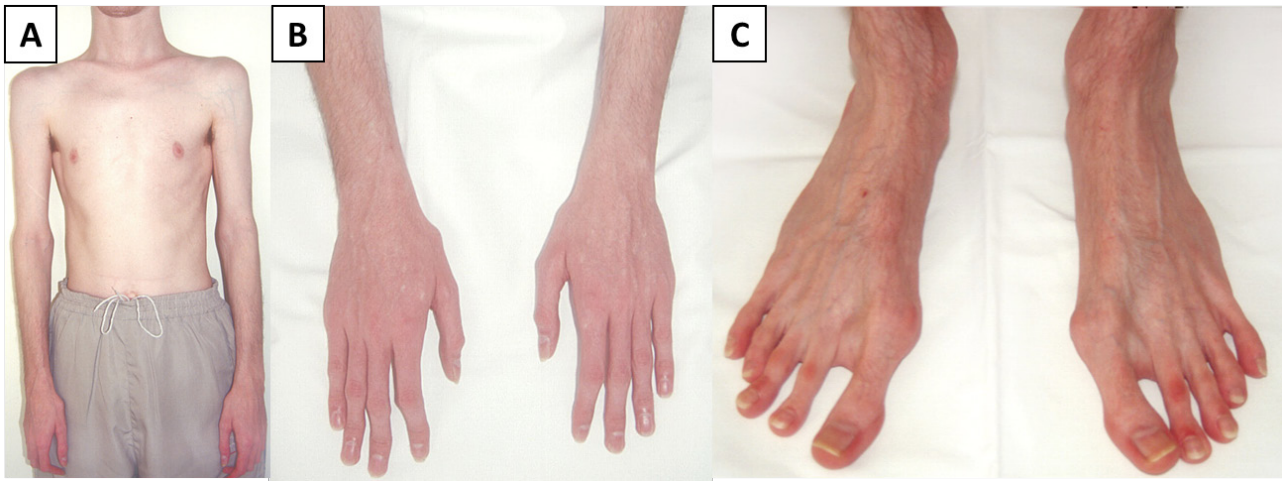

Fig. 2. Physical appearance of the patient with brittle cornea syndrome. (A) asthenic habitus (age 26); (B) hands with clinodactyly (age 26); (C) feet with hallux valgus (age 26).

(Illumina). FASTQ reads were aligned to the GRCh38/hg38 human reference sequence using the Burrows-Wheeler Alignment tool[7]. Variant calling was performed with HaplotypeCaller[8]. Sequence changes with a minor allele frequency <0.005 in *ZNF469* and *PRDM5* were prioritized for further evaluation. Conventional Sanger sequencing was applied to show segregation of the detected mutation within the family[9].

Sequence variants previously reported as causing BCS1 were searched in the literature, manually curated and aligned to the reference sequence NM_001127464.2. Missense variants were subjected to *in silico* analysis using 6 different tools. The population frequency of the variants was retrieved from the Genome Aggregation Database (gnomAD), providing sequencing data from more than 138,000 unrelated individuals of various ethnic backgrounds[10], and 4,528 Czech control chromosomes available through the projects of the National Center for Medical Genomics (https://ncmg.cz/en).

RESULTS

CASE REPORT

The proband of Czech/Polish descent was under ophthalmic review from his 3rd birthday because of progressive myopia. According to his clinical notes, he was diagnosed with bilateral corneal ectasia before the age of

Table 1. Ocular surgeries performed in the proband reviewed for 26 years.

Eye	Age (years)	Procedure	Reason	Preoperative BCVA	Postoperative BCVA (3 months after surgery)	Comment
RE	26.0	Tectonic PK	Large corneal perforation after blunt trauma	LP	0.16	Graft size 8.5 mm, aphakia (lens lost during trauma)
	26.0	AMT	Wound leakage	0.16	0.16	
	26.5	PPV + SO	Retinal detachment	0.10	0.25	
	28.5	CCK	Secondary glaucoma	LP	LP	
LE	16.5	PK	Corneal hydrops	LP	0.16	Graft size 9.0 mm
	17.5	rePK	Graft failure	0.01	0.01	
	17.5	TE	Secondary glaucoma	0.01	NA	Performed 11 days after rePK
	20.0	rePK	Graft failure	LP	0.16	Graft size 6.2 mm

AMT - amniotic membrane transplantation; BCVA - best corrected visual acuity (measured on Snellen charts and extrapolated to decimal values); CCK – cyclocryocoagulation; LE - left eye; LP – light projection; PK - penetrating keratoplasty; PPV - pars plana vitrectomy; RE - right eye; rePK – repeated penetrating keratoplasty; SO - silicone oil tamponade; TE – trabeculectomy

Table 2. Summary of *ZNF469* mutations and individual families with brittle cornea syndrome reported to date.

DNA level	Protein level	No of affected subjects/with hearing loss	No. of families	Origin	Zygosity	Consanguinity	Ref.
c.1402_1411del c.1705C>T	p.(Pro468Alafs*31) p.(Gln569*)	1/1	1	Caucasian Czech/ Polish	Compound HET	N	Current study
c.1963dup c. 6360dup	p.(His655Profs*83) p.(Gln2121Alafs*42)	1/0	1	Not provided	Compound HET	N	17
c.2029G>T	p.(Gly677*)	2/0	1	Saudi Arabian	HOM	Y	1,13
c.2150del	p.(Phe717Serfs*15)	3/0	2	Saudi Arabian	HOM	Y/1, N/1[#]	1,13[#],18
c.3220G>T	p.(Glu1074*)	1/1	1	Yemenish	HOM	Y	1,13
c.3392del	p.(Gly1131Alafs*105)	1/1	1	Indian	HOM	Y	13
c.4174G>T	p.(Glu1392*)	2/0	1	Syrian	HOM	Y	19
c.5269C>T	p.(Gln1757*)	3/3	2	Syrian	HOM	Y	1,13
c.5704del c.5704dup	p.(Gln1902Argfs*6) p.(Gln1902Profs*133)	1/1	1	Caucasian British	Compound HET	N	13
c.5943del	p.(Gly1983Alafs*16)	6/NA	4	Tunisian Jewish	HOM	Y/3, N/1[#]	3,20
c.6360del	p.(Gln2121Serfs*51)	1/0	1	Pakistani	HOM	Y	1,13
c.6644delA deletion of 1q24.1 including *ZNF469*	p.(Asp2215Alafs*8). p.?	1/0	1	Caucasian	Compound HET	N	12
c.6563del	p.(Gln2188Argfs*21)	2/0	1	Syrian	HOM	Y	1,13
c.8817_8830dup	p.(Glu2944Glyfs*50)	8/4	2	Saudi Arabian	HOM	Y	1,13,21
c.9399del	p.(His3134Thrfs*20)	1/0	1	Saudi Arabian	HOM	Y	1,13
c.9531del	p.(Gln3178Argfs*23)	6/NA	1	Palestinian	HOM	Y	3
c.10016G>A	p.(Cys3339Tyr)	2/2	1	Norwegian	HOM	Y	2
c.10022G>C	p.(Arg3341Pro)	1/0	1	Syrian	HOM	Y	1,13

HOM = homozygous, HET = heterozygous, Y= yes, N = no, NA = not available
[#]common founder with other families carrying the same mutation
All mutations were curated based on original publications and are listed according to the reference sequence NM_001127464.2. Recommendations of Human Genome Variation Society were used for description. Information on origin was mined from published reports.

Table 3. *In silico* analysis of two missense variants in *ZNF469*.

DNA level	Protein level	PolyPhen2 (ref.[22])	PROVEAN (ref.[23])	SIFT (ref.[23])	MutPred2 (ref.[24])	Mutation Taster (ref.[25])	SNP&GO (ref.[26])
c.10016G>A	p.(Cys3339Tyr)	Probably damaging	Disease	Damaging	Disease causing	Disease causing	Disease
c.10022G>C	p.(Arg3341Pro)	Probably damaging	Neutral	Damaging	Disease causing	Polymorphism	Disease

Both mutations were detected in a compound heterozygous state with a truncating mutation in patients with BCS1 (NM_001127464.2).

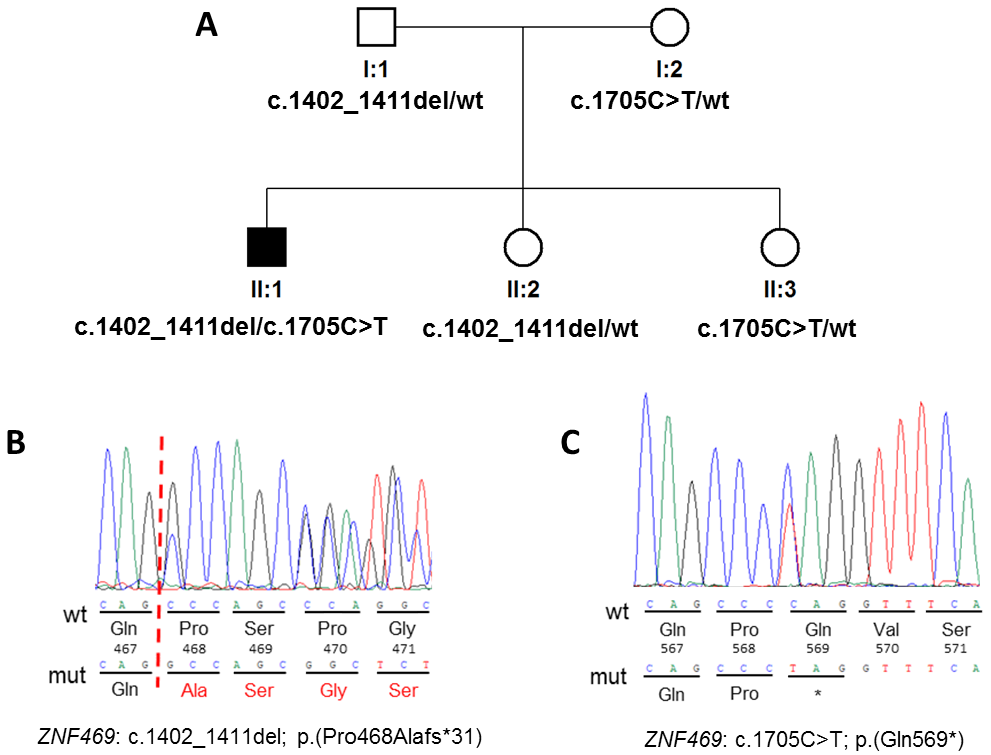

Fig. 3. Pedigree and results of molecular genetic testing. (A) Pedigree of the investigated family, sequence chromatograms of the heterozygous mutations identified in *ZNF469* (B) c.1402_1411del and (C) c.1705C>T. Wild type is referred as "wt".

13 years. Best corrected visual acuity (BCVA) at the age of 16 was 0.1 (Snellen decimal conversion) with -23 dioptre sphere (DS) in the right eye, and 0.06 with -23 DS x -4.0 dioptre cylinder in the left eye. At the age of 16.5 years he was referred to the Department of Ophthalmology, General University Hospital in Prague, with acute corneal hydrops in the left eye (Fig. 1E). Blue sclerae were also noticed bilaterally (Fig. 1B, H). Right cornea was ectatic (Fig. 1A). No other abnormalities of iris, pupil, lens or retina were noted. Penetrating keratoplasty was performed two months later in view of persistence of the corneal edema and light perception visual acuity in the affected eye. Unfortunately, the patient suffered from immunological rejection and graft failure (Fig. 1F). Two repeated keratoplasties were therefore performed at the age of 17.5 and 20 years complicated by increased intraocular pressure (IOP) necessitating trabeculectomy. Eighteen months after the third keratoplasty, BCVA was 0.16 in the left eye. Thereafter the graft gradually failed (Fig. 1G) and 23 years following his examination (now aged 42) BCVA in the left eye was light perception. IOP remained controlled.

At the age of 26, the patient experienced right corneal rupture with lens dislocation after blunt trauma. Tectonic penetrating keratoplasty was performed. Five months after the surgery, the right retina detached and the patient underwent pars plana vitrectomy and silicone oil tamponade. Unfortunately, uncontrollable secondary glaucoma caused progressive BCVA decline. The corneal graft in the right also failed and became opaque (Fig. 1C). Since the age of 32, the right eye was totally blind. Progression of scleral ectasia was documented (Fig. 1B,C,D). Table 1 lists all surgeries the patient underwent since the age of 16.5 years.

In addition, the proband had been followed up since childhood (11 years of age) for sensorineural hearing loss, managed with a hearing aid. Repeated audiometry confirmed the presence of moderate symmetrical non-progressive impairment in both ears with a loss in the range of 45-65 dB. Mild worsening was observed with age and deemed to be age-associated.

Transthoracic echocardiography was performed at the age of 17 and 26 years. Mitral and tricuspid valve insufficiencies were noted but not deemed functionally important. Incomplete right bundle branch block was also detected on electrocardiography and considered benign, not requiring treatment. Aged 26 years the patient's height was 190 cm and his weight was 60 kg, with concomitant mild kyphoscoliosis, clinodactyly and hallux valgus (Fig. 2). No joint subluxations, fractures, abnormal contractures or severe bone deformities were found. No skin striae, excessive scarring, bruising or abnormal laxity were observed. At the age of 31, the proband underwent surgery for right scrotal hernia. Of note, he also suffered from excessive dental caries since childhood. Details of dental examinations were however unavailable.

Importantly, since the age of 13 he had been considered to be a *de novo* case of Stickler syndrome. This diagnosis remained unchallenged until the age of 40, when a clinical diagnosis of BCS based on careful review of his past clinical notes was suspected.

Molecular genetic diagnosis uncovered compound heterozygosity for c.1705C>T; p.(Gln569*) and

c.1402_1411del; p.(Pro468Alafs*31) in *ZNF469* (Fig.3), absent from gnomAD as well as from white Czech control chromosomes, confirming BCS1. As truncating mutations have been previously associated with BCS1 (Table 2), these variants were considered pathogenic. Consistent with autosomal recessive disease, both parents were heterozygous carriers of each detected variants. Two unaffected sisters were also heterozygous carriers (Fig. 3).

Summary of *ZNF469* mutations causing BCS1

Including this study, there are 22 different sequence variants reported as pathogenic in 24 families with more than 40 family members affected by BCS1 (Table 2). Only four probands were compound heterozygotes, the rest were homozygotes.

None of the mutations had an entry in gnomAD. Sixteen reported variants are predicted to result in the interruption of translation, consequently leading either to a truncation of the encoded protein, or degradation of aberrant transcripts by nonsense-mediated mRNA decay[11]. One mutation was a large deletion encompassing the whole *ZNF469* gene. Two variants were missense mutations[1,12,13]. Pathogenicity predictions using six software tools supported the disease-causing role of the two missense mutations (Table 3).

One additional variant reported as disease-causing c.7424C>A; p.(Ala2475Glu) (ref.[13]) was discarded because of its high prevalence in the general population (minor allele frequency 0.07422, with 567 homozygotes reported as per gnomAD), not matching the rarity of BCS1.

DISCUSSION

BCS1 is an ultra-rare disease. In addition to a comprehensive curation and summary of all 22 disease-causing mutations in *ZNF469* associated with BCS1 reported to date, we present a case harbouring two novel pathogenic variants detected by genome sequencing.

Analysis using current bioinformatic tools, especially interrogation of publicly available minor allele frequencies, allowed us to dismiss one *ZNF469* variant previously associated with BCS1 highlighting the general fact that there is a need of re-evaluation of mutational findings published before the era of large datasets. BCS1 has been caused by homozygous mutations in the great majority of families, which is consistent with consanguinity and/or marriages within endogamous populations. The function of ZNF469 has not been fully resolved, however the importance of the protein on corneal structure and development has been recently confirmed, showing association with keratoconus and central corneal thickness[9,14].

Although the phenotype in our proband was typical it took more than two decades to make the correct diagnosis. His clinical course confirms the fact that management of corneal rupture in BCS is difficult and outcomes are usually unsatisfactory despite state-of-the-art treatment[15,16]. It is therefore of utmost importance to recognize BCS early, in order to apply preventive measures. As a part of our long-term follow-up we have also documented sensorineural hearing impairment with no progression other than age-related mild decline.

CONCLUSION

BCS1 occurs very rarely in outbred populations which may cause diagnostic errors due to poor awareness of the disease. Molecular genetic analysis evolved to be an essential part of the diagnostic process in many rare diseases including BCS, and in some cases, it may even lead after many years to a correction of the clinical diagnosis.

Search strategy and selection criteria

Our research strategy was aimed at identifying studies reporting on *ZNF469* mutations associated with BCS1. Scientific articles from 1999 to December 2018 were searched using the PubMed and Scopus databases. The search terms used included “brittle cornea syndrome”, “*ZNF469*“, “mutation“, “variant“. All relevant articles were reviewed.

Acknowledgement: This work was supported by GAUK 250361/2017. Institutional support was provided by UNCE 204011, SVV 260367/2017 and PROGRES Q26/LF1 programs of the Charles University. LFP is a clinical lecturer funded by NIHR. FM was supported by OP VVV MEYS funded project CZ.02.1.01/0.0/0.0/16_019/0000765 "Research Center for Informatics". We thank The National Center for Medical Genomics (LM2015091) providing ethnically matched population frequency data (project CZ.02.1.01/0.0/0.0/16_013/0001634).

Author contributions: PS: manuscript writing, data collection; LFP: manuscript writing, data collection and analysis, KB: manuscript writing, figure preparation and literature search, FM: manuscript writing, statistical analysis, LD: manuscript writing, figure preparation and PL manuscript writing, study design.

Conflict of interest statement: The authors state that there are no conflicts of interest regarding the publication of this article.

REFERENCES

1. Al-Hussain H, Zeisberger SM, Huber PR, Giunta C, Steinmann B. Brittle cornea syndrome and its delineation from the kyphoscoliotic type of Ehlers-Danlos syndrome (EDS VI): report on 23 patients and review of the literature. Am J Med Genet A 2004;124A:28-34.
2. Christensen AE, Knappskog PM, Midtbo M, Gjesdal CG, Mengel-From J, Morling N, Rødahl E, Boman H. Brittle cornea syndrome associated with a missense mutation in the zinc-finger 469 gene. Invest Ophthalmol Vis Sci 2010;51:47-52.
3. Abu A, Frydman M, Marek D, Pras E, Nir U, Reznik-Wolf H, Pras E. Deleterious mutations in the Zinc-Finger 469 gene cause brittle cornea syndrome. Am J Hum Genet 2008;82:1217-22.
4. Burkitt Wright EMM, Spencer HL, Daly SB, Manson FDC, Zeef LAH, Urquhart J, Zoppi N, Bonshek R, Tosounidis I, Mohan M, Madden C, Dodds A, Chandler KE, Banka S, Au L, Clayton-Smith J, Khan N, Biesecker LG, Wilson M, Rohrbach M, Colombi M, Giunta C, Black

GCM. Mutations in PRDM5 in brittle cornea syndrome identify a pathway regulating extracellular matrix development and maintenance. Am J Hum Genet 2011;88:767-77.
5. Porter LF, Gallego-Pinazo R, Keeling CL, Kamieniorz M, Zoppi N, Colombi M, Giunta C, Bonshek R, Manson FD, Black GCM. Bruch's membrane abnormalities in PRDM5-related brittle cornea syndrome. Orphanet J Rare Dis 2015;10:145.
6. Galli GG, Honnens de Lichtenberg K, Carrara M, Hans W, Wuelling M, Mentz B, Multhaupt HA, Fog CK, Jensen KT, Rappsilber J, Vortkamp A, Coulton L, Fuchs H, Gailus-Durner V, Hrabě de Angelis M, Calogero RA, Couchman JR, Lund. Prdm5 regulates collagen gene transcription by association with RNA polymerase II in developing bone. PLoS Genet 2012;8:e1002711.
7. Li H, Durbin R. Fast and accurate long-read alignment with Burrows-Wheeler transform. Bioinformatics 2010;26:589-95.
8. Van der Auwera GA, Carneiro MO, Hartl C, Poplin R, Del Angel G, Levy-Moonshine A, Jordan T, Shakir K, Roazen D, Thibault J, Banks E, Garimella KV, Altshuler D, Gabriel S, DePristo MA. From FastQ data to high confidence variant calls: the Genome Analysis Toolkit best practices pipeline. Curr Protoc Bioinformatics 2013;43:11.10.1-11.10.33. doi: 10.1002/0471250953.bi1110s43
9. Lechner J, Porter LF, Rice A, Vitart V, Armstrong DJ, Schorderet DF, Munier FL, Wright AF, Inglehearn CF, Black GC, Simpson DA, Manson F, Willoughby CE. Enrichment of pathogenic alleles in the brittle cornea gene, ZNF469, in keratoconus. Hum Mol Genet 2014;23:5527-5535.
10. Lek M, Karczewski KJ, Minikel EV, Samocha KE, Banks E, Fennell T, O'Donnell-Luria AH, Ware JS, Hill AJ, Cummings BB, Tukiainen T, Birnbaum DP, Kosmicki JA, Duncan LE, Estrada K, Zhao F, Zou J, Pierce-Hoffman E, Berghout J, Cooper DN, Deflaux N, DePristo M, Do, Flannick J, Fromer M, Gauthier L, Goldstein J, Gupta N, Howrigan D, Kiezun A, Kurki MI, Moonshine AL, Natarajan P, Orozco L, Peloso GM, Poplin R, Rivas MA, Ruano-Rubio V, Rose SA, Ruderfer DM, Shakir K, Stenson PD, Stevens C, Thomas BP, Tiao G, Tusie-Luna MT, Weisburd B, Won HH, Yu D, Altshuler DM, Ardissino D, Boehnke M, Danesh J, Donnelly S, Elosua R, Florez JC, Gabriel SB, Getz G, Glatt SJ, Hultman CM, Kathiresan S, Laakso M, McCarroll S, McCarthy MI, McGovern D, McPherson R, Neale BM, Palotie A, Purcell SM, Saleheen D, Scharf JM, Sklar P, Sullivan PF, Tuomilehto J, Tsuang MT, Watkins HC, Wilson JG, Daly MJ, MacArthur DG; Exome Aggregation Consortium. Analysis of protein-coding genetic variation in 60,706 humans. Nature 2016;536:285-91.
11. Hug N, Longman D, Caceres JF. Mechanism and regulation of the nonsense-mediated decay pathway. Nucleic Acids Res 2016;44:1483-95.
12. Ramappa M, Wilson ME, Rogers RC, Trivedi RH. Brittle cornea syndrome: a case report and comparison with Ehlers Danlos syndrome. J AAPOS 2014;18:509-11.
13. Rohrbach M, Spencer HL, Porter LF, Burkitt-Wright EM, Bürer C, Janecke A, Bakshi M, Sillence D, Al-Hussain H, Baumgartner M, Steinmann B, Black GC, Manson FD, Giunta C. ZNF469 frequently mutated in the brittle cornea syndrome (BCS) is a single exon gene possibly regulating the expression of several extracellular matrix components. Mol Genet Metab 2013;109:289-95.
14. Davidson AE, Borasio E, Liskova P, Khan AO, Hassan H, Cheetham ME, Plagnol V, Alkuraya FS, Tuft SJ, Hardcastle AJ. Brittle cornea syndrome ZNF469 mutation carrier phenotype and segregation analysis of rare ZNF469 variants in familial keratoconus. Invest Ophthalmol Vis Sci 2015;56:578-86.
15. Burkitt Wright EM, Porter LF, Spencer HL, Clayton-Smith J, Au L, Munier FL, Smithson S, Suri M, Rohrbach M, Manson FD, Black GC. Brittle cornea syndrome: recognition, molecular diagnosis and management. Orphanet J Rare Dis 2013;8:68.
16. Izquierdo L, Jr., Mannis MJ, Marsh PB, Yang SP, McCarthy JM. Bilateral spontaneous corneal rupture in brittle cornea syndrome: a case report. Cornea 1999;18:621-4.
17. Menzel-Severing J, Meiller R, Kraus C, Trollmann R, Atalay D. Brittle cornea syndrome type 1 caused by compound heterozygosity of two mutations in the ZNF469 gene. Ophthalmologe 2018 Oct 18. doi: 10.1007/s00347-018-0796-8 [Epub ahead of print] [Article in German]
18. Khan AO, Aldahmesh MA, Alkuraya FS. Brittle cornea without clinically-evident extraocular findings in an adult harboring a novel homozygous ZNF469 mutation. Ophthalmic Genet 2012;33:257-9.
19. Khan AO, Aldahmesh MA, Mohamed JN, Alkuraya FS. Blue sclera with and without corneal fragility (brittle cornea syndrome) in a consanguineous family harboring ZNF469 mutation (p.E1392X). Arch Ophthalmol 2010;128:1376-9.
20. Abu A, Frydman M, Marek D, Pras E, Stolovitch C, Aviram-Goldring A, Rienstein S, Reznik-Wolf H, Pras E. Mapping of a gene causing brittle cornea syndrome in Tunisian jews to 16q24. Invest Ophthalmol Vis Sci 2006;47:5283-7.
21. Al-Owain M, Al-Dosari MS, Sunker A, Shuaib T, Alkuraya FS. Identification of a novel ZNF469 mutation in a large family with Ehlers-Danlos phenotype. Gene 2012;511:447-50.
22. PolyPhen-2. Prediction of functional effects of human nsSNPs. http://genetics.bwh.harvard.edu/pph2/ (accessed12/2018).
23. PROVEAN (Protein Variation Effect Analyzer): a software tool which predicting whether an amino acid substitution or indel has an impact on the biological function of a protein. It also shows SIFT predictions when precomputed scores are available. http://provean.jcvi.org/protein_batch_submit.php?species=human (accessed 12/2018).
24. MutPred2. Predict the pathogenicity of amino acid substitutions and their molecular mechanisms. http://mutpred.mutdb.org/#qform
25. Mutation Taster: The free web-based application to evaluate DNA sequence variants for their disease-causing potential. http://www.mutationtaster.org/ (accessed 12/2018)
26. SNP&GO: Predicting disease associated variations using GO terms. http://snps.biofold.org/snps-and-go/snps-and-go.html (accessed 12/2018)